The effects of *Neisseria meningitidis* infection on endothelial E-selectin, and consequences for neutrophil adhesion and transmigration

Philip James Dusart

This thesis is submitted for the degree of Doctor of Philosophy
at University College London

Division of Infection and Immunity
UCL

July 2014

Declaration:

I, Philip Dusart, confirm that the work presented in this thesis is my own. Where information and help has been obtained from other sources, this has been indicated in the text.

Abstract

Severe septicaemia due to the bacterium *Neisseria meningitidis* is characterised by substantial recruitment and activation of neutrophils on inflamed endothelium, and is associated with vascular damage. *N.meningitidis* associates with endothelial cells, E-selectin, and neutrophils in patient biopsies, and E-selectin can co-localise beneath adherent bacteria *in vitro*. This thesis aims to investigate whether *N.meningitidis* affects E-selectin distribution on the endothelial surface and whether meningococcal-E-selectin interactions have functional consequences on neutrophil rolling, adhesion and transmigration across vascular endothelium.

Lentiviral constructs were created containing full-length E-selectin (ES) or a cytoplasmic domain deficient mutant (ΔC). Transfection of primary HUVEC demonstrated that ES E-selectin forms spontaneous clusters, while ΔC is expressed in a diffuse membrane pattern. Capsulated *N.meningitidis* was unreliable at inducing E-selectin clustering and co-localisation. In contrast, an unencapsulated *SiaD*- strain could co-localise with endogenous IL-1β induced E-selectin, although not with transfected ES or ΔC. Thus the E-selectin cytoplasmic domain affects both the molecule's distribution on the endothelial membrane, and also *N.meningitidis* mediated redistribution, which additionally requires some factor present on IL-1β stimulated, but not ES or ΔC transfected, endothelium.

Functional aspects of *N.meningitidis* interactions with E-selectin on neutrophil behaviour were also investigated. Brief co-culture of *N.meningitidis* with ES transfected HUVEC induced increased neutrophil adhesion under static conditions and greater transmigration under physiological flow. Neutrophil adhesion to *N.meningitidis* stimulated ΔC transfected HUVEC however, was no greater than untransfected cells. ΔC HUVEC also only saw a small increase in transmigration despite having comparable adhesion and rolling velocity to ES cells under flow. Taken together these results show that the E-selectin cytoplasmic domain has an important yet unstudied role in neutrophil adhesion and transmigration. These data should lead to a better understanding of the underlying processes surrounding neutrophil mediated endothelial damage caused by *N.meningitidis*, and could have broader relevance for other inflammatory responses, particularly in sepsis.

Acknowledgements

First of all I would like to my supervisor, Garth Dixon, for his guidance throughout the project, and always being a good source of motivation, especially when I was having trouble seeing the end product of my experiments. I would also like to thank my secondary supervisor Nigel Klein, for his help during my PhD, and along with Garth, for giving me the opportunity to take on this project.

The other fellow members of Team Meningococcus at ICH, Marianne Jacobsen, Hannah Jones and Alastair Copland, have been invaluable support, especially Marianne who helped to teach me everything to do with the endothelium at the start of this project, and also for holding lab meetings with a drink or two!

The lentivirus work in this thesis would have been impossible without the assistance and advice of Emma Chan and Waseem Qasim, who both provided the plasmids and taught me how to use them to make the virus. All of the microscope work in this thesis owes a large amount of gratitude to Bertrand Vernay, who appears to know everything there is to know about microscopy, and almost always had a solution when the microscopes were playing up.

Aleksander Ivetic from King's College London was a great help when developing the transmigration experiments, and speaking with him helped to spark many interesting ideas as well as experiments to investigate neutrophil adhesion and transmigration.

I would also like to thank all of my friends, especially those who convinced me to do a PhD in the first place. And a massive thanks to everyone in office 646, both past and present, who have both helped keep me sane throughout the project, and were usually willing to go down the pub when things got too bad; Shaz, Joanna, Sarah, Marianne, Lisa, Ronan, Hannah P and Hannah J, Arianne, Alastair, Eva, anyone I may have forgotten, and of course Vania who keeps the whole department running.

Finally I would like to thank my family; my parents, who were always supportive of everything I do even if they don't understand it, and Lesley who is always good at keeping me down to earth when I start talking too much science! Last of all I want to thank Celine for everything over the last few years; for putting up with my working late and getting stressed, for asking "so are you working?" when I am busy procrastinating, and most of all for looking forward with me for where we're going next.

Table of Contents

Table of Figures

Table of Videos (On CD)

Abbreviations

AAV	Adeno-associated virus
ATF-2	Activating Transcription Factor 2
BBB	Blood Brain Barrier
C4bp	C4 binding protein
CAMP	Cationic antimicrobial peptide
CCP	Complement control protein
cDNA	Coding Deoxyribonucleic Acid
CEACAM	Carcinoembryonic antigen-related cell adhesion molecule
CHO	Chinese Hamster Ovary (cell line)
CSF	Cerebro Spinal Fluid
DAPI	4',6-diamidino-2-phenylindole
DNA	Deoxyribonucleic Acid
ERK	Extracellular-signal-regulated Kinase
erm	Erythromycin ribosomal methylase
ES	Full length transfected E-selectin
ESL-1	E-selectin Ligand 1
EU	Endotoxin Unit
FCS	Foetal Calf Serum
fH	Complement factor H
fHbp	Factor H binding protein
FITC	Fluorescein isothiocyanate
FPS	Frames per second
GFP	Green Fluorescent Protein
HEK293T	Human Embryonic Kidney cell line
HMEC-1	Human Microvascular Endothelial Cell line
HUVEC	Human Umbilical Vein Endothelial Cell
ICAM-1	Intracellular Adhesion Molecule 1
IL-1β	Interleukin 1 β
LFA-1	Lymphocyte function-associated antigen 1
LOS	Lipooligosaccharide
LPS	Lipopolysaccharide
MAC	Membrane Attack Complex
MAPK	Mitogen-activated protein kinase
MASP-2	MBL-associated serine protease-2
MBL	Mannose Binding Lectin
MFI	Median Fluorescence Intensity
mRNA	Messenger RNA
Msf	Meningococcal surface fibril
NadA	Neisserial adhesin A
NADPH	Nicotinamide adenine dinucleotide phosphate
NCAM	Neural Cell Adhesion Molecule
NET	Neutrophil Extracellular Trap
NFκB	Nuclear Factor κB
NHBA	Neisseria heparin binding antigen
Nhha	Neisseria hia homologue

OMP	Outer Membrane Protein
OMV	Outer membrane vesicle
PAMP	Pathogen Associated Molecular Pattern
PBS	Phosphate Buffered Saline
PCR	Polymerase Chain Reaction
PRR	Pattern Recognition Receptor
PSGL-1	P-selectin glycoprotein ligand-1
qPCR	Real-time Quantitative PCR
RNA	Ribonucleic Acid
ROS	Reactive Oxygen Species
RPE	R-phycoerythrin
RT	Room Temperature
SD	Standard deviation
SEM	Standard error of the mean
SHP2	Src Homology Phosphatase 2
SiaD	Polysialyltransferase
Tbp	Transferrin binding protein
TLR	Toll-like Receptor
TNFα	Tumour necrosis factor α
TSAP	Thermostable Shrimp Alkaline Phosphatase
VCAM-1	Vascular cell adhesion molecule 1
vWF	von Willibrand factor
WT	Wild Type
ΔC	Tail-less mutant transfected E-selectin (delta-cytoplasmic region)

1 Introduction

1.1 Epidemiology of meningococcal disease

1.1.1 Geographical spread of disease and serotypes

Neisseria meningitidis (*N.meningitidis*) is a gram-negative diplococcus, specific to humans, which can cause both meningitis and septicaemia. The incidence of meningococcal disease in the UK is 1.63 cases per 100,000 people, which is the third highest in Europe behind Ireland and Lithuania(European Centre for Disease Prevention and Control, 2013; Jafri et al., 2013). The disease burden however falls disproportionally on the very young, with those under 5 having much greater incidence than the greater population(European Centre for Disease Prevention and Control, 2013; Public Health England, PHE, 2014; Trotter et al., 2007).

Meningococcal disease rates are similar across Europe and the Americas (Incidence 0.2-2.0/100,000), with a few large outbreaks in Uruguay, Brazil and Cuba (1-5 cases/100,000). Meningococcal disease is rarer in East Asian countries such as China and Japan, as well as some south-east Asian countries such as Thailand (Incidence <0.2/100,000 population)(Jafri et al., 2013; Vyse et al., 2011). The low disease burden across Europe, America and some East Asian countries is largely attributable to extensive vaccination programs, and historical incidence is much higher(Vyse et al., 2011). Accurate data is not available for many less developed Asian countries such as India, Pakistan and Indonesia, although outbreaks have been reported in some regions and cities, and the disease burden there may be higher than currently suspected. (Vyse et al., 2011)

The largest disease burden of *N.meningitidis* however is in Africa; particularly in the group of African countries spanning from the western African coast, across the southern Saharan desert and into western Ethiopia, which make up a region known as the "meningitis belt" as shown on the map in Figure 1.1.(Molesworth et al., 2002)

Countries in the meningitis belt have a much greater incidence of infection compared to developed countries, as well as the rest of Africa, with regular seasonal epidemics (defined as incidence of >10/100,000), and severe epidemics causing infection rates of over 100 cases per 100,000 people and up to 500-1000/100,000in the worst events(Jafri et al., 2013; Rosenstein et al., 2001).

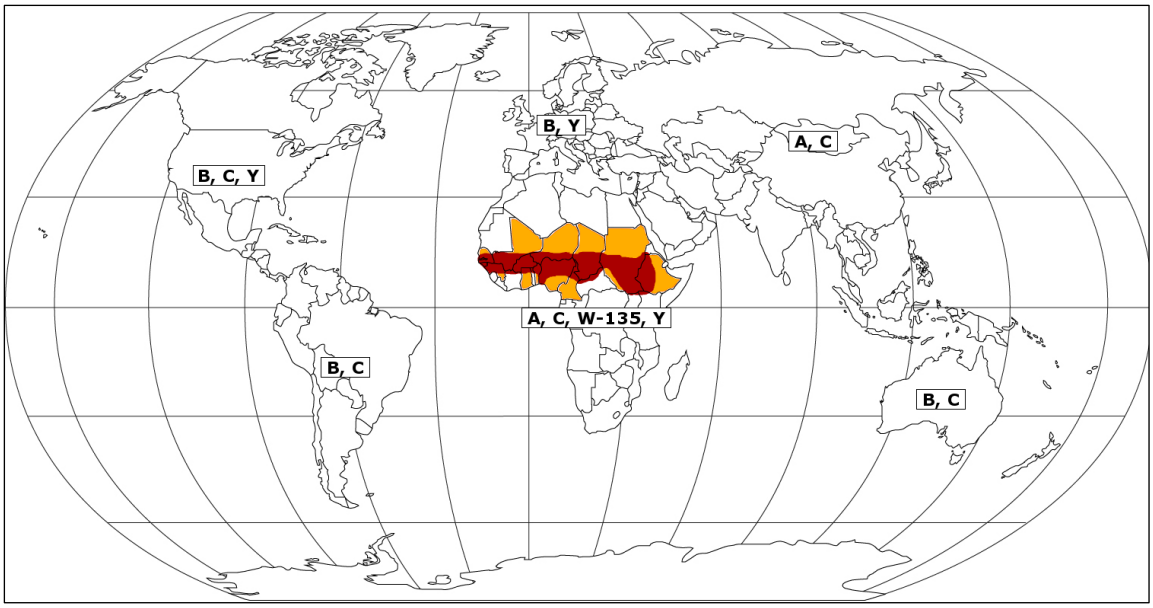

Figure 1.1: Map of the world highlighting the Meningitis Belt as well as the prevalent meningococcal serotypes across different continents.

Red shaded area shows the meningitis belt region of highly increased incidence of meningococcal disease. Orange shading shows outlines of countries considered part of the meningitis belt. (Map adapted from Stephens et al, 2007)(Stephens et al., 2007)

The pathogenic *N.meningitidis* strains responsible for almost all meningococcal disease can be separated into six distinct serogroups; A, B, C, X, Y and W-135, based on the structure of their polysaccharide capsule. The prevalent serotypes vary from region to region around the world (Figure 1.1).

Since 1999 the epidemiology of meningococcal disease in the UK and Europe has changed significantly. Before 1999 groups B and C were responsible for the majority of infections in Europe and other industrialised countries, however since the introduction of a vaccine for type C in 1999 to combat a growing epidemic, group C infections have fallen steadily, and group B meningococcus is now responsible for up to 90% of infections in the UK, and 70% across the whole of Europe(European Centre for Disease Prevention and Control, 2013; Gray et al., 2006; Halperin et al., 2012; Public Health England, PHE, 2014). Alongside the decrease in group C infections, the incidence of group B has also fallen by more than half, reducing total meningococcal infections in the UK to less than a third of the levels in 1999(Public Health England, PHE, 2014).

While group C infections have fallen dramatically since the introduction of the vaccine, meningococcal group Y has been recently increasing in incidence in western Europe, and is now the second most common serotype in the UK behind group B, accounting for almost 8% of cases in the UK compared to less than 2% 10 years ago(Ladhani et al., 2012; Public Health

England, PHE, 2014), incidence in other European countries has also increased, and now accounts for over 20% of cases in Scandinavia and Switzerland(Bröker et al., 2012). The increase in serogroup Y infection was also seen in North America several years ago, and it now causes over a third of all cases in the USA(Cohn et al., 2010). Unusually, given meningococcal disease is usually associated with the under 5s, serogroup Y appears to have greater incidence amongst older individuals, with a much greater infection rate amongst those over 60 years than the other serotypes common in North America and Europe.

The majority of meningococcal disease across the meningitis belt and the rest of Africa is caused by serotype A, which is responsible for between 70-96% of African cases(Marc LaForce et al., 2009). Recent efforts to introduce an affordable vaccine against type A have produced the vaccine MenAfriVac, which in trials has shown carriage rates fall to near zero in Burkina Faso, and reduced incidence of disease by up to 90% in vaccinated areas of Chad(Daugla et al., 2014; Kristiansen et al., 2013). As this vaccine is introduced in other countries across the meningitis belt, and studies of the long-term protection are carried out, the prevalence of group A meningococcal disease will hopefully be reduced significantly.

Meningococcal groups W-135 and X have also been determined as the cause of some epidemics in Africa(Delrieu et al., 2011; Koumaré et al., 2007), although are relatively rare compared to Group A; being responsible for around 10% and 1.6% of cases, respectively (Marc LaForce et al., 2009). Group W-135 (along with groups A, C and Y) is included in the quadrivalent meningococcal vaccine used in the USA and some other countries(Reisinger et al., 2010), however there is no current vaccine against group X.

Individual outbreaks of meningococcal disease have been reported in Asia, however widespread surveillance is not common in many areas. Most known Asian outbreaks have been due to serogroup A, however increasing cases of group C have also been reported in recent years in China, perhaps due to widespread group A vaccination in that country in recent years(Halperin et al., 2012; Sinclair et al., 2010; Vyse et al., 2011).

1.1.2 Disease carriage and mortality

Humans are the only natural reservoir for *N.meningitidis*. The bacterium colonises the nasopharynx of around 10-35% of the normal population in both westernised countries and regions with a high proportion of epidemics (Cartwright et al., 1987; Caugant et al., 1994; Orr et al., 2003; Trotter and Greenwood, 2007). Carriage generally peaks between the ages of 15-24 and declines thereafter, it also increases dramatically in certain populations such as military recruits(Caugant et al., 1992; Tyski et al., 2001), new university students(Neal et al.,

2000), and in pilgrims during the annual Hajj in Mecca(Wilder-Smith et al., 2002); due to the sudden close proximity mixing of large groups of people from different regions.

Disease caused by *N.meningitidis* has a mortality rate with treatment of between 10-15% in developed countries(Rosenstein et al., 1999; Sharip et al., 2006; Stein-Zamir et al., 2014), and up to 20% in the developing world(World Health Organisation, 2011). Before the advent of antibiotics in the 20th century, mortality was over 70% in many outbreaks(Cartwright, 2006).

As well as the high fatality rate, 15-57% of survivors can have significant long-term sequelae, ranging from limb ischemia requiring amputation or skin grafting, cognitive dysfunction, and hearing or kidney problems(Borg et al., 2009; Erickson and De Wals, 1998; Stein-Zamir et al., 2014). Patients with meningococcal septicaemia alone have fewer long term sequelae then those with meningitis alone, but a higher mortality rate(van Brakel et al., 2000; Van Deuren et al., 2000).

The epidemiology of *N.meningitidis* infection creates a minor paradox; it is a bacterium with a relatively high carriage rate combined with a much lower incidence of disease, however when disease does occur, it is devastating. The severity of disease does not promote meningococcal spread, and probably hinders it given the fast onset and combined mortality and morbidity of over 20%. The epidemiology implies that *N.meningitidis* is a commensal organism that only causes disease on accidental occasions. The transformation of an asymptomatic commensal bacteria into a devastating disease appears to occur suddenly(Maiden and Caugant, 2006), and for an accidental pathogen, *N.meningitidis* is remarkably well evolved to evade the immune system and cause damage.

1.2 The *Neisseria meningitidis* bacterium in meningococcal disease

As discussed in the previous section, progression from asymptomatic carriage to invasive meningococcal disease is a relatively rare event. This section will discuss the sequence of events that can lead to traversal of the nasopharyngeal epithelium and invasion of underlying tissues, as well as the bacterial components that allow adhesion to and manipulation of host cells and avoidance of clearance by the immune system.

1.2.1 Major components of the *N.meningitidis* bacterium and their role in meningococcal disease

As in all gram-negative bacteria, *N.meningitidis* has a double cell membrane separated by a periplasmic space. Many of the properties that allow epithelial adhesion and invasion rest on components of the outer membrane, shown in Figure 1.2. The polymeric type IV pili, as

well as outer membrane adhesins such as Opa and Opc, control adhesion to the nasopharyngeal epithelium. The Lipo-oligosaccharide (LOS) that makes up a large proportion of the outer membrane is responsible for much of the severe inflammatory response that characterises meningococcal infection, and the entire bacteria is encapsulated by a protective polysaccharide capsule. The functions of the various meningococcal surface components responsible for adhesion to host cells and evasion of the human immune system are described in more detail below, and summarised in Table 1-1 at the end of the section.

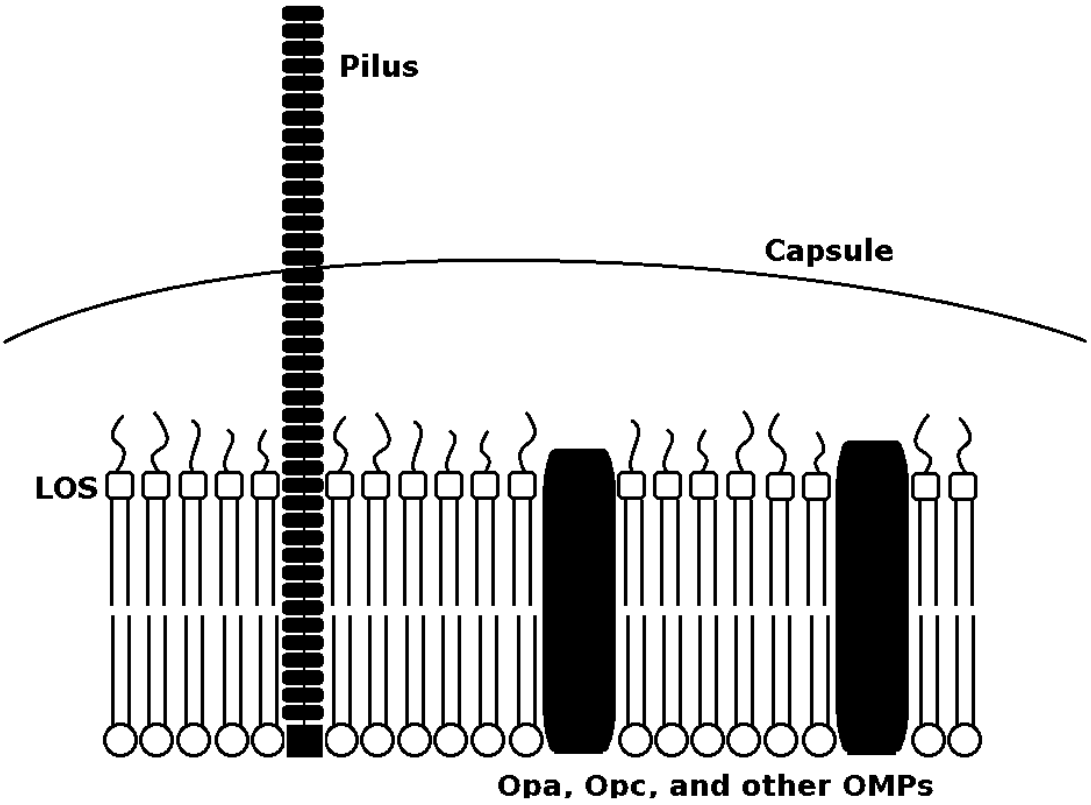

Figure 1.2: Basic diagram of the outer membrane structure of *N.meningitidis*.

Outer Membrane Proteins (OMP) such as Opa and Opc span the outer membrane, which consists partially of Lipo-Oligosaccharide (LOS). The entire bacterium is encapsulated in a capsular polysaccharide, however the long type IV pilus, essential for bacterial adhesion, extends outside the capsule.

1.2.1.1 Type IV Pilus

One of the main adhesion molecules involved in attachment of *N.meningitidis* to host cells, whether to the nasopharyngeal epithelium in normal carriage, or to the vascular endothelium when the infection reaches the bloodstream, is the type IV pilus. Pili are long, polymeric, filamentous structures, made up of many identical PilE subunits along with several other components responsible for pilus stabilisation and modulation (PilC1, PilC2). The PilC subunit is also implicated in the adhesive properties of pili to specific host cell

receptors(Kirchner and Meyer, 2005), although only PilC1 appears to be essential for adhesion to host cells. Very recently, PilE and PilV have been implicated in specific binding to the endothelium via CD147(Bernard et al., 2014). Other important pilus proteins responsible for assembly, retraction and anchorage of the pilus are found in both the outer and inner membranes. PilQ forms a stable pore in the outer membrane through which the pilus is extruded, while PilD and PilG are located in the inner membrane and are responsible for pilus assembly. PilF and PilT are ATPases that provide energy for the assembly or retraction of the pilus, respectively.(Morand and Rudel, 2006)

The multiple pili on each bacterium extend well beyond the surface and capsule and can be several micrometres long, longer than the diameter of a *N.meningitidis* cell(Merz et al., 2000). The main function of pili is adhesion, both to host cells and to other meningococci with which it can form aggregates, and pilus mediated adhesion is essential for encapsulated strains whose other adhesion proteins are masked by the polysaccharide capsule. The pilus is also involved in a type of cell motility, called twitching motility: when the tip of the pilus tethers to something, the pilus can be rapidly disassembled from the base, reeling in the bacteria at speeds up to 1μm/s(Merz et al., 2000; Morand and Rudel, 2006). Type IV pili are also involved in the uptake of DNA by bacterial cells, which in meningococci can enable phase switching of capsular and LOS serotypes.

The prospective receptor for pili on human cells was thought to be CD46, which is expressed in many cell types including both epithelium and endothelium. CD46 antibodies have blocked *N.meningitidis* adhesion to cells(Källström et al., 1998), and CD46 transgenic mice have increased meningococcal invasion and disease compared to controls(Sjölinder and Jonsson, 2007). However more recent studies have shown no effect of CD46 expression at all on meningococcal invasion and disease(Kirchner et al., 2005), so the true extent of CD46-pilus binding on meningococcal adhesion to cells, as well as the presence of other adhesion receptors, is currently unknown(Morand and Rudel, 2006). Very recently, some studies have shown the potential of the β2 Adrenoreceptor(Coureuil et al., 2010) as well as CD147(Bernard et al., 2014) as potential receptors for the meningococcal pilin on the endothelium.

1.2.1.2 Outer Membrane Proteins: Opa and Opc

Although pili are thought to be the major component in meningococcal adhesion to host cells, pilus negative mutants have also been shown to adhere to host cells, mainly through the actions of the opacity proteins: Opa and Opc; so named due to the opacity of colonies

expressing these proteins in vitro. The meningococcal Opa family consists of 3-4 genes in meningococci, and up to 11 in gonococci, which all undergo extensive phase variation within both species and individual bacteria (Aho et al., 1991; Hill et al., 2010). Opc expression however is specific to *N.meningitidis*, and is encoded by a single gene(Hill et al., 2010). Opa and Opc are outer membrane proteins (OMP), and have a variety of different binding partners. The ability of the meningococcus to bind to host cells via several different mechanisms shows multiple redundancy, so if one mechanism of attachment fails, another can be used instead to similar effect.

Opc does not appear to bind to host receptors directly, instead binding to serum components such as Heparin(De Vries et al., 1998), fibronectin(Unkmeir et al., 2002) and vitronectin(Sa E Cunha et al., 2010; Virji et al., 1994), the latter alongside another OMP called Nhha (also known as Msf)(Griffiths et al., 2011). While coating itself in these serum factors can help disguise the bacteria from the immune system, as discussed later, it also allows the bacteria to interact with integrin receptors for these serum components on epithelial and endothelial cells, promoting adhesion and cellular invasion. After cellular invasion has taken place, Opc has also been shown to bind directly to a number of cytoskeletal molecules, assisting in its survival and dissemination within and beneath the epithelial or endothelial layer(Sa E Cunha et al., 2009; Virji et al., 1994).

While Opc binds to components of human serum, the main interactions of the Opa proteins occur with the CD66/CEACAM family of receptors expressed on the surface of human cells(Virji et al., 1996). The CEACAM proteins are encoded by several genes with multiple splice variants, each with a conserved N-terminal region; however only CEACAM1, 3, 5 and 6 have been shown to bind Opa proteins(Muenzner et al., 2000; Sadarangani et al., 2011; Virji et al., 1999). CEACAM1 is expressed in a large number of different cell types, including leucocytes, endothelium, and the epithelium of many organs including the respiratory tract. Neutrophils express both CEACAM3 and CEACAM6, of which the latter is additionally expressed in gastric epithelia alongside CEACAM5 (Hammarström, 1999).

Opa mediated adherence to host cells is directly dependent on the concentration of CEACAM1 expressed on the surface(Bradley et al., 2005; Rowe et al., 2007; Virji et al., 1996). CEACAM1 expression is increased upon inflammatory stimulation, which allows both unencapsulated and capsulate *N.meningitidis* to adhere to inflamed epithelia(Bradley et al., 2005; Griffiths et al., 2007; Rowe et al., 2007). The increased adhesion of encapsulated bacteria under inflammatory conditions allows much greater adhesion and invasion without the bacteria needing to downregulate its protective capsule. It also means that the rate of

invasive meningococcal disease can be increased in patients with inflammation or mucosal damage from sources such as infection, smoking, or dry atmospheric conditions(Derrick et al., 2006; Griffiths et al., 2007; Rowe et al., 2007).

The inflammatory response to invasive *N.meningitidis* can therefore increase its own infectivity; inflammation stimulates CEACAM1 expression, which allows closer bacteria adhesion and tissue penetration, and helps disseminate the bacteria around the body. Alongside this, Opa binding to CEACAM1 can actively inhibit immune activation by inhibiting the TLR2 activated NFκB pathway(Derrick et al., 2006; Slevogt et al., 2008). Opa appears to be particularly important in the later stages of invasive meningococcal disease, with Opa+ bacteria being selected for in several disease models(Sjölinder and Jonsson, 2007; Virji et al., 1996).

1.2.1.3 Lipo-oligosaccharide (LOS)

As in all gram-negative bacteria, a large proportion of the outer membrane of *N.meningitidis* is comprised of Lipo-polysaccharide (LPS), also called endotoxin, whose major function is to stabilise the outer membrane and preserve the structural integrity of the bacteria. Due to the chemical nature of the *N.meningitidis* LPS, it lacks the highly repetitive side chains characteristic of LPS from many other bacteria, and is often referred to as Lipo-oligosaccharide (LOS) instead. The LOS molecule has two distinct regions: the lipid A lipophilic region, and the hydrophilic oligosaccharide tail. The chemical composition of the latter can vary due to phase variation, and *N.meningitidis* can display several different LOS structures at once(Jennings et al., 1999; Wright et al., 2006).

There are 12 major immunotypes of Neisserial LOS(Jennings et al., 1999; Scholten et al., 1994), the structure of which can affect whether the bacteria remains commensal or becomes invasive. In one study 97% of disease isolates were found to have the same L3, 7, 9 immunotype, while strains from carriers were much more heterogeneous(Jones et al., 1992). In another study, invasive disease caused by other immunotypes was found to only occur after switching to the L3, 7, 9 immunotype(Mackinnon et al., 1993).

LOS is one of the major bacterial components responsible for the severe inflammatory response seen in patients with meningococcal disease, and the concentration of LOS in the blood is predictive of the outcome of disease(Brandtzaeg et al., 1989). LOS is a major proinflammatory molecule, stimulating endothelial cells and monocytes mainly via TLR4, and causing severe inflammatory activation. The major pathological effect in meningococcal disease is vascular damage, the main cause of which is thought to be due to the over-

activation of the immune system by the massive amounts of LOS released, over 100 EU/ml in many of the most severe cases(Brandtzaeg, 2006; Brandtzaeg et al., 2001; Wright et al., 2006).

Until recently, LOS was considered to be the only major meningococcal component responsible for stimulating the inflammatory damage caused by the immune system. Despite the important functions of LOS in stabilising the bacterial outer membrane, a viable *N.meningitidis* mutant (LpxA) has been created that does not express LOS (Steeghs et al., 1998, 2001), which was the first gram negative bacteria successfully found to be viable without it. When stimulated with high concentrations (>10^7 bacteria/ml, equivalent to concentrations found in the blood in severe meningococcal disease) of both WT and the LOS negative mutant *N.meningitidis*, a comparable inflammatory response was seen in PBMCs(Sprong et al., 2001) and endothelial cells(Dixon et al., 2004); while monocyte and dendritic cell responses were attenuated but still caused activation and maturation(Dixon et al., 2001; Pridmore et al., 2001). Although several bacterial components were found to have impaired function, such as pili and surface lipoproteins, (Albiger et al., 2003; Ley and Steeghs, 2003), and some factors of the immune response were attenuated, these results showed that not all the host's inflammatory pathways induced by *N.meningitidis* are due to LOS, and that there is still much that is yet unknown about the LOS mediated inflammatory response.

1.2.1.4 Meningococcal capsule

Meningococcal bacteria are usually coated in a capsule that surrounds the bacteria with a protective polysaccharide layer. This helps prevent the bacteria from desiccation during spread between hosts, as well as helping to protect the bacteria from recognition by the immune system(Frosch and Vogel, 2006; Ram and Vogel, 2006). While *N.meningitidis* isolated from the nasopharynx of carriers can be both capsulate or acapsulate, almost all *N.meningitidis* bacteria isolated from the blood or cerebrospinal fluid (CSF) of patients with meningococcal disease express a polysaccharide capsule(Cartwright et al., 1987; Mackinnon et al., 1993), indicating its importance in invasive disease. The chemical composition of the capsule forms the basis of separating meningococci into the different serogroups described in section 1.1.1.

The capsule's main role in the progression of meningococcal disease is to inhibit the targeting of the immune system against the bacteria; by preventing membrane-targeting antimicrobial molecules from reaching the bacterial membrane, and inhibiting the

deposition of opsonising molecules such as complement and antibodies. The immunoprotective properties of meningococcal capsule are discussed in more detail in section 1.2.2.2.3.

As well as helping to mask the *N.meningitidis* bacteria from the immune system, the capsule also masks the action of many outer membrane proteins from the environment. The long pili extend beyond the capsule, and are essential for bacterial adhesion in capsulate strains; Opa and Opc however are embedded in the bacterial outer membrane, as seen in Figure 1.2, and therefore are largely prevented from binding to host receptors. The sialylation state of both LOS and capsule also appears to have an effect on pathogenesis, with sialylated, unencapsulated bacteria able to adhere to host cells using both pili and the Opa and Opc proteins, and sialylated bacteria only able to use pili(Virji et al., 1995a).

These functions combine to show a picture where encapsulated bacteria survive for longer in the host, but have more difficulty attaching to and invading host cells compared to unencapsulated bacteria. *In vivo* it appears that the benefits of immune evasion outweigh the reduced adhesion to host cells, as almost all meningococcal isolates from disease patients are encapsulated. However it has also been shown that *N.meningitidis* can modulate the production of capsule and other surface molecules, switching production on and off during different phases of infection(Deghmane et al., 2002), and even switching serotype if in close proximity to other strains(Hill et al., 2010; Swartley et al., 1997).

1.2.1.5 Molecular basis of human specificity of N.meningitidis infection

The meningococcal components described above have a range of functions that contribute to meningococcal survival and that can lead to disease in humans. The underlying reasons behind the human specificity of *N.meningitidis* are not completely understood, however there are a number of Neisserial ligands that are specific to human, and not other species, receptors.

Opa mediated CEACAM1 binding, as mentioned in section 1.2.1.2, is highly specific to humans in both *N.meningitidis* and the closely related N.*gonorrhoeae* (Voges et al., 2010), while the Porin proteins in *N.gonorrhoeae* also interact species-specifically with human C4bp (C4 binding protein) to inhibit complement activation(Ngampasutadol et al., 2005).

NalP is a Neisserial protein that specifically degrades human complement C3(Del Tordello et al., 2014), while meningococcal NspA has been shown to bind specifically to human complement factor H (fH)(Lewis et al., 2010). *N.meningitidis* and *N.gonorrhoeae* binding of human (and small amounts of chimpanzee) fH blocks the activation of both the human

complement system, as well as complement activation from serum of both rabbits and rats (Granoff et al., 2009; Ngampasutadol et al., 2008). The Neisserial receptors are specific for binding to human fH, however human fH can block activation of the complement system from other species.

One particular group of human proteins that *N.meningitidis* appears to target very specifically are those involved in iron transport and storage. Iron inside the human body is stored and contained very securely in a range of iron containing proteins, leaving very little free iron for invading organisms to utilise. To thrive within the body, *N.meningitidis* has evolved receptors that target the human iron storage proteins Lactoferrin and Transferrin(Schryvers and Morris, 1988). Transferrin appears to be the major Neisserial target for iron acquisition, and *N.meningitidis* has two receptors, TbpA and TbpB (Transferrin binding protein A + B), that bind specifically to human transferrin(Boulton et al., 1999; Cornelissen and Sparling, 1994), although studies have also shown that *N.meningitidis* can bind, albeit with much lower affinity, to transferrin from closely related primates(Gray-Owen and Schryvers, 1993).

When introduced into other species, *N.meningitidis* bacteria may cause transient infection, but are usually cleared within 48 hours with few long term sequelae (Oftung et al., 1999). As a consequence of this, almost all data on meningococcal pathogenesis has been gathered either from human patients or *in vitro* cell studies.

N.meningitidis can cause disease in some animal models either after injection of an iron source such as transferrin(Oftung et al., 1999; Yi et al., 2003), or transgenic expression of human transferrin(Zarantonelli et al., 2007), CEACAM1(Johswich et al., 2013), CD46 (mild disease) (Johansson et al., 2005), or human immune factors such as fH(Vu et al., 2012). Given the many species-specific interactions of *N.meningitidis* with human receptors however, it is unlikely that even transgenic mouse models will be entirely representative of disease. Possibly the most reliable animal model so far is in a very recent model involving mice which were xenografted with patches of human skin(Join-Lambert et al., 2013; Melican et al., 2013). These mice developed severe invasive meningococcal disease, however the infectious meningococci specifically targeted only the grafted human tissues, while the mouse tissues remained healthy. This potentially provides a model for meningococcal disease that can be used to study both the disease itself and new treatments in far greater detail than previously possible.

Table 1-1: Summary of the adhesive properties and immune interactions of various *N.meningitidis* membrane components.

	Adhesion properties	Immune system interactions
Pilus	•Major adhesion factor in encapsulated and unencapsulated meningococci, but essential in encapsulated strains. •Host receptor is currently unclear, although one recent study suggests CD147 may be the main receptor.	
Outer Membrane Proteins (OMP)	•**Opa** ○Enhances adhesion in addition to the pilus, but much more effective in unencapsulated strains ○Important for survival inside host cells, and after initial pilus adhesion ○Binds to CEACAM proteins on epithelial cells ○CEACAM1 important in invasion of epithelial and endothelial cells, and has increased expression under inflammatory conditions •**Opc** ○Enables adhesion in unencapsulated bacteria ○Interacts with serum factors such as fibronectin, vitronectin and heparin, which facilitates adhesion to their endothelial receptors	• <u>Immune activation</u> • **Opa** o Binds to CEACAM3 on neutrophils, enhancing bacterial phagocytosis and killing. o Along with **PorB3,** binds to MBL, activating complement o Covalently binds to C3b and C4b, opsonising bacteria • <u>Immune evasion</u> • **PorA**-binds C4bp component, inhibiting complement activation • **PorB**-bcan inhibit neutrophil activation • **Opc + Nhha**-binds to heparin, fibronectin and vitronectin, inhibiting binding of complement components. • **fHbp + NspA**-bind factor H to the bacteria surface, inhibiting complement activation and binding.
LOS	•Sialyation of LOS inhibits Opa and Opc mediated adhesion •L3, 7, 9 immunotype associated with 97% of invasive strains	•Sialyated LOS inhibits MBL and C3b complement binding in most common serotypes •Sialyated LOS can also assist in the binding of fH to the bacteria •PEA modification of LOS ihelps resist bacterial killing by CAMPs
Capsule	•Present in nearly all invasive strains, but not essential in carriage strains. •Inhibits Opa and Opc, but not pilus, mediated adhesion	•Sialyated capsule inhibits MBL and C3b complement binding in most common serotypes •Sialyated capsule from some serotypes resembles sialyated host molecules, especially serotype B, which can diminish effective adaptive immune response and make vaccine development difficult

1.2.2 Meningococcal disease symptoms and manifestations

Disease caused by *N.meningitidis* presents in two main clinically recognisable ways: meningococcal meningitis caused by inflammation of the meninges, a fluid filled space between the brain and the circulatory system; and meningococcal septicaemia, a systemic meningococcal infection throughout the body, although patients can also present with both types. Typical symptoms of meningococcal disease include headache, fever, photosensitivity and neck stiffness (particularly in meningitis), as well as the characteristic non-blanching meningococcal rash(Pollard and Nadel, 2006).

Patients with systemic meningococcal disease have a lower survival rate than patients with disease confined to the meninges, however patients with symptoms of meningitis often have more long term neurological morbidity such as deafness or neurological impairment due to the sensitivity of the brain to damage(van Brakel et al., 2000; Brandtzaeg et al., 2001; Brandtzaeg, 2006; Van Deuren et al., 2000).

There is also an inverse relationship between the duration of pre-admission symptoms and the disease severity. With fast bacterial growth leading to high bacterial load (>10^7 bacteria/ml), the onset of disease is very quick (<12 hours) and can lead to severe systemic meningococcal disease resulting in overwhelming systemic septic shock. If the bacterial load is lower, there is a longer time before the onset of disease (>24 hours), but bacteria can

attach to and cross the brain microvasculature, causing meningitis (Van Deuren et al., 1995; Brandtzaeg et al., 2001; Brandtzaeg, 2006).

This section will cover the progression of meningococcal disease and the body's attempts to mount an immune response against it.

1.2.2.1 Meningococcal carriage and traversal of the epithelium

Meningococcal disease only occurs in a very small proportion of those carrying the bacterium. The natural habitat of *N.meningitidis* is in the human nasopharynx, where it can divide and be easily spread from person to person by close contact and mucus droplets. Carriage of *N.meningitidis* in the nasopharynx is generally asymptomatic, perhaps causing a mild irritation sometimes reported a few days before full meningococcal disease symptoms(Brandtzaeg, 2006).

The reasons for progression from carriage to invasive meningococcal disease in some patients and not others are unclear. Although damage to the nasopharyngeal epithelium due to other infections, particularly influenza, smoking, or environmental factors such as changes in humidity, temperature, and the level of dusty particulate matter in the air, have been shown to increase incidence of disease(Kinlin et al., 2009; Molesworth et al., 2003; Pace et al., 2009). The age of patients (<5, and between 15-19 years)(Trotter et al., 2007) is also an important factor in disease susceptibility, and immune deficiencies in various aspects of the complement pathway(Ross and Densen, 1984; Mathew and Overturf, 2006; Ram et al., 2010) are also associated with increased incidence of meningococcal disease.

In order for bacterial carriage to progress to disease, the bacteria must traverse the respiratory epithelium to reach the bloodstream, evade the immune system, and remain able to divide and spread around the body. Meningococcal disease symptoms occur when the bacteria induce major inflammatory responses in various sites around the body.

Initial adhesion to the respiratory epithelium is mediated by the long filamentous type IV pili. Other bacterial adhesins such as the Opa and Opc proteins can also assist in Neisserial adhesion; however the presence of capsule inhibits the interactions of Opa and other outer membrane proteins with host cells. The contributions of various Neisserial membrane components to the binding of host cells were summarised in Table 1-1 above along with their functions in immune evasion.

Progression from carriage to disease requires the additional step of traversing the epithelium and entering the bloodstream. Traversal of the epithelial layer is not fully

understood, but is thought to primarily take place by transcellular pathways(Merz et al., 1996; Pujol et al., 1997; Sutherland et al., 2010) i.e. through the cellular cytoplasm, although paracellular (between cells) transmigration has also been seen(Birkness et al., 1995).

The bacteria are reliant on expression of both pili and capsule for successful traversal of the epithelial layer(Merz et al., 1996; Sutherland et al., 2010); pili for adhesion and contact with the epithelial cells, and capsule enhancing intracellular survival by providing resistance to a range of host cell defence mechanisms, including cationic antimicrobial peptides (CAMPs) and defensins(Spinosa et al., 2007).

1.2.2.2 Immune response to N.meningitidis and complement activation

Both before and after traversing the epithelium, the bacteria re exposed to a hostile immune system; from both antibody mediated adaptive immunity, important in the mucosal immunity of the nasopharynx, and serum components such as the complement system and phagocytic neutrophils in the bloodstream.

To avoid the various host responses targeting the invasive bacteria for destruction, *N.meningitidis* has evolved a number of factors, with overlapping and redundant functions, in order to evade, deplete, and prevent the immune system from inhibiting its spread. The reasons why a usually commensal organism living in the respiratory system has evolved such potent and specific immune modulation pathways are still unclear.

1.2.2.2.1 Adaptive immunity and recognition of meningococci

Adaptive immunity plays an important role in protection against meningococcal disease, preventing the progression from carriage to disease. The age range with the highest incidence of disease are infants at around 6-24 months, which is also the age at which the children have lost the protective maternal antibodies but not yet gained the ability to make their own. This is also the age group with the lowest titre of anti-meningococcal antibodies and serum bactericidal activity, as well as a very low carriage rate(Gold et al., 1978; Goldschneider et al., 1969a); suggesting that the proportion of infections proceeding from carriage to disease is also much higher amongst infants and individuals without protective antibodies.

The outbreak of meningococcal disease amongst military recruits is also associated with low amounts of protective antibody against the specific strain acquired, and acquisition of protective antibody concentrations is facilitated by meningococcal carriage(Goldschneider et al., 1969a, 1969b; Reller et al., 1973). Although natural immunity produces antibodies

against a variety of meningococcal antigens, most meningococcal vaccines produce antibodies against the polysaccharide meningococcal capsule, which is essential for bacterial survival in the bloodstream and therefore expression is less variable in invasive strains(Goldschneider et al., 1972; Gotschlich et al., 1969a, 1969b; Reller et al., 1973). Switching of capsular phenotype has been seen in some pathogenic strains during co-infection however, which can hinder the effectiveness of acquired immunity(Swartley et al., 1997).

The heavily sialylated capsule of serogroup B *N.meningitidis* has a structure that closely resembles a component of Neural Cell Adhesion Molecule (NCAM)(Finne et al., 1987; Hill et al., 2010), an important adhesion molecule in the human foetal brain. This makes it difficult to mount an adaptive immune response against, as antibodies directed against it can potentially target the host, and are therefore selected against. This is also the main reason why vaccines against type B were unavailable until very recently.

More recent group B vaccines have concentrated on inducing antibodies against other meningococcal antigens including factor H binding protein (fHbp), Neisserial adhesin A (NadA), Neisseria heparin binding antigen (NHBA) in combination with outer membrane vesicles (OMV) from a specific MenB strain that contain the protein PorA(Gorringe and Pajón, 2012). This vaccine has only recently been licenced, and although initial trials were promising in terms of strain coverage, the eventual effectiveness in the country-wide population is not yet known(Christensen et al., 2013; Snape et al., 2013; Vogel et al., 2013).

The four antigens used in the novel MenB vaccine were selected due to their occurrence in the majority of invasive strains, as well as their relatively low variability. *N.meningitidis* has the ability to vary many of its other surface molecules such as Opa, pili, and LOS to evade specific immune targeting(Criss and Seifert, 2012; Virji, 2009).

The expression of Neisserial Opa genes can be regulated closely, and expression of each of the genes can be turned on or off as required, reducing their exposure to the immune system(Virji, 2009). *N.meningitidis* can also vary the structure and type of LOS expressed on the surface by modulating the activity of various glycosyltransferases to produce different LOS moieties(Jennings et al., 1999). Pili can change their structure frequently via gene polymorphism and phase variation of glycosylation enzymes(Banerjee and Ghosh, 2003; Virji, 2009), resulting in antibodies created against the pili sequences becoming useless against bacteria that have already changed their epitopes. There is also evidence that pilus expression is downregulated after invasion of host cells, reducing exposure of recognisable

bacterial proteins to host defence mechanisms(Deghmane et al., 2002; Sutherland et al., 2010).

As well as phase variation of surface molecules, meningococci can also secrete a protease that actively degrades human IgA, which is most prominently present in the respiratory mucosa where *N.meningitidis* usually thrives(Mulks et al., 1980). Live meningococci can also actively suppress activation of antigen presenting cells such as dendritic cells (Jones et al., 2007). These active methods of inhibition and evasion of the adaptive response, as well as the rapid progression of meningococcal disease, mean that the innate immune system is equally as important in preventing the progression of meningococcal disease.

1.2.2.2.2 The complement system in meningococcal infection

The complement system is a major element of innate immunity that is controlled by an inter-related collection of serum proteins, and can activate several bactericidal pathways. The much greater rate of meningococcal infection, and poorer prognosis, in patients with deficiencies in various components of the complement pathway indicate that the complement system is a fundamental barrier to meningococcal infection.

There are three major pathways that lead to complement activation: the Classical, Lectin and the Alternative pathway, all of which result in the activation of a C3 convertase and formation of the Membrane Attack Complex (MAC). The Classical and Lectin pathways are initiated by recognition of bacterial components by pattern recognition receptors (PRR), whereas the Alternative pathway is a positive feedback loop that amplifies the complement signalling (Schneider et al., 2007; Ricklin et al., 2010). Figure 1.3 shows a diagram outlining the major events in the complement pathway; as well various methods that *N.meningitidis* can use to evade and inhibit complement activation.

The Classical pathway is initiated by the binding of the C1 complex to bacterial structures such as Lipid A; this activates a protease ability, which cleaves the C4 and C2 fragments to form the C4b2a complex. Initiation of the Lectin pathway on the other hand involves Mannose Binding Lectin (MBL) binding to carbohydrate structures on the bacterial surface, and then forming a complex with MASP-2 (MBL-associated serine protease-2), which cleaves C4 and C2 to form the same C4b2a complex as the Classical pathway(Schneider et al., 2007; Ricklin et al., 2010).

The C4b2a complex functions as a C3 convertase, catalysing the cleavage of the inert C3 to form the active fragments C3a and C3b. C3a mainly acts as a chemoattractant, helping to recruit and cause degranulation of leucocytes, while C3b has three major, and related,

functions. Firstly, it interacts with Complement factor B, forming the C3 convertase C3bBb, which can then catalyse cleavage of more C3 resulting in the Alternative pathway positive feedback loop. Secondly c3b binds covalently to bacterial cells, opsonising them for recognition by phagocytic cells. Finally, C3b can form additional complexes with either of the C3 convertases to form C5 convertases (C4b2a3b or C3bBbC3b), which cleave C5 into C5a and C5b(Schneider et al., 2007; Ricklin et al., 2010). C5b recruits several other components (C6, C7, C8 and C9) to form the C5b-9 MAC, which forms a pore and inserts itself into the membrane of targeted bacteria, initiating cell lysis.

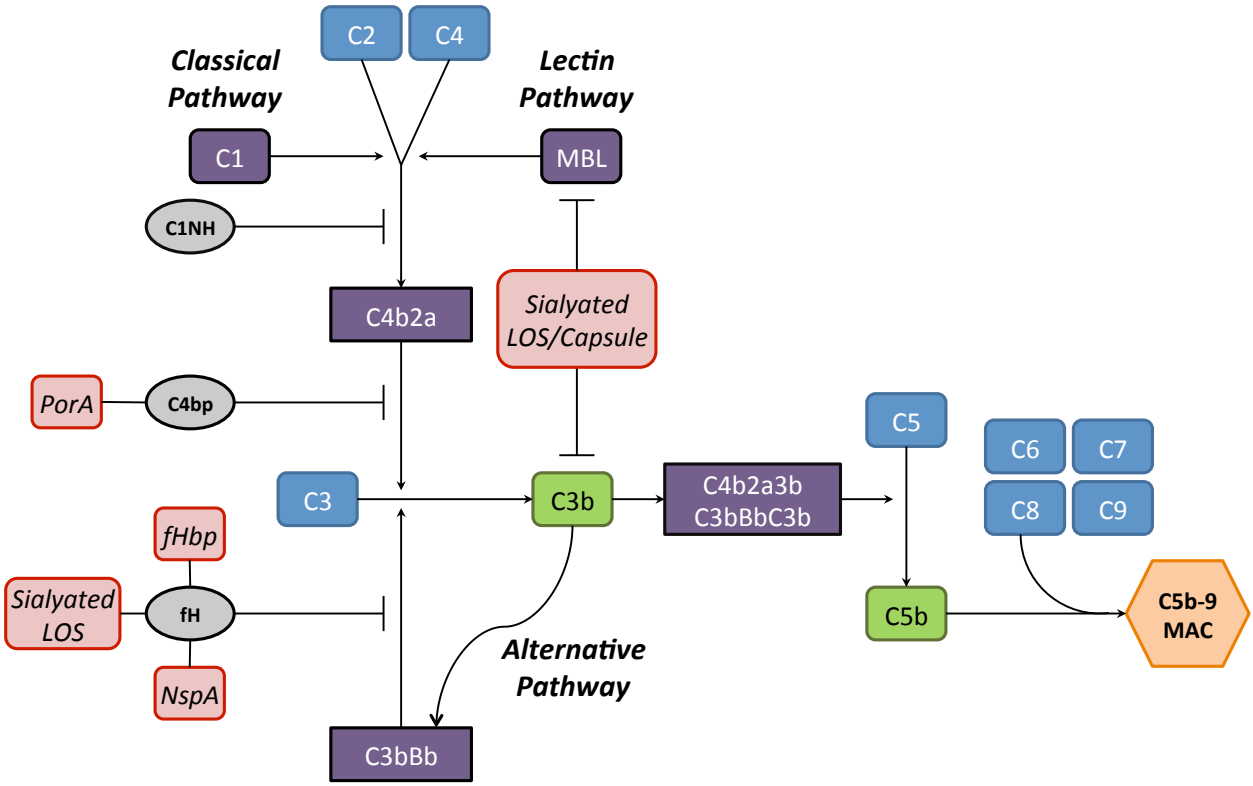

Figure 1.3: Diagram showing the activation cascade of the complement system and methods of its inhibition by *N.meningitidis*.

Inactive precursor proteins are shown in blue, while activated enzymes are in purple. The end products of the complement pathway are the membrane attack complex (MAC) in orange, and the opsonins C3b and C5b, which are green. Methods by which *N.meningitidis* can interfere and inhibit the complement pathway are shown in red, and mostly act to recruit host complement inhibitory proteins, which are in grey.

1.2.2.2.3 Meningococcal evasion of the complement system

Deficiencies in most sections of the complement pathway have been associated with meningococcal disease, but particularly in both the MAC and C3 convertase(Mathew and Overturf, 2006; Schneider et al., 2007), indicating the importance of the complement pathway in defence against meningococcal disease. To combat this *N.meningitidis* has evolved numerous methods for the evasion of the complement pathway.

Mannose Binding Lectin (MBL) usually binds to carbohydrate structures on the surface of bacteria causing activation of Lectin pathway, and has been shown to bind to Opa and PorB in *N.meningitidis*(Estabrook et al., 2004). However, sialylation of LOS and capsule on pathogenic *N.meningitidis* can inhibit binding of MBL(Jack et al., 1998). Around 97% of invasive strains have been shown to express sialylated LOS, indicating its importance in bacterial survival.

The C3b and C4b complement fragments are major antibacterial molecules that can covalently bind to and opsonise Opa proteins on the surface of meningococci(Lewis et al., 2008). Sialylation of LOS and capsule can inhibit binding of the opsonising C3b and C4b fragments(Jarvis and Vedros, 1987; Vogel et al., 1997; Schneider et al., 2007); although this has been shown to be highly variable depending on the capsular serotype, with serotypes Y and W-135 paradoxically causing large increases in complement activation(Ram et al., 2011). The relative contributions of sialylated LOS or capsule to C3b binding and serum resistance have still to be elucidated fully, as many studies give conflicting results, seeing either very little effect, or confusion between C3b and other complement proteins (Kahler et al., 1998; Ram et al., 2003). It is likely that while sialylated LOS and capsule contribute to C3b inactivation, there are also other components that provide overlapping and multiple redundant methods of C3b inactivation(Hill et al., 2010; Schneider et al., 2007; Wright et al., 2006).

Various outer membrane proteins of *N.meningitidis* are responsible for complement evasion by binding host components and using them to disguise the bacteria from the immune system. The meningococcal outer membrane protein PorA binds the C4bp (C4 binding protein) fragment, which confers resistance to complement activation and promotes degradation of C4b(Jarva et al., 2005; Schneider et al., 2007). As discussed in section 1.2.1.2, the outer membrane protein Opc can bind to heparin, fibronectin and vitronectin from the bloodstream. As well as facilitating adherence to the endothelial receptors for those blood components as mentioned previously, complement binding to the bacteria coated in these host factors is inhibited(Griffiths et al., 2011).

Another major factor responsible for complement evasion by *N.meningitidis* involves the binding and coating of the bacteria in human factor H (fH). Human fH blocks the activation of the complement system by preventing the activation and binding of the C3b fragment and promoting its cleavage. Meningococci have evolved several overlapping and redundant fH recruitment mechanisms. Factor H binding protein (fHbp)(Madico et al., 2006; Schneider et al., 2009) and Neisserial surface protein A (NspA)(Lewis et al., 2010) are two outer

membrane proteins that can bind fH and inhibit activation of C3b. In addition, sialylated LOS appears to enhance fH binding to the bacteria, although it is not as important in fH binding than the two outer membrane proteins(Vu et al., 2012; Lewis et al., 2012). The actions of these two proteins, as well as the novel action of LOS, were only discovered relatively recently, showing that there is still much that is not understood about the molecular basis for the progression of meningococcal disease.

1.2.2.2.4 Neutrophil responses to meningococcal infection and extracellular killing

While complement mediated killing is a major component of the innate immune response against *N.meningitidis*, neutrophil activation is essential for the successful clearance of meningococcal bacteria; and one of the one of the most characteristic signs of meningococcal infection is the activation and extravasion of neutrophils into the periphery, most notably sterile spaces such as the CSF and meninges.

Typically, neutrophils recognise pathogens by binding of Toll-like receptors(TLR) or other PRRs to foreign structures such as LPS, as well as binding to opsonised bacteria coated with complement or antibodies. The neutrophils can then cause bacterial killing either by phagocytosis; taking up the bacteria into phagolysosomes and exposing them to antimicrobial enzymes and reactive chemicals such as superoxide, or by extracellular release of cytotoxic granules and microorganism trapping NETs(Criss and Seifert, 2012; Lacy and Eitzen, 2008).

Despite causing extensive neutrophil activation during meningococcal infection, *N.meningitidis* has also evolved many methods to evade extracellular killing and NETs, prevent phagocytosis, and survive and even replicate within neutrophils once they have been phagocytosed.

1.2.2.2.5 N.meningitidis resistance and survival of neutrophil mediated killing

Phagocytosis of *N.meningitidis* can be initiated via bacterial opsonisation by complement components or antibodies, or by direct binding to bacterial PAMPs. Methods of *N.meningitidis* resistance to antibody and complement mediated opsonisation were outlined in sections 1.2.2.2.1 and 1.2.2.2.3 respectively, recognition of bacterial components such as LOS and glycosylated antigens by TLRs and other PRRs is also an important factor in neutrophil recognition of bacteria. Of particular importance in non-opsonic phagocytosis of *N.meningitidis* by neutrophils are the Opa proteins.

The Opa proteins are Neisserial outer membrane proteins that can bind to various members of the CEACAM family of receptors on human cells, most notably CEACAM1 on epithelial and endothelial cells, and CEACAM3 on neutrophils. Opa binding to CEACAM1 assists in adhesion and invasion of epithelial and endothelial cells as described earlier, whereas binding to CEACAM3 on neutrophils appears to lead to rapid phagocytosis (McCaw et al., 2003; Sarantis and Gray-Owen, 2007; Virji et al., 1999). As CEACAM3 has no other known non-bacterial ligands, it has been proposed that CEACAM3 has evolved as a decoy receptor, to utilise the bacterial affinity for CEACAMs against itself. Some Neisseria strains have been isolated which appear to have further evolved their Opa proteins to selectively bind CEACAM1 while avoiding CEACAM3(Sadarangani et al., 2011; Schmitter et al., 2004).

Phagocytosed bacteria are contained within small membrane bound compartments called phagosomes inside neutrophils. Neutrophils can then release Reactive Oxygen Species (ROS) such as superoxide into the phagosomes to attack the bacteria, as well as a range of granules containing bactericidal enzymes such as elastase and the cathepsins, and toxic cationic peptides such as defensins(Borregaard and Cowland, 1997; Lacy and Eitzen, 2008; Urban et al., 2006). This burst of ROS and toxic molecules into the compartment is usually enough to kill and break down most phagocytosed organisms.

Although most phagocytosed meningococci appear to be transported to phagolysosomes and killed, there is evidence that some phagocytosed bacteria of the closely related *Neisseria gonorrhoeae* are able to survive and even replicate within the neutrophils(Derrick et al., 2006; Hauck et al., 1998).

Mechanisms of Neisserial survival within neutrophils include the breakdown of ROS and inhibition of ROS production(Criss and Seifert, 2012), LOS and capsule modification to protect against CAMPs and other toxic molecules(Spinosa et al., 2007; Tzeng et al., 2005), and prevention of neutrophil apoptosis by translocation of porins, which increases neutrophil lifespan and assists neutrophil and bacterial dissemination around the host.(Bjerknes et al., 1995; Criss and Seifert, 2012; Derrick et al., 2006)(Criss and Seifert, 2012)

N.meningitidis can escape killing by the extracellular release of granules by many of the same mechanisms, as well as resisting NET (Neutrophil Extracellular Trap) mediated killing by expression of high-affinity zinc uptake receptor ZnuD and release of OMVs that bind the NETs in place of the bacteria, allowing bacteria to escape their killing effects(Lappann et al., 2013). The extracellular release of bactericidal granules and NETs causes damage not only to

the bacteria, but also to the surrounding tissues. The meningococcal resistance to neutrophil-mediated killing, and subsequent over-activation of neutrophils and excessive granule release is responsible for much of the vascular damage and symptoms characteristic of meningococcal disease (Criss and Seifert, 2012; Heyderman et al., 1999; Klein et al., 1996; Westlin and Gimbrone, 1993). One of the key indicators of poor prognosis in patients is a lowered circulating neutrophil count due to excessive peripheral recruitment and activation induced by the *N.meningitidis*(Gedde-Dahl et al., 1990).

1.2.2.3 Bacterial growth, tissue damage, and dissemination around the body causing meningococcal disease

Initial symptoms of meningococcal disease begin to occur once the bacteria have reached the bloodstream and evaded the immune system well enough to be able to divide. The severity of disease correlates directly with the concentration of bacteria and LOS in the blood(Brandtzaeg et al., 2001; Darton et al., 2009). Interestingly, more severe disease appears to have a much faster onset (12-13 hours) than milder disease (24-29 hours), as well as involving 10-10^3-fold higher concentrations of bacteria and LOS in the blood(Van Deuren et al., 1995; Brandtzaeg et al., 2001; Brandtzaeg, 2006); indicating that the ability of the body to restrict the rate of bacterial growth is essential for preventing severe disease onset, and that the ability of a meningococcal strain to quickly divide and disseminate is directly linked to its ability to cause disease.

Although *N.meningitidis* bacteria have numerous ways for evading the human immune system, the majority of the bacteria detected in the bloodstream are dead. For every live *N.meningitidis* bacteria found in the bloodstream (as determined by being capable of forming colonies on chocolate agar), around 10^2-10^3 non-viable ones are present (as determined by the number of copies of meningococcal DNA found in the blood of infected patients)(Øvstebø et al., 2004).

These high quantities of both live and dead bacteria, as well as LOS, in the bloodstream (up to 10^8 bacteria/ml, and over 100EU/ml of LOS in many cases (Brandtzaeg et al., 2001; Øvstebø et al., 2004)) lead to hyper-activation of neutrophils, and extensive release of the cytotoxic neutrophil granules mentioned previously. A significant proportion of damage caused in meningococcal disease is likely to be due to this excessive neutrophil activation on vascular endothelium (Criss and Seifert, 2012; Klein et al., 1996; Pathan et al., 2003; Sotto et al., 1976) leading to vascular and tissue damage. The ensuing effects of this damage involve loss of vascular integrity and increase in capillary leakage through the damaged blood vessels, leading to reduced blood volume and endothelial dysfunction. Microthrombosis and

tissue hypoxia are the main conditions responsible for the patho-physiological manifestations of septic shock seen in severe meningococcal disease.

1.2.2.3.1 Disease symptoms

The most characteristic meningococcal disease symptom; the haemorrhagic rash (Shown in Figure 1.4), referred to as petechiae or purpura, is seen in roughly 40-80% of patients with meningococcal infections, and almost all patients with meningococcal septicaemia; with number and size increasing with time from onset of disease(Marzouk et al., 1991; Thompson et al., 2006). Biopsies taken from these regions show large numbers of bacteria associated with the capillary walls(Mairey et al., 2006), along with activated immune cells, coagulation and thrombosis (Faust et al., 2001; Hazelzet, 2005; Pollard and Nadel, 2006). An example of a patient with extensive meningococcal rash and purpura at the limb extremities is shown in Figure 1.4.

Figure 1.4: Photographs from a young patient with meningococcal disease, showing characteristic meningococcal rash purpura rash in the limb extremities.

Accumulation and activation of neutrophils and bacteria, as well as expression of procoagulant factors such as Tissue Factor and inhibition of anti-coagulant mediators such as

Thrombomodulin, Protein C, and plasminogen activator (Bevilacqua et al., 1986; Moore et al., 1987; Mirlashari et al., 2001; Faust et al., 2001), causes vascular damage and capillary leakage; which can lead to extensive necrosis of the surrounding tissue and skin and result in much of the morbidity seen in many survivors of the disease, such as amputation, deafness and neurological impairment. As well as excessive inflammation and coagulation, the capillary leakage can cause a reduced blood volume leading to hypotension (low blood pressure) and septic shock, which along with the other symptoms can cause multiple organ failure and eventual death.

The other major disease manifestation of meningococcal infection is meningitis, where the bacteria manage to cross the blood brain barrier (BBB) and cause inflammation of the meninges. This can cause swelling of the meninges, leading to neck stiffness, photophobia and headaches, and can cause long term neurological impairment or deafness in some survivors.

1.3 Endothelial function and contribution to meningococcal disease

The vascular endothelium is a vital human component in the pathogenesis of meningococcal disease; both in meningitis, when the bacterium binds to and crosses the blood brain barrier and infects the meninges, and also in meningococcal septicaemia when *N.meningitidis* adheres to endothelial cells causing the characteristic intense systemic inflammation and neutrophil activation.

The endothelium consists of the thin layer of cells that line the inside of every blood vessel; helping to control blood homeostasis, cellular and nutrient trafficking in surrounding tissues, and contributing to the inflammatory response(Aird, 2003; Rubanyi, 1993). Capillaries consist of a single layer of endothelial cells and little sub-endothelial material. Their thin walls allow them to control the microenvironment of the tissues in which they are located, forming a semi-permeable barrier between the blood and surrounding tissues and selectively filtering which chemicals and cells can pass through.

The main location of meningococcal adhesion in the brain is thought to be in capillaries, where the Blood Brain Barrier is at its weakest at the junctions between capillaries and post-capillary venules (Coureuil et al., 2012; Mairey et al., 2006; Pron et al., 1997). Systemically however, capillary diameter is only just wide enough for neutrophils to squeeze through, making adhesion of the neutrophils that cause the majority of vascular damage in meningococcal infection much more difficult without disrupting flow. In meningococcal septicaemia, post-capillary venules are thought to be the more common sites of neutrophil

mediated damage (DeVoe et al., 1977; Join-Lambert et al., 2013; Springer, 1994; Witko-Sarsat et al., 2000). At sites of adhesion, the meningococcus can induce rearrangement of endothelial tight junction molecules, enabling the passage of bacteria through the endothelial layer(Coureuil et al., 2012; Doulet et al., 2006; Join-Lambert et al., 2013).

1.3.1 Differing states of endothelium around the body

Rather than being just one homogenous organ, endothelium from different types of vessels in different regions of the body are arranged and behave differently(Aird, 2006; Stevens et al., 2001). For example; brain endothelial cells have tight junctions that maintain the blood-brain barrier, whereas endothelium in liver and spleen are arranged in a discontinuous layer, allowing extensive cell trafficking(Aird, 2003).

Different endothelial cells can also differ in expression of many endothelial genes. For example; Thrombomodulin is expressed at high levels in the lung, but not expressed at all in brain endothelial cells(Ishii et al., 1986), and von Willibrand factor (vWf) is highly expressed in large vessels, but at much lower levels in the small capillaries of the kidney, lung and spleen(Pusztaszeri et al., 2006). Similarly in cultured cells; vWf is highly expressed in HUVEC (Human Umbilical Vein Endothelial Cells), but at much lower levels in HPMEC (Human pulmonary vascular endothelial cells)(Müller et al., 2002), and E-selectin is expressed for significantly longer time periods on microvascular endothelial cells such as HDMEC (Human Dermal Microvascular Endothelial Cells) than on endothelial cells from larger vessels such as HUVEC(Kluger et al., 1997). A large number of other endothelial genes have also been shown to be differentially regulated, based on vascular type, location, and size(Aird, 2003, 2006; Chi et al., 2003; Deng et al., 2006).

1.3.2 Response of endothelial cells to inflammatory conditions

Endothelial cells provide a vital role in the response of the body to inflammatory stimuli. They can finely control activation from different stimuli, differentially co-ordinate the recruitment and activation of immune cells and vasomotor tone, as well as regulating the coagulation pathways that lead to thrombostasis (Aird, 2003).

In response to inflammatory stimuli, such as endogenous cytokines TNFα and IL-1β or bacterial products such as LPS, endothelial cells can release and express a variety of factors with different functions; including pro-coagulation factors Tissue Factor and vWF (Mantovani et al., 1997; Schorer et al., 1987), cytokines such as IL-8 (Baggiolini, 1993; Sica et al., 1990), and cell adhesion molecules (CAMs) including E-selectin, ICAM-1 and VCAM-1 (Bevilacqua, 1993; Cotran and Pober, 1990), essential for the recruitment of leucocytes.

1.3.2.1 Role of Cell adhesion molecules in leucocyte recruitment

The recruitment of leucocytes to sites of inflammation via the endothelium is a stepwise process, involving multiple adhesion molecules on both the endothelium and circulating leucocytes. The major steps in neutrophil recruitment are outlined in Figure 1.5, and described in more detail below.

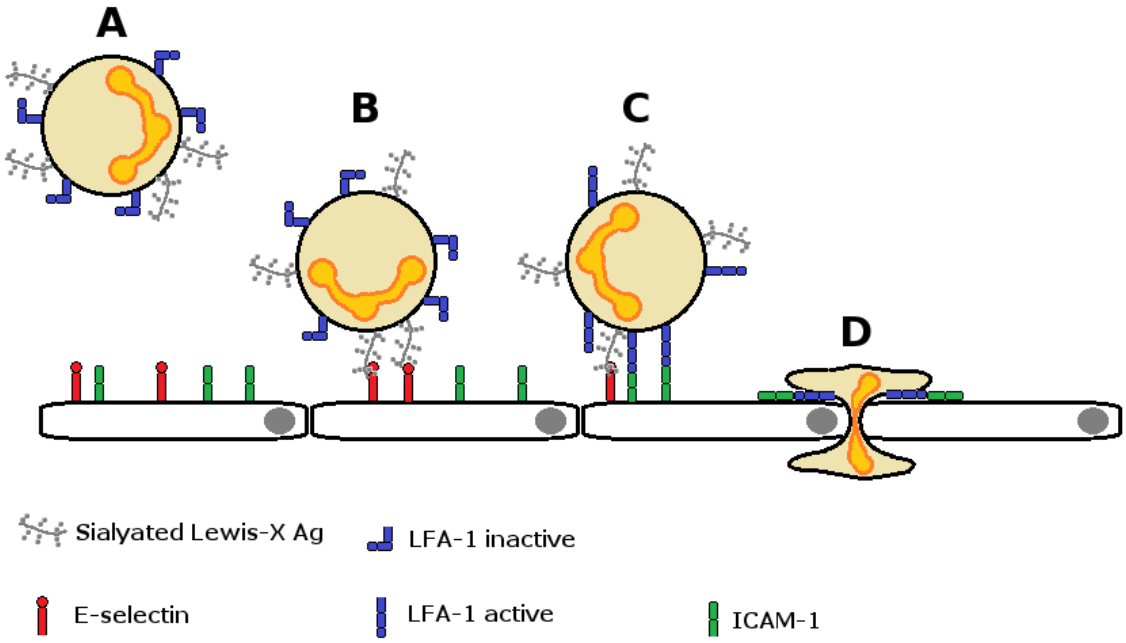

Figure 1.5: Sequence of events in neutrophil rolling, adhesion and migration through endothelium.

Sialylated Lewis-X Antigen ligands on free flowing neutrophils (A) bind to E-selectin expressed on endothelial cells under inflammatory conditions, causing the neutrophils to slow and roll along the endothelium (B). The binding of E-selectin to its sialylated ligands activates neutrophil intracellular signalling pathways, resulting in conformational changes in the structure of integrins such as LFA-1, allowing it to interact with ICAM-1 on the endothelium (C). These bonds provide tight adhesion and bring the rolling neutrophil to a halt, allowing it to then migrate between endothelial cells (D)

Initial contacts between leucocytes and endothelial cells involve a class of adhesion molecule called selectins. There are three known members of the selectin family; L-selectin, P-selectin, and E-selectin. They each have very similar structures, but differ in length, expression and ligand binding specificities. L-selectin is constitutively expressed on circulating leucocytes, whilst both P- and E-selectin are both expressed on the endothelium upon inflammatory stimulation, and P-selectin is additionally expressed on platelets. Although both P- and E-selectin expression is inducible, P-selectin is stored in granules and is released to the cell surface within minutes of inflammatory stimulation, whereas E-selectin must be produced *de novo*, and typically reaches a peak of expression 4-6 hours after stimulation before declining to basal levels around 24 hours later(Tedder et al., 1995).

During the initial tethering of circulating neutrophils to the endothelium E-selectin binds to sialylated Lewis X Ag ligands, such as ESL-1, PSGL-1 and CD44 (Hidalgo et al., 2007), present on the surface of circulating leucocytes (Figure 1.5A). These bonds are weak and break very quickly, but the process of multiple bonds being made and broken in short succession cause the leucocyte to slow, and then begin to roll along the endothelium (Figure 1.5B).

At the same time, the action of E-selectin binding to PSGL-1 and CD44 activates signalling pathways in the neutrophils involving Src family kinases, Syk and p38(Zarbock et al., 2007; Yago et al., 2010). These signalling pathways result in conformational changes in the structure of neutrophil adhesion molecules, most notably the integrin LFA-1 (also known as CD11a/CD18, or $\alpha_L\beta_2$)(Smith et al., 2004; Zarbock et al., 2007; Yago et al., 2010; Simon et al., 2000). This conformational change to a high affinity state allows the formation of tight bonds between LFA-1 and endothelial integrin receptors such as ICAM-1, bringing the rolling neutrophils to a halt (Figure 1.5C), and also assisting in initiation of neutrophil migration (Green et al., 2006). While initial adhesion and rolling of neutrophils along the endothelium can be mediated by all three selectins, leucocyte signalling resulting in integrin conformational change is a function specific to E-selectin(Ma et al., 2004).

In addition to E-selectin, the activation of firm adhesion of neutrophils to the endothelium is also induced by chemokine stimulation; the endothelium releases the chemokine CXCL1, which activates CXCR2 on neutrophils, leading to the same increased affinity conformational changes in LFA-1. The E-selectin and CXCR2 mediated firm adhesion are thought to be additive, with blocking of either pathway reducing adhesion by around 50%, and blocking of both inhibiting adhesion almost entirely(Lefort and Ley, 2012; Smith et al., 2004; Zarbock et al., 2007).

Once firmly adhered to the endothelium, the next stage in neutrophil migration involves transmigration through the endothelium to enter the sub-endothelial space, although not all neutrophils that adhere transmigrate. During transmigration the leucocyte flattens itself against the endothelium and extends pseudopodia between endothelial cells, the leucocyte then pulls itself through the gaps created (Figure 1.5D).

Clustering of the adhesion molecules ICAM-1 and VCAM-1 by integrin binding can activate a range of pathways within endothelial cells that reduce the activity of adhesion molecules at the endothelial cell junctions such as VE-cadherin(Nottebaum et al., 2008; Turowski et al., 2008; Muller, 2009), as well as enhance actin-myosin contraction(Hixenbaugh et al., 1997), which contributes to the loosening of the endothelial cell junctions(Muller, 2009). Adhesion

molecules such as PEACAM-1 (CD31), JAM-A and ICAM-2 can then co-operate to help pull the leucocyte through the endothelium(Dejana, 2004; Mamdouh et al., 2003; Woodfin et al., 2009). The exact interactions between the many molecules involved in neutrophil transmigration is not fully understood, but the process is complex and tightly controlled, as one would expect from a process involving disruption of a vital organ such as the endothelium(Muller, 2009).

Chemokines such as CXCL8 (IL-8) are also produced both by endothelial cells and macrophages, and can be displayed on surface receptors of endothelial cells(Middleton et al., 1997; Mukaida, 2003). This creates a concentration gradient, which the extravasated leucocytes can follow to the source of the inflammation, and activates the neutrophils, inducing them to attack and damage the endothelium and surrounding tissues.

1.3.3 *N.meningitidis* interactions with the endothelium

The interactions of *N.meningitidis* with the vascular endothelium are likely to be crucial to the pathogenesis of the systemic inflammatory response seen in meningococcal disease. The level of endothelial activation controls the extensive neutrophil recruitment that is typical of meningococcal disease; and the subsequent over-activation of the recruited neutrophils causes widespread damage to the vasculature that leads to the capillary leakage and haemorrhagic rash characteristic of meningococcal disease(Klein et al., 1996; Pathan et al., 2003).

Meningococcal adhesion to the endothelium is controlled by many of the same proteins and mechanisms that mediate epithelial adhesion and invasion, including pili as well as outer membrane proteins such as Opa and Opc(Muenzner et al., 2000; Virji et al., 1991, 1992). While Opa and Opc have similar levels of contribution during epithelial adhesion and invasion, Opc appears to be more significant than Opa to endothelial adhesion, although pili are important in both(Virji et al., 1993).

After binding to the endothelium, *N.meningitidis* bacteria can continue to grow and divide while still adherent, forming microcolonies on the surface of the endothelial cells(Pujol et al., 1997). These microcolonies have been shown to affect the expression and organisation of various cytoskeletal molecules, such as ezrin, moesin, and cortactin(Doulet et al., 2006; Eugène et al., 2002; Lambotin et al., 2005), adhesion molecules including E-selectin, ICAM-1 and VCAM-1(Doulet et al., 2006), and also the Par3/Par6/PKC polarity complex that controls the tight junctions between endothelial cells(Coureuil et al., 2009), as well as the receptor tyrosine kinase ErbB2(Hoffmann et al., 2001). This complex rearrangement and control of

endothelial cellular function is apparently activated by *N.meningitidis* hijacking the β2 adrenoreceptor/β adhesion pathway(Coureuil et al., 2010).

This complex reorganisation of cytoskeletal, transmembrane and adhesion molecules creates a nest of microvilli-like structures around the adhered bacteria that both protect the microcolony from the effects of sheer blood pressure, and assist the bacteria's migration through, or into the endothelium(Coureuil et al., 2009; Eugène et al., 2002; Hoffmann et al., 2001).

Formation of these microcolonies appears to be controlled by pilus mediated adhesion, as the majority of experiments showing microcolony formation thus far have been carried out with an unusual encapsulated, piliated Opa-, Opc- Meningitis C strain (2C43). Whether this recruitment of endothelial components beneath adherent microcolonies also occurs beneath wild type strains expressing a full complement of outer membrane molecules, or other meningococcal strains remains to be seen; however meningococcal activation of other endothelial pathways leading to sphingomyelinase and ceramide mediated internalisation of the bacteria require Opc expression (Simonis et al., 2014).

1.3.3.1 Endothelial inflammatory response to N.meningitidis

Endothelial exposure to *N.meningitidis* causes large amounts of inflammatory activation, despite the immune modulation capabilities of the bacteria.

The LOS present in the meningococcal outer membrane is a potent proinflammatory molecule, as described in section 1.2.1.3, and can activate endothelial cells via TLR4. Non-LOS components of *N.meningitidis* have also been shown to be important in inflammatory stimulation, as LOS-deficient mutants can stimulate an equivalent inflammatory response in endothelial cells at high bacterial concentrations(Dixon et al., 2004).

The conventional pathway of proinflammatory stimulation in endothelial cells involves stimulation by cytokines such as IL-1β or TNFα, or direct pathogen recognition by PRRs such as TLR2 or TLR4; which activate signalling pathways such as MAPK/ERK and p38 resulting in translocation of the transcription factor NFκB to the nucleus(Constantin et al., 2004; Denk et al., 2001; Kempe et al., 2005). *N.meningitidis* can also activate endothelial cells via a different mechanism: LOS and non-LOS components may signal via non TLR2 or TLR4 mechanisms in human meningeal cells(Humphries et al., 2005), and LOS-deficient meningococci can activate endothelial cells via a pathway separate from NFκB(Dixon et al., 2004), utilising the transcription factor ATF-2 instead (Jacobsen et al, manuscript in preparation).

Adhesion molecule expression in *N.meningitidis* infection is influenced by both the capsular and LPS structures of the bacteria(Dixon et al., 1999). At high concentrations (10^7-10^8 bacteria/ml), an LOS-deficient *N.meningitidis* mutant induces E-selectin and other adhesion molecule expression to a similar level to that induced by WT *N.meningitidis*, while E-selectin expression due to stimulation by just LOS is significantly lower than that induced by either bacteria (Dixon et al., 2004).

This observation contributes to the growing idea that both LPS-dependent and LPS-independent mechanisms contribute to endothelial activation and inflammation in meningococcal disease. In particular the non-LPS component of Nm signalling is thought to act via p38 MAPK mediated activation of the ATF-2 transcription factor (Jacobsen et al, manuscript in preparation). It is also interesting to note that the concentration of LOS-deficient *N.meningitidis* required to elicit endothelial inflammatory response is similar to that associated with the severest forms of meningococcal septicaemia(Hackett et al., 2002; Hellerud et al., 2008; Øvstebø et al., 2004).

1.3.4 E-selectin structure and functions

E-selectin expression on endothelial cells is differentially induced by *N.meningitidis* stimulation compared to other endothelial adhesion molecules(Dixon et al., 2004), which implies that E-selectin may somehow be involved in the progression of *N.meningitidis* infection. The structures of the three members of the human selectin family are shown in Figure 1.6A. The extracellular region of each selectin consists of a C-type lectin domain, a single EGF-like domain, and between 2-8 CCP-like domains (also called sushi domains). A transmembrane domain holds the molecule in the cell membrane, and each selectin has a short intracellular region.

The N-terminal lectin domain of E-selectin binds to sialylated Lewis X Ag moieties, present on E-selectin ligands such as ESL-1, PSGL-1 and CD44(Hidalgo et al., 2007), expressed on the surface of circulating leucocytes. This binding leads to slow rolling and the neutrophil adhesion cascade as described above. While the structures of the extracellular regions are similar between different selectins, varying in the number of CCP-like domains, as well as the precise binding specificities of the lectin domains, the Intracellular domain is not conserved between selectins. The C-terminal intracellular tail of E-selectin is 31 amino acids long and contains several known potential phosphorylation sites (Figure 1.6B).

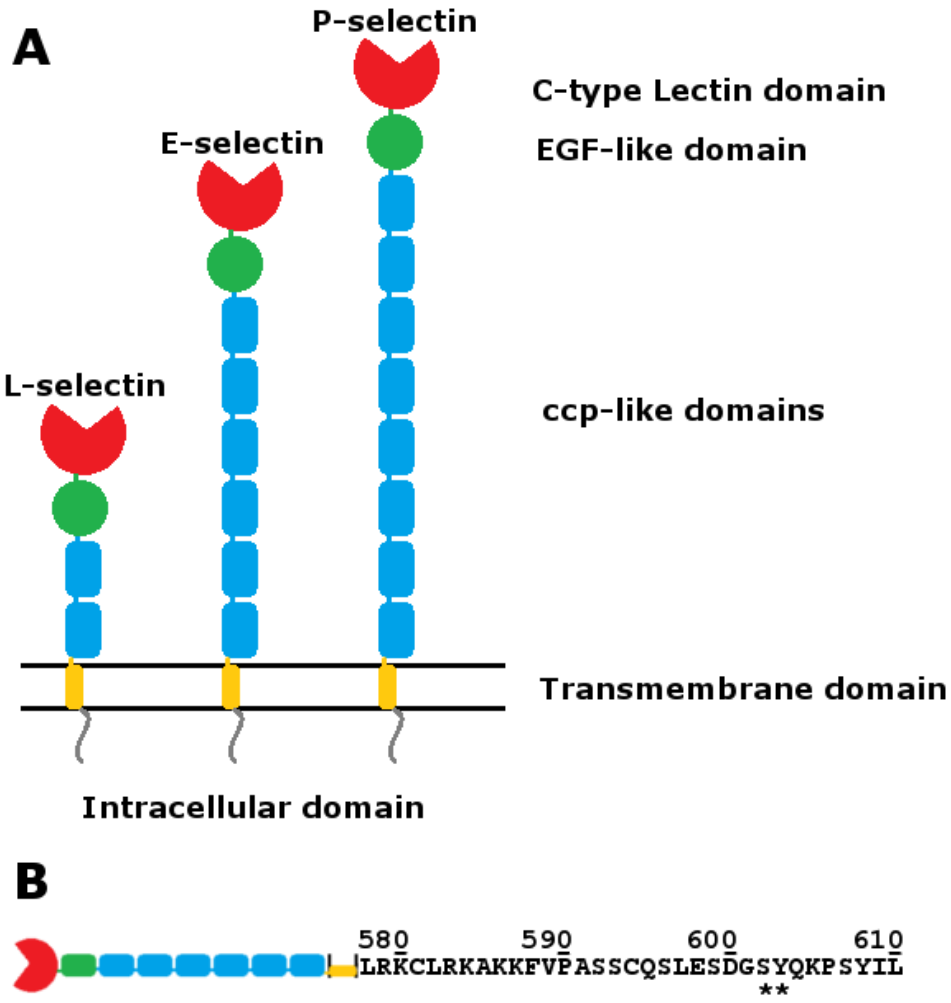

Figure 1.6: Structures of the three selectin proteins as well as the cytoplasmic sequence of E-selectin.

(A) Domain Structure of selectins. The selectins have a rigid structure that protrudes from the cytoplasmic membrane. They are composed of an N-terminal Lectin domain, an Epidermal Growth Factor (EGF)-like domain and between 2-8 complement control protein (CCP) domains. There is a single transmembrane domain, and a short C-terminal intracellular region(Varki et al., c1999). (B) Amino acid sequence of the E-selectin intracellular domain, phosphorylation sites labelled as *.

The three selectins have overlapping functions and specificities. Mice deficient in one of the selectins appear to have only mild reductions in immune response, whereas mice deficient in all three selectins showed severe impairment of neutrophil recruitment and spontaneous skin infections. Double mutants with only one functioning selectin show that L- and P-selectin are more responsible for initial capture of leucocytes from the bloodstream, while E-selectin is more responsible for slow rolling over the endothelium(Homeister et al., 1998; Jung and Ley, 1999), as well as the activation and conformational changes in LFA-1.

Despite the overlapping functions of the selectin family, the selectins have been shown to have differences in the specific class of leucocytes they recruit. L-selectin is important for recruitment of most leucocyte subsets (although it is downregulated in memory T-cells), and is rapidly shed upon leucocyte activation highlighting its importance in the very early stages

of recruitment(Bochner, 2000; Hafezi-Moghadam et al., 2001). E-selectin has approximately 10x higher affinity for neutrophils compared to P-selectin, while P-selectin has a higher affinity for eosinophils. This is due to the relative abundance of their ligands expressed on the relevant leucocytes; neutrophils have a higher concentration of the E-selectin ligand sialylated Lewis X Ag(Bochner, 2000; Bochner et al., 1994), whereas eosinophils have a higher affinity for P-selectin, due to increased levels of P-selectin ligand PSGL-1 on eosinophils(Bochner, 2000; Woltmann et al., 2000).

1.3.4.1 Functional aspects of the E-selectin cytoplasmic tail

As well as its main known function in the recruitment and activation of neutrophil binding, the E-selectin tail has also been shown to be able to activate signalling pathways within the endothelium, triggered by clustering of the adhesion molecule upon neutrophil binding. Several of the amino acid residues in the cytoplasmic tail are able to become phosphorylated and consequently modulate a number of important signalling pathways.

Upon Leucocyte rolling and adhesion, E-selectin rearranges into larger clusters, which become associated with cytoskeletal components such as actin and Src cortactin (Tilghman and Hoover, 2002a; Yoshida et al., 1996). Clustering can also initiate several signalling mechanisms including the p38 and ERK MAPK pathways(Hu et al., 2000, 2001; Yoshida et al., 2003), Phospholipase Cγ(Kiely et al., 2003), and increases in Calcium signalling(Kaplanski et al., 1994; Kiely et al., 2003; Lorenzon et al., 1998). Summaries of the signalling pathways activated by E-selectin clustering are shown in Figure 1.7.

These clusters of E-selectin have also been visualised upon exposure to other E-selectin binding molecules, such as cross linking antibodies (Kiely et al., 2003) or artificial E-selectin binding aptamers (Mann et al., 2010). Antibody cross-linking of E-selectin is observed as bright clusters on the surface of the cells, while leucocyte-mediated clustering is seen as a ring of E-selectin around the point of contact of the leucocyte with the endothelium(Doulet et al., 2006; Tilghman and Hoover, 2002a; Wójciak-Stothard et al., 1999) under fluorescent or confocal microscopy.

The Ser602 residue on the E-selectin tail is constitutively phosphorylated upon normal E-selectin expression, this phosphorylation is essential for the re-internalisation of E-selectin, alongside a di-leucine motif at Ile609 and Leu610(Chuang et al., 1997; Kluger et al., 2002; Yoshida et al., 1998). Upon E-selectin cross-linking however, the serine becomes de-phosphorylated, which maintains the presence of E-selectin on the cell surface.

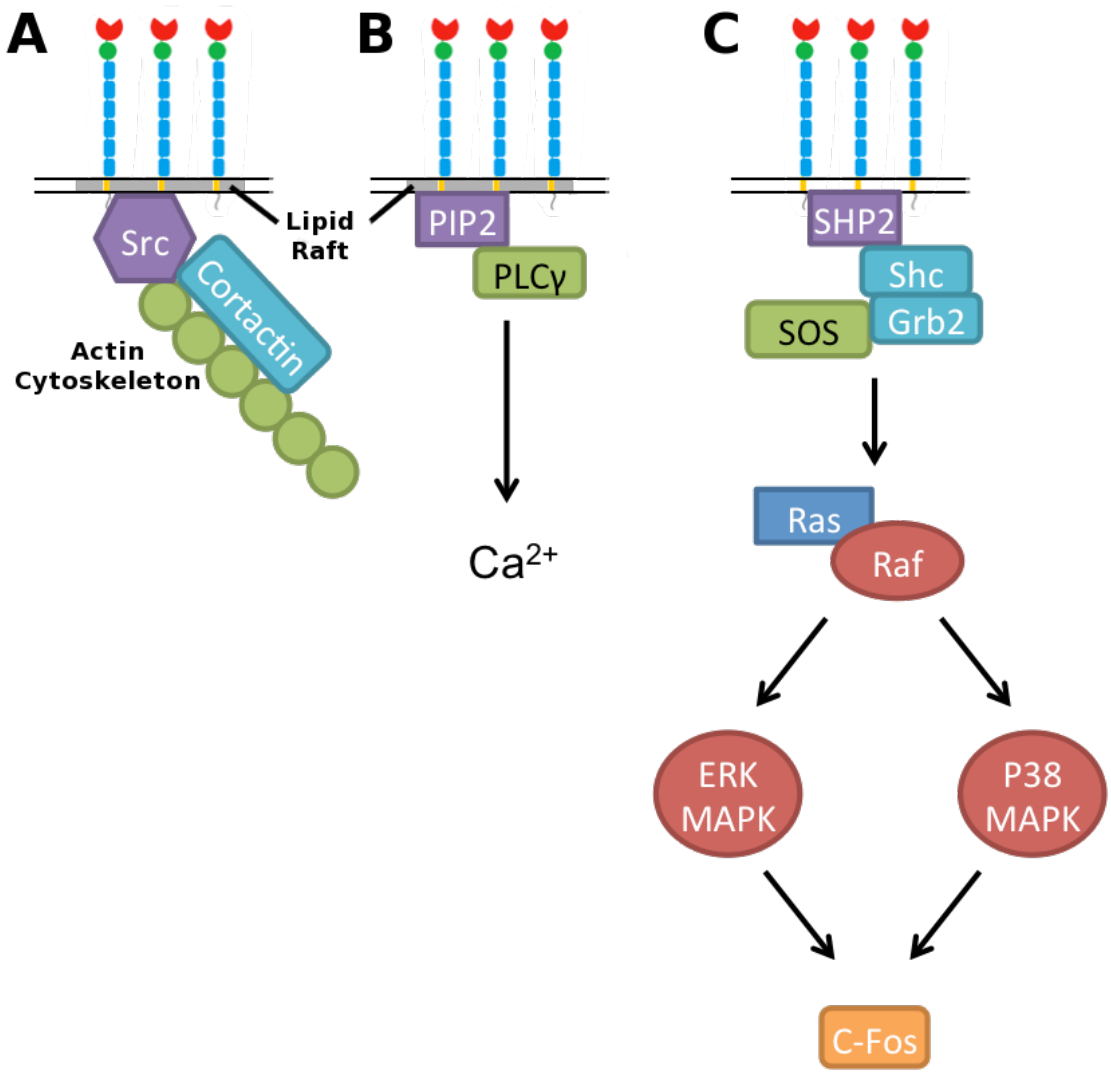

Figure 1.7: Summary of signalling pathways activated by E-selectin clustering.

(A) E-selectin clustering in lipid rafts de-phosphorylates Ser 602 on the intracellular domain, which increases interactions with the cytoskeleton and is associated with the Src-Cortactin phosphorylation pathway. (B) Clustering of E-selectin in lipid rafts can also recruit PLCγ, and can increase intracellular Ca2+ signalling. (C) The ERK/p38/MAPK pathways can be activated by E-selectin clustering causing phosphorylation of Tyr 603 on the E-selectin cytoplasmic tail, leading to the recruitment of a large complex of signalling proteins beneath the clustered E-selectin, activating both the ERK and p38 MAPK pathways and leading to c-Fos transcription factor activation. MAPK signalling does not require specific lipid raft localisation of E-selectin.

E-selectin is expressed in both lipid rafts and clathrin-coated pits on endothelial cells(Kiely et al., 2003; Setiadi and McEver, 2008; Tilghman and Hoover, 2002b). Expression and clustering in these cell surface locations is essential for efficient tethering and rolling of leucocytes along the endothelium. Disruption of E-selectin clustering in either location drastically reduces neutrophil rolling, highlighting the important role of E-selectin clustering in leucocyte adhesion (Setiadi and McEver, 2008; Tilghman and Hoover, 2002a). Association of Src and cortactin with E-selectin appears to be essential for clustering and cytoskeletal interactions (Figure 1.7A), although the interconnectivity of this with other E-selectin signalling pathways is unclear(Tilghman and Hoover, 2002a, 2002b).

Clustering of E-selectin in lipid rafts has also been shown to cause Phospholipase-Cγ (PLCγ) activation (Figure 1.7B); disruption of lipid rafts prevents E-selectin mediated activation of PLCγ, but not E-selectin mediated activation of other pathways such as the MAPK/ERK pathway (Kiely et al., 2003), indicating that the signalling properties of E-selectin can vary depending on its cell surface location. Disruption of lipid rafts has also been shown to inhibit E-selectin and ICAM-1 interactions with cortactin and Src, which are essential for the clustering of E-selectin around adhered leucocytes and antibodies(Tilghman and Hoover, 2002a, 2002b), perhaps due to disruption of cytoskeletal interactions.

Probably the best-characterised E-selectin mediated signalling pathway however is the ERK1/2 pathway, outlined in Figure 1.7C. Upon clustering of E-selectin, Tyr603 in the E-selectin cytoplasmic tail becomes phosphorylated and associated with the protein-tyrosine phosphatase SHP2. SHP2 itself becomes phosphorylated, and recruits the complex of Shc, Grb2 and Sos, allowing activation of the Ras/Raf-Phospho-MEK signalling complex. This activates the MAPK/ERK signalling pathway, resulting in upregulation of the transcription factor c-fos(Hu et al., 2000, 2001; Yoshida et al., 1998). C-fos has been shown to upregulate a wide variety of genes, involved in activities such as cell division, differentiation and, perhaps most relevantly, suppression of inflammatory response(Ray et al., 2006).

Interestingly, there is some evidence that the activation of the ERK/MAPK as well as p38 can regulate the migration of leucocytes and metastasising colon cancer cells across the endothelium. HT-29 colon cancer cells have been shown to roll along E-selectin on endothelium and activate the ERK and p38 signalling pathways in a manner very similar to neutrophils, and blocking either signalling pathway in endothelial cells also prevented colon cancer cell transmigration(Tremblay et al., 2006, 2008). Endothelial ERK activation has also been shown to be important in neutrophil activation(Stein et al., 2003); indicating an important role for the two E-selectin activated signalling pathways in cell transmigration.

1.4 Aims and Objectives

Preliminary work by other members of this group has shown high levels of association of *N.meningitidis* bacteria, neutrophils and E-selectin in skin biopsies from patients with meningococcal disease, as well as a much greater increase in E-selectin expression on endothelial cells compared to other inflammatory stimuli (Dixon et al., 1999, 2004). Other publications have shown E-selectin associated with *N.meningitidis* microcolonies on the endothelial surface(Doulet et al., 2006), and actin cytoskeleton mediated rearrangement of E-selectin expression on the endothelial surface (Tilghman and Hoover, 2002b; Yoshida et al., 1996).

The primary aims of this project were to investigate whether exposure to the gram negative bacterium *Neisseria meningitidis* can influence the distribution and function of the cell adhesion molecule E-selectin on the endothelium; and if so, the level of involvement of the E-selectin intracellular domain in this process, as well as the consequences this may have on the regulation of neutrophil recruitment and activation; which are the key pathophysiological processes in the development of the vascular damage that is characteristic of meningococcal disease.

In order to establish and accomplish these aims, the following procedures and investigations were carried out:

1. Creation of a lentiviral vector system in order to transfect both full-length and cytoplasmic tail-less mutant E-selectin into host cells.
2. Evaluation of the lentiviral vector system by examination of E-selectin expression in lentiviral transfected cells compared to inflammatory stimuli, and also whether infection by the lentivirus results in additional inflammatory stimulation.
3. Investigation of whether *N.meningitidis* can influence redistribution of E-selectin on primary endothelial cells, either directly or indirectly, and the involvement of E-selectin cytoplasmic signalling in the endothelial response to the bacteria.
4. To study the influence of *N.meningitidis* on the E-selectin mediated recruitment and subsequent transmigration of neutrophils under both static and physiological flow conditions, as well as the contribution of the E-selectin cytoplasmic region to these processes.

2 Materials and Methods

2.1 List of reagents

Reagent	Company	Code
Cell Culture		
Foetal Bovine Serum, PAA Clone	PAA	A15-102
RPMI 1640 Medium + HEPES	Gibco	52400-041
MCDB 131 Medium	Gibco	10372-019
Accutase	Sigma	A6964
Fungizone antimycotic	Gibco	15290-026
200mM L-Glutamine	Gibco	25030-024
Penicillin-Streptomycin (10,000 U/mL)	Gibco	15140-122
Collagenase type II powder	Gibco	17101-015
Fibronectin from human plasma	Sigma	F2006
Polymorphprep	Axis Shield	1114683
Lentiviral Cloning		
QIAquick PCR Purification Kit	Qiagen	28104
QIAquick Gel Extraction Kit	Qiagen	28704
QIAprep Spin Miniprep Kit	Qiagen	27104
BIOTAQ DNA Polymerase	Bioline	BIO-21040
T4 DNA ligase	Promega	M180A
PfuUltra™ High Fidelity DNA polymerase (2.5 U/ µl)	Stratagene	600380
TSAP Alkaline Phosphatase	Promega	M9910
BclI	Promega	R6651
BamHI	Promega	R6021
SspI	Promega	R6601
One Shot TOP10 Chemically Competent *E. coli*	Invitrogen	C404003
1Kb Plus DNA Ladder	Invitrogen	10787-018
GelRed Nucleic Acid Gel Stain, 10,000X in water	Biotium	41003
Lentivirus Creation		
QIAfilter Plasmid Maxi Kit	Qiagen	12262
Opti-MEM media	Gibco	31985-062
PEI (polyethylenimine)	Sigma	P3143
Confocal Staining		
TO-PRO3 Iodide (642/661)	Molecular Probes	T3605
Fluorescein isothiocyanate isomer I	Sigma	F7250
Slowfade Gold Antifade Reagent	Molecular Probes	S36936
Triton X-100	Sigma	T8787
Nunc Thermanox Coverslips	NUNC	174942
µ-Slide VI 0.4, ibiTreat, tissue culture treated, sterile	Ibidi	80606
VECTASHIELD Mounting Medium with DAPI	Vector Laboratories	H-1200

Bacterial Culture		
GC Agar Base	BD Difco	228950
Vitox Supplement	Oxoid	SR090A
Mueller Hinton Broth	Oxoid	CM045B
General Other		
Paraformaldehyde powder	Sigma	P6148
BD Cellfix 10x concentrate	BD	340181
Recombinant human IL-1β	Invivogen	rhil-1b
Dulbecco's phosphate buffered saline (DPBS) tablets	Oxoid	BR0014
Sterile DPBS, No Calcium, No Magnesium	Gibco	14190-094
Bovine Serum Albumin	Sigma	A4503
Polybrene	Santa Cruz Biotechnology	sc-134220

2.2 Plasticware

Cell Culture Plasticware	Company	Code
T25 flasks	Corning	CLS3056
6 well plates	Corning	CLS3506
24 well plates	Corning	CLS3527
15ml centrifuge tube	Corning	430791
50ml centrifuge tube	Corning	430829
5ml stripette	Corning	CLS4487
10ml stripette	Corning	CLS4488

2.3 List of antibodies

Antigen	Antibody	Clone	Company	Code
FACS				
ICAM-1	PE-Cy5 mouse anti-human CD54	HA48	BD	555512
VCAM-1	FITC mouse anti-human CD106	51-10C9	BD	551146
E-selectin	PE mouse anti-human CD62E	68-5H11	BD	551145
E-selectin	mouse anti-human CD62E	1.2B6	AbD Serotec	MCA883
Mouse IgG	RPE Anti-mouse IgG	Polyclonal	Dako	R0480
CD66b	FITC Mouse anti-Human CD66b	80H3	AbD Serotec	MCA216F
Confocal microscopy				
E-selectin	Human E-selectin/P-selectin Mab	BBIG-E6	R&D Systems	BBIG-E6
E-selectin	Human E-selectin Mab	BBIG-E4	R&D Systems	BBIG-E4
Mouse IgG	FITC goat anti-mouse IgG	Polyclonal	Sigma	F2012
Mouse IgG	Alexa Fluor 546 Goat anti-mouse IgG	Polyclonal	Molecular Probes	A-11003
Mouse IgG	Alexa Fluor 568 Goat anti-mouse IgG	Polyclonal	Molecular Probes	A-11004

2.4 Buffers and Media

HUVEC Media: 20% FCS in MCDB medium supplemented with 100μg/ml Penicillin-Streptomycin, 2mM L-Glutamine and 0.25μg/ml Fungizone.

HMEC-1 Media: 10% FCS in MCDB medium supplemented with 2mM L-Glutamine.

Resting Media: 10% FCS in RPMI medium supplemented with 2mM L-Glutamine.

FACS Buffer: 10% FCS in PBS

2.5 Software used for analysis and acquisition of data

All of the graphs in this thesis were prepared using Graphpad Prism (Graphpad Software), which was also used to carry out appropriate statistical tests on the data. Flow cytometry data was captured using BD Cellquest Pro software (BD Biosciences), and analysed using FlowJo data analysis software (Flowjo LLC). Confocal microscopy images were captured using Carl Zeiss Zen 2009 software (Carl Zeiss Microscopy), and both time lapse and still images of neutrophil adhesion under flow were captured using Volocity 3D image analysis software (PerkinElmer). Both confocal and phase contrast microscopy images were analysed using the Open Source image processing software Fiji ImageJ(Schindelin, 2008; Schindelin et al., 2012). The ImageJ 'Analyse Particles' plugin was used to count the number of bright adherent neutrophils on thresholded phase contrast images. The Fiji 'MTrackJ' plugin was used to track rolling neutrophils and measure their velocity, and the external plugin 'Cell Counter' was used to manually count transmigrated cells(De Vos, Kurt, 2008).

2.6 Preparation of 4% PFA

A 4% solution of paraformaldehyde (PFA) was prepared for use in fixing cells for confocal microscopy as well as dilution to 0.5% to kill *N.meningitidis* bacteria in suspension. 4grams of paraformaldehyde power (Sigma) were added to 80ml non-sterile PBS solution (Oxoid: one tablet per 100ml MilliQ water) and heated gently on a hot plate to around 60°C. NaOH solution was added dropwise to the solution while stirring until the powder was completely dissolved. Once dissolved, HCl was added dropwise until the Ph returned to around 7.6. The volume of the solution was made up to 100ml using PBS, and the solution was cooled, filtered and aliquoted before storing at 4°C.

2.7 Cell culture

HMEC-1 cells are an endothelial cell line, derived from human dermal microvascular cells and immortalised by transfection with a PBR-322-based plasmid containing simian virus 40A gene product(Ades et al., 1992). HMEC-1 cells were thawed from stocks in liquid nitrogen, and grown in HMEC-1 media in T-25 flasks. Cells were split when around 90% confluent using Accutase (Millipore), which was around every 3-4 days.

HUVEC were isolated from umbilical cords collected by midwives from consented patients in the labour ward at West Middlesex University Hospital and placed in RPMI collection media:

RPMI media supplemented with 100μg/ml Penicillin-Streptomycin, 2mM L-Glutamine and 1.25μg/ml Fungizone (Life Technologies) at 4°C. Cords were retrieved from the hospital for endothelial cell preparation every 3-4 days. Ethics approval for anonymous use of human tissue was obtained, and no data from patients was gathered or kept.

To prepare HUVEC from the umbilical cords; excess blood in the cord was squeezed out, and the cord flushed through with RPMI to wash most of the clotted blood away. Cords were then filled with 0.1% collagenase type II (Life Technologies) in RPMI and incubated at 37°C for 10 minutes. Cords were removed from incubator and massaged gently to aid mechanical removal of endothelial cells from basement membrane. The cell suspension was emptied into a 50ml falcon tube, and the cord was flushed through with RPMI containing 20% FCS into the same falcon tube to inactivate the collagenase. Suspensions were centrifuged at 900g for 5 minutes and supernatant discarded. Cells were resuspended in 5ml HUVEC media and grown in T25 flasks (passage 0). In all experiments HUVEC were used at passage 1, and HMEC-1 at passage 7-8.

2.8 Neutrophil isolation

Neutrophils were isolated from healthy donors using Polymorphprep (Axis-shield), a solution of 8% dextran-500 and 13.8% sodium diatrizoate. 5ml of heparin treated whole blood was layered on top of an equal volume of Polymorphprep and centrifuged at 400g for 40 minutes at room temperature. The blood cells separate by cell density, with the erythrocytes losing water to the Polymorphprep, becoming more dense, and sinking to the bottom. The granulocytes form a band midway through the sodium diatrizoate gradient formed by the sinking erythrocytes, while the mononuclear leucocytes remain at the boundary between the blood plasma and the Polymorphprep. Diagram of the blood layers before and after centrifugation are shown in Figure 2.1.

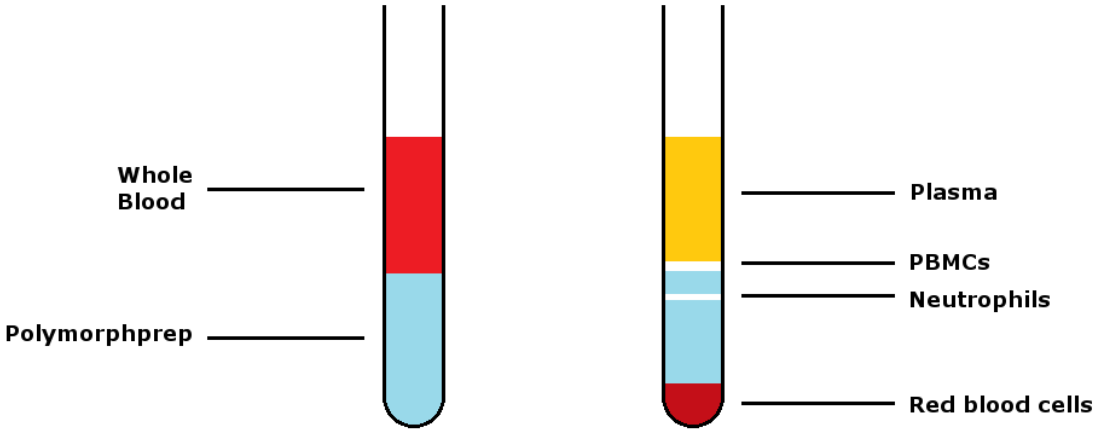

Figure 2.1: Diagram of the three layers of cells produced after centrifugation of whole blood layered over an equal volume of polymorphprep.

The granulocyte band was removed (after first removing the mononuclear band on top of it, to minimise contamination) using a sterile Pasteur pipette, and washed in 10% FCS RPMI.

At this stage the cell pellets were often red or pink coloured due to erythrocyte contamination; to remove erythrocytes the pellet was resuspended in 1ml sterile filtered water for 15 seconds, to rapidly lyse the red blood cells, before quickly adding 15ml 10% RPMI to return the granulocytes to an isotonic solution before they could be killed themselves(Thorson et al., 1995). After washing again the cells were resuspended in 1ml 10% FCS RPMI, counted and diluted to the appropriate concentration in 10% FCS RPMI.

2.8.1 Confirmation that the neutrophil isolation protocol resulted in a pure population of granulocytes by flow cytometry

In order to confirm neutrophil purity following isolation, cell were analysed by Flow Cytomtery. $1x10^6$ cells were prepared using polymorphprep and counted using a Neubauer counting chamber after 1:1 mixing with Trypan blue to detect dead cells. Neutrophils were stained for the granulocyte marker CD66b, and checked for staining and expression via flow cytometry. Leucocytes were separated from dead cells and debris using a Forward scatter/Side scatter gate (Figure 2.2A), and CD66b expression was seen on around 90-93% of gated leucocytes (Figure 2.2B), which corresponds well to the published data on polymorphprep isolated granulocyte purity rates (Degel and Shokrani, 2010; Zhou et al., 2012). Although it was unclear whether the small cell population seen below the granulocyte population in Figure 2.2A were debris or lymphocytes, only 4.01% of the total cell population were CD3 positive (Figure 2.2C), showing that any potential lymphocyte contamination was small.

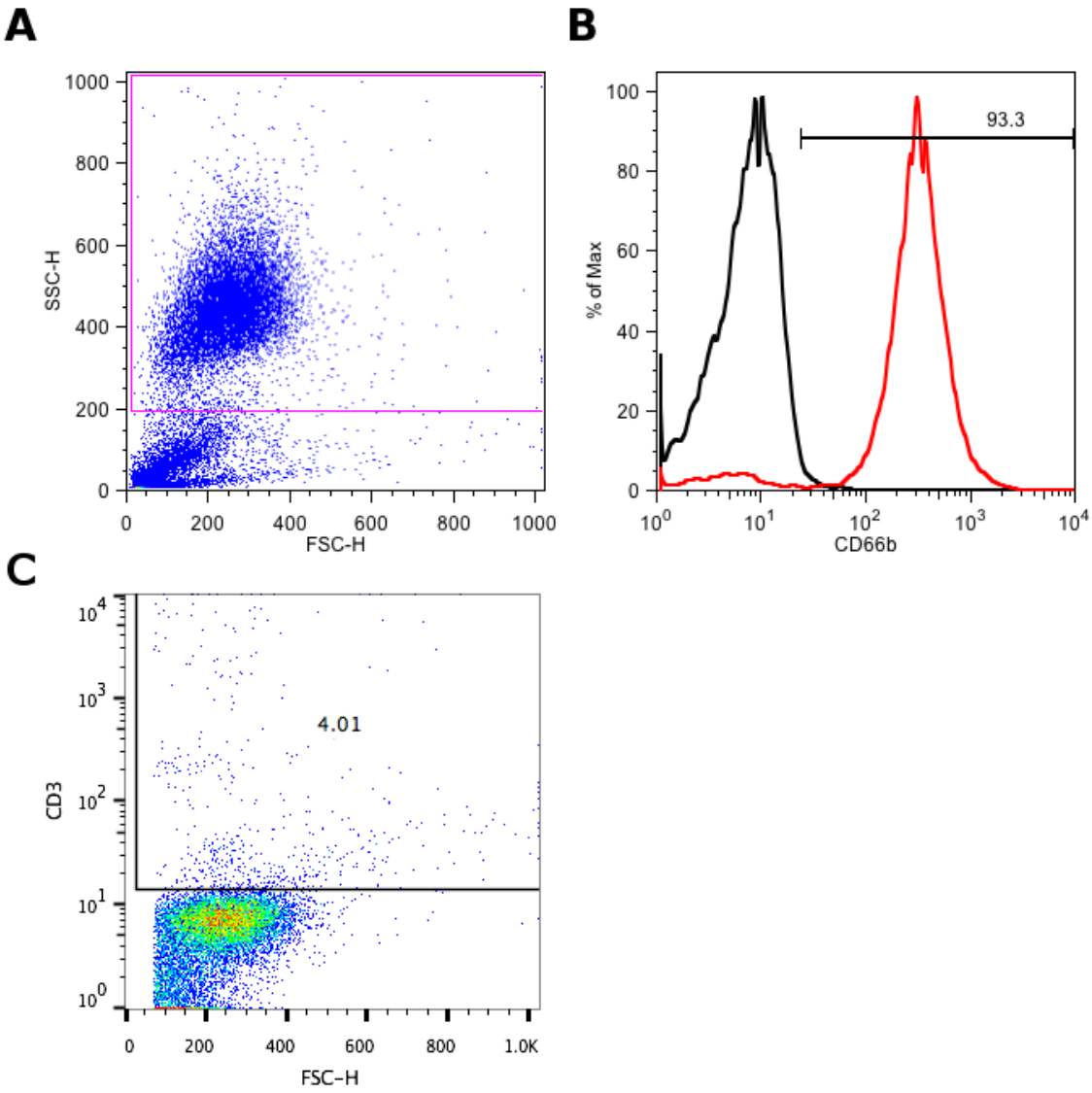

Figure 2.2: Representative flow cytometry graphs showing neutrophil purity after leucocyte separation using polymorphprep.

(A) Neutrophil gate on a Forward Scatter vs. Side scatter dot blot excluding dead cells and debris. (B) Histogram showing both unstained cells (black) and CD66b+ stained cells (red) within the gated area, 93.3% of gated cells were CD66b+, and thus identified as neutrophils. (C) CD3 gate showing that only 4.01% of the total cell count was CD3+, and that lymphocyte contamination was low. Figures representative of 2 donors.

2.9 Virus transfection

HUVEC or HMEC-1 cells were detached from flasks using 1ml Accutase and seeded into 24 well plates at $5x10^4$ cells/well in either HUVEC media or HMEC-1 media, and incubated at 37°C, 5% CO_2 overnight. The next day, media was replaced by 0.5ml of the relevant HUVEC or HMEC-1 medium containing 5µg/ml Polybrene (Millipore), and the lentivirus was added to the relevant concentration based on the experiment. (After the viral titre was determined as outlined in chapter 4.3.4, the concentration of virus used was at 1µl of stock virus/ml, or $7x10^4$ virus particles/ml). Plates were then incubated at 37°C 5% CO_2.

Media was changed after 24 hours to remove polybrene, which can be toxic to the cells, and incubated for a further 48 hours. 72 hours post-transfection, expression of ES or ΔC lentiviral inserts will have reached sufficient levels for analysis. Media was replaced with Resting media 24 hours prior to experiment to rest the cells.

2.10 HUVEC preparation for immunofluorescent confocal microscopy

13mm diameter, #1.5 circular glass cover slips were coated with 100μl fibronectin at concentration of 25μg/ml (approx. 2μg/cm^2) and incubated at RT for 45 minutes. Cover slips were then washed with PBS (without Mg^{2+} and Ca^{2+}) and placed one per well in the bottom of a 24 well plate while still wet.

HUVEC were seeded at 5x10^4 cells/well in HUVEC media on top of the fibronectin coated cover slips. The HUVEC were grown on cover slips until confluent, when the media was replaced by resting media for 24 hours before the experiment to rest the cells.

Two staining methods were used for immunofluorescence staining, method A and method B. In staining method A; after stimulation, cover slips were washed in PBS, then fixed for 10 minutes in 4% PFA. The cells were then washed twice again in PBS and blocked with 1% BSA in PBS for 30 minutes. Cells were then stained with 20μl 10μg/ml anti-human E-selectin/P-selectin (BBIG-E6, R&D systems) for 20 minutes at RT. A 20μl drop of 10μg/ml antibody was placed on a sheet of parafilm, and the cover slip was removed from the well and placed face-down onto the droplet, ensuring no air bubbles between the cover slip and parafilm, creating contact between the whole slide and the drop containing the antibody.

The cover slips were returned to their wells, washed again 3 times in PBS, then stained again for 20 minutes with both 20μl FITC-conjugated goat anti-mouse antibody (F2012, Sigma) as well as 1μl/ml TO-PRO3 Iodide (Molecular Probes) using the same method, then washed again 3 times in PBS.

Staining method B was similar to method A, except that staining with the primary antibody took place before fixing the cells with 4% PFA. To reduce the possibility of the live cells dissociating from the glass slide during staining, the slides were laid face-up on the parafilm and 40μl of the antibody solution was applied to their surface for 20 minutes, the droplet was kept in place by surface tension.

For antibody cross-linking of E-selectin, the staining followed the same protocol except the and cells were fixed with PFA only after staining with the two antibodies, as the PFA fixes the surface proteins in place and doesn't allow for cross-linking rearrangement of proteins.

Slides stained for cross-linking were laid face-up on the parafilm for staining in the same way as the live cells in staining method B.

After staining the cells were mounted on clear glass slides in mounting media (Slowfade Gold Antifade Reagent, Molecular Probes) and sealed in place using nail varnish. In some early experiments a mounting media containing DAPI stain (Vectashield) was used instead, and the TO-PRO3 stain was not used, these experiments are clearly indicated in the figure legends.

Photographs were taken using a Zeiss LSM 710 confocal microscope and Zen 2009 capture software. Images were processed using Fiji ImageJ image processing software(Schindelin et al., 2012). Images in Chapter 5 were taken using x63 oil-immersion objective, and those in Chapter 6 using a 10x objective.

2.11 Bacterial strains and preparation

All strains used in the experiments in this thesis were constructed and characterised by Peter Van Der Ley (Laboratory of Vaccine Research, RIVM, Bilthoven, Netherlands). The Wild Type bacterial strain was the serotype B strain *N.meningitidis* H44/76 (sero (sub)-type (B: 15:P1.7, 16), ET-5 complex, Pilus^{+}, Opa^{+}, Opc^{+}, *SiaD*$^{+}$), first isolated from a patient in Norway in 1978 (Holten, 1979). The *SiaD* deletion mutant (Pilus^{+}, Opa^{+}, Opc^{+}, *SiaD*$^{-}$), was created by insertional inactivation of the polysialyltransferase gene using an erm (*erythromycin ribosomal methylase*) resistance cassette (Jones et al., 2014), and were assessed for the absence of capsule expression using an enzyme-linked immunosorbent assay (ELISA) (Hammerschmidt et al., 1994, 1996).

All *N.meningitidis* strains were stored in Muller-Hinton broth with 10% glycerol at -80C, and grown on GC agar (BD) supplemented with Vitox (SR0090A, Oxoid) at 37°C overnight. Single colonies were subcultured onto a second GC agar plate and incubated overnight a second time, *N.meningitidis* prepared from this second subculture were used in experiments. To prepare killed *N.meningitidis*, bacteria were resuspended in 0.5% PFA in PBS at RT for 10 min to kill them. The bacteria were pelleted and washed three times in PBS, before being resuspended in sterile PBS at 10^{9} bacteria/ml, as determined by an absorbance value of 1.0 at a wavelength of 600nm. To prepare live *N.meningitidis*, the bacteria were directly resuspended in PBS without PFA, washed once, and then diluted to absorbance of 1.0 at 600nm.

To stain bacteria with FITC, a saturated solution of FITC was created by absorbing 0.2g of FITC in 5ml PBS, then passing through a 0.22µm filter to remove solid lumps. A bacterial

pellet was resuspended in the FITC solution and incubated at 37°C for 15 minutes. Bacteria were then washed in PBS 3-4 times before being used.

2.12 Statistics

Where indicated in the text and figures, statistical significance of results was analysed using the Student's T-test to determine whether the data gathered from two different conditions was statistically different from each other. In Figure 6.11 a Friedman test was used to determine whether the E-selectin blocking antibody led to a consistent reduction in adhesion in transfected cells under all conditions, rather than analysing all conditions individually.

3 Design and creation of Lentivirus vectors containing full length and tail-less E-selectin

3.1 Introduction

E-selectin is expressed on endothelial cells following stimulation with inflammatory mediators such as TNFα and LPS, and to a significantly greater level upon stimulation with *N.meningitidis* bacteria(Dixon et al., 1999, 2004). However, these powerful inflammatory stimuli also activate multiple pathways and enhance the expression of many more cellular response mechanisms than just E-selectin.

In order to investigate the effects of E-selectin engagement with minimal interference from other endothelial inflammatory molecules; various methods of transducing E-selectin into cells, both primary HUVEC and non-endothelial cell lines, have been used in the past. Specifically, the use of adenovirus vectors to transfect both HUVEC and CHO cells with E-selectin have been used by several groups to investigate both intracellular signalling ability and the lipid raft subcellular location of E-selectin expression(Yoshida et al., 1998; Hu et al., 2000; Setiadi and McEver, 2008).

More recently, the use of lentiviruses for transfecting cells to express proteins of interest has become more commonplace. Lentiviruses have several advantages over adenoviruses for transfection; including more stable expression due to integration into the target cell genome, and much reduced inflammatory activation of transfected cells(Blömer et al., 1997; Copreni et al., 2009; Nayak and Herzog, 2010). Conversely however, lentivectors have lower expression of their packaged gene, as well as a much smaller limit to the size of insert they are capable of expressing (8kb compared to 36kb)(Kay et al., 2001; Nayak and Herzog, 2010). The fact that adenovirus vectors can cause inflammatory activation of transfected cells is a particular concern when studying molecules involved in inflammation, such as E-selectin. For this reason we aimed to create new lentiviral vectors for transfection of both primary cells and cell lines, rather than use existing adenoviral vectors.

E-selectin is a transmembrane protein located on the plasma membrane. Its intracellular domain is known to be important for some signalling processes, as well as attachment to the cytoskeleton. When investigating interactions of E-selectin on the surface of the endothelium, it is important to be able to distinguish the effects of extracellular binding to the E-selectin, and the influence of rearrangement or activation of the adhesion molecule via its intracellular and cytoskeletal interactions. To this end, an E-selectin mutant that lacks the intracellular domain responsible for both intracellular signalling and interaction with the

cytoskeleton has also been used in the publications utilising adenovirus transfection outlined above, and both the full-length and tail-less mutant sequences were obtained for this project.

3.1.1 Aims and Objectives

The aims of the experiments carried out in this chapter were to clone the full length (ES) and tail-less mutant (ΔC) E-selectin sequences from an adenovirus vector into a lentiviral vector, in order to allow the transduction of both primary HUVEC and cell lines with both full-length E-selectin and a mutant form that lacks the intracellular domain.

3.2 Methods

3.2.1 Lentivector PCR and transformation

To extract the cDNA sequences from the adenovirus vector (provided by Jeanne-Marie Keily and Michael Gimbrone: Department of Pathology, Brigham and Women's Hospital, Boston) the cDNA was amplified by PCR using PfuUltra high fidelity DNA polymerase (Stratagene) and two primers shown in Figure 3.1. The forward primer contained the 5' E-selectin sequence along with both a BclI restriction enzyme site and the consensus Kozak translation initiation sequence; the reverse primer contained just the BclI restriction sequence alongside the 3' E-selectin sequence. The Kozak sequence enhances translation, while the BclI sequence allows ligation of the sequence into plasmid site cut with BamHI.

```
                BclI    Kozak          E-selectin
Forward: CTAG TGATCA GCCACC ATGATTGCTTCACAGTTTCTCTCAGC
Reverse: CTAG TGATCA        TTAAAGGATGTAAGAAGGCTTTTGGTAGC
```

Figure 3.1: Primer sequences for amplification of E-selectin cDNA from adenovirus vectors

Amplified cDNA was purified (QIAquick PCR Purification Kit, Qiagen) and cut with BclI restriction enzyme (Promega). At the same time the lentiviral vector pLNT-SIN-SIEW was cut with BamHI restriction enzyme (Promega), before being treated with TSAP alkaline phosphatase (Promega) to dephosphorylate the cut DNA, preventing the cut vector re-annealing to itself without the insert.

Cut cDNA and vector DNA were gel-purified (QIAquick gel extraction kit, Qiagen) to remove proteins and shorter DNA sequences. The cDNA was ligated into the cut vector using T4 DNA ligase (Promega) and heat shock transformed into One-shot top10 competent *E.Coli* cells (Invitrogen). Positive transformants were selected on LB agar plates containing 50μg/ml ampicillin.

3.2.2 Restriction digestion, Colony PCR and sequencing

The presence of lentivector plasmid and cDNA inserts in the ampicillin resistant clones was confirmed by both restriction digestion and colony PCR. For the restriction digestion the colonies were subcultured into 5ml LB broth containing 50μg/ml ampicillin and grown overnight. The plasmid DNA was isolated (QIAprep spin miniprep kit) and cut with BamHI and SspI restriction enzymes (Promega) before being run on a 1% agarose gel containing GelRed (Biotium) detection agent and photographed under UV light alongside a 1Kb Plus DNA ladder for size comparison (Invitrogen). For colony PCR confirmation the primers in Figure 3.7A were used with Biotaq DNA polymerase (Bioline). Sequence and direction of insert was confirmed by sequencing at the UCL Wolfson Institute for Biomedical Research also using the primers in Figure 3.7A. The ClustalW2 Sequence Alignment tool from the EMBL-EBI website were used to analyse the sequenced data(Goujon et al., 2010; Larkin et al., 2007).

3.2.3 Creation of lentivirus

A clone containing each sequence (ES-64 and ΔC-4) was grown up in 500ml LB broth with 50μg/ml ampicillin; and large quantities of lentivector plasmid DNA prepared with a plasmid maxiprep kit using manufacturer's instructions (Qiagen).

To create lentivirus particles; 200μg lentivector DNA was added to 40ml Opti-MEM media (Invitrogen) along with 140μg pMDG envelope plasmid DNA (expressing VSV-G coat protein) and 260μg pCMVΔ8.74 packaging plasmid DNA (expressing gag-pol, tet and rev accessory genes). The solution was passed through a 0.47μm filter and mixed 1:1 with 40ml 2μM polyethylenimine (PEI, Sigma) in Opti-MEM, also filtered, and left at room temperature for 20 minutes. The two packaging plasmids were a gift from Emma Chan and Waseem Qasim (Molecular Immunology, Institute of Child Health, UCL), who also provided the lentivirus production protocol(Chan et al., 2012).

Six T175 flasks of 90% confluent HEK293T cells were prepared in advance. HEK293T cells are a cell line derived from Human Embryonic Kidney cells immortalised by transfection with human adenovirus 5(Graham et al., 1977), and then subsequently transfected with the SV40 T-antigen which increases production of transfected proteins(Rio et al., 1985). The HEK293T cells were washed with 10ml opti-MEM before addition of 10ml of the plasmid-PEI mixture and incubation at 37°C 5% CO_2. The media was replaced with 17ml Opti-MEM once after 24 hours, and virus was harvested twice, at 48 and 72 hours post-infection. Supernatant was removed from cells and centrifuged at 2000g for 10 minutes, pellet was discarded and the

supernatant passed through 0.47µm filter before ultra-centrifugation at 50,000g for 2 hours in 33ml polyallomer tubes.

Supernatant was discarded and each pellet covered in 150µl MCDB (Invitrogen), the tube was sealed with parafilm and incubated on ice for 30 minutes. The pellet was then resuspended, transferred to another tube and centrifuged at 2000g for 10m to remove cell debris; supernatant containing the virus particles was aliquoted to cryovials and stored in 20µl aliquots at -80°C.

The techniques used in the creation of the lentivirus particles were carried out with the assistance and guidance of Emma Chan and Waseem Qasim of the Molecular and Cellular Immunology department at ICH, however all labwork was carried out by myself.

3.3 Experimental design and cloning of E-selectin and mutant lentiviral vectors

3.3.1 Cloning of ES and ΔC cDNA sequences

The cDNA coding sequences for both the full length E-selectin (ES) and the tail-less mutant (ΔC) were received in separate pAdRSV4 adenovirus vectors as a gift from Jeanne-Marie Keily and Michael Gimbrone, (department of Pathology, Brigham and Women's Hospital, Boston)(Yoshida et al., 1998). Rather than use the adenovirus vectors supplied, a lentiviral vector system was chosen instead, to reduce the amount of inflammatory stimulation caused by the virus itself, as well as induce longer term ES and ΔC expression(Blömer et al., 1997; Copreni et al., 2009).

The mutant E-selectin contains a nonsense STOP mutation at the beginning of the transmembrane region, transforming an AAA Lysine codon into a UAA stop codon. This prevents the 30 amino acid intracellular region from being transcribed, although the sequence is still present in the cDNA. It would theoretically be possible for a point mutation to revert the ΔC sequence back to the ES sequence, however this is very unlikely. Protein sequence of the intracellular domains of both ES and ΔC are shown in Figure 3.2.

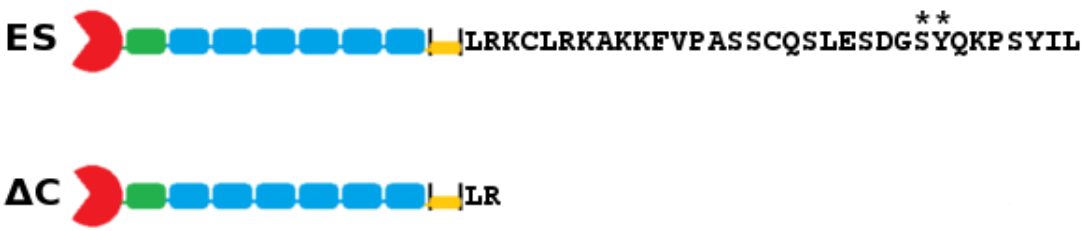

Figure 3.2: Amino acid sequence of the E-selectin cytoplasmic tail.

Known phosphorylation sites are marked with *, and the location of the STOP mutation in the ΔC mutant is shown directly after Arg579. Figure adapted from Yoshida et al, 1998(Yoshida et al., 1998)

3.3.1.1 Design of cloning strategy for ES and ΔC cloning from adenovirus vectors

The lentiviral vector plasmid (pLNT-SIN-SIEW) was received as a gift from Emma Chan and Waseem Qasim (Molecular Immunology, Institute of Child Health, UCL); the plasmid map of which is shown in Figure 3.3A. This vector is self-inactivating (SIN) HIV-1 derived vector, containing a Multiple Cloning Site (MCS) between base pair 8231-8257 as well as an Ampicillin resistance gene to enable clonal selection. The plasmid also contains the spleen focus-forming virus (SFFV) promoter sequence and the woodchuck posttranscriptional regulatory element (WPRE), which both enhance the expression of transfected genes, as well as the central polypurine tract (cPPT) sequence from HIV-1 which enables the lentivirus to achieve high levels of transduction into host cells(Demaison et al., 2002).

All of the genes required for making new lentiviral particles are not included in the packaging plasmid for safety reasons. In order to make viral particles capable of transfecting human cells the packaging plasmid must be transduced into a host cell line along with two helper plasmids, containing sequences for the envelope proteins and packaging genes required to form virus particles.

The E-selectin coding sequence in Figure 3.3B highlights the location of the point mutation that separates the ES and ΔC mutants, a single A>T substitution at base pair 1738. To insert the ES and ΔC coding DNA into the lentivector, the BamHI restriction site in the MCS was selected as the insertion site, however the E-selectin sequence also contains a BamHI restriction site at base 1216, and so the BamHI enzyme could not be used to create the sticky ends on the ends of E-selectin required for sequence ligation into the vector.

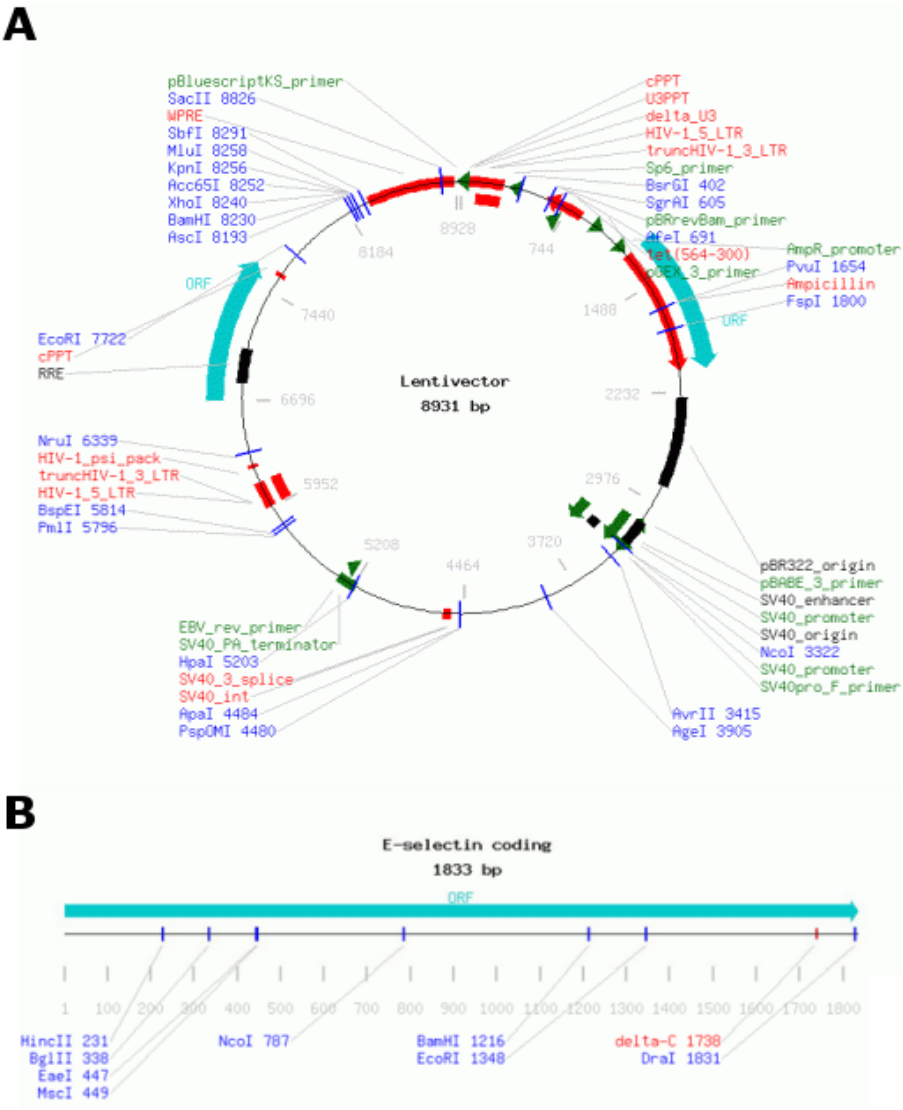

Figure 3.3: Map of the lentivirus vector and E-selectin cDNA coding sequences.

(A) Detailed map of the lentiviral vector that the ES and ΔC sequences were inserted into. Note the Multiple Cloning Site between bases 8193-8291. (B) E-selectin coding sequence, showing BamHI restriction site (1216) and location of the ΔC (delta-C) mutation (1738). Maps drawn using the plasmid tool at Lablife.org

Other restriction enzymes that create complementary sticky ends to BamHI include BglII, XhoII and BclI. However XhoII also cuts at the BamHI site, and BglII also has its own restriction site within the E-selectin gene; therefore BclI was chosen as the replacement restriction enzyme to create the sticky ends. BclI cuts at a different site to BamHI (shown in Figure 3.4), but creates the same 5' GATC overhang; allowing DNA cut by the two enzymes to be ligated easily to each other. However BclI requires a different buffer and temperature to function, necessitating an extra step in the cloning process.

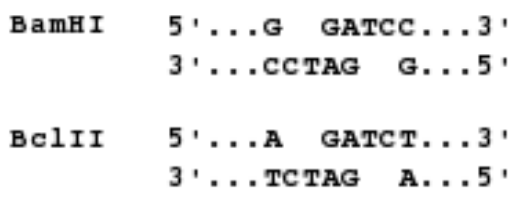

Figure 3.4: Restriction sites of the enzymes BamHI and BclI, showing their overlapping sticky ends.

3.3.1.2 Amplification of ES and ΔC cDNA from adenovirus vectors

The cDNA of ES and the mutant ΔC was amplified from the pAdRSV4 adenovector by high fidelity PCR. The forward and reverse primers were designed to be complimentary to either the beginning or end of the E-selectin sequence, respectively, and are shown in Figure 3.1. The forward primer also contained a Kozak sequence before the start codon, which enhances initiation of translation in eukaryotic cells, and both primers contained sequences for BclII restriction sites either side of the gene.

The vector was cut with BamHI and treated with TSAP Alkaline Phosphatase to dephosphorylate the sticky ends of the cut DNA, preventing spontaneous re-annealing of the cut ends without the insert. The amplified cDNA was cut with BclI, but not dephosphorylated, and ligated into the cut BamHI site in the vector. A brief flowchart describing the steps in lentivector creation is shown in Figure 3.5.

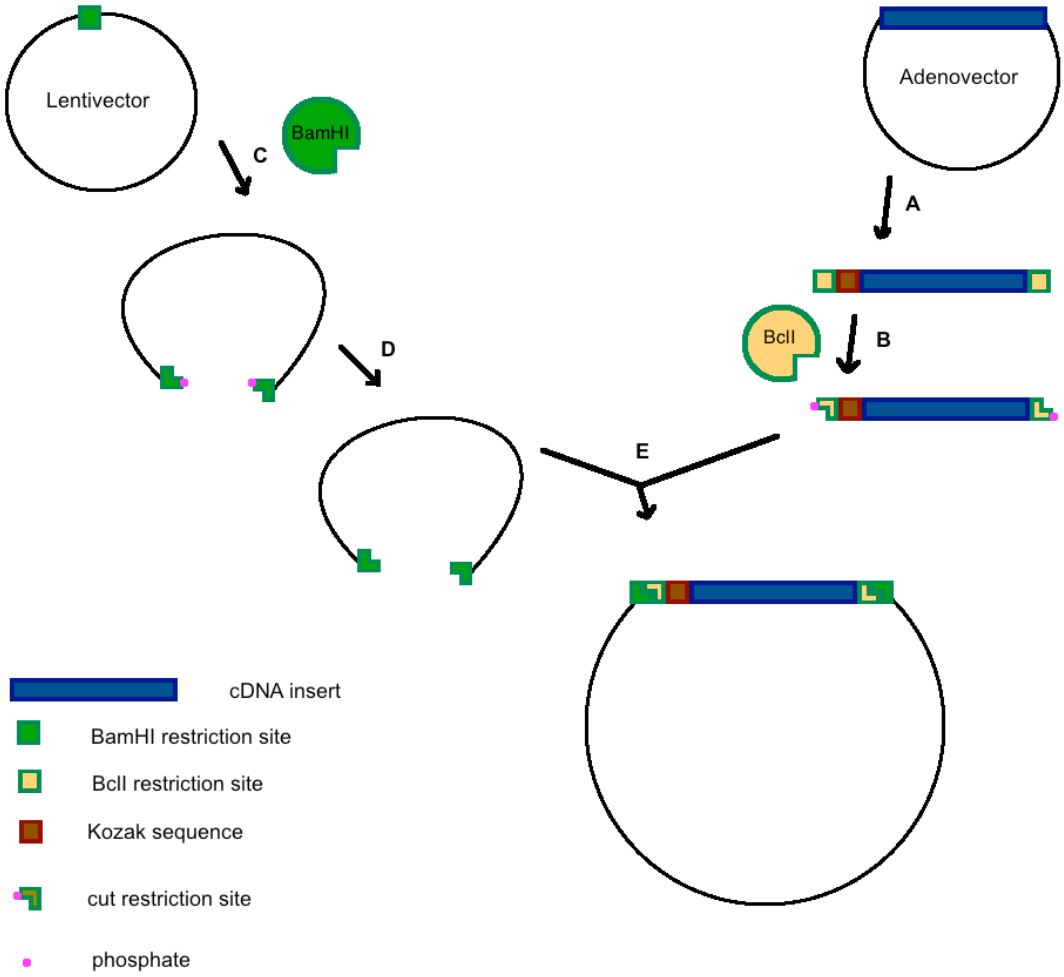

Figure 3.5: Flow diagram showing the sequence of steps in the creation of the ES and ΔC lentivector constructs.

(A) ES or ΔC cDNA is amplified from adenovirus vector via PCR, using primers that also attach a Kozak sequence and two BclI restriction sites. Amplified cDNA (B) and lentivector plasmid (C) are cut using BclI or BamHI restriction enzyme respectively, exposing sticky ends. (D) Cut lentivector DNA is treated with TSAP alkaline phosphatase to remove phosphate groups and prevent re-ligation to itself. (E) Cut cDNA insert and lentivector are ligated together to form a whole plasmid that will express the inserted ES or ΔC gene.

3.3.2 Selection of positive clones containing ES and ΔC cDNA

Ligated vectors were transformed into competent *E.coli* bacteria, and positive transformants were selected on agar plates containing 50μg/ml ampicillin. Presence and direction of cDNA inserts were confirmed by both restriction digest and colony PCR, and the clonal inserts were sequenced to confirm the correct insert was present.

3.3.2.1 Confirmation of cDNA insert by restriction digest

In the first method used to confirm the directionality of the cDNA inserted into the vector, the purified plasmids from the Ampicillin resistant clones were digested with a combination of enzymes. The enzyme SspI cuts at three sites (bases 1218, 4918 and 5071) in the vector, while the enzyme BamHI cuts at base 8230 in the vector, and base 1217 in E-selectin.

However the BamHI site in the vector is destroyed when the E-selectin cDNA is ligated into it. The different relative positions of these sites when the E-selectin gene is reversed or not present create different sized digest products that are described in Table 3-1.

Table 3-1: Size of DNA fragments produced when the lentiviral vector is digested with the restriction enzymes BamHI and SspI, depending on the presence and directionality of the E-selectin insert.

	Always present	Variable lengths
Empty vector, no insert	153, 3700	1919, 3159
Vector + insert in correct direction	153, 3700	2537, 4386
Vector + insert in reverse direction	153, 3700	3136, 3787

Colony PCR was used to confirm the presence of the E-selectin insert in the lentiviral plasmid, while larger quantities of the plasmid DNA were isolated via miniprep followed by incubation with the two restriction enzymes. After incubation the digested DNA solutions were run on a 1% agarose gel containing GelRed and viewed under a UV light.

Figure 3.6 shows the representative colony PCR and restriction digest results from the 4 ΔC transformants. Images of the restriction digestion products from colonies containing the ES insert are in Appendix A-1.

In Figure 3.6A the results of the colony PCR using primers a-b (Figure 3.7A) showed that all 4 ΔC transformants contained the insert, as all have bands at the same size as the E-selectin gene (1833bp). However in Figure 3.6B, after the BamHI/SspI double digest of the plasmid DNA, it can be seen that only clone 4 contained the insert in the correct direction. Clones 1-3 have two bands (the lighter band of 3136bp and the heavier band containing the 3787bp and 3700bp fragments merging together), while clone 4 has three bands (The same 3700bp fragment as in clones 1-3, plus a lighter band of 2537bp and a heavier one of 4386bp).

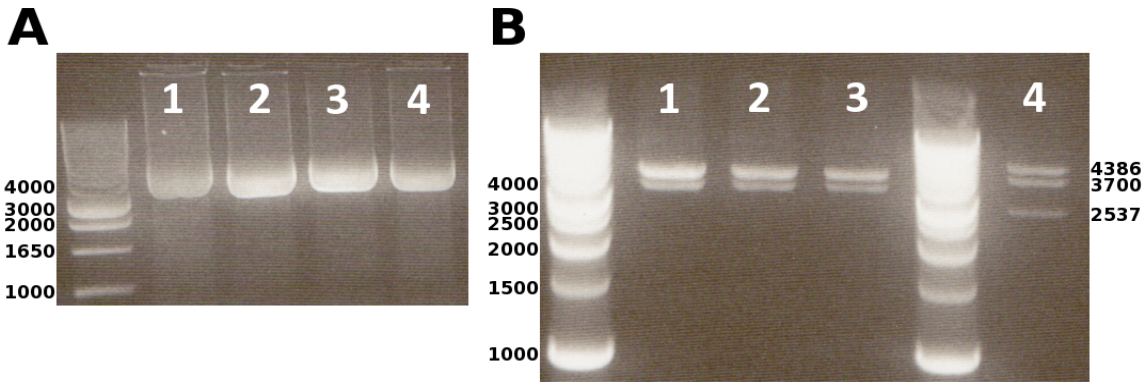

Figure 3.6: PCR and double restriction digest of clones transformed with lentivirus vector plasmids containing the ΔC mutant E-selectin cDNA sequence.

(A) Colony PCR using primer pair a-b and (B) restriction digest using enzymes BamHI and SspI (B) of the 4 ampicillin resistant transformants ligated with the mutant ΔC E-selectin sequence. Clones 1-3 have the insert in the reverse direction; clone 4 has the insert in the correct direction.

A

a– CAATCAGCCTGCTTCTCGC
b– CCACATAGCGTAAAAGGAGC
c– GTGCTCCTATTCCAGCCTG

B

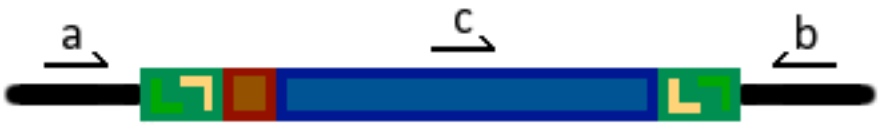

Figure 3.7: Sequence (A) and complimentary position and direction on the inserted E-selectin cDNA (B) of the three primers used for colony PCR of transformants.

3.3.2.2 Confirmation of cDNA insert by colony PCR

As the differences in size between the bands were small, and the DNA ladder became smeared in the agarose gel around the larger band sizes, making direct size determination difficult. A second method was used to confirm the presence and directionality of the E-selectin insert, by using colony PCR with different primers.

Three primers were designed and used in combination, the sequences of which are shown in Figure 3.7A. Firstly, primer pair a-b was used to determine the presence of the ES or ΔC insert in the transformed colonies in the same way as in Figure 3.6A. Vectors with an insert would have a large band around 2Kbp; those without the insert would have much smaller band only around 100-200bp.

Colonies that were positive for the insert then underwent two more rounds of colony PCR with the primer combinations a-c or c-b. If a band was seen with primer pair c-b then the insert was in the correct direction, as shown in the diagram in Figure 3.7B, if a band was seen with primer pair a-c then the insert had been ligated into the vector backwards, and the direction of the primer c was reversed from that in Figure 3.7B.

Figure 3.8A shows the colony PCR results using primer pair a-b of the 65 colonies grown on ampicillin after transformation with ES containing lentivector plasmid. 19 of the clones produced a band of DNA with the a-b primers, of which 6 had a heavy band of around 2Kbp, and the other 13 had smaller bands around 250bp. Colony PCR results for the ΔC clones are in Appendix A-2.

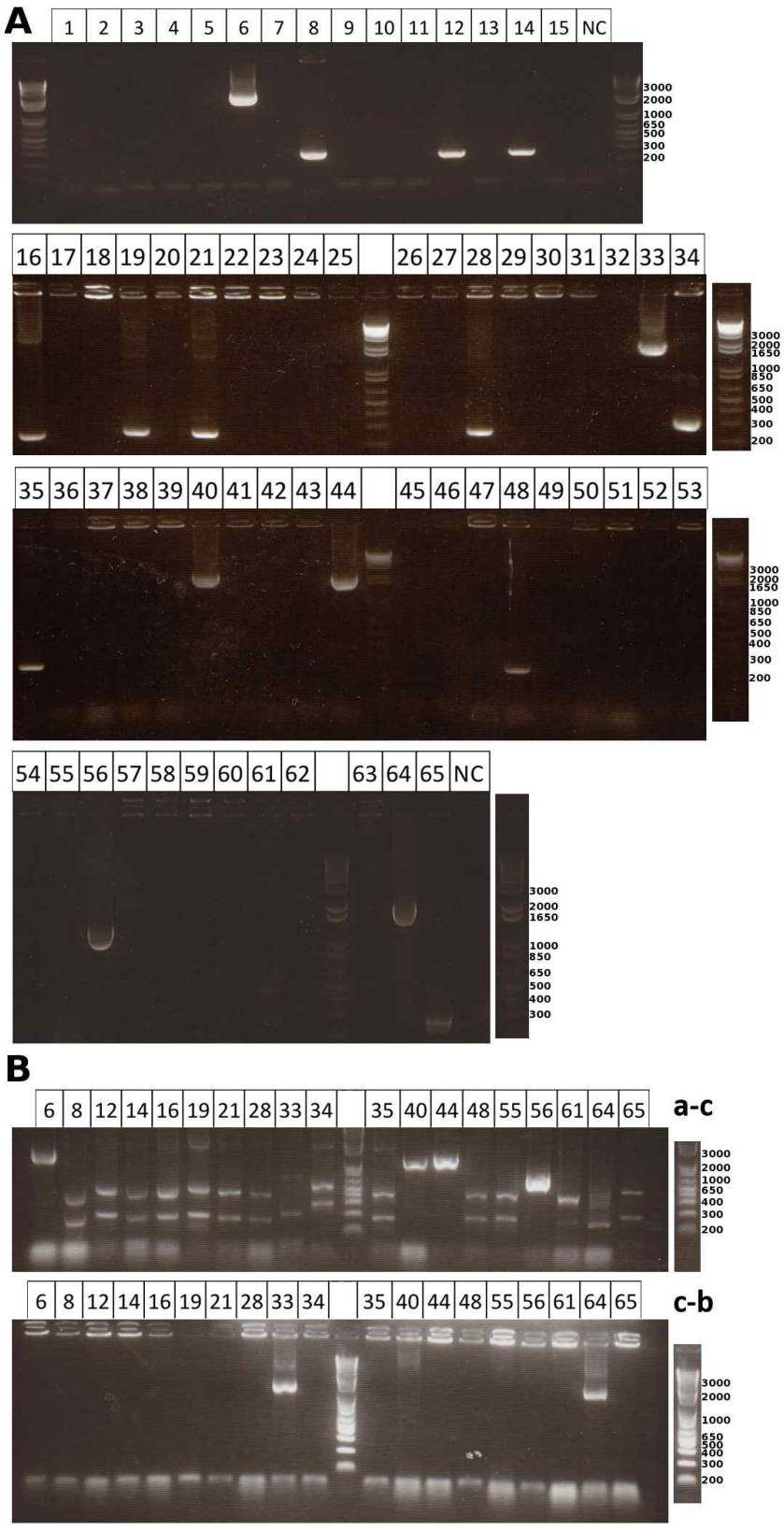

Figure 3.8: PCR of 65 E.coli colonies isolated after transformation with lentivirus vector plasmids containing the ES E-selectin cDNA sequence.

65 ES transformed colonies grew on an ampicillin plate, 19 of these clones produced colony PCR products when amplified using primer pair a-b (A). Six of these colonies also produced bands when amplified using primer pairs a-c and c-b to check for inserts in the correct direction (B), colonies 6, 40, 44 and 56 produced bands of the correct size with primer pair a-c, while colonies 33 and 64 produced bands with primer pair c-b.

The 19 colonies that produced DNA bands after PCR with primer pair a-b were then put through colony PCR again, this time with the primer pairs a-c or c-b. Figure 3.8B shows 4 colonies containing plasmids with inserts in the wrong direction (clones 6, 40, 44 and 56), as PCR formed large bands only with primer pair a-c; while two colonies (33 and 64) formed large bands only with primer pair c-b and so had the ES insert in the correct direction. The 13 colonies that formed light PCR fragments with primers a-b but nothing with a-c or b-c were probably transformed with an empty lentivector, although this does not explain why the other 46 colonies from the transformation were ampicillin resistant if they did not contain the lentiviral plasmid.

Although the reason for the large number of colonies that did not form PCR products was unexplained, the experiment produced two clones containing the ES cDNA insert in the correct direction, and the additional colonies were not investigated further.

3.3.2.3 Confirmation of cDNA inserts by DNA sequencing

In the experiments outlined above, three clones were identified containing the cDNA insert in the correct direction. Full-length E-selectin clones ES-33 and ES-64, and a single tail-less mutant clone ΔC-4.

To confirm the sequences of the inserted cDNA, the entire insert region in each plasmid was sequenced using the primers a-b. This would also confirm the directionality again in case there had been an error in the restriction digest and colony PCR experiments. Sequencing was carried out at the Wolfson Institute at UCL, and resultant sequences were aligned with the reference E-selectin sequence(Bevilacqua et al., 1989) using the Clustal W2 sequence alignment tool on the EMBL-EBI website(Goujon et al., 2010; Larkin et al., 2007).

Figure 3.9 shows the final 60 bases of the ES-64 and ΔC-4 sequences aligned with the reference sequence; the full sequence alignment of the ES-64 and ΔC-4 with the reference E-selectin sequence is in Appendix B-1. The sequence of ES-64 was identical to the published E-selectin sequence, whereas the ES-33 clone (not shown) was discovered to have a spontaneous STOP mutation at amino acid position 55, which would destroy the function of the 610 amino acid long protein. The ΔC-4 insert also contained two mutations; one at the expected mutation site 1738 (AAA>TAA), creating a stop codon and preventing the translation of the intracellular region, but also a second mutation at position 1833, that replaces the WT stop codon with a Tyrosine codon (TAA>TAT), both are highlighted in red in Figure 3.9. If this second mutation at site 1833 occurred in the WT sequence, then this would extend translation creating a longer protein with possibly abnormal function;

however as this mutation occurs in the ΔC mutant, translation has already been terminated by the first mutation at site 1738, so this second mutation should have no functional effect.

```
E-selectin      GCACCATTTCTCCTCTGGCTTCGGAAATGCTTACGGAAAGCAAAGAAATTTGTTCCTGCC 1773
ES-64           GCACCATTTCTCCTCTGGCTTCGGAAATGCTTACGGAAAGCAAAGAAATTTGTTCCTGCC 1773
AC-4            GCACCATTTCTCCTCTGGCTTCGGTAATGCTTACGGAAAGCAAAGAAATTTGTTCCTGCC 1773
                ********************** ***********************************

E-selectin      AGCAGCTGCCAAAGCCTTGAATCAGACGGAAGCTACCAAAAGCCTTCTTACATCCTTTAA 1833
ES-64           AGCAGCTGCCAAAGCCTTGAATCAGACGGAAGCTACCAAAAGCCTTCTTACATCCTTTAA 1833
AC-4            AGCAGCTGCCAAAGCCTTGAATCAGACGGAAGCTACCAAAAGCCTTCTTACATCCTTTAT 1833
                ************************************************************
```

Figure 3.9: Comparison of the last 120 bases of E-selectin (ELAM-1) cDNA (Bevilacqua et al., 1989), compared to the sequenced data of both the ES-64 and ΔC-4 inserts in the lentiviral constructs.

The ES sequence is identical to that of WT E-selectin, whereas the ΔC mutant has two mutations (highlighted in red): the 1738A>T nonsense mutation, which prevents translation of the cytoplasmic tail, and an additional 1833A>T mutation which removes the WT stop codon.

The suitable clones for each construct: ES-64 and ΔC-4, were transfected into the HEK 293T packaging cell line alongside two helper plasmids to create a stock of lentivirus particles, which were then stored at -80C until required.

3.4 Conclusions and Discussion

This chapter documented the design and creation of two lentiviral vectors, expressing either full length (ES) or tail-less mutant (ΔC) E-selectin. The cDNA coding sequences were extracted from adenoviral vectors using high fidelity PCR and inserted into lentiviral vectors. Correct insertion and directionality of the ES and ΔC cDNA was confirmed by restriction digestion, colony PCR and DNA sequencing; and after sequence confirmation, the lentivirus particles themselves were created by transfection into a packaging cell line.

The ES sequence proved to be more difficult than the ΔC sequence to clone successfully, for unknown reasons. The ES sequence required several rounds of cloning experiments, and was eventually isolated from a single colony out of 64 ampicillin resistant transformants, whereas the ΔC was cloned successfully on the first attempt. It was unclear whether this was due to random chance or due to another experimental reason; it may be that the mutation in the ΔC sequence renders it easier for it to be transformed into the bacteria, or more simply that the PCR amplification of the ES sequence was less efficient than for the ΔC sequence. The reasons behind this difference in cloning efficiency were not investigated further after successful lentiviral clones of both sequences were obtained.

4 Investigation of the transfection efficiency of E-selectin lentiviral construct in HUVEC and HMEC-1 cells

4.1 Introduction

Chapter 3 detailed the creation of lentivirus constructs containing both full length (ES) and tail-less mutant (ΔC) E-selectin. In order to use the virus to investigate the effects of full length ES and tail-less ΔC E-selectin expressed in transfected human cells, it was first necessary to evaluate their transfection efficiency in the cell types I would be using, and calculate an infectious titre for replicable transfection in future experiments.

The transfection efficiency of lentiviral vectors can vary between different cell types; previous publications suggest that HUVEC are compliant to lentiviral transfection, with transfection efficiencies up to 70% (Dishart et al., 2003; Totsugawa et al., 2002), however it was essential to determine the titre and efficiency of the specific lentiviruses created in Chapter 3.

Lentiviral transfection into human cells is known to cause much lower inflammatory stimulation compared to other transfection techniques. Adenovirus or other viral vectors such as Adeno-associated virus (AAV) have much higher immunogenicity than lentivirus, as determined by their ability to induce NFκB activation and cytokine production in endothelial cells (Blömer et al., 1997; Copreni et al., 2009; Nayak and Herzog, 2010).

Transfection of an adhesion molecule important in the inflammatory response such as E-selectin however, may have effects on the wider endothelial inflammatory response as well. Several other adhesion molecules, including ICAM-1 and VCAM-1, are expressed in response to the same inflammatory stimuli as E-selectin, and expression of all three adhesion molecules peaks around 4-6 hours after stimulation. E-selectin expression however, decreases to basal levels after 24 hours, whereas the expression of ICAM-1 and VCAM-1 plateau, and remain on the surface of cells for several days. It is important to elucidate the expression of these adhesion molecules at both the peak inflammatory expression period of 4-6 hours post-stimulation, as well as 72 hours later at the peak of transfected gene expression(Liu et al., 2006) in order to determine whether the inflammatory response to the lentivirus will interfere with future experiments.

4.1.1 Aims and Objectives

The two major aims of the experiments described in this chapter were to evaluate the titre and transfection efficiency of the lentiviral vectors described in Chapter 3, as well as to determine the level of endothelial E-selectin, ICAM-1 and VCAM-1 responses to the lentivirus construct. Titration of serial dilutions of ES and ΔC lentivirus constructs on both HMEC-1 cell line and primary HUVEC will be conducted, and the amount of stimulated expression of the adhesion molecules E-selectin, ICAM-1 and VCAM-1 after 4 hours and 72 hours post-transfection will be measured. This titration will be used to determine the optimal lentiviral dilution for sufficient transfection with minimum inflammatory activation. A lentivirus containing the GFP gene will be used as a control to measure any induction of endogenous E-selectin expression due to an inflammatory response to the lentivirus instead of expression of the transfected E-selectin gene.

4.2 Methods

4.2.1 Flow Cytometry

Cells were washed with 1ml PBS, and then removed from wells using 100µl accutase, incubated for 3-4 minutes at 37°C. 1ml of FACS buffer was added to each well to inactivate the accutase and wash the cells. Cells were removed from the wells using a Pasteur pipette to scrape the cells from the bottom of the well and deposit them into polystyrene NUNC tubes; tubes were then spun for 5 minutes at 900g and supernatant discarded.

The relevant antibodies was added to each tube at a suitable concentration, vortexed, and incubated in the dark at RT for 20 minutes. Cells were washed with 2ml FACS buffer and spun again. When staining using the unconjugated anti-E-selectin antibody, a secondary PE conjugated anti-mouse antibody was added, vortexed and incubated again for 20 minutes at RT in the dark. Cells were washed again in 2ml FACS buffer before being resuspended in 100µl Cellfix (BD), vortexed, and stored in the dark at 4°C. Flow cytometry analysis was carried out within 1-3 days on a BD FACScalibur machine, and data was analysed using FlowJo cytometric analysis software.

Unless otherwise indicated, E-selectin was stained using a primary mouse anti-human CD62E antibody (AbD Serotec), followed by a secondary RPE conjugated anti-mouse IgG (Dako). FITC-conjugated mouse anti-VCAM-1 and PE-Cy5 conjugated mouse anti-ICAM-1 antibodies (BD) were used to stain VCAM-1 and ICAM-1 respectively.

4.3 Results

4.3.1 72 hours transfection with ES and ΔC lentiviral constructs produced high levels of E-selectin expression on both HMEC-1 and HUVEC

Following the construction of the lentivirus vector and particles in the previous chapter, the first objective was to measure the infectious titre of each construct by transfecting serial dilutions of the virus onto endothelial cells. 10-fold serial dilutions of virus, ranging from 10μl-0.01μl stock solution in 500μl media (dilution factors of $2x10^{-2}$-$2x10^{-5}$), were transfected into primary HUVEC and HMEC-1, incubated for 3 days, and E- selectin expression measured by flow cytometry.

Although a lentiviral vector was available which contained a GFP expression sequence alongside the inserted E-selectin gene, which allowed for simple identification and counting of expression rates, the lentivector chosen to make the ES and ΔC constructs did not contain the GFP marker. The non-GFP containing vector was chosen as it allowed for greater flexibility to use multiple fluorophores for immunofluorescence microscopy and flow cytometry. This meant that staining of the cells using anti-E-selectin antibodies was required to determine whether they were transfected successfully or not.

Figure 4.1A shows a representative histogram of E-selectin expression on HMEC-1 72 hours post-infection with ES lentivirus construct. There was very low expression of E-selectin when high dilutions of virus ($2x10^{-4}$ and $2x10^{-5}$) were used, a clear population shift creating a positive peak at the $2x10^{-3}$ dilution, and at dilution of $2x10^{-2}$ almost all the HMEC-1 cells had shifted to the positive peak.

Figure 4.1B shows a representative histogram of E-selectin expression on HUVEC 72 hours post infection with ES lentivirus construct. Similar to HMEC-1, there was very low E-selectin expression at dilutions of $2x10^{-4}$ and $2x10^{-5}$, and a clear shift in E-selectin positive cells when transfected with dilutions of $2x10^{-2}$ and $2x10^{-3}$; however there was still a small negative population, even after transfection with the highest concentration of virus. This was not observed in transfected HMEC-1.

TNFα stimulation for 72 hours resulted in a very small increase in E-selectin expression on HUVEC (Figure 4.1B), but no increase over unstimulated cells in HMEC-1 (Figure 4.1A). The histograms showing E-selectin expression after transfection with ΔC lentivirus were very similar in shape to the representative ES lentivirus histograms in Figure 4.1 (data not shown).

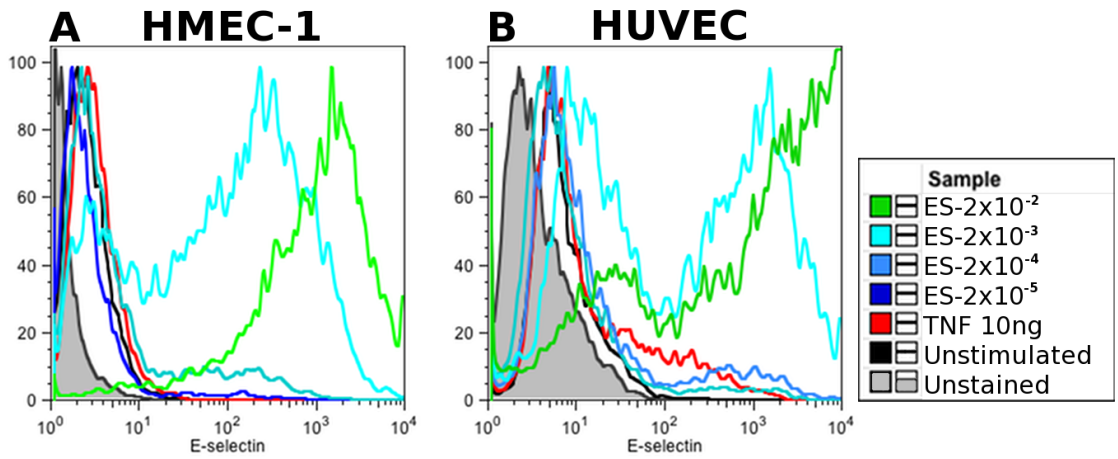

Figure 4.1: Representative histograms of E-selectin expression on HMEC-1 (A) and HUVEC (B), 72 hours after transfection with 10-fold serial dilutions of ES lentiviral constructs, or stimulation with 10ng/ml TNFα.

The proportion of transfected cells expressing E-selectin and their staining fluorescence intensity were measured, and the results shown in Figure 4.2.

HMEC-1 cells had very high transfection efficiency at the higher viral concentrations, with over 90% of cells expressing ES or ΔC at viral dilutions of $2x10^{-2}$ and $2x10^{-3}$. HMEC-1 cells do not normally express E-selectin upon inflammatory stimulation; therefore the low levels of E-selectin expression after 72 hours TNFα stimulation were expected (Figure 4.2A).

Over 70% of HUVEC were transfected with the ES and ΔC constructs at dilutions between $2x10^{-2}$ and $2x10^{-3}$(Figure 4.2B), which was significantly greater than the 22% of cells expressing E-selectin after 72 hours of stimulation with TNFα (ES: P=0.0048, ΔC: P=0.006, Student's t-test). Low E-selectin expression after 72 hours TNFα stimulation was expected, as E-selectin expression normally peaks after 4-6 hours post-inflammatory stimulation on HUVEC, and degrades back to basal levels by 24-48 hours.

E-selectin expression as measured by MFI (Median Fluorescence Intensity) showed that the total E-selectin expression of the HMEC-1 and HUVEC cells also increased at a similar rate to the % of transfected cells, although while the proportion of transfected cells appeared to level be similar at dilutions between $2x10^{-2}$ and $2x10^{-3}$, the total amount of expressed E-selectin increased.

There was a noticeable trend that at the highest concentrations, cells transfected with ΔC appeared to express more E-selectin compared to those transfected with ES, as seen in the difference in MFI (ΔC-1900 compared to ES-1500 in HMEC-1 (Figure 4.2C), and ΔC-650 compared to ES-450 in HUVEC (Figure 4.2D)). Although these differences in E-selectin

expression were not significant, they indicated a possible trend of the ΔC construct producing higher levels of E-selectin expression than ES on both HMEC-1 and HUVEC.

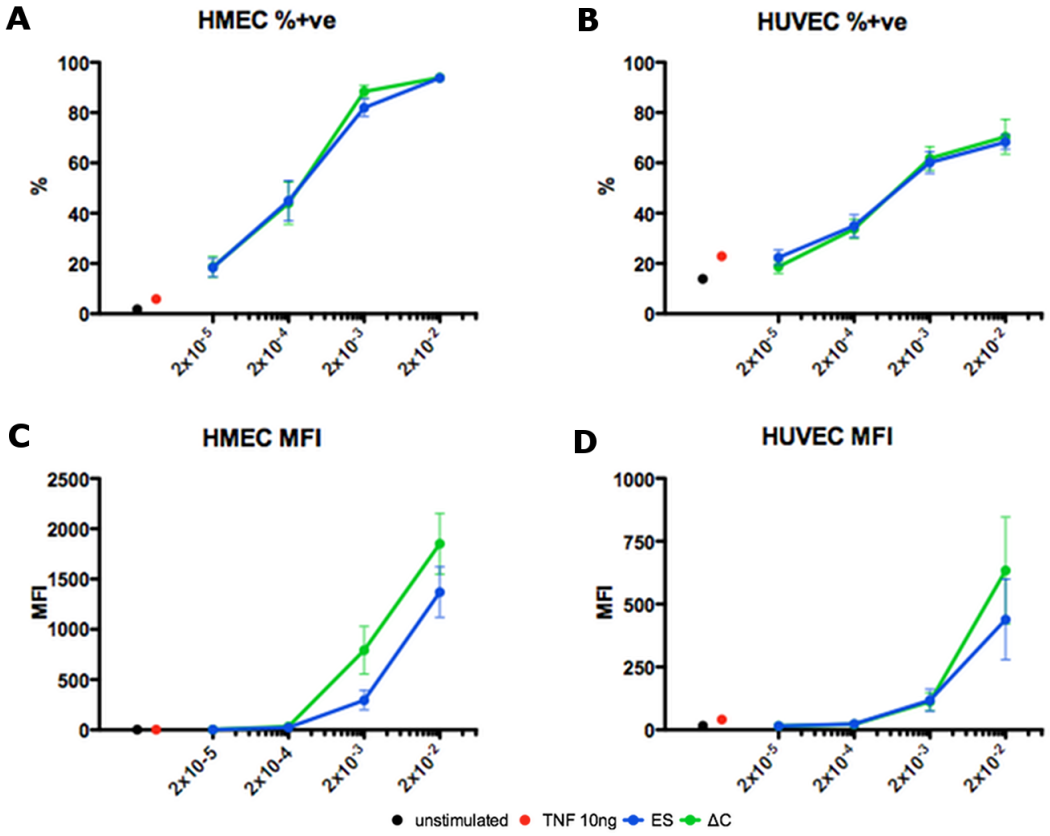

Figure 4.2: Graphs showing E-selectin expression on both HMEC-1 (A+C) and HUVEC (B+D) cells, 72 hours after transfection with 10-fold serial dilutions of ES or ΔC lentiviral constructs, or stimulation with 10ng/ml TNFα. (HMEC-1: n=8, HUVEC: n=11)

Expression of E-selectin was measured as percentage of cells expressing E-selectin (A+B) and the Median Fluorescence Intensity (MFI) of all the cells (C+D).

Next, we confirmed the presence of E-selectin on the cell surface of transfected HMEC-1 and HUVEC by immunofluorescence microscopy. Confocal microscopy images of HMEC-1 infected with ES (Figure 4.3A) and ΔC (Figure 4.3B) lentiviral constructs show E-selectin expression on the cell surface. The E-selectin staining on the cells infected with the ΔC construct appeared to be brighter compared to those infected with the ES construct, backing up Flow Cytometry data in Figure 4.2C.

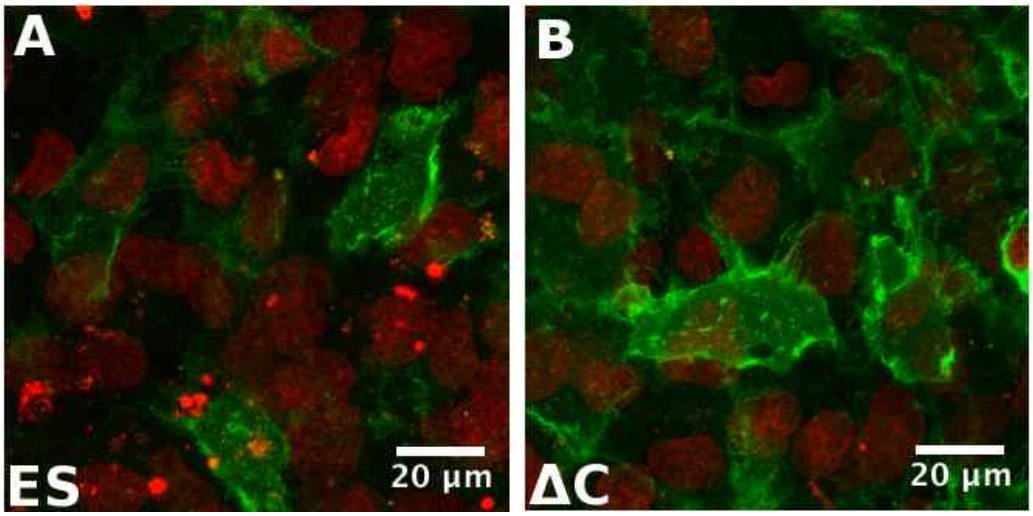

Figure 4.3: Confocal microscopy images of HMEC-1 cells 72 hours post-infection with either ES (A) or ΔC (B) lentiviral constructs. Nuclei stained with DAPI (Red) and E-selectin with FITC (green).

The titration graphs appear to show the number of HUVEC expressing E-selectin after transfection reaching a plateau at around 70%, with a viral dilution factor of $2x10^{-3}$(1µl virus in 0.5ml media). Assuming the initial number of seeded cells doubled from the time they were seeded to the time they were infected with the lentivirus ($5x10^4$ cells to $1x10^5$ cells), 70% of the 10^5 cells were transfected at this dilution, using 1µl of the virus, corresponding to a stock viral titre of $7x10^7$/ml.

In conclusion, lentiviral transfection increased E-selectin expression as detected by percentage expression and MFI on HMEC-1 at all viral concentrations, and on HUVEC at concentrations between $2x10^{-2}$ and $2x10^{-3}$. TNFα stimulation only slightly increased E-selectin expression after 72 hours, and E-selectin expression on cells transfected with lentivirus concentrations greater than $2x10^{-4}$ was greater than on cells stimulated for 72 hours with TNFα.

4.3.2 72 hours transfection with ES and ΔC lentiviral constructs increased ICAM-1 expression on HUVEC, but not HMEC-1

As the lentivirus can potentially cause inflammatory stimulation, endothelial inflammatory markers were measured to investigate whether the lentivirus constructs were inducing an inflammatory response or not. Although E-selectin expression usually peaks around 4-6 hours post-stimulation then declines back towards baseline levels(Bevilacqua et al., 1989), other adhesion molecules expressed on the endothelium, such as VCAM-1 and ICAM-1, can stay activated for over 72 hours after inflammatory stimulation(Bevilacqua, 1993). As the transfected lentiviral constructs take 72 hours to achieve maximal expression of the inserted

genes(Liu et al., 2006), it was important to see if transfection affected the expression of inflammation-associated adhesion molecules at this time point.

ICAM-1 is an adhesion molecule that is constitutively expressed on endothelial cells; expression levels increase after inflammatory stimulation and can remain elevated for several days.

Figure 4.4A shows a representative histogram of ICAM-1 expression on HMEC-1 cells 72 hours after infection with 10-fold dilutions of ES lentivirus constructs and stimulation with TNFα. There was constitutive low level ICAM-1 expression in unstimulated cells, and only the highest concentration of lentivirus used in the titration (dilution factor $2x10^{-2}$) appeared to increase ICAM-1 expression. However, the ICAM-1 expression induced by 72 hours exposure to TNFα was much greater than that induced by any concentration of virus.

Figure 4.4B shows ICAM-1 expression on HUVEC 72 hours after transfection with ES lentivirus. In contrast with the transfected HMEC-1 cells, transfection with all concentrations of virus increased ICAM-1 expression above resting levels, with the highest lentiviral concentration appearing to increase expression to a higher level than that induced by 72 hours exposure to TNFα. The histograms showing ICAM-1 expression on cells transfected with ΔC lentivirus were similar to the representative ES lentivirus histograms in Figure 4.4 (data not shown).

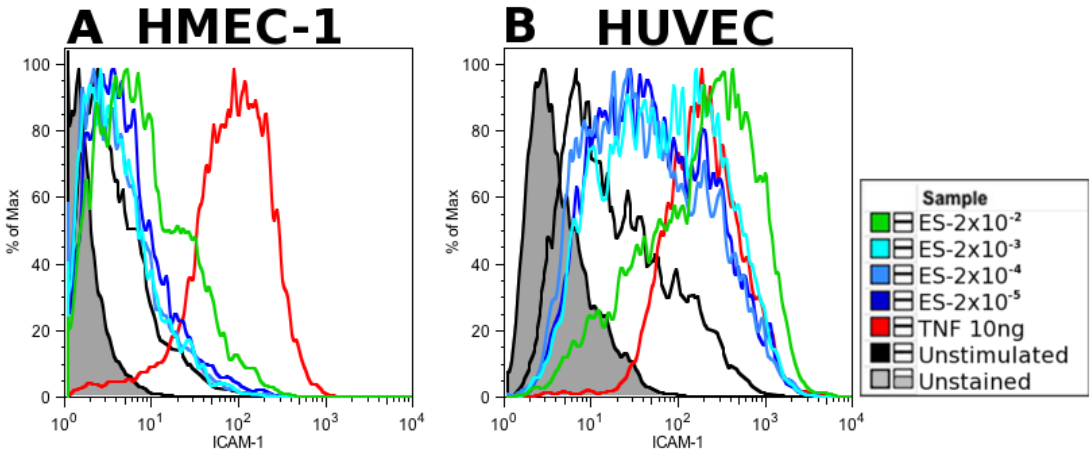

Figure 4.4: Representative histograms of ICAM-1 expression on HMEC-1 (A) and HUVEC (B) 72 hours after transfection with 10-fold serial dilutions of ES lentiviral constructs, or stimulation with 10ng/ml TNFα.

The proportion of transfected cells expressing ICAM-1 and their staining fluorescence intensity were measured, and the results shown in Figure 4.5.

Constitutive ICAM-1 expression was seen in around 30% of unstimulated HMEC-1, which increased to almost 100% expression after 72 hours of TNFα stimulation (Figure 4.5A). There

was a 10% increase in ICAM-1 expression over untransfected cells after 72 hours infection with the highest concentration of the lentiviral constructs ($2x10^{-2}$ dilution), while lower concentrations of the lentivirus raised ICAM-1 expression by only 5% above unstimulated levels. The MFI of ICAM-1 expression on untransfected HMEC-1 was 11.4, and upon TNFα stimulation, ICAM-1 MFI levels increased to 90.6. In response to viral transfection however, ICAM-1 MFI levels remained almost unchanged at an MFI between 7-16, even at high viral transfection concentrations (Figure 2.5C).

In HUVEC, 50% of untransfected cells expressed ICAM-1, which increased to almost 100% of cells in response to 72 hours TNFα. When exposed to the virus construct, over 60% of cells expressed ICAM-1 on the cell surface, which was increased to 70% in the highest concentration of virus (Figure 4.5B).

Figure 4.5D shows the MFI of ICAM-1 expression in unstimulated HUVEC is 41.4, compared to 188.0 in response to 10ng/ml TNFα. As can be seen, the same pattern of ICAM-1 expression on HUVEC was observed as with the percentage data, with all concentrations of virus causing increased MFI of ICAM-1 expression. The highest MFI levels (114.8) were detected in response to the highest concentration ($2x10^{-2}$) of lentiviral construct, however the MFI in response to other viral concentrations was only around 54-60. MFI levels of ICAM-1 expression were lower in response to all concentrations of lentivirus in response to TNFα.

In conclusion, ICAM-1 expression, as detected by both percentage expression and MFI, was increased by lentiviral transfection only at the highest concentration of virus in HMEC-1; however, all concentrations of virus construct induced ICAM-1 expression on HUVEC. Expression levels were lower at all virus concentrations however than in response to TNF-alpha.

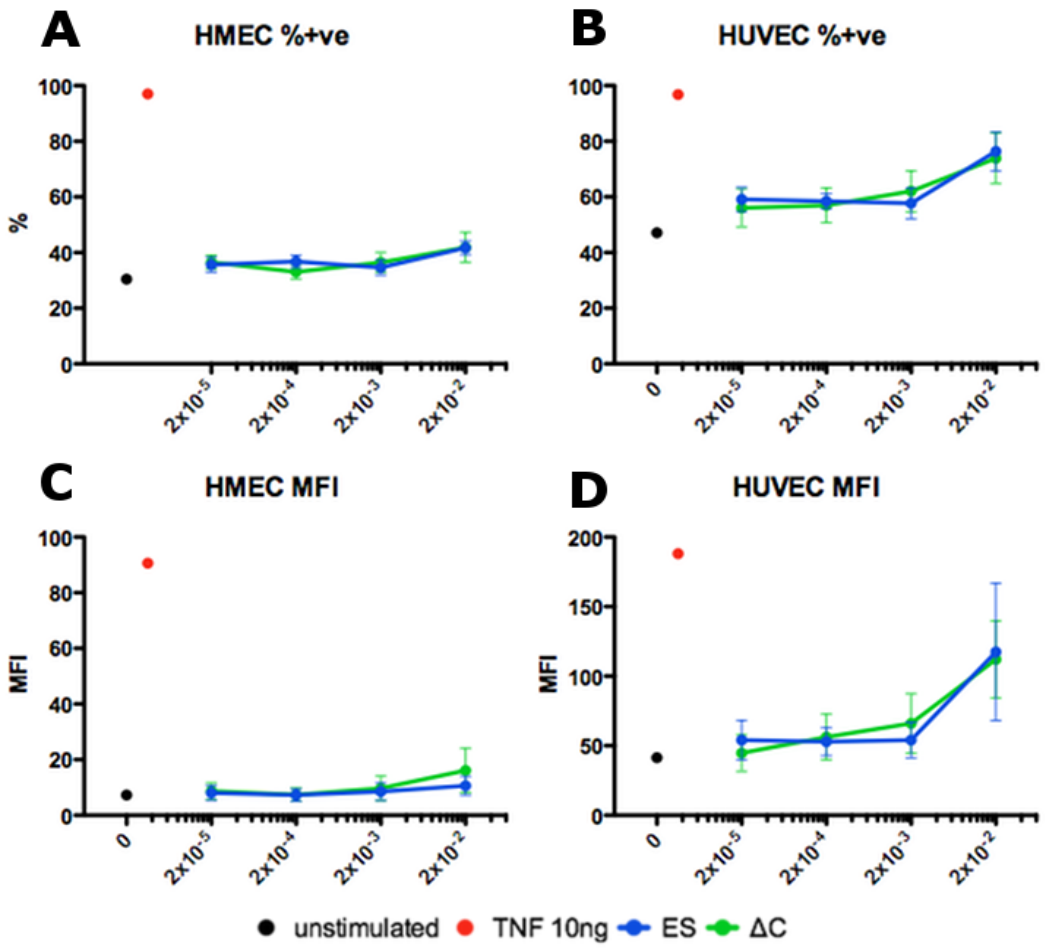

Figure 4.5: Graphs showing ICAM-1 expression on HMEC-1 (A+C) and HUVEC (B+D) 72 hours after transfection with 10-fold serial dilutions of ES lentiviral constructs, or stimulation with 10ng/ml TNFα. (HMEC-1: n=6, HUVEC: n=3)

Expression of ICAM-1 was measured as percentage of cells expressing ICAM-1 (A+B) and the Median Fluorescence Intensity (MFI) of the stained cells (C+D).

4.3.3 72 hours transfection with ES and ΔC lentiviral constructs did not increase VCAM-1 expression on either HMEC-1 or HUVEC

While ICAM-1 is constitutively expressed on both HMEC-1 and HUVEC, VCAM-1 is only expressed after inflammatory stimulation but then remains elevated for up to 72 hours (Bevilacqua, 1993).

Figure 4.6A shows a representative histogram of VCAM-1 expression on HMEC-1 72 hours post-infection with 10-fold dilutions of ES lentivirus constructs. There was a small increase in VCAM-1 expression after 72 hours of TNFα stimulation. At low lentiviral concentrations there was no detectable VCAM-1 expression on HMEC-1 cells, however levels of VCAM-1 expression increased in response to the highest lentiviral concentration ($2x10^{-2}$).

Figure 4.6B shows a representative histogram of VCAM-1 expression on HUVEC. There was a large shift in VCAM-1 expression after 72 hours of 10ng/ml TNFα stimulation. There was no

obvious population shift in VCAM-1 expression above that in unstimulated cells 72 hours after transfection with ES lentivirus at dilutions of $2x10^{-5}$ – $2x10^{-3}$, however VCAM-1 expression was detected on HUVEC in response to the highest $2x10^{-2}$ lentiviral concentration.

The histograms showing VCAM-1 expression on cells transfected with ΔC lentivirus were similar in shape to the representative ES lentivirus histograms in Figure 4.6 (data not shown).

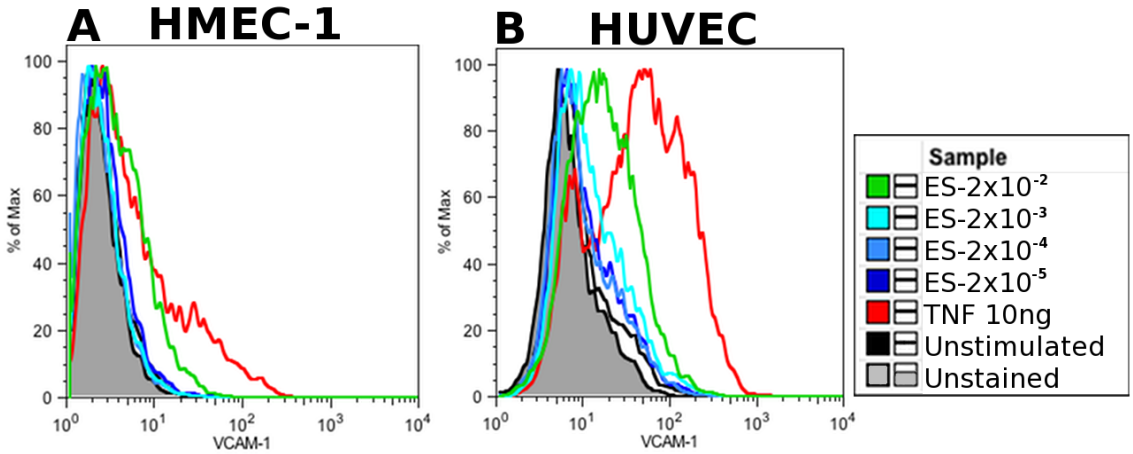

Figure 4.6: Representative histograms of VCAM-1 expression on HMEC-1 (A) and HUVEC (B) 72 hours after transfection with 10-fold serial dilutions of ES lentiviral constructs, or stimulation with 10ng/ml TNFα.

The proportion of transfected cells expressing ICAM-1 and their staining fluorescence intensity were measured, and the results shown in Figure 4.7.

The proportion of unstimulated HMEC-1 expressing VCAM-1 was only 6%, which increased to 30% after 72 hours TNFα stimulation. Lower concentrations of lentivirus construct did not increase the amount of VCAM-1 expression, however VCAM-1 did increase slightly to 8% after transfection with $2x10^{-2}$ dilution of ES or ΔC virus (Figure 4.7A). In Figure 4.7C, The MFI of VCAM-1 expression in unstimulated HMEC-1 was 2.3, and was only increased to 4.2 in TNFα stimulated cells. The MFI of VCAM expression did not increase upon lentivirus transfection, and remained at around 2.3-2.5 at all concentrations of virus.

Figure 4.7B shows 6% of unstimulated HUVEC expressing VCAM-1, which increases to 52% upon 72 hours TNFα stimulation. At lower concentrations of lentivirus transfection, VCAM-1 expression was the same as in untransfected cells, however VCAM-1 expression rose slightly to 11% in HUVEC transfected with viral concentration of $2x10^{-2}$. VCAM-1 expression as measured by MFI was similar in Figure 4.7D; the VCAM-1 MFI in untransfected cells was 6.4, and rose to 44.5 in HUVEC stimulated with TNFα. Upon transfection with the lentivirus

construct MFI remained at between 6-8 for the lower virus concentrations, before rising to 10.9 at the highest $2x10^{-2}$ concentration.

VCAM-1 expression did not appear to be significantly affected by infection with either of the lentiviral constructs at viral concentrations lower than $2x10^{-2}$. Even when exposed to the highest concentrations of virus used, VCAM-1 expression was much less than the levels seen upon endothelial stimulation with the inflammatory cytokine TNFα.

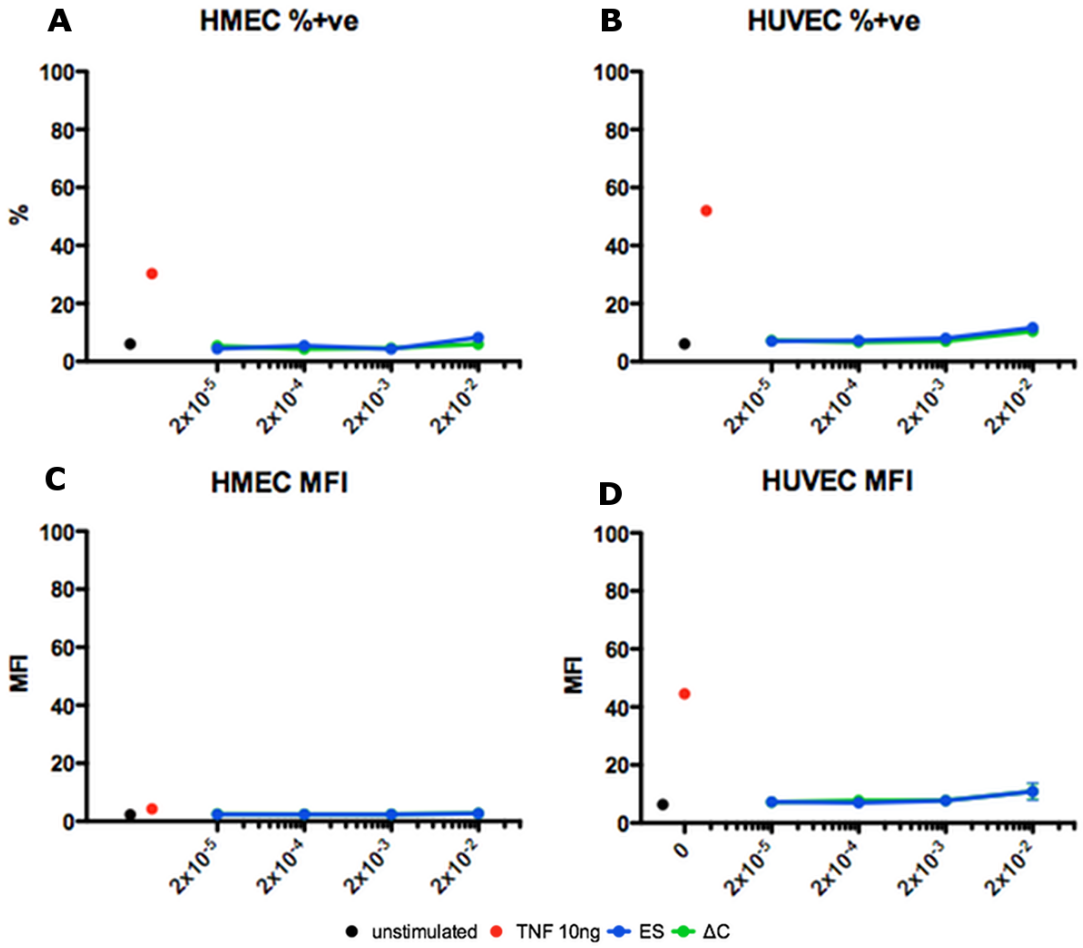

Figure 4.7: Graphs showing VCAM-1 expression on HMEC-1 (A+C) and HUVEC (B+D) 72 hours after transfection with 10-fold serial dilutions of ES lentiviral constructs, or stimulation with 10ng/ml TNFα. (HMEC-1: n=4, HUVEC: n=3)

Expression of VCAM-1 was measured as percentage of cells expressing VCAM-1 (A+B) and the Median Fluorescence Intensity (MFI) of the stained cells (C+D).

4.3.4 Determination of optimal lentiviral construct concentration

The highest concentration of lentivirus used to transfect HUVEC and HMEC-1 cells was at a dilution of $2x10^{-2}$. This produced E-selectin expression rates of over 90% in HMEC-1 cells and 70% in HUVEC (Figure 4.2A and B). However this concentration also appeared to stimulate increased expression of the inflammatory markers ICAM-1 and VCAM-1 (Figure 4.5 and Figure 4.7).

A 10-fold dilution of the virus ($2x10^{-3}$) appeared to transfect only a slightly lower proportion of cells, and still had high levels of transfected E-selectin expression; while stimulating no observable increase in VCAM-1 expression, and only a slight increase in ICAM-1 expression above unstimulated cells. Dilutions higher than this had decreased E-selectin expression, with equal levels of ICAM-1 expression. Therefore the viral dilution of $2x10^{-3}$ was chosen as the lentiviral dilution used in future transfection experiments. Despite the potential data showing increased ΔC expression over ES at the same infection concentration in Figure 4.2, the differences were not significant, and both viruses were used at the same concentration.

4.3.5 72 hours transfection with GFP lentiviral construct did not increase E-selectin expression on HUVEC

Although lentiviral induced VCAM-1 and ICAM-1 expression could be investigated by looking at HUVEC and HMEC-1 responses to transfection by ES or ΔC constructs, this was not possible for investigating whether E-selectin itself was upregulated by the infection protocol, as the anti-E-selectin antibodies would stain both endogenous and transfected E-selectin. Instead, a control lentivirus that contained a GFP (Green Fluorescent Protein) coding insert was used, this made the infected cells easy to count via flow cytometry, and allowed investigation of E-selectin expression without staining the transfected ES or ΔC as well.

HUVEC were transfected with a $2x10^{-3}$ dilution of the GFP lentiviral construct, as well as the constructs containing the ES and ΔC genes at the same concentration. After 72 hours incubation with the viral constructs, the cells were stained for analysis of E-selectin expression via flow cytometry.

Figure 4.8A shows a histogram of E-selectin expression on HUVEC 72 hours after infection with ES, ΔC and GFP lentiviral constructs. The level of E-selectin expression upon infection with GFP construct was similar to its expression on unstimulated cells, whereas infection by ES or ΔC constructs resulted in an increase in E-selectin expression, as expected.

Analysis of the proportion of transfected cells expressing E-selectin and their staining fluorescence intensity are shown in Figure 4.8B. E-selectin expression in cells infected with GFP construct was the same as in unstimulated cells, at around 15-20%, whereas between 40-45% of ES and ΔC transfected cells expressed E-selectin, approximately double the amount than unstimulated cells. E-selectin expression as measured by MFI is shown in Figure 4.8C, and shows a similar pattern. Unstimulated and GFP transfected cells had a similar MFI of around 5-6, whereas ES and ΔC transfected HUVEC had MFI of between 15-25.

The reason for the apparent reduced amount of E-selectin expression in response to lentiviral transfection in Figure 4.8 compared to Figure 4.1 and Figure 4.2 is due to the fact that a different antibody was used (PE conjugated mouse anti-CD62E (BD)). The differences in expression between transfected and untransfected cells were still clear, however the intensity of staining was reduced, meaning that the MFI of ES and ΔC was reduced from over 500 in Figure 4.2D to only 25 in Figure 4.8C.

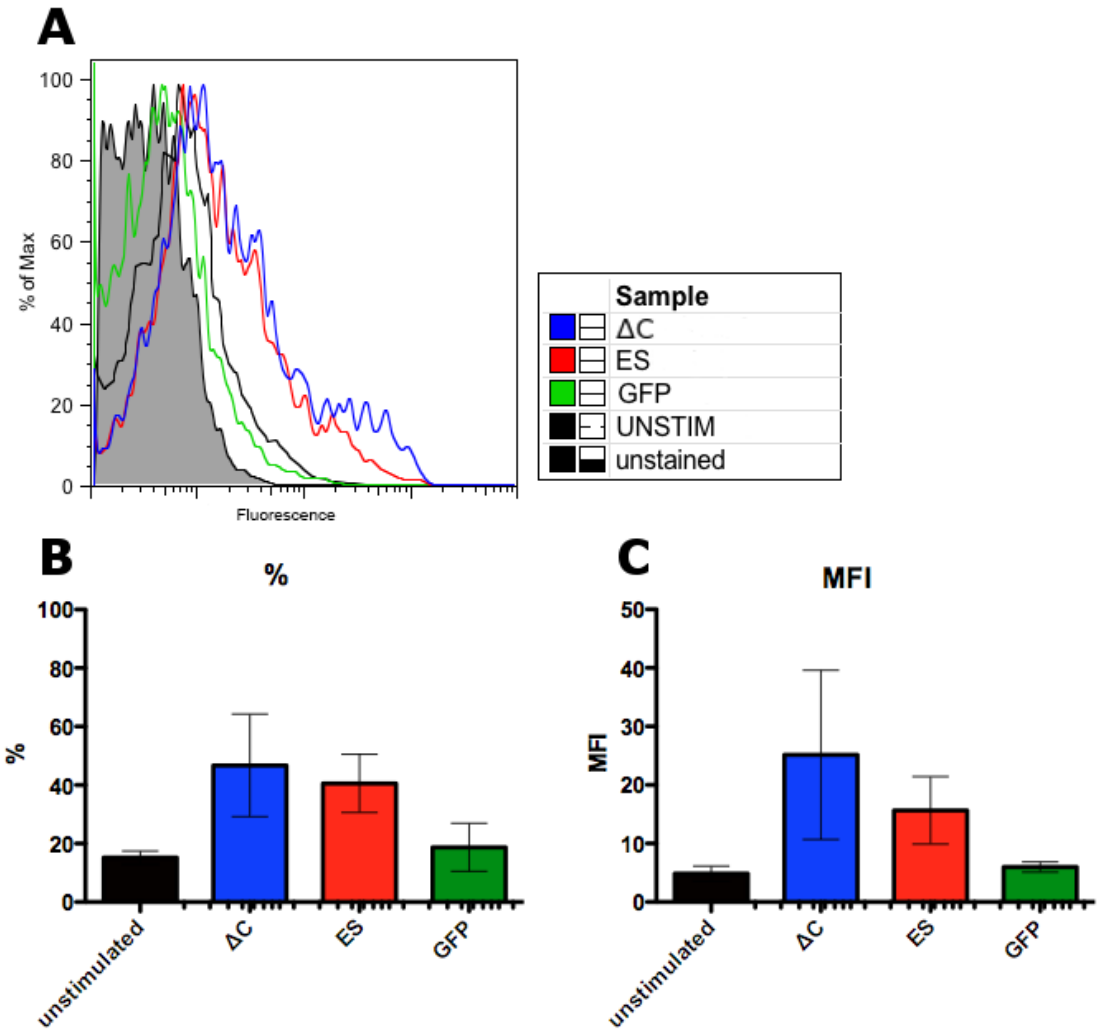

Figure 4.8: Histogram and graphs showing E-selectin expression on HUVEC 72 hours after transfection with either ES, ΔC or GFP lentiviral constructs. (n=2)

(A) Representative histogram of E-selectin expression on HUVEC 72 hours after infection with ES, ΔC or GFP lentiviral constructs. E-selectin expression was measured by the percentage of cells expressing E-selectin (B) and Median Fluorescence Intensity of the stained cells (C).

4.3.6 Low concentrations of E-selectin are expressed on HUVEC 4 hours after transfection with the lentiviral constructs

While previous experiments showed that inflammatory markers are not significantly upregulated 72 hours after transfection with lentivirus, the peak expression of many

inflammatory markers such as E-selectin is between 4-6 hours after inflammatory stimulation. Although future experiments would be carried out at 72 hours after lentiviral transfection, when the transfected ES and ΔC genes are maximally expressed, it was important to ensure that there was as little inflammatory stimulation of the HUVEC as possible. Therefore, the expression of endothelial inflammatory markers 4 hours post-transfection was investigated. HUVEC cells were infected with ES and ΔC lentivirus, alongside a positive TNFα control, and expression of E-selectin, VCAM-1 and ICAM-1 were measured after 4 hours.

Figure 4.11A shows a histogram of E-selectin expression on HUVEC 4 hours after infection with ES and ΔC lentivirus or stimulation with 10ng TNFα. E-selectin expression was greatly increased on 90% of cells after TNFα stimulation (Figure 4.11B), however expression was also slightly increased 4 hours after exposure to ES or ΔC lentivirus, from 10% to 30-40% expression. TNFα also increased E-selectin expression as measured by MFI, from 6.4 in unstimulated HUVEC to 436 in TNFα stimulated cells (Figure 4.9C). The MFI increase due to lentivirus transfection was only 12.9.

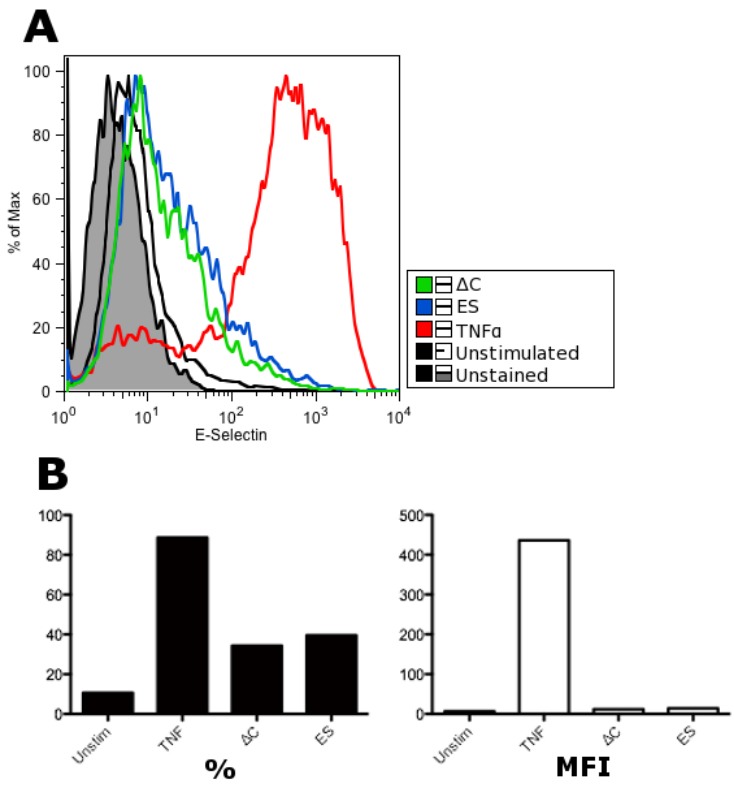

Figure 4.9: Histogram and graphs showing E-selectin expression 4 hours after either stimulation with 10ng/ml TNFα, or transfection with ES or ΔC lentivirus. (n=1)

(A) Histogram of HUVEC stained for E-selectin 4 hours after stimulation with 10ng TNFα or infection with lentivirus containing ES or ΔC cDNA. (B) E-selectin expression was measured by percentage of cells expressing the molecule and the MFI of all the cells stained.

Figure 4.10A shows a histogram of ICAM-1 expression on HUVEC 4 hours after infection with ES and ΔC lentivirus or stimulation with 10ng TNFα. ICAM-1 expression is almost 100% in all conditions (Figure 4.10B), although TNFα stimulation does shift the histogram upwards, increasing the MFI value from around 180 to 790, which is not seen with lentiviral transfection (Figure 4.10C).

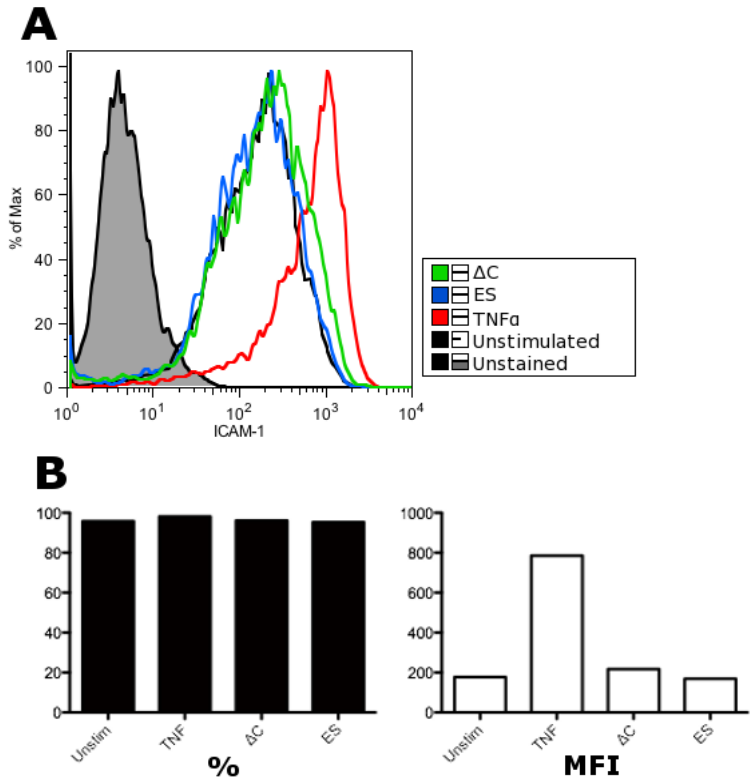

Figure 4.10: Histogram and graphs showing ICAM-1 expression 4 hours after either stimulation with 10ng/ml TNFα, or transfection with ES or ΔC lentivirus. (n=1)

(A) Histogram of HUVEC stained for ICAM-1 4 hours after stimulation with 10ng TNFα or infection with lentivirus containing ES or ΔC cDNA. (B) ICAM-1 expression was measured by percentage of cells expressing the molecule and the MFI of all the cells stained.

Figure 4.11A shows a histogram of VCAM-1 expression on HUVEC 4 hours after infection with ES and ΔC lentivirus, or stimulation with 10ng TNFα. TNFα stimulation causes a significant shift in the proportion of VCAM-1 expressing HUVEC, from 8% to 60% of cells, and an increase from 3.9 to 64.4 as measured by MFI. Infection by ES or ΔC constructs however did not produce any increase in VCAM-1 expression after 4 hours.

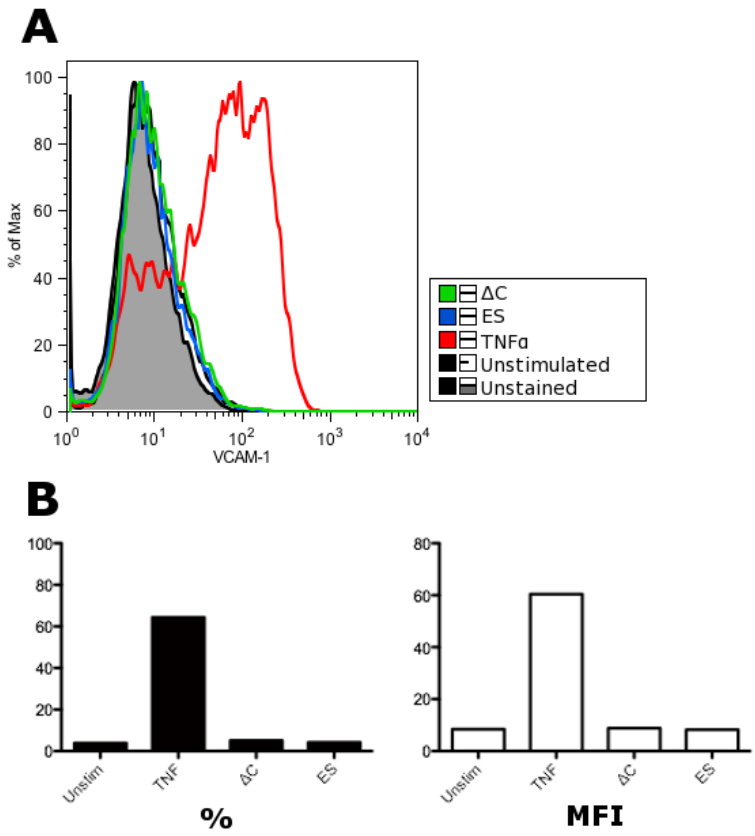

Figure 4.11: Histogram and graphs showing VCAM-1 expression 4 hours after either stimulation with 10ng/ml TNFα, or transfection with ES or ΔC lentivirus. (n=1)

(A) Histogram of HUVEC stained for VCAM-1 4 hours after stimulation with 10ng TNFα or infection with lentivirus containing ES or ΔC cDNA. (B) VCAM-1 expression was measured by percentage of cells expressing the molecule and the MFI of all the cells stained.

These figures show low level expression of E-selectin in HUVEC 4 hours after transfection with lentivirus. It is, however, unclear whether this was due to an endogenous response to the lentiviral vector, or whether it was early expression of the lentivirus itself. The lack of ICAM-1 and VCAM-1 expression after 4 hours of lentiviral transfection indicates that there was little to no inflammatory response to the transfection, especially compared to the very high inflammatory response seen to TNFα. It can be concluded that the lentiviral transfection induces a minimal inflammatory response on HUVEC, and it was deemed that this system was acceptable to use for further studies.

4.4 Conclusions and discussion

Both the cell line HMEC-1 and primary HUVEC were transfected successfully by both ES and ΔC lentiviral vectors, and resulted in significant expression of the gene constructs after 72 hours (Figure 4.2). The expression rate of 70% at the viral dilution of $2x10^{-3}$ for both the ES and ΔC constructs in HUVEC was particularly impressive as primary cells such as HUVEC have

been shown to be difficult to transfect by non-viral means(Gerszten et al., 1996; Sipehia and Martucci, 1995; Uchida et al., 2002; Writer et al., 2004).

There were some differences in the relative expression of ES and ΔC E-selectin after lentiviral transfection. The proportion of HMEC-1 or HUVEC cells expressing E-selectin is the same whether transfected with ES or ΔC virus (Figure 4.2A+B), but different when measured using MFI (Figure 4.2C+D), implying that the same proportion of cells are transfected by both viruses, but more ΔC E-selectin is expressed per cell than ES. It has been shown that the cytoplasmic domain is important in the endocytosis and recycling of endogenous E-selectin in endothelial cells, especially via clathrin-coated pits (Von Asmuth et al., 1992; Chuang et al., 1997; Kluger et al., 2002; Setiadi and McEver, 2008). This raises the possibility that the ES E-selectin may be being internalised and degraded at a faster rate than the ΔC E-selectin, leading to apparent decreased levels on the cell surface despite the same proportion of cells being transfected.

To investigate this further, real-time quantitative PCR (qPCR) could be used to measure the relative concentrations of E-selectin mRNA transcripts in ES and ΔC transfected cells, and compare whether this more precise measurement of E-selectin transcription and translation rates correlates with the surface expression. In the context of this thesis however, the differences were judged to be non-significant and were ignored during the experiments carried out later in the project.

At concentrations of virus below $2x10^{-2}$ there is no observed induction of VCAM-1 on HMEC-1 or HUVEC (Figure 4.7) or ICAM-1 on HMEC-1 cells (Figure 4.5A+C), although some ICAM-1 expression in transfected HUVEC after 72 hours infection was observed (Figure 4.5B+D). Increased ICAM-1 expression upon viral infection has previously been observed in HUVEC transfected using adenovirus (Gerszten et al., 1996; Rafii et al., 2001).

No E-selectin expression was seen on HUVEC 72 hours after transfection with lentiviral constructs expressing the gene coding for GFP (Figure 4.8), which indicates that all of the E-selectin expression seen on HUVEC infected with the ES or ΔC lentivirus at the $2x10^{-3}$ dilution used was due to the construct and not activation of endogenous E-selectin pathways. E-selectin expression was only very slightly raised after 4 hours exposure to the lentivirus constructs (Figure 4.9), and other adhesion molecules were not increased at all.

Taken together, these results show that lentiviral transfection does not have significant inflammatory effects on the endothelium, either after 4 hours, when inflammatory stimulation is detected, or at 72 hours, when the ES and ΔC transfected cells are used.

Although some ICAM-1 upregulation is seen after 72 hours, in general the inflammatory effects of lentiviral transfection observed were much lower than the equivalent response to adenovirus vectors(Copreni et al., 2009; Gerszten et al., 1996; Nayak and Herzog, 2010).

These results were encouraging for the use of HMEC-1 and HUVEC transfected with ES and ΔC lentivirus as a model for E-selectin expression in otherwise resting cells. Despite some activation of ICAM-1 in transfected HUVEC, very little expression of inflammatory markers were detected as a result of lentiviral transfection, indicating that there is minimal inflammatory activation when transfected with ES or ΔC lentiviral constructs. This was important as E-selectin is itself an inflammatory marker, and inflammatory activation by other means must be avoided as much as possible in future experiments. Expression of transfected E-selectin or other induced adhesion molecules were not regularly checked in subsequent experiments however.

Transfection with lentivirus at a dilution of $2x10^{-3}$ appears to be the ideal concentration for use in future experiments. E-selectin expression is high, 90% and 70% in HMEC-1 and HUVEC cells respectively; and using concentrations of virus higher than this shows only a small increase in E-selectin expression while increasing the expression of other inflammatory markers. Transfection experiments in later chapters used this concentration of virus for both ES and ΔC expression.

5 Exploring the E-selectin clustering properties of *Neisseria meningitidis*

5.1 Introduction

5.1.1 Leucocyte adhesion can cause clustering of E-selectin leading to endothelial intracellular signalling

Upon inflammatory stimulation, endothelial cells upregulate expression of E-selectin alongside other cell adhesion molecules. E-selectin forms transient tethers with Sialyl Lewis X ligands on circulating neutrophils, causing the cells to slow down and roll along the endothelium. At the same time, binding to their ligands causes conformational changes on neutrophil integrins, allowing them to bind tightly to receptors such as ICAM-1 and VCAM-1 on the endothelium and leading to firm adhesion. The binding to adherent leucocytes also causes E-selectin clustering around the point of contact with the leucocyte(Yoshida et al., 1996), as can be seen in Figure 5.1.

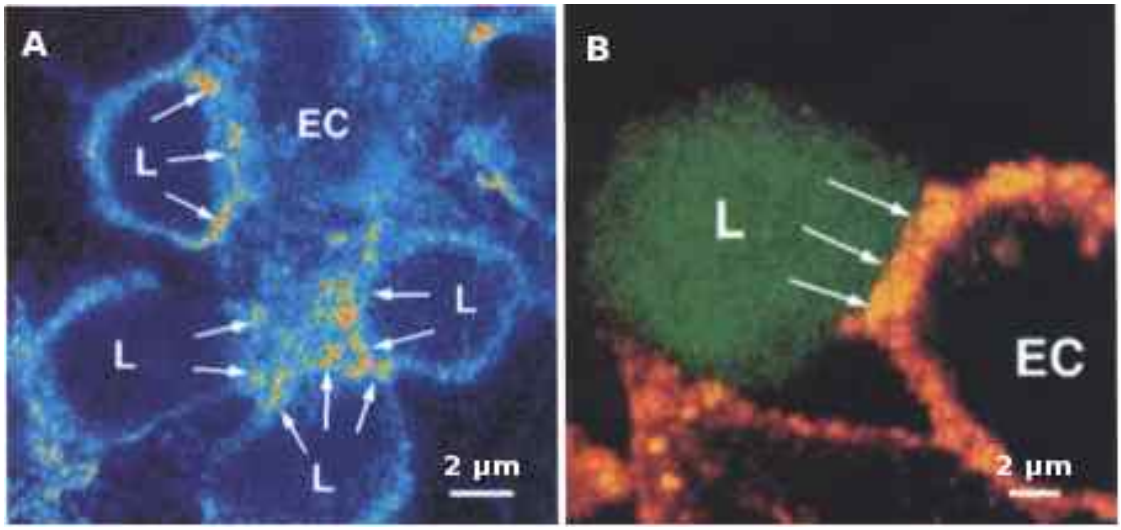

Figure 5.1: Representative image of E-selectin clustering at the point of contact between leucocytes and endothelial cells reproduced from Yoshida et al, 1996.

Endothelial cells (EC) in a HUVEC monolayer adhere to the leucocyte cell line HL-60 (L) which expresses ligands to E-selectin. Cells were stained with anti-E-selectin antibody, and E-selectin clustering can be seen at the site of leucocyte-endothelial contact in both A (blue staining) and B (orange staining).

This leucocyte initiated E-selectin clustering activates signalling pathways within endothelial cells, which can be mimicked by antibody cross-linking. E-selectin mediated signalling pathways are controlled by the phosphorylation status of specific amino acid residues on the E-selectin intracellular domain, and are known to lead to increased interactions with the endothelial cytoskeleton as well as activation of several intracellular signalling pathways including PLCγ and ERK/MAPK leading to activation of c-fos transcription factor (Hu et al., 2000; Kiely et al., 2003). The exact outcome of these signalling pathways has not been

extensively studied, but ERK/MAPK activation has been shown to be involved in neutrophil adhesion and transmigration(Stein et al., 2003; Tremblay et al., 2006).

5.1.2 Interactions of *Neisseria meningitidis* with the endothelium

E-selectin is the major endothelial cell adhesion molecule involved in neutrophil recruitment and activation on the endothelium, and previous studies have shown that *N.meningitidis* stimulates significantly greater E-selectin expression on the surface of endothelial cells than seen in response to LPS, TNFα, or other inflammatory cytokines (Dixon et al., 2004).

In addition, preliminary work by other members of the Klein/Dixon laboratory showed that recombinant soluble E-selectin could directly bind to *N.meningitidis* bacteria without LOS interactions, implying an intimate connection between them (personal communication). Other preliminary work has shown high levels of E-selectin and neutrophil staining in skin biopsies from patients with meningococcal sepsis (Faust et al., 2001; unpublished data-personal communication), and has also hinted that *N.meningitidis* can cause the clustering of E-selectin on the endothelial surface. Publications such as Doulet et al, 2006, have shown that *N.meningitidis* can adhere and multiply on the endothelial surface, forming microcolonies that can recruit and cluster E-selectin as well as other adhesion molecules and cytoskeletal proteins.

Meningococcal disease induces a severe inflammatory response (Chapter 1); and the widespread neutrophil recruitment to vascular endothelium and resultant release of cytotoxic granules could account for the tissue damage observed in severe cases of the disease(Klein et al., 1996). While it is known that high level expression of E-selectin can be induced in response to *N.meningitidis;* the redistribution and clustering of E-selectin can activate signalling pathways such as ERK/MAPK and PLCγ, as mentioned above; and affect the extent of neutrophil recruitment and activation, potentially providing a mechanism through which meningococci could directly influence the inflammatory response that is characteristic of this disease. The experiments in this chapter sought to determine whether meningococci can directly influence E-selectin surface distribution and clustering.

5.1.3 Aims and Objectives

The aims of the initial experiments outlined in this chapter were to evaluate and confirm the normal expression patterns of E-selectin on HUVEC endothelial cells, and compare the surface distribution of IL-1β induced E-selectin with the distribution on lentiviral transfected HUVEC expressing ES (full-length) and ΔC (tail-less) E-selectin. In addition, the endogenous and transfected E-selectin clustering response to both leucocyte adhesion and antibody

cross-linking would be examined. This would also serve to provide further validation of the lentivirus transfection method for further functional studies described in the next chapter.

In order to investigate E-selectin behaviour during meningococcal disease, one of the main aims of this chapter was to examine redistribution of E-selectin in response to brief exposure (<60 minutes) to wild type *N.meningitidis* bacteria. As well as exploring the intracellular or extracellular mechanisms regulating E-selectin reorganisation in transfected ES and ΔC as well as endogenous E-selectin to *N.meningitidis* bacteria.

Finally; adhesion of *N.meningitidis* to the endothelium and the effects of this adhesion on E-selectin localisation using bacteria with different endothelial properties would be explored. Encapsulated bacteria have been shown to have low levels of interaction with host cells, as the capsule blocks interactions of bacterial outer membrane proteins such as Opa and Opc(Dixon et al., 1999; Virji et al., 1995b). Unencapsulated bacteria have both greater adhesion and stimulation of endothelial cells, therefore an unencapsulated *SiaD*- mutant would also be used to investigate the effects of meningococcal adhesion on E-selectin distribution.

5.2 Methods

5.2.1 Cell culture

HUVEC preparation and cell culture protocol is outlined in detail in the Materials and Methods chapter section 2.5 of this thesis. Preparation of neutrophils using polymorphprep is described in Methods chapter section 2.6.

5.2.2 Lentivirus transfection of HUVEC

Lentivirus transfection of endothelial cells is outlined in detail in the Materials and Methods chapter section 2.7 of this thesis as well as Chapter 4.

5.2.3 Preparation and staining for immunofluorescence confocal microscopy

The staining protocols which methods A and B are based on are described in detail in section 2.8 of the Materials and Methods chapter. Briefly: in staining method A the cells were fixed in 4% PFA for 10 minutes before blocking in 1% BSA for 30 minutes. After blocking, the cells were stained with the primary anti E-selectin antibody for 30 minutes at room temperature, washed, and then stained with the FITC-linked secondary anti-mouse antibody and TO-PRO3 DNA stain for a further 20 minutes. After Secondary antibody staining, cover slips were mounted on glass slides and affixed in place using nail varnish. Method B follows a similar

process, except that the primary antibody staining is carried out before fixation of the cells in 4% PFA. Figure 5.2 shows the key differences between staining methods A and B together with the cross-linking protocol. The purpose of comparing these two staining methods was to investigate and account for any spontaneous receptor clustering that could be induced by the antibody staining protocol.

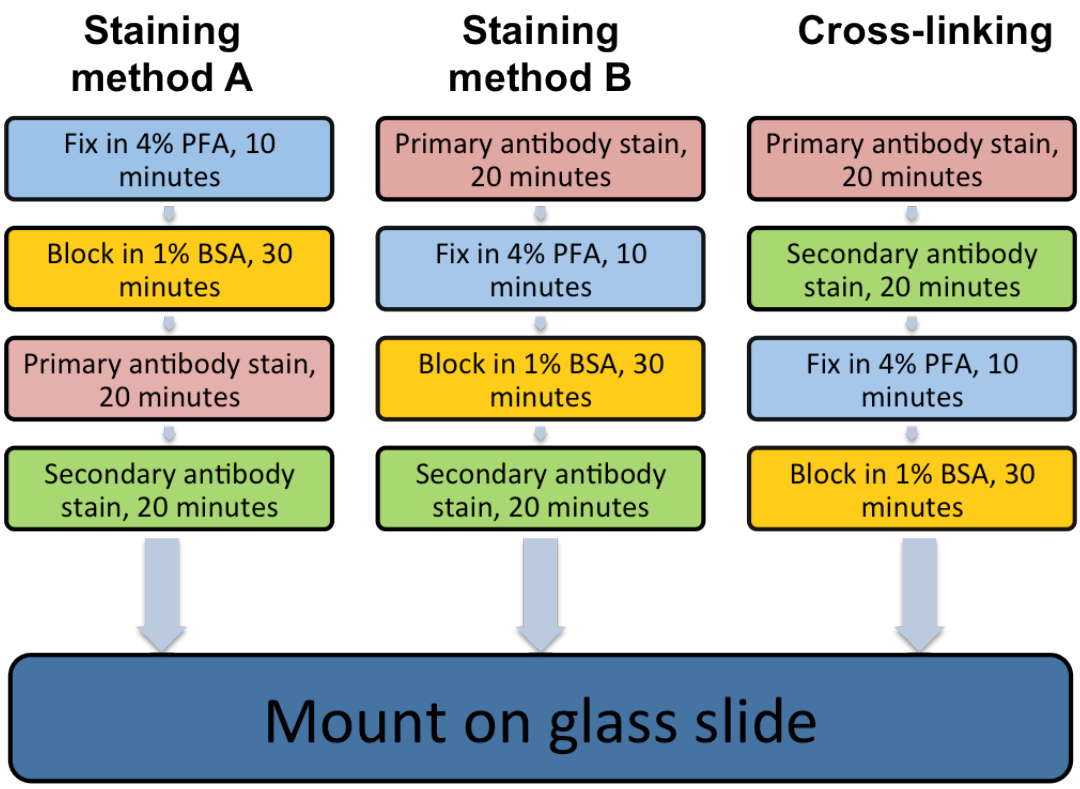

Figure 5.2: Diagram describing the different staining protocols Method A, Method B and Antibody cross-linking of the E-selectin, which differ in the order of addition of reagents.

5.2.4 Cell permeabilisation

For intracellular staining in some experiments, Method A was modified by the addition of a permeabilisation step (0.1% Triton X100 in PBS 1-2 min) following 4% PFA fixation. Cells were subsequently washed with PBS and blocked and stained as outlined above.

5.3 Results

5.3.1 Both endogenous and transfected E-selectin form large clusters upon neutrophil adhesion and cross-linking with anti-E-selectin antibodies

5.3.1.1 The expression pattern of ES, but not ΔC, transfected E-selectin resembles that of endogenous IL-1β stimulated E-selectin

E-selectin is normally only expressed on endothelial cells after exposure to inflammatory stimuli such as IL-1β, TNFα or LPS. Expression peaks around 4-6 hours post-stimulation, and

E-selectin is expressed in a punctate pattern, evenly spread in small spots across the surface of the endothelium. To compare the expression pattern of lentiviral transfected E-selectin with endogenous E-selectin, HUVEC were either transfected with ES or ΔC lentivirus, or stimulated for 4 hours with IL-1β.

HUVEC stimulated with IL-1β for 4 hours expressed E-selectin in the punctate pattern described above, with a few spontaneous clusters appearing randomly across the cell surface (Figure 5.3A). Both the full length ES (Figure 5.3B) and the tail-less ΔC (Figure 5.3C) mutant E-selectin transfected into HUVEC also appeared to be expressed evenly across the transfected cells, although not all cells were transfected. While the ES appeared to form small spontaneous clusters in a similar pattern to the IL-1β induced E-selectin, the ΔC did not; indicating that the spontaneous clusters may be controlled by a mechanism involving the intracellular domain.

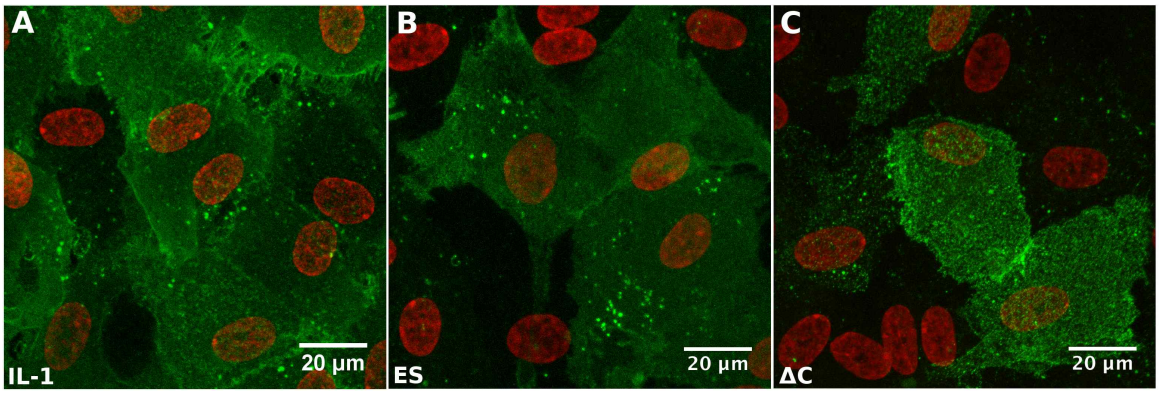

Figure 5.3: Expression of E-selectin on HUVEC either stimulated with 10ng/ml IL-1β, or transfected with ES or ΔC lentiviral constructs.

E-selectin expression on HUVEC stimulated with 10ng/ml IL-1β for 4 hours (A), or transfected with lentivirus containing either full length ES (B) or tail-less ΔC (C) E-selectin cDNA. E-selectin shown in green, nuclei in red.

5.3.1.2 Large clusters of E-selectin are formed beneath adherent Neutrophils in IL-1β stimulated or ES and ΔC transfected endothelial cells

Endogenous E-selectin has been reported to form large clusters beneath adhered neutrophils and other leucocytes expressing E-selectin ligands, and also form smaller clusters upon antibody mediated cross-linking(Kiely et al., 2003; Yoshida et al., 1996). These observations wee confirmed for both endogenous IL-1β induced E-selectin as well as transfected ES or ΔC. Figure 5.4A shows the clustering of IL-1β induced E-selectin under adherent leucocytes on a HUVEC monolayer. E-selectin was expressed in a punctate pattern across the whole endothelial cell (E) with some small spontaneous point clusters, but then gathered in large congregations associated with the adherent neutrophils (N).

Figure 5.4B shows a 3D image, made from a confocal image Z-stack, showing E-selectin specifically gathering around the point of contact of neutrophils with the endothelium. A 3D rotation video of Figure 5.4B is shown in Video 5.1, showing more detail of both the underside of the endothelium and the large patches of neutrophil and E-selectin clustering. Patches of green staining around the neutrophils and above the plane of the endothelium also appear to show that the plasma membrane of the endothelium was being drawn around the adherent neutrophils.

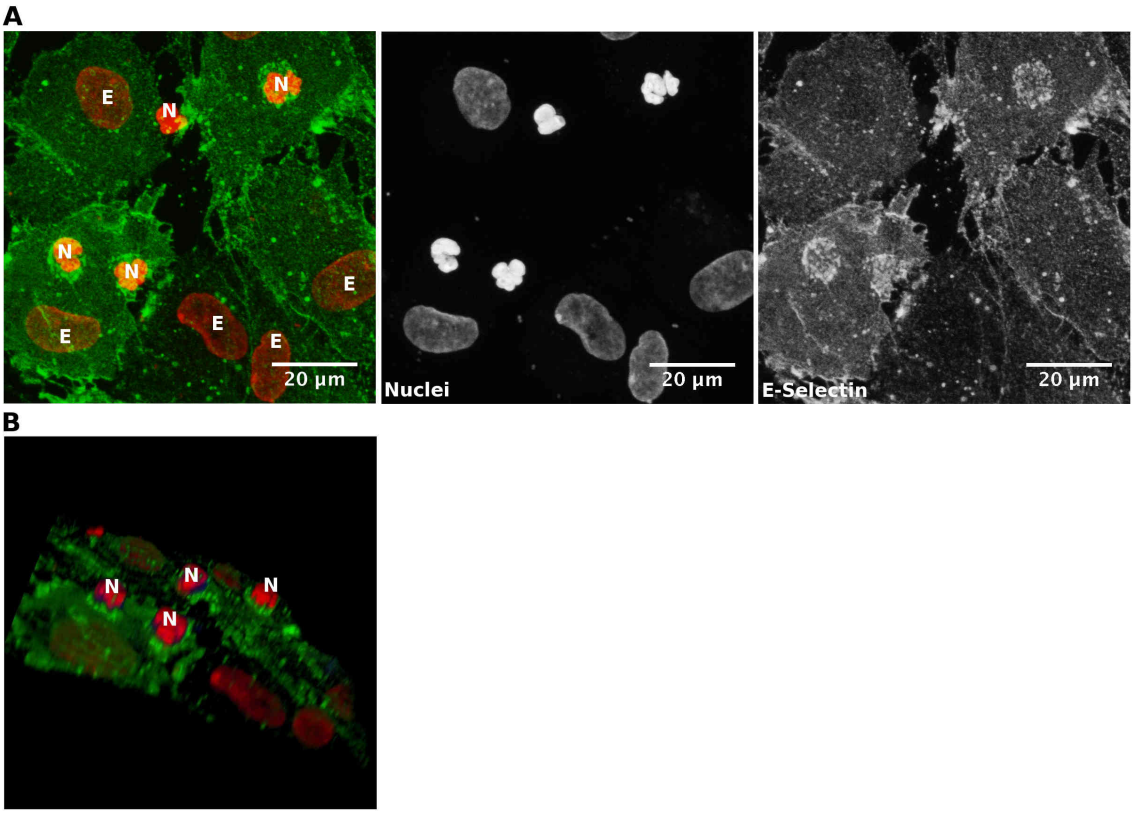

Figure 5.4: Confocal microscopy images showing clustering of endogenous IL-1β induced E-selectin beneath adhered neutrophils.

(A) Composite image of neutrophils bound to primary HUVEC after 4 hours IL-1β stimulation, showing E-selectin (green) clustering around the adherent neutrophils. Nuclei (red) of both HUVEC and neutrophils are visible, with neutrophil nuclei distinguished by their smaller size, brighter staining and multi-lobed appearance. Both E-selectin and Nuclei are also shown as separate grayscale images (B) 3D image made from a multi-image z-stack showing large amounts of E-selectin clustering beneath adhered neutrophils. Rotation video of the 3D image can be found in Video 5.1.

To investigate whether the transfected ES and ΔC E-selectin behaved in the same manner, the effects of leucocyte mediated clustering were investigated on both endogenous and transfected E-selectin in HUVEC. Figure 5.5A and B show that transfected ES and ΔC E-selectin undergo the same clustering beneath adherent leucocytes as endogenous E-selectin does in Figure 5.4A, forming the same large clusters of E-selectin around the neutrophil adhesion site. It is notable that both ES and the mutant ΔC E-selectin form clusters beneath

the adherent neutrophils, indicating that the clustering is directly mediated by adhesion of the neutrophil, and not via a mechanism requiring the intracellular domain of E-selectin.

As with the IL-1β induced endogenous E-selectin, 3D images of neutrophils adherent to ES and ΔC transfected endothelium are shown in Figure 5.5C and D, with 3D rotation videos shown in Video 5.2 and Video 5.3. E-selectin staining was also seen above the plane of the endothelial layer with both full-length and mutant E-selectin, in a similar pattern seen with IL-1β induced E-selectin in Figure 5.4B, confirming that these effects are also not regulated by the E-selectin intracellular domain.

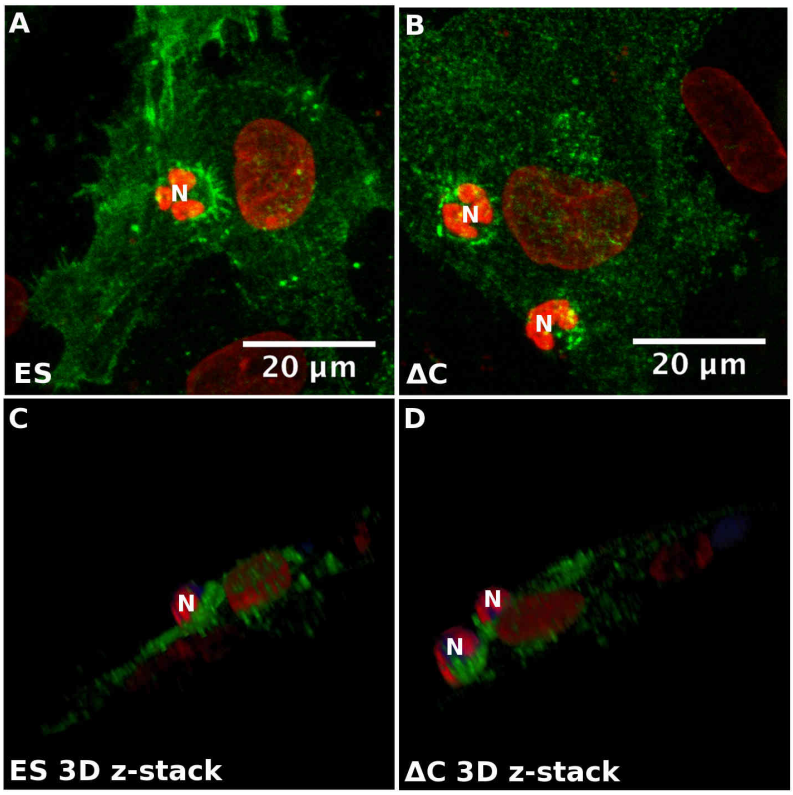

Figure 5.5: Confocal microscopy images showing clustering of transfected ES and ΔC E-selectin beneath adhered neutrophils.

Composite images of neutrophils bound to primary HUVEC transfected with either ES (A+C) or ΔC (B+D) E-selectin, showing E-selectin (green) clustering around the adherent neutrophils. Nuclei of both HUVEC and neutrophils are shown in red, with neutrophil nuclei distinguished by their smaller size, brighter staining and multi-lobed appearance. The confocal Z-stacks are displayed as both 2D (A+B) and 3D (C+D) images. 3D rotational videos can be found in Video 5.2 and Video 5.3 on the DVD.

5.3.1.3 Antibody cross-linking of E-selectin causes clustering on both endogenous and ES and ΔC transfected E-selectin

Leucocyte-mediated E-selectin clustering occurs via an outside-in mechanism, i.e. the leucocyte binds to the E-selectin extracellular domain and induces receptor clustering beneath it. Antibody cross-linking can mimic this by binding E-selectin with a primary anti-

human E-selectin antibody, followed by a secondary anti-mouse IgG antibody to cross-link multiple E-selectin molecules together to form clusters.

The clustering induced by anti-E-selectin antibody cross-linking was examined on both endogenous E-selectin expressed on IL-1β stimulated HUVEC, as well as in ES and ΔC transfected HUVEC. As can be seen in Figure 5.6A, antibody cross-linking triggers cluster formation on the endogenous E-selectin. Furthermore, Figure 5.6B and C show that full length ES and mutant ΔC transfected E-selectin also form the same pattern of clusters upon antibody mediated cross-linking as endogenous IL-1β induced E-selectin. Antibody mediated cross-linking can therefore be used as a positive control for clustering caused by binding to the external region of E-selectin.

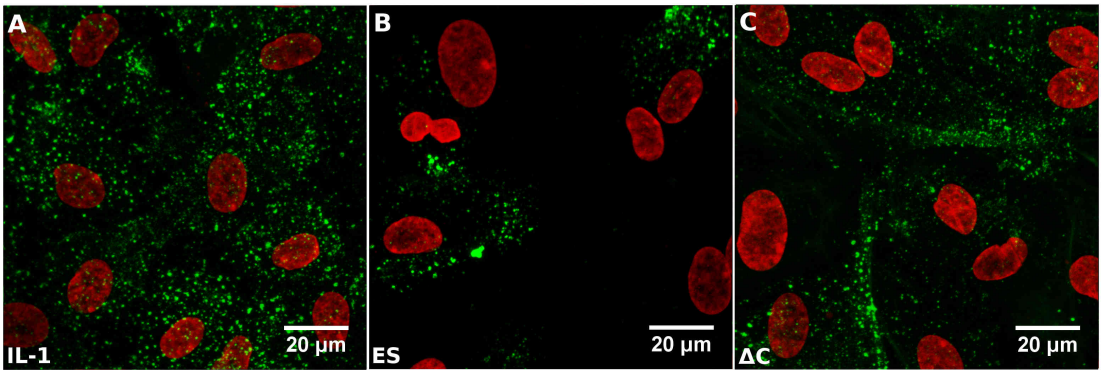

Figure 5.6: Confocal microscopy images showing clustering of both endogenous IL-1β induced E-selectin and transfected ES and ΔC E-selectin upon antibody cross-linking.

Confocal microscopy image of antibody mediated cross-linking of E-selectin expressed on HUVEC (A) stimulated with IL-1β for 4 hours, or (B+C) transfected with full-length ES or mutant ΔC. E-selectin is shown in green and nuclei in red.

Interestingly, the clusters formed by antibody cross-linking are a different shape to those formed by leucocyte adhesion. Clusters beneath the adherent leucocytes cover only the point of contact between the leucocyte and the HUVEC, whereas antibody mediated clusters form points beneath the antibody immunocomplex, which are smaller than the leucocyte cells, so form smaller, brighter focal points. This also has the effect of involving almost all of the E-selectin present in the endothelial cell, as there are many more antibody complexes present than adherent leucocytes.

Although the shape of the leucocyte or antibody mediated clusters differ, the internal signalling caused by the clustering remains the same. E-selectin clustering, whether by leucocyte binding or antibody cross-linking, can activate various signalling pathways within the endothelial cells, such as ERK1/2 MAPK and Phospholipase Cγ, as described in greater detail in section 1.3.4.1 of the Introduction chapter.

In conclusion, both endogenous E-selectin, as well as transfected full-length ES and tail-less ΔC E-selectin can form clusters beneath adhered neutrophils and upon antibody cross-linking. The results show that the lack of intracellular domain on ΔC transfected E-selectin does not affect the clustering caused by cross-linking of the extracellular domain by binding of E-selectin ligands on neutrophils, or specific anti-E-selectin antibodies.

5.3.2 *Neisseria meningitidis* induced E-selectin clustering on endothelial cells

5.3.2.1 Exposure to Neisseria meningitidis for 60 minutes can produce an E-selectin clustering response on endothelial cells

In section 5.3.1, the clustering effects of leucocyte adhesion and antibody cross-linking were studied on both IL-1β induced endogenous E-selectin, and lentiviral transfected ES and ΔC E-selectin. To investigate whether clustering of E-selectin may also be initiated by meningococci, the effects of the *N.meningitidis* bacterium on the pattern of E-selectin surface expression was studied. Figure 5.7A shows E-selectin expression on HUVEC from four different donors (numbered 1-4) after 4 hours stimulation with 10ng/ml IL-1β; E-selectin was expressed in a punctate pattern across the surface of the cell, as seen previously in Figure 5.3A. When exposed to killed *N.meningitidis* for 60 minutes, the E-selectin on the IL-1β stimulated HUVEC appeared to form large, bright clusters (Figure 5.7B), in a similar pattern to the clusters seen upon antibody cross linking in Figure 5.7C.

The E-selectin expression appeared to form slightly different arrangements in each of the donors, implying a degree of donor variation in E-selectin expression rates and patterns. E-selectin staining in donor 3 appeared to be brighter in IL-1β stimulated cells, both with and without *N.meningitidis* exposure compared to the other donors, however this is probably due to natural variation seen in human donors.

The *N.meningitidis* induced clusters, although similar in shape to the antibody cross-linked E-selectin clusters, formed a distinct clustering pattern. Antibody cross-linking rearranged almost all the E-selectin into very bright clusters of varying sizes, with very little E-selectin staining between individual clusters. *N.meningitidis* induced more sporadic clustering, that did not involve all the E-selectin on the HUVEC, with some punctate and diffuse staining still visible between the clusters, akin to that induced by the leucocyte binding in Figure 5.4A.

In conclusion, the E-selectin expression pattern was distinctly altered under both antibody mediated cross-linking and *N. meningitides* induced clustering, as compared to the more diffuse staining seen on IL-1β stimulated HUVEC with no secondary stimuli. Furthermore,

there were differences in the pattern of E-selectin clustering mediated by antibody cross-linking compared to the pattern observed in response to killed WT *N.meningitidis*.

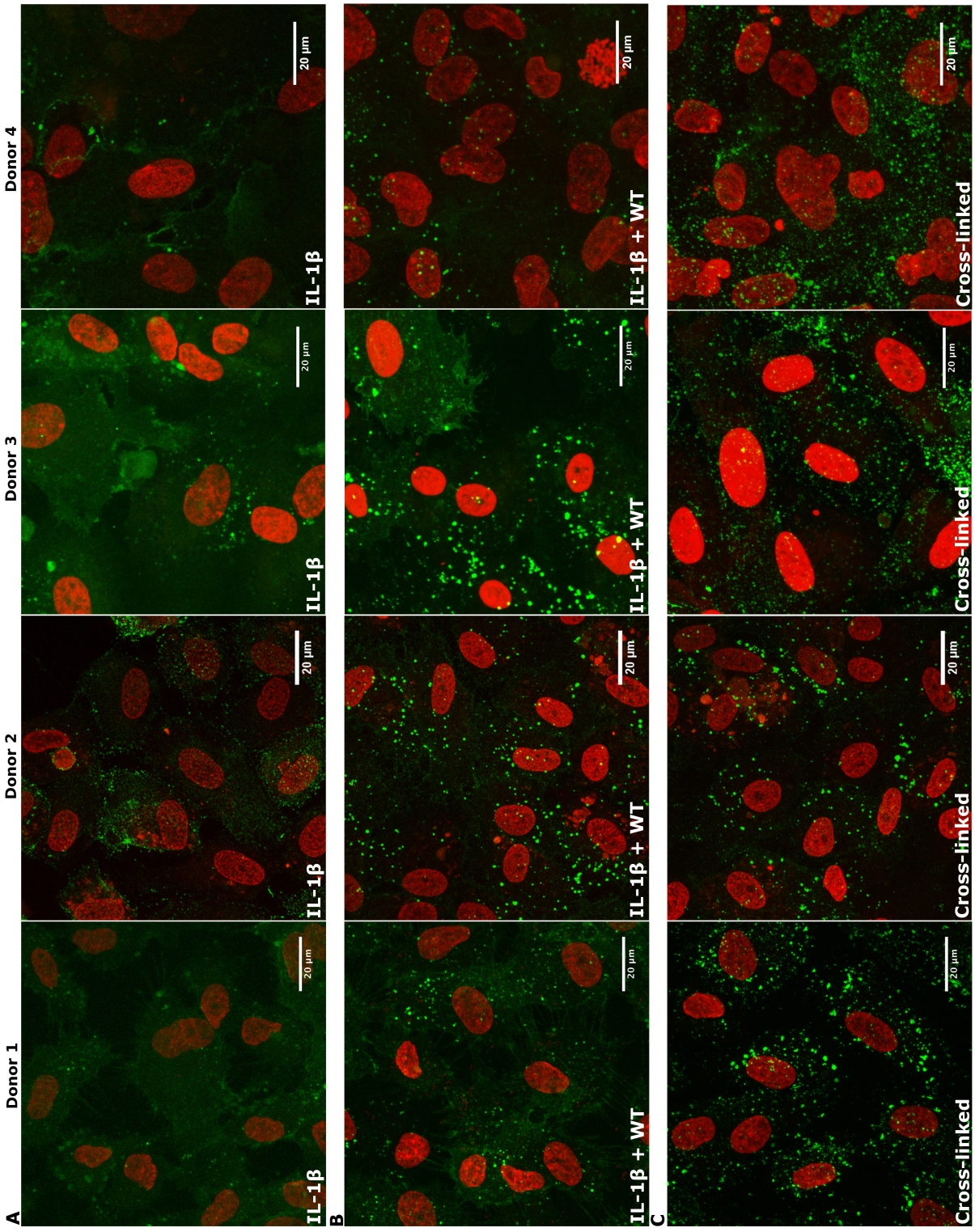

Figure 5.7: Confocal microscopy images showing formation of clusters of IL-1β induced E-selectin on HUVEC after exposure to killed *N.meningitidis* in 4 donors.

Representative images of four donors showing E-selectin expression after 4 hours IL-1β stimulation (A), followed by further exposure to either 10^7 bacteria/ml of killed *N.meningitidis* for 60 minutes (B) or cross-linking by anti-E-selectin antibodies (C). E-selectin shown in green, TO-PRO3 DNA staining in red.

5.3.2.2 E-selectin clustering induced by N.meningitidis is not consistent, and clusters can also form spontaneously under other conditions

The HUVEC isolated from four donors shown in Figure 5.7 show consistent E-selectin clustering in response to *N.meningitidis*. However the E-selectin expression pattern due to IL-1β stimulation was not always consistent, and varied between different donors. Figure 5.8 shows four additional experiments where E-selectin clustering due to *N.meningitidis* exposure was much less evident than in the images shown in Figure 5.7.

All four donors in Figure 5.8 show bright clusters of E-selectin staining in both the IL-1β stimulated control (Figure 5.8A) and the IL-1β stimulated cells exposed to killed *N.meningitidis* (Figure 5.8B); the size and distribution of which resembles the distribution of clusters seen in the *N.meningitidis* exposed cells in Figure 5.7B. This spontaneous clustering of E-selectin upon IL-1β stimulation masked any observations of additional *N.meningitidis* induced clustering on HUVEC. The clustering of E-selectin observed upon antibody cross-linking was still evident in all the donors (Figure 5.8C), although the exact pattern varied between experiments.

Some spontaneous clustering of E-selectin was expected, and was seen in most donors even where there was also *N.meningitidis* induced clustering, as shown in the experiments depicted in Figure 5.7. However, the level of spontaneous clustering seen in Figure 5.8 was much greater, and obscured the effects of *N.meningitidis* on the expression of E-selectin. The reasons for this spontaneous clustering were unclear at this stage; however, one possibility is that it could be attributable to variation between HUVEC from different donors.

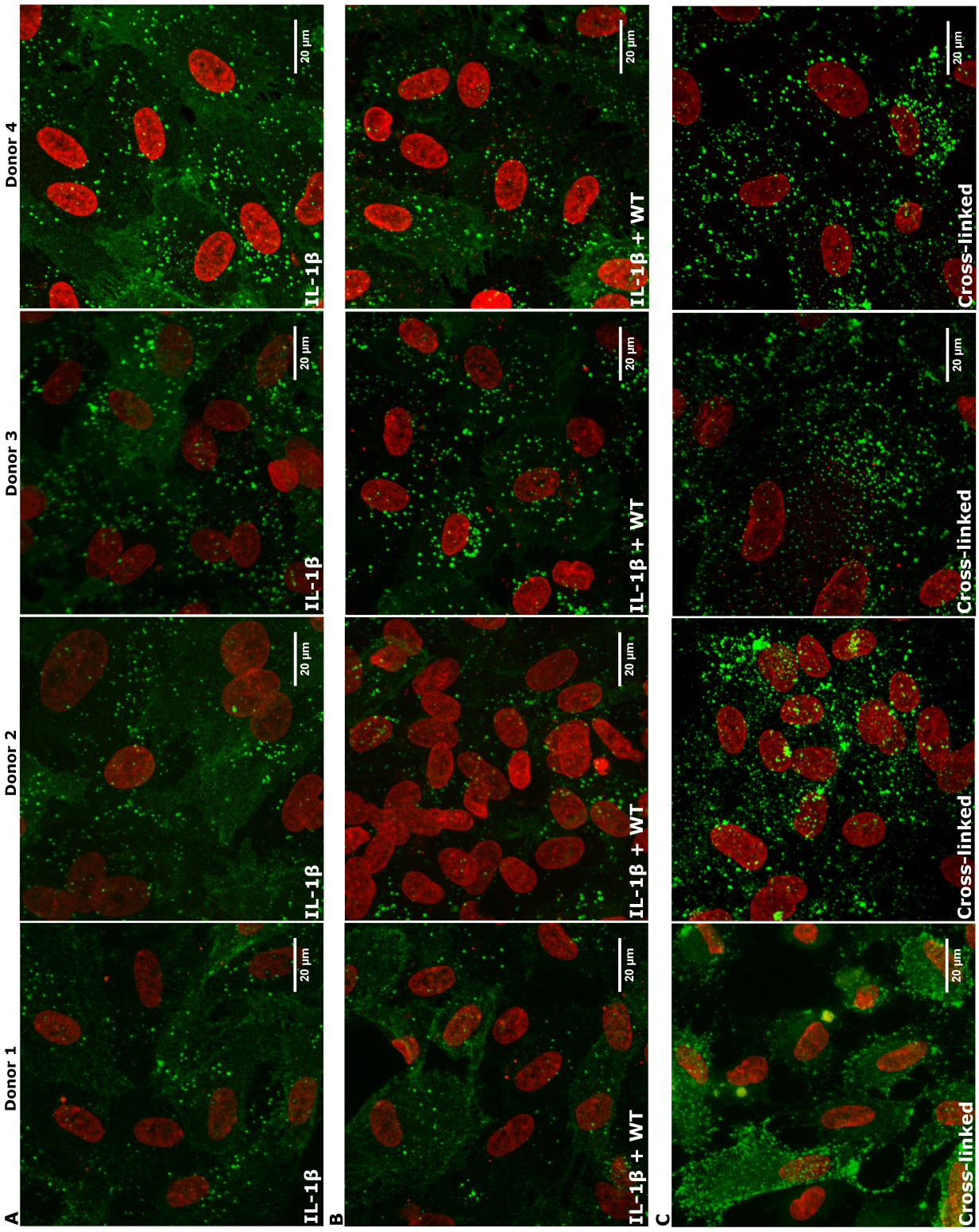

Figure 5.8: Confocal microscopy images showing spontaneous clustering of IL-1β induced E-selectin in 4 donors, preventing the observance of *N.meningitidis* induced clustering.

Representative images of four additional donors showing E-selectin expression and spontaneous clustering after 4 hours IL-1β stimulation (A), and after exposure to 10^7 bacteria/ml of killed *N.meningitidis* (B) or cross-linking by an anti-E-selectin antibody (C). E-selectin shown in green, TO-PRO3 DNA staining in red.

5.3.2.3 ES and ΔC transfected HUVEC were used to investigate the nature of spontaneous and N.meningitidis induced E-selectin clustering

The extent of the spontaneous clustering of IL-1β induced E-selectin was variable across different HUVEC donors, but was usually widespread enough that any *N.meningitidis* induced clustering was not noticeably enhanced over spontaneous cluster formation, as seen in Figure 5.8. Low levels of spontaneous E-selectin clustering, with no additional stimuli were also seen in HUVEC transfected with full length ES, but not ΔC E-selectin mutant, as shown in Figure 5.3B. In order to establish whether transfected E-selectin had similar levels of variability in expression between experiments as IL-1β induced endogenous E-selectin; HUVEC were transfected with the ES and ΔC lentiviral constructs, and then exposed to 10^7/ml *N.meningitidis*.

The expression and clustering patterns of both ES and ΔC E-selectin on three transfected donors are shown in Figure 5.9. ES E-selectin on donor 1 formed the punctate expression pattern, similar to that seen in endogenous E-selectin, whereas the mutant ΔC was expressed in a more diffuse pattern with fewer spontaneous clusters, as also observed in Figure 5.3. On donor 2 neither ES nor ΔC E-selectin appeared to form spontaneous clusters, and both ES and ΔC were expressed in a relatively diffuse pattern throughout the cell. Donor 3, however, showed spontaneous clustering with both ES and ΔC E-selectin, although far more clustering was seen with ES, while ΔC had brighter staining in the areas between the clusters.

The level of ES or ΔC clustering was not observably increased upon *N.meningitidis* exposure and binding (Figure 5.9, middle row). Donor 1 demonstrated some localised clustering compared to the unexposed control cells. Donor 2 demonstrated no observable clustering in response to *N. meningitidis*, compared to unexposed control, finally, donor 3 had high levels of spontaneous E-selectin clustering in unexposed cells, and it was impossible to discern any difference between unexposed and *N. meningitidis* exposed cells. All three donors still demonstrated extensive clustering of both ES and ΔC E-selectin upon antibody cross-linking.

Figure 5.9: Confocal microscopy images showing expression of ES and ΔC transfected E-selectin on HUVEC from three donors after either *N.meningitidis* exposure or antibody cross-linking.

Images from three representative donors showing E-selectin expression on HUVEC after transfection with ES and ΔC lentivirus after 60 minutes exposure to 10^7 bacteria/ml killed *N.meningitidis* or cross-linking by an anti-E-selectin antibody. E-selectin shown in green, TO-PRO3 DNA staining in red.

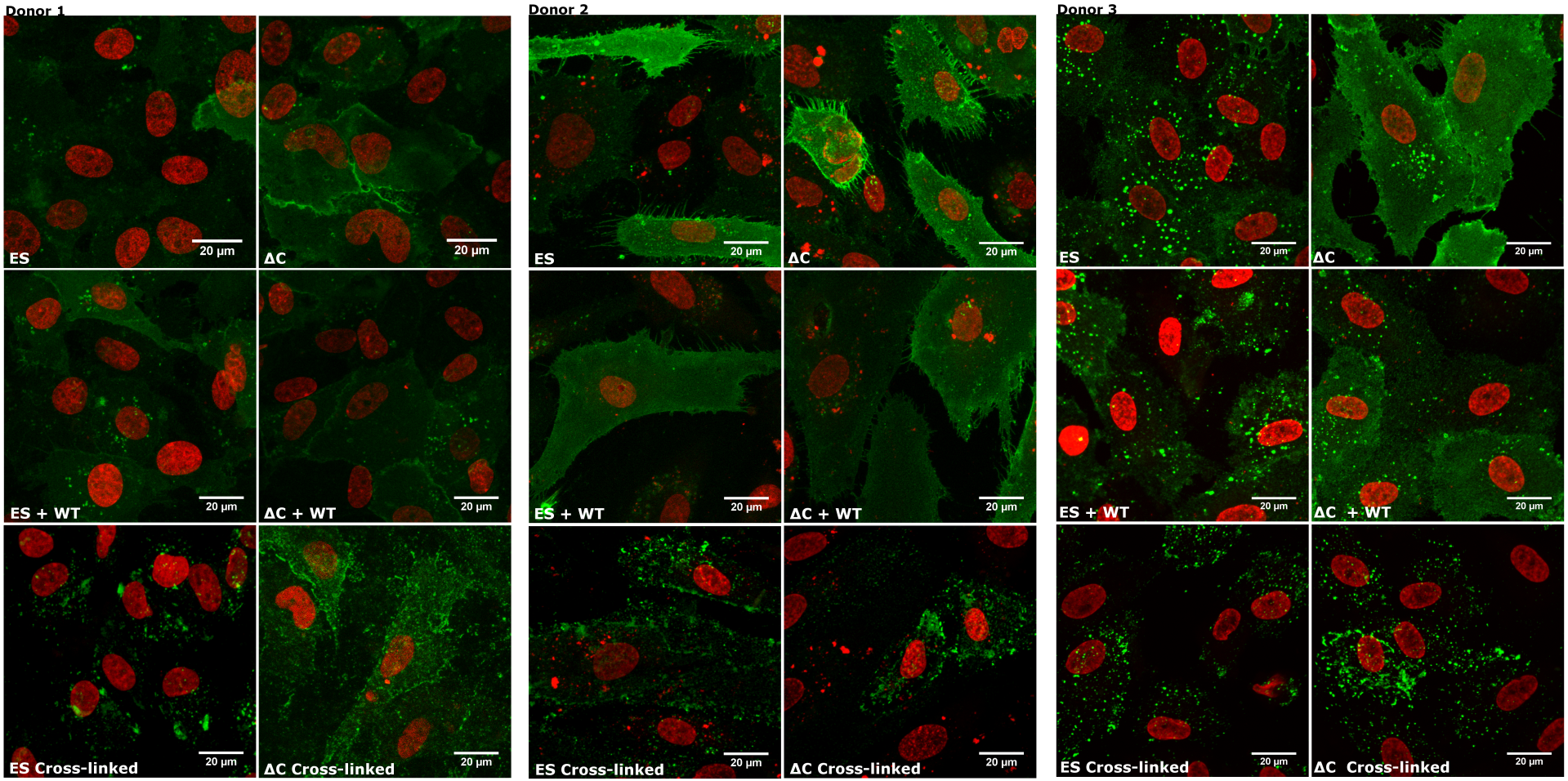
Donor 1
Donor 2
Donor 3
ES
ΔC
ES + WT
ΔC + WT
ES Cross-linked
ΔC Cross-linked
ΔC + WT
20 µm

There were distinct differences in the distribution of ES compared to ΔC E-selectin, in that ΔC formed fewer spontaneous clusters than ES or IL-1β induced E-selectin. This implies that the spontaneous clustering of E-selectin involves a mechanism requiring the intracellular domain. These would presumably involve interactions with the actin cytoskeleton, rather than the extracellular domain clustering seen with neutrophil binding or antibody cross-linking which does not require an intact intracellular tail.

The variability observed of spontaneous E-selectin clustering in cells expressing both endogenous and transfected E-selectin obscured clustering in response to *N. meningitidis* shown in Figure 5.7. This made it difficult to make any conclusive comments on *N. meningitidis* induced clustering of E-selectin, as any clustering seen could be explained as spontaneous clustering also present in control conditions. They do demonstrate, however, the difficulties faced when conducting experiments on primary cells, which may have unknown confounding genetic and environmental factors interfering with the experimental procedure.

5.3.3 Use of an acapsulate *N.meningitidis* mutant (*SiaD*-) to further explore E-selectin redistribution on HUVEC

5.3.3.1 Investigating endogenous and transfected E-selectin clustering in response to a N.meningitidis capsular mutant

Adherence to the endothelium is an important step in meningococcal infection. The meningococcal capsule is known to influence many interactions between bacteria and the endothelium; and unencapsulated strains both adhere to and stimulate endothelial cells to a much greater extent than WT strains(Dixon et al., 1999; Virji et al., 1995b). Natural variation of capsule expression is known to occur amongst strains isolated from carriers and patients. Although most invasive strains are encapsulated due to the large advantage in immune evasion afforded by the capsule; *N.meningitidis* has also been shown to vary capsular expression under different conditions(Deghmane et al., 2002; Hammerschmidt et al., 1996). The strain of *N.meningitidis* used in experiments thus far was an encapsulated WT strain of *N.meningitidis* serogroup B. Given the difficulties experienced thus far with the reproducibility of induced E-selectin clustering due to WT *N.meningitidis* exposure, unencapsulated bacteria were used to explore E-selectin expression patterns.

The *N.meningitidis* mutant used had an ERM resistance cassette inserted into the *SiaD* gene in order to disrupt its function(Edwards et al., 1994; Steeghs et al., 2001). The *SiaD* gene encodes a polysialyltransferase involved in polymerisation of capsule components. The non-

functional capsular mutant still expresses LOS and pili, and allows greater interactions between outer membrane components of the bacteria such as Opa and Opc with the endothelium, which are usually physically impeded by the presence of the capsular coat.

Figure 5.10A shows E-selectin expression on IL-1β stimulated endothelial cells in response to IL-1β alone, exposure to WT and killed *SiaD- N.meningitidis*, or after cross-linking with anti-E-selectin antibody. There was some spontaneous clustering seen upon IL-1β stimulation alone, and clustering was greatly increased upon addition of the cross-linking antibody. Although some E-selectin clustering was seen in the presence of killed WT *N. meningitidis*, the level of clustering was not enhanced compared to the spontaneous clustering seen upon IL-1β stimulation alone. Similarly, exposure to the *SiaD* mutant did not appear to produce levels of E-selectin clustering distinct from that seen upon IL-1β stimulation alone or following exposure to the WT bacteria.

Figure 5.10B and C show ES and ΔC transfected E-selectin respectively, under the same conditions as IL-1β stimulated HUVEC in Figure 5.10A. The ES transfected E-selectin appeared to form spontaneous clusters without any additional stimuli, while the transfected ΔC showed more diffuse expression, as seen previously in Figure 5.3 and Figure 5.9. The level of spontaneous clustering of transfected ES E-selectin appeared much lower than the endogenous IL-1β induced E-selectin in this donor, suggesting there is a degree of donor variation in the expression of transfected ES E-selectin. Both ES and ΔC transfected E-selectin formed more clusters upon antibody cross-linking.

The expression patterns of ES and ΔC transfected E-selectin upon 60 minutes exposure to WT *N.meningitidis* did not appear to differ from unexposed ES or ΔC transfected cells. *N.meningitidis* exposed ES transfected HUVEC formed similar levels of spontaneous clusters to unexposed cells, and ΔC was expressed in the same diffuse pattern on both exposed and unexposed HUVEC. Upon exposure to *SiaD*- mutant *N.meningitidis* the expression pattern of ΔC transfected cells did not change. Interestingly however, there did appear to be slightly fewer clusters seen on the *SiaD* exposed ES cells compared to cells exposed with WT bacteria, however it was unclear how much this was due to general variation in spontaneous clustering.

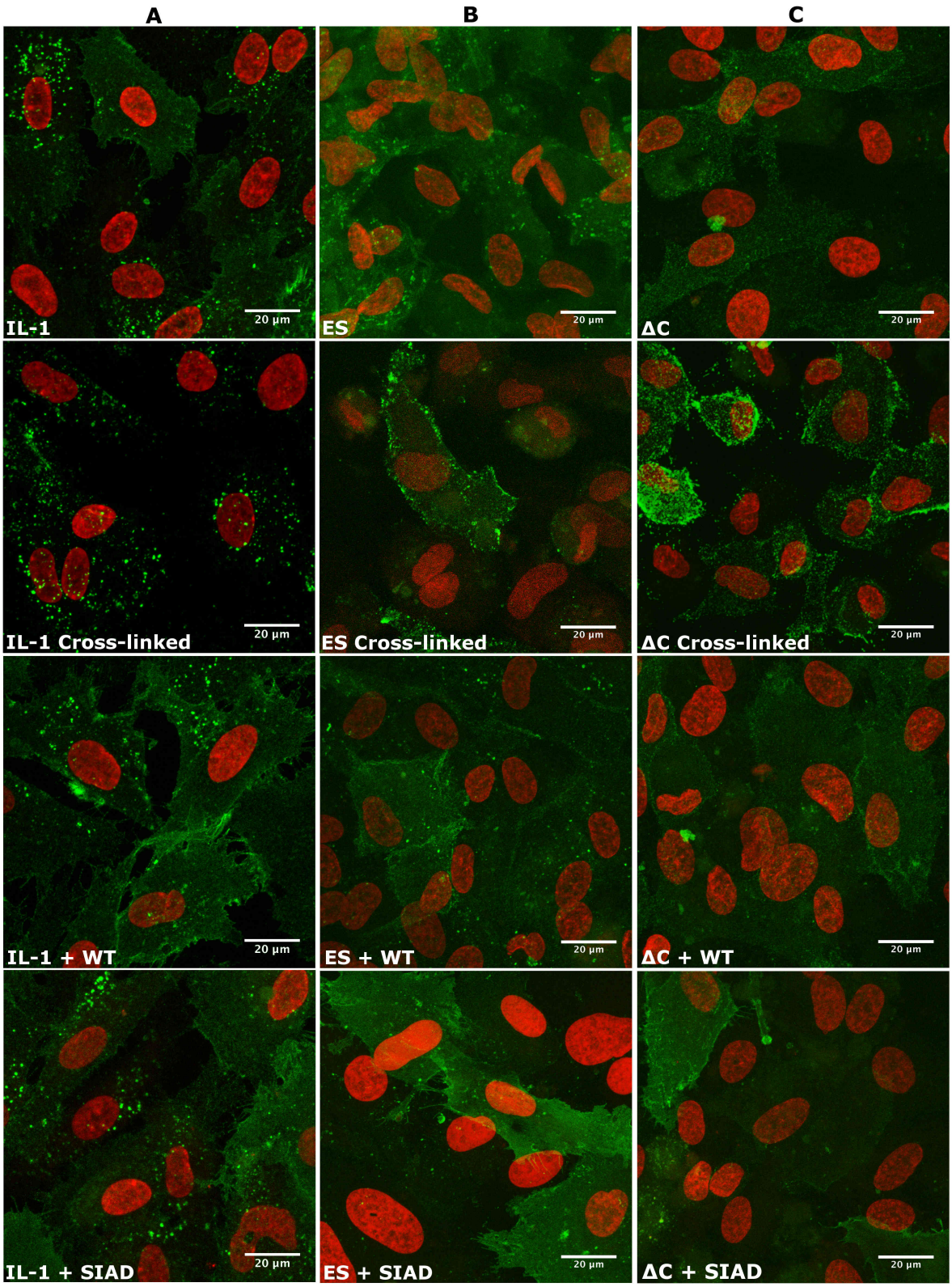

Figure 5.10: Confocal microscopy images showing endogenous IL-1β induced E-selectin expression after 60 minutes exposure to WT or *SiaD* mutant *N.meningitidis*.

Representative images showing E-selectin expression on HUVEC after stimulation with 10ng/ml IL-1β (A), or transfected with ES (B) or ΔC (C) lentivirus after 60 minutes exposure to 10^7 bacteria/ml killed WT or *SiaD* mutant *N.meningitidis*. E-selectin shown in green, TO-PRO3 DNA staining in red.

These results suggest that the clustering response of both endogenous and transfected E-selectin to exposure to the unencapsulated *SiaD* mutant does not differ greatly from their response to WT, and neither strain of *N.meningitidis* appeared to induce any more clustering than that seen occurring spontaneously. These experiments however were only looking at the general clustering response of E-selectin, and other E-selectin redistribution mechanisms may still occur.

5.3.3.2 Endogenous E-selectin can co-localise beneath SiaD N.meningitidis, but not WT, after 120 minutes exposure

The clustering of both endogenous and transfected E-selectin did not consistently increase upon exposure to WT or *SiaD*- mutant *N.meningitidis* bacteria. Adhesion of *SiaD N.meningitidis* to the endothelium however, is much greater than WT due to the removal of the capsular barrier preventing outer membrane adhesion protein interactions with host cells (Nikulin et al., 2006; Virji et al., 1993, 1995a).

In order to see how bacterial adhesion influences local E-selectin redistribution, E-selectin expression was examined in relation to adherent *SiaD* and WT bacteria. For these experiments, live bacteria were used and exposure time to these live *N.meningitidis* bacteria were extended, to allow more bacteria to adhere. Killed bacteria were used in previous experiments for both safety and ease of use, as N.meningitidis mutants are classed as category 3 organisms.

The DNA-binding TO-PRO3 stain used to stain nuclei, as seen in the confocal images above, can also stain the DNA in adherent *N.meningitidis*, which appear as small red spots up to 1μm in diameter on the confocal images. The small bacteria are not as bright as the nuclei, and so were more difficult to see on the confocal images shown above.

Experiments using live FITC labelled bacteria were therefore carried out to prove that the small structures stained with TO-PRO3 were indeed bacteria (Figure 5.11). Bacteria were labelled with FITC, before being incubated on HUVEC for 2 hours to adhere and form colonies. After fixation, HUVEC were labelled with TO-PRO3 DNA stain, and studied under a fluorescent confocal microscope. As can be seen, there is co-localisation (yellow) of the FITC stained bacteria (green) with the small 1μm TO-PRO3 stained structures (red), but not with the large nuclei. It was also noticeable that while all bacteria appeared to be stained to a similar brightness with the TO-PRO3 stain (applied after fixation), the brightness of the FITC staining (applied before addition of live bacteria to the endothelium) varied between different bacteria. This was most likely due to bacterial division forming microcolonies on

the cell surface. As the bacteria divide, the levels of FITC within a single bacterium are split between the two daughter bacteria produced by mitosis. In Figure 5.11, it can be seen that the brightest bacteria occur singly, the next-brightest bacteria occur in pairs, the next-brightest in fours, the next in eights, and so on.

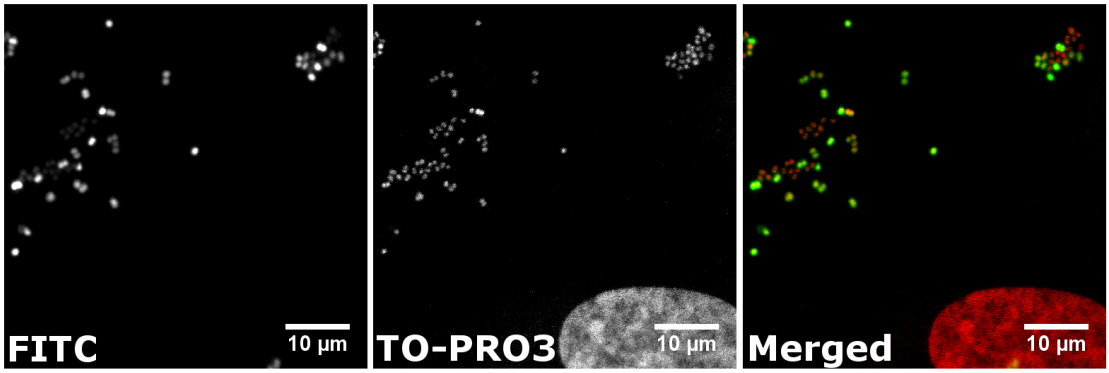

Figure 5.11: Confocal images showing co-localisation of FITC stained adherent *N.meningitidis* bacteria (green) with the TO-PRO3 DNA stain (red).

10^7/ml Live *N.meningitidis* bacteria were stained with FITC before addition to HUVEC for 2 hours. After 2 hours incubation, the cells were fixed in 4% PFA, and stained using TO-PRO3 DNA stain, which stained the nuclear DNA in the HUVEC, as well as bacterial DNA in the adhered *N.meningitidis*.

Next, the co-localisation of E-selectin with live *N.meningitidis* bacteria were investigated. Figure 5.12A shows IL-1β stimulated HUVEC expressing E-selectin and forming some spontaneous clusters. Addition of cross-linking antibodies in Figure 5.12B caused extensive clustering of E-selectin across the entire endothelium, as had been seen previously.

Exposure of IL-1β stimulated HUVEC to either WT or *SiaD N.meningitidis* bacteria for 60 minutes (Figure 5.12C and D) was associated with slightly greater levels of E-selectin clustering, however the variability in *N.meningitidis* induced clustering as seen in previous experiments, made it difficult to ascertain whether this was significant. Adherent WT and *SiaD* bacteria could be seen bound to the endothelial surface. The WT bacteria were bound in smaller groups, most commonly in pairs, while the *SiaD* bacteria formed larger bacterial colonies, presumably due to the increased adherence properties of the *SiaD- N.meningitidis*.

After 120 minutes exposure to either WT or the *SiaD- N.meningitidis* (Figure 5.12E and F), there did not appear to be any additional clustering beyond that seen on IL-1β stimulated HUVEC. Larger numbers of both WT and *SiaD* bacteria were adherent to the endothelium after 120 minutes compared to 60 minutes exposure, and more significantly; co-localisation of E-selectin staining beneath the adherent *SiaD* bacteria was now visible (Figure 5.12F). No co-localisation was seen beneath the WT bacteria at the same time point, indicating that this appeared to be specific to the unencapsulated *SiaD- N.meningitidis* mutant. No E-selectin

co-localisation was seen after 1 hour exposure with either WT or *SiaD N.meningitidis* in Figure 5.12C or D, despite bacteria from both strains adhering to the endothelium.

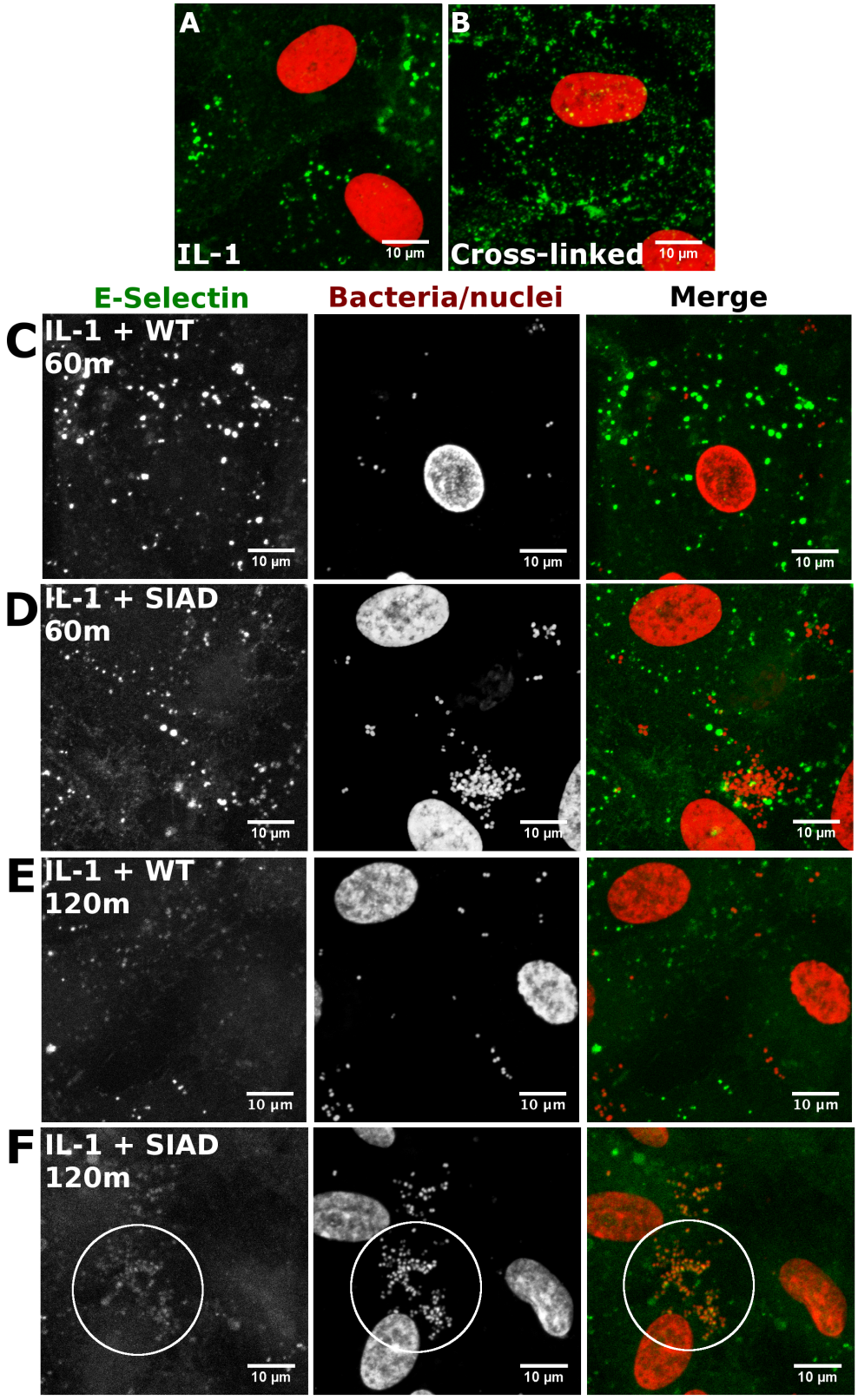

Figure 5.12: Confocal microscopy images showing co-localisation of endogenous E-selectin beneath adherent *SiaD N.meningitidis* on HUVEC after 120 minutes, but not 60 minutes, exposure.

HUVEC were stimulated with IL-1β for 4 hours (A), and were incubated with anti-E-selectin cross-linking antibodies (B). IL-1β stimulated HUVEC were incubated with 10^7/ml live WT (C + E), or *SiaD*- mutant (D + F) *N.meningitidis* for 60 (C + D) or 120 (E + F) minutes. Cells were stained for E-selectin (green) and DNA (red). Co-localisation of E-selectin with adherent bacteria is circled.

Not all expressed E-selectin co-localised with the adherent *SiaD* mutant bacteria after 2 hours, as diffuse E-selectin staining was still visible across the rest of the HUVEC. The fact that co-localisation was seen after 2 hours exposure but not 1 hour implies that the interaction is more complex than the clustering seen with leucocyte and antibody mediated cross-linking, which involve direct binding of either E-selectin specific antibody or E-selectin ligands and can typically be seen after only 10-15 minutes exposure and binding.

It is also interesting to note that the amount of spontaneous E-selectin clustering appeared much reduced upon exposure of HUVEC to *SiaD N.meningitidis* for 120 minutes as shown in Figure 5.12F compared to the IL-1β control in Figure 5.12A. The clustering of E-selectin was mostly restricted to areas beneath the adherent bacteria. This may imply that the spontaneous clustering of full length E-selectin is disrupted by the redistribution of E-selectin beneath the adherent *SiaD* colonies.

5.3.3.3 Co-localisation of E-selectin beneath adherent SiaD N.meningitidis occurs after 120 minutes exposure, but not 60 minutes or 240 minutes

Co-localisation of E-selectin beneath *SiaD*- mutant bacteria as seen in Figure 5.12F, occurred after 120 minutes of bacterial exposure, but was not seen after only 60 minutes. In order to investigate whether increased bacterial exposure time further increased E-selectin co-localisation or clustering, the exposure time of HUVEC to WT or *SiaD N.meningitidis* was increased up to 240 minutes.

In the IL-1β stimulated HUVEC control shown in Figure 5.13A, the induced E-selectin formed several spontaneous clusters, as seen in previous experiments. After 120 minutes exposure to WT *N.meningitidis,* clumps of adherent bacteria could be seen on the HUVEC in Figure 5.13B, but the clustering pattern was similar to the spontaneous clustering seen without bacterial exposure, and no co-localisation of E-selectin with the adherent bacteria was seen. After 120 minutes exposure to the *SiaD* mutant bacteria in Figure 5.13C, spontaneous clustering of E-selectin decreased, while co-localisation beneath the adhered bacteria was visible. Upon 240 minutes exposure to either WT or *SiaD* bacteria (Figure 5.13D and E), faint co-localisation of E-selectin beneath the adherent bacteria can be seen. The level of bacterial adhesion and co-localisation with E-selectin in this second donor appeared fainter than in Figure 5.12, and the amount of adhesion of the *SiaD* bacteria in Figure 5.13E is particularly low. This highlights the amount of donor variation in the level of endothelial adhesion and E-selectin expression.

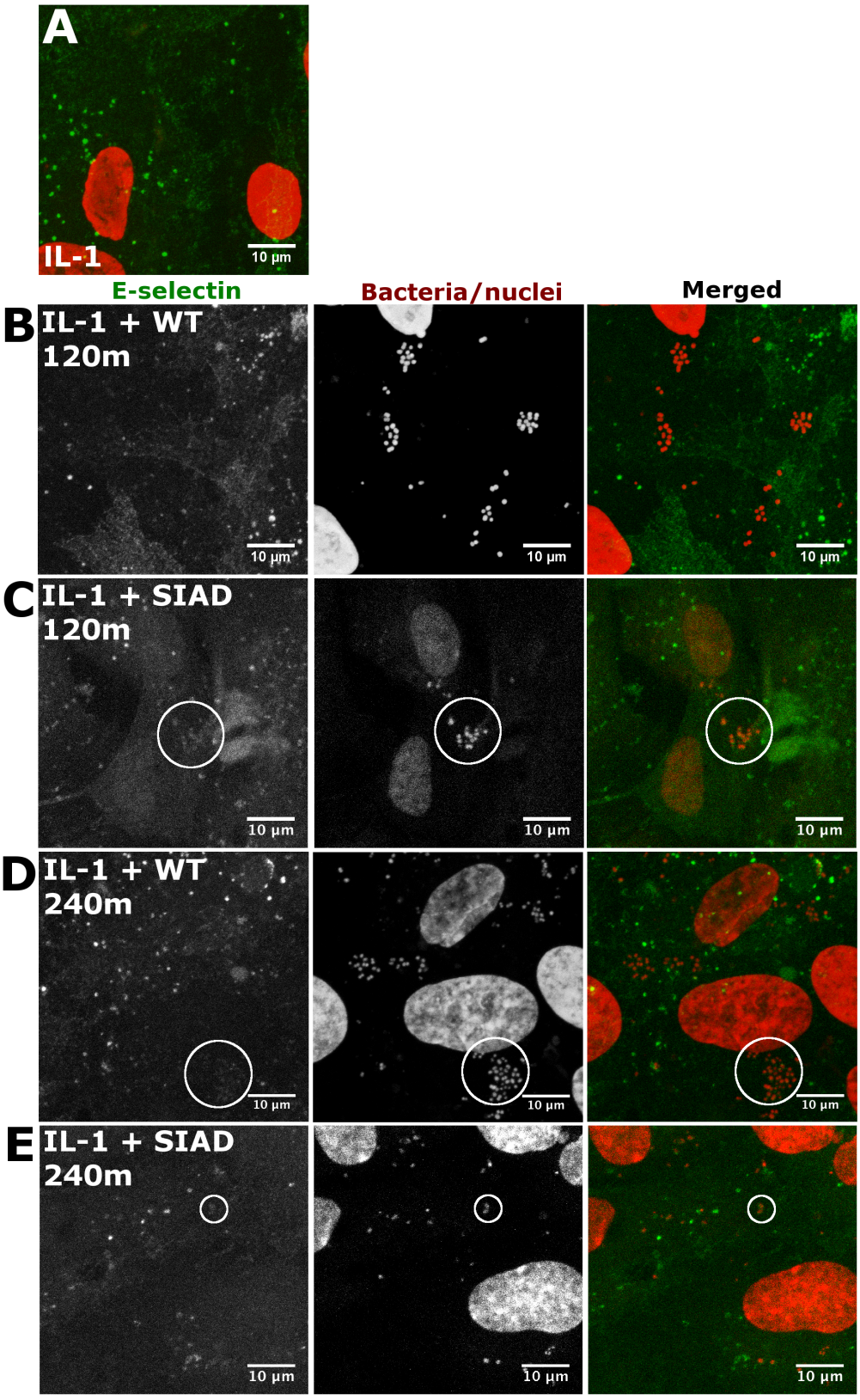

Figure 5.13: Confocal microscopy images showing co-localisation of endogenous E-selectin beneath WT and *SiaD N.meningitidis* after 240 minutes exposure, but only *SiaD N.meningitidis* after 120 minutes exposure.

HUVEC were stimulated with IL-1β for 4 hours (A), and exposed to 10^7/ml WT (B+D) or *SiaD* (C+E) *N.meningitidis* for either 120m (B+C) or 240m (D+E). Co-localisation of E-selectin with adhered bacteria (circled) occurs after 120m *SiaD* exposure (C) and faintly after 240m WT or *SiaD* exposure (D+E). Cells were stained for E-selectin (green) and DNA (red).

Increased exposure time to the *SiaD* mutant did not appear to increase co-localisation of E-selectin, or its clearance from other areas of the cell to beneath adherent bacteria. The 240 minute exposure time did however appear to show faint co-localisation of E-selectin with WT (Figure 5.13D+E), indicating E-selectin co-localisation is still possible with WT bacteria, but requires longer time.

The size of the *SiaD* microcolonies and bacterial complexes also appeared smaller in Figure 5.13 compared to Figure 5.12, with the associated clusters of co-localised E-selectin similarly smaller. In Figure 5.13E in particular, the number of adherent bacteria is much lower, and they do not appear to form large microcolonies. This may be due to donor variation in receptors for meningococcal adhesion or other factors required for bacterial adhesion. Co-localisation of E-selectin with adherent bacteria was still visible, but the clumps were smaller and had dimmer staining.

In accordance with observations in Figure 5.12F, levels of spontaneous bright E-selectin clusters on cells exposed to *SiaD N.meningitidis* for 120 minutes (Figure 5.13C) appeared reduced compared to the IL-1β stimulated cells shown in Figure 5.13A. Bright clusters were still seen on cells exposed to WT *N.meningitidis* for 120 minutes. Whether this reduced level of spontaneous E-selectin clustering was attributable to the *SiaD* mediated redistribution of E-selectin is unknown, however, the rest of the endothelial monolayer shown in Figure 5.13C also showed very little spontaneous E-selectin clustering.

5.3.3.4 ES and ΔC transfected E-selectin does not co-localise beneath adherent unencapsulated N.meningitidis

The co-localisation of E-selectin beneath adherent *SiaD* mutant bacteria did not appear to be due to direct binding, as the process of co-localisation was much slower than the clustering seen following exposure to E-selectin cross-linking antibodies or binding by adherent neutrophils, which can be seen after only 10-15 minutes of exposure.

E-selectin is known to be expressed in specific cell membrane locations such as lipid rafts and clathrin pits (Kiely et al., 2003; Setiadi and McEver, 2008), and the intracellular E-selectin tail can interact with the cytoskeleton(Yoshida et al., 1996). Given these interactions, it is possible that the E-selectin co-localisation beneath adhered *N.meningitidis* is due to *N.meningitidis* signalling through an alternative pathway and causing E-selectin redistribution by intracellular signalling and interactions with the cytoplasmic tail rather than direct extracellular binding.

In order to investigate whether intracellular signalling regulates the redistribution of E-selectin to co-localise beneath adhered *SiaD* bacteria, ES and ΔC E-selectin were transfected into HUVEC and exposed to live *SiaD* mutant *N.meningitidis* for 120 minutes.

After 120 minutes exposure, microcolonies of *SiaD* bacteria could be seen adhering to E-selectin transfected endothelial cells, however, neither the ES nor the ΔC E-selectin was seen co-localising beneath the adhered bacteria (Figure 5.14).

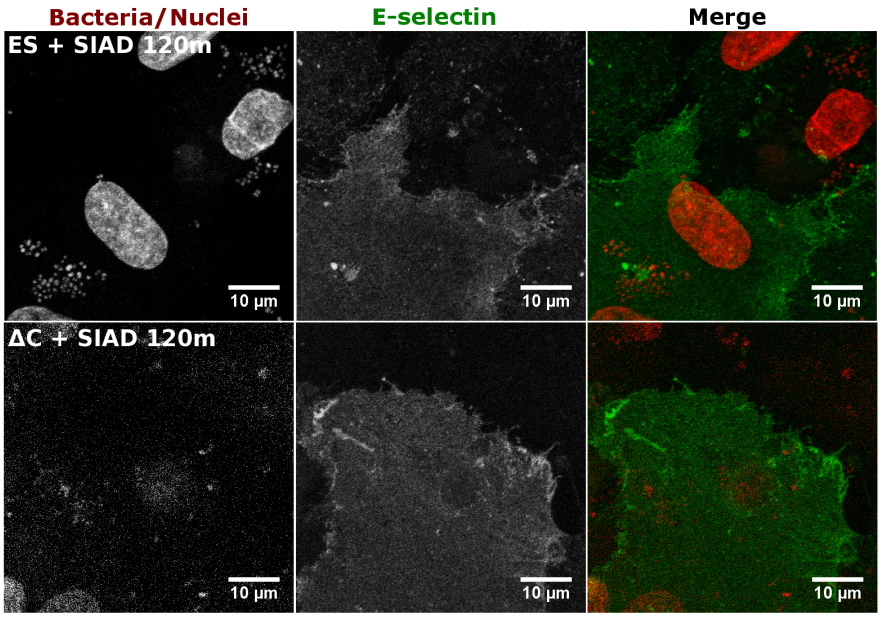

Figure 5.14: Representative images of 10^7/ml adherent *SiaD*- mutant *N.meningitidis* bacteria after 120 minutes exposure on HUVEC transfected with either full length ES or tail-less mutant ΔC E-selectin, with no co-localisation. Cells were stained for E-selectin (green) and DNA (red).

If the co-localisation of E-selectin with *SiaD* bacteria seen in Figure 5.12 and Figure 5.13 were due to intracellular signalling within the endothelial cells, then the lack of E-selectin redistribution in ΔC transfected cells would be expected, but not in ES transfected HUVEC as well. As E-selectin co-localisation was not seen in is HUVEC transfected with full length E-selectin either, it appears that there are additional elements to the co-localisation mechanism that have yet to be discovered.

One hypothesis is that transfected E-selectin is not expressed in the same cellular location as endogenous E-selectin. E-selectin transfected into CHO cells using an adenovirus vector was expressed in clathrin pits, but not in lipid rafts, whereas endogenous E-selectin is known to be expressed in both surface microdomains(Setiadi and McEver, 2008). If the expression of lentiviral transfected ES and ΔC in HUVEC follows that of adenovirial transfected E-selectin in CHO cells, then it could affect E-selectin signalling and redistribution upon *N.meningitidis* exposure. Alternatively, IL-1β stimulation upregulates a large number of different adhesion

molecules and signalling pathways, and the endothelial response that leads to E-selectin co-localisation beneath adherent bacteria could require the contribution of one or more of these other pathways that are not activated in ES or ΔC transfected HUVEC.

To summarise the experimental findings of HUVEC exposure to the *SiaD N.meningitidis* in this section; the adhesion of *N.meningitidis* bacteria to the endothelium is enhanced by the lack of capsule due to deletion of the *SiaD* gene and the subsequent exposure of outer membrane proteins. Upon binding to the endothelium, the bacteria appear to co-localise with endogenous E-selectin, and sequester it beneath microcolonies that form as the adhered bacteria divide. Although the bacterial colonies co-localise E-selectin, staining still occurs across the rest of the cell and is not cleared from the rest of the cell surface as antibody cross-linking does; the E-selectin co-localisation pattern is more similar to that seen on leucocyte binding. In addition, ES and ΔC transfected E-selectin do not appear to co-localise with adhered *SiaD N.meningitidis*.

Interestingly there also appears to be fewer bright clusters of E-selectin on the endothelial cells exposed for 120 minutes to *SiaD N.meningitidis* compared to the control IL-1β stimulated HUVEC; although it is unclear if this was due to the co-localisation re-distributing the E-selectin from the clusters, or just due to donor variation.

5.3.4 Optimisation of experimental methodology to improve reproducibility

5.3.4.1 Investigation of HUVEC permeabilisation and intracellular staining of E-selectin as a cause of spontaneous E-selectin clustering

The co-localisation of endogenous E-selectin beneath adhered *SiaD* mutant bacteria showed that redistribution due to *N.meningitidis* exposure and binding can occur, despite spontaneous E-selectin clustering with no associated stimuli also being seen. The spontaneous formation of E-selectin clusters made it difficult to make conclusions about the role of bacteria in causing E-selectin clustering. It was therefore attempted to modify the experimental technique in order to investigate the potential causes and reduce the impact of spontaneous clustering.

It was hypothesised that the staining method used may also be staining intracellular E-selectin, contained within compartments or vesicles inside the cells. This would explain the appearance of E-selectin clusters despite there being no obvious stimuli to cause clustering.

The E-selectin staining method used in the experiments described so far was Method A, as described in the materials and methods section and summarised in Figure 5.2. Whilst this

method would not be expected to stain intracellular E-Selectin, as there was no permeabilisation step, we wanted to confirm that this was the case. The effect of actual permeabilisation with Triton-X 100 on E Selectin staining was therefore determined.

The intracellular E-selectin staining results from two donors are shown in Figure 5.15; in both donors bright clusters of E-selectin resembling those seen on cross-linked cells could be seen in the HUVEC stimulated with IL-1β (Figure 5.15A), and similar clusters could be seen upon exposure to *N.meningitidis* (Figure 5.15B). A single very large aggregation of E-selectin staining was also seen directly adjacent to the nucleus in many of the cells (white arrows), which was not seen in non-permeabilised cells in previous experiments. Cells were not permeabilised before cross-linking, so all E-selectin clusters on the cross-linked cells were extracellular, and the large clump adjacent to the nucleus was not seen (Figure 5.15C).

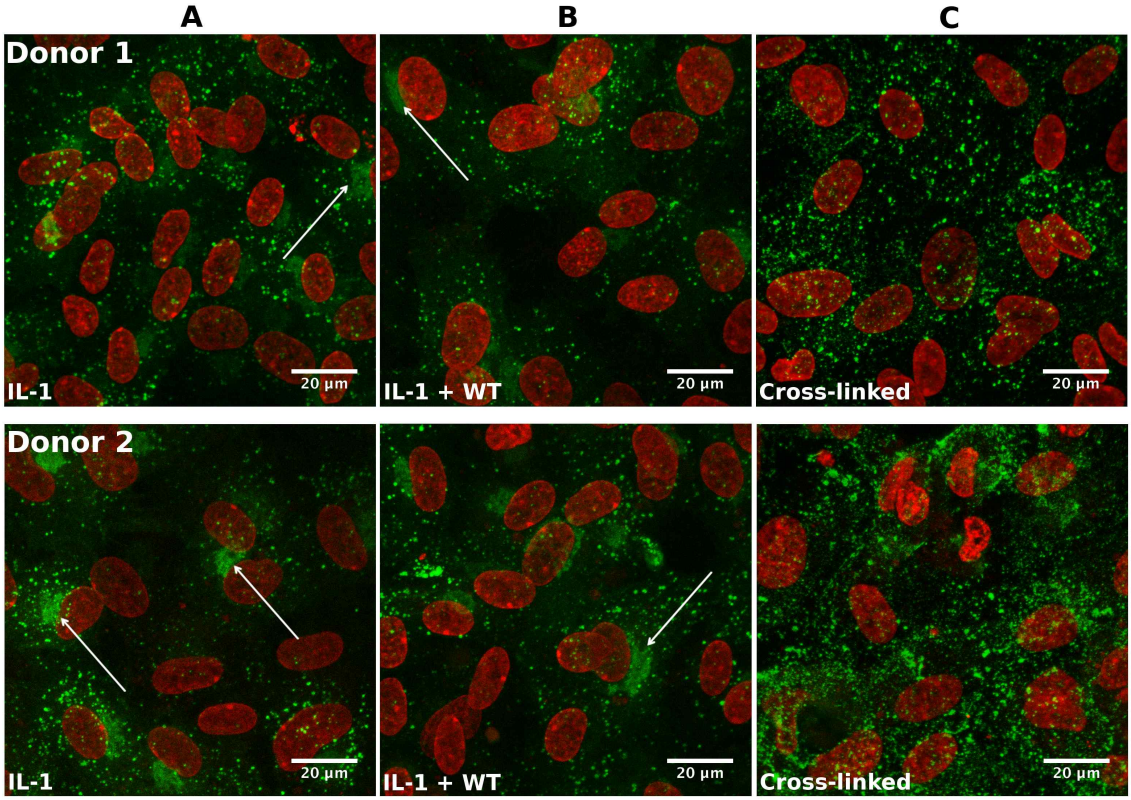

Figure 5.15: Confocal microscopy images showing endogenous E-selectin expression on both the plasma membrane and in the Golgi apparatus in HUVEC permeabilised with Triton-X100

HUVEC from donors 1 and 2 were stimulated with IL-1β for 4 hours (A), before being exposed to either 10^7/ml WT *N.meningitidis* for 1 hour (B) or E-selectin cross-linking antibodies (C). After fixation with 4% PFA, cells were permeabilised with 0.1% Triton-X 100 and then stained as normal. Cells that were cross-linked for E-selectin were not permeabilised and therefore only show extracellular E-selectin. White arrows point to large perinuclear E-selectin aggregates. E-selectin shown in green, TO-PRO3 DNA staining in red.

The perinuclear location of E-selectin seen upon intracellular staining has been described previously(Von Asmuth et al., 1992), and was investigated further using electron microscopy to show that the perinuclear E-selectin was associated with the Golgi apparatus(Von Asmuth

et al., 1992; Yoshida et al., 1996), which is important in packaging proteins before they are delivered to the cellular location where they are expressed. This distinctive structure was not stained in the cross-linked cells, or the non-permeabilised experiments shown in Figure 5.7 and Figure 5.8. This implies that the staining Method A used previously does not permeabilise cells, and the large clusters of E-selectin seen in Figure 5.7 and Figure 5.8 were indeed on the HUVEC surface.

Intracellular E-selectin staining was also investigated on ES and ΔC transfected HUVEC. Cells were transfected with ES or ΔC, or stimulated with IL-1β for 4 hours as a control (Figure 5.16A), before being exposed to WT *N.meningitidis* for 1 hour (Figure 5.16B). E-selectin staining of the IL-1β stimulated HUVEC was similar to that seen in Figure 5.15, and both ES and ΔC E-selectin were stained in a similar pattern: numerous bright clusters of E-selectin staining were seen across the cell, as well as a single large structure next to the nucleus. However, in both ES and ΔC transfected cells there was also additional extensive cytoplasmic staining, suggesting that translation and subcellular location of the transfected E-selectin may be less tightly controlled than E-selectin expressed after inflammatory stimuli such as IL-1β. There did not appear to be any observable intracellular redistribution of E-selectin staining on any of the cells upon 1 hour *N.meningitidis* exposure.

Interestingly, the bright clusters of E-selectin staining could be seen in both ES and ΔC transfected cells in Figure 5.16, despite spontaneous E-selectin clustering rarely being seen on non-permeabilised ΔC transfected cells. This suggests that many of the clusters seen in the permeabilised cells may in fact be intracellular, possibly E-selectin contained within vesicles or other intracellular compartments. In previous studies of E-selectin intracellular staining, vesicles were seen containing endocytosed E-selectin (Von Asmuth et al., 1992), contributing to the observations showing rapid E-selectin internalisation and recycling in endothelial cells. This may explain why extensive numbers of E-selectin clusters can be seen under all conditions in both Figure 5.15 and Figure 5.16, as many of the clusters of E-selectin are not on the surface of the cell but contained within intracellular vesicles.

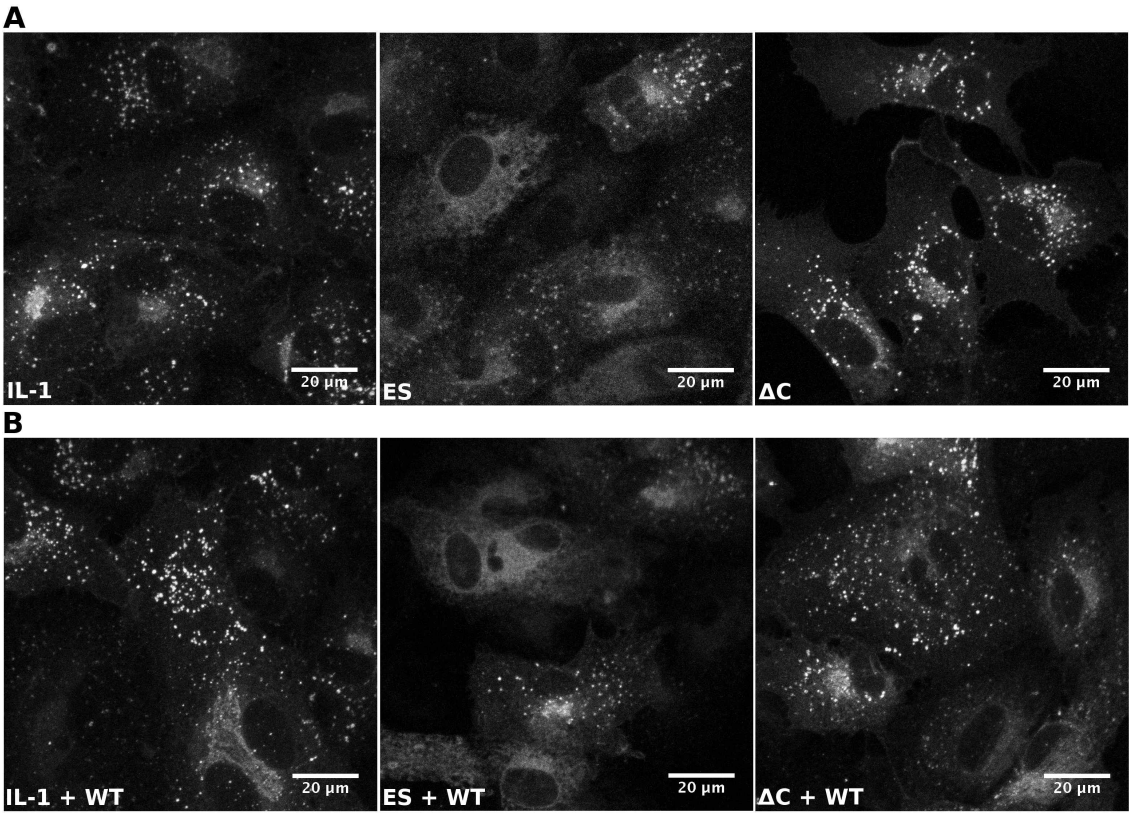

Figure 5.16: Confocal microscopy images showing expression of ES and ΔC transfected E-selectin on the plasma membrane and the Golgi apparatus in HUVEC permeabilised with Triton-X100.

HUVEC from a single donor were stimulated with IL-1β for 4 hours or transfected with ES or ΔC E-selectin (A), then exposed to 10^7/ml WT *N.meningitidis* for 1 hour (B). Cells were fixed in 4% PFA before permeabilisation with 0.1% Triton-X 100 and E-selectin staining.

In conclusion, permeabilisation of the endothelium before E-selectin staining results in a distinct staining pattern that shows both cytoplasmic and surface location of E-selectin. The distinctive E-selectin staining of a large structure next to the nucleus when the fixed cells are treated with Triton-X 100, described previously as the Golgi apparatus, is not visible in non-Triton-X 100 treated cells such as those with cross-linked E-selectin or seen in experiments earlier in the chapter. This indicates that the normal staining Method A does not permeabilise the cells, and all E-selectin staining on these cells is expressed on the cell surface.

5.3.4.2 Modification of E-selectin staining technique to remove potential spontaneous E-selectin clustering artefacts

Permeabilisation of the HUVEC with Triton-X 100 prior to staining with E-selectin antibody had shown that the spontaneous E-selectin clusters seen in the experiments so far was on the cell membrane and was not intracellular. In order to investigate whether other aspects of the experimental protocol were influencing the distribution of E-selectin staining and causing spontaneous clustering, further modifications were made to the experimental

protocol, including altering the order of some experimental steps. Additionally, alternative primary and secondary antibody clones were tested to see whether the specific antibodies used made a difference to the E-selectin staining, however the use of different primary and secondary antibodies did not appear to reduce the level of spontaneous clustering at all (Appendix C-1).

It was hypothesised that while the fixation of endothelial cells using 4% PFA does not permeabilise the cells, it may change the structure and distribution of the epitopes recognised by the anti-E-selectin antibody, which has been described previously for other antigens (Brock et al., 1999; Schnell et al., 2012). In order to investigate whether this was having an affect on the E-selectin staining, a second staining technique was developed (Method B, described in more detail in section 5.2.3 and Figure 5.2). Briefly, the cells were stained with the primary antibody before fixation with 4% PFA, and then after primary antibody staining, cells were fixed and stained with secondary antibody as previously described.

Figure 5.17 shows HUVEC from a single donor either stimulated with IL-1β for 4 hours or transfected with ES or ΔC E-selectin, and stained using either Method A (Figure 5.17A), the original staining protocol used in the figures up to this point, or Method B (Figure 5.17B-D).

In both IL-1β stimulated and ES transfected HUVEC, but not ΔC transfected, there was considerable spontaneous clustering of E-selectin on the cell surface when stained using Method A (Figure 5.17A). The level of spontaneous clustering in all conditions however appeared to be greatly reduced when stained using Method B (Figure 5.17B). E-selectin could be seen in a more dispersed pattern throughout the cells, with only a few spontaneous clusters rather than the large number seen in the cells stained with Method A. There was not much difference however in the staining of ΔC E-selectin between Method A or B, as spontaneous clusters were rarely seen with either staining method.

When exposed to WT *N.meningitidis* for 60 minutes in Figure 5.17C there did not appear to be any additional induced clustering of E-selectin seen on any of the cells, whether the expressed E-selectin was endogenously induced by IL-1β, or transfected by lentivirus. The method for the antibody cross-linking control shown in Figure 5.17D was not changed, and showed that both endogenous and transfected ES and ΔC E-selectin could still form clusters upon antibody cross-linking.

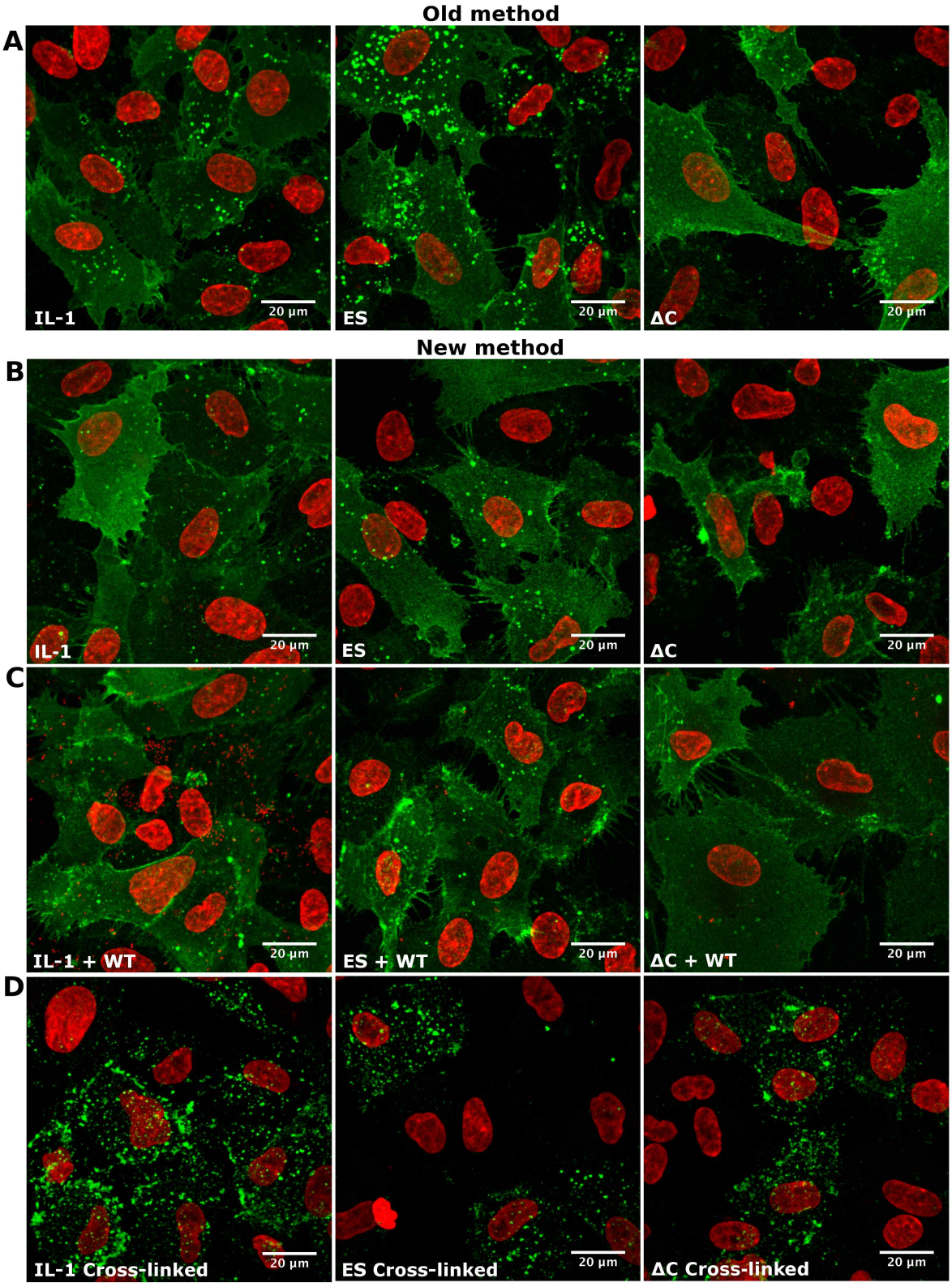

Figure 5.17: Confocal microscopy images comparing the staining of endogenous and transfected E-selectin using the three staining methods: Method A, Method B, or antibody cross-linking.

Representative images showing the difference in E-selectin staining between two different staining protocols, Method A (A) and method B (B, C, D), described in section 5.2.3. E-selectin expression was induced on HUVEC by either IL-1β stimulation or transfection with ES or ΔC lentivirus (A and B), and then exposed to 10^7/ml WT *N.meningitidis* for 60 minutes (C) or incubated with cross-linking antibodies (D). E-selectin shown in green, TO-PRO3 DNA staining in red.

There were concerns that addition of the primary antibody while the cells were still alive would lead to greater E-selectin clustering, as had been seen in a previous publication (Wójciak-Stothard et al., 1999). However lower levels of E-selectin clustering were seen in the experiments above, and cross-linking of E-selectin was found to require addition of both the primary and secondary antibodies before cell fixation. The primary antibody binds to E-selectin, before the secondary antibody cross-links the bound primary antibodies to create large complexes, forming the extensive clustering pattern seen in Figure 5.17D.

Although the results in Figure 5.12 showed co-localisation of E-selectin beneath adherent *SiaD N.meningitidis* colonies that were stained using Method A, there was unfortunately not enough time towards the end of the project to attempt these co-localisation experiments using the different staining Method B.

Despite the challenges regarding the staining methodology and donor variation in affecting E-selectin staining, the conclusions from these modifications of the experimental technique show that staining with the primary antibody before fixation in 4% PFA reduced the level of spontaneous clustering compared to staining after fixation. Addition of both antibodies while the cells were alive however results in cross-linking and clustering of almost all the expressed E-selectin. Despite the different staining method, exposure to WT N.meningitidis for 60 minutes still failed to initiate observable further E-selectin clustering using the Method B staining method, both in Figure 5.17C and additional repeats.

5.4 Conclusions and Discussion

5.4.1 Formation of large E-selectin clusters is not consistently observed as a result of *Neisseria meningitidis* exposure on endothelial cells

Although endogenous IL-1β induced E-selectin clustering was seen in response to *N.meningitidis* exposure in some donors (Figure 5.7), the result was not reproducible. This was largely due to spontaneous clustering in the control conditions making the data hard to interpret (Figure 5.8). These results do not disprove the hypothesis that *N.meningitidis* can cause redistribution of E-selectin on the surface of endothelial cells, but equally the evidence is too unreliable to prove the hypothesis true.

This variation in E-selectin clustering would have been more easily explained by simple donor variation had it only occurred in a minority of experiments; however, a large number of repeat experiments were carried out while attempting to identify a factor that may have caused this spontaneous clustering, and over time the majority of experiments showed aberrant spontaneous clustering under IL-1β stimulated conditions.

Other publications that show E-selectin immunofluorescence microscopy staining also show a range of different staining patterns under similar conditions, some of which appear to show fairly diffuse E-selectin staining(Setiadi and McEver, 2008; Wójciak-Stothard et al., 1999; Yoshida et al., 1996), while others show more spontaneous clusters(Kiely et al., 2003; Tremblay et al., 2006; Wójciak-Stothard et al., 1999). This reinforces the idea that E-selectin expression and distribution can be extremely variable depending on both donor variation and staining techniques, as well as additional unknown confounding factors.

5.4.2 Changing the E-selectin staining method reduced E-selectin spontaneous clustering

Attempts were made to modify the E-selectin staining technique in order to investigate and reduce the spontaneous E-selectin clustering, and therefore allow a clearer view of the E-selectin redistribution caused by endothelial-meningococcal interactions.

The spontaneous clustering was shown to be unrelated to artefacts caused by the specific E-selectin antibody clone used, as other primary and secondary antibodies were tested and found to form similar staining patterns (Appendix Figure C-1). The clusters were also shown to occur on the cell surface, as endothelial cells permeabilised with Triton-X 100 showed E-selectin staining within a large structure next to the nucleus, which has been described previously only in permeabilised endothelial cells and is thought to be the Golgi apparatus (Von Asmuth et al., 1992); this structure would have been seen in previous experiments had the staining Method A been permeabilising cells (Figure 5.15).

Changing the staining technique by altering the order of incubation with the reagents, i.e. by switching from Method A to Method B, however does appear to alter the observed E-selectin expression pattern on the HUVEC, and reduces the extensive spontaneous clustering seen with both full-length IL-1β induced and ES transfected E-selectin when stained with Method A (Figure 5.17).

The original hypothesis that led to the change in staining method was that fixation of the HUVEC in 4% PFA may modify the E-selectin epitopes in some way, leading to aberrant clustering staining; which has been reported for certain cell membrane components previously(Brock et al., 1999; Schnell et al., 2012). It was unclear whether this was the reason for the reduced clustering seen with Method B staining, however, this should be taken into consideration when interpreting data and may help explain data variability.

An alternative explanation for the reduction in spontaneous clustering when staining with Method B however is that the spontaneous clusters were caused by some other factor

present in the media or experiment, and the binding of primary antibody to E-selectin on the live cell membrane may somehow interfere with the molecular interactions causing E-selectin spontaneous clustering; subsequently disrupting the clusters. The epitope recognised by the primary antibody may be involved in the clustering reaction, and blocking it may have blocked the interactions. Alternative anti-E-selectin antibodies were not used to test the staining Method B; so alternative epitopes were not evaluated.

This hypothesis has additional implications when assessing the experiments showing co-localisation of adhered *SiaD* with E-selectin, as the fact that spontaneous clustering of E-selectin appears to be reduced both upon addition of anti-E-selectin antibody prior to fixation, and co-localisation of E-selectin beneath adherent *SiaD N.meningitidis* may imply that both stimuli can inhibit the interactions that cause spontaneous E-selectin clustering.

In order to potentially mitigate the effects of disruption of E-selectin expression pattern on the endothelial surface by fixation in future experiments, a possible future approach may be to evaluate E-selectin expression patterns in real time using live cell imaging. Labelling of E-selectin using a fluorescent-conjugated antibody to a non-essential epitope on the surface(Runnels et al., 2006), or intracellular labelling using a fluorescent protein such as GFP could be used to investigate the redistribution of E-selectin upon exposure to both *N.meningitidis* and neutrophil adhesion. Experiments investigating other endothelial cell adhesion molecules such as ICAM-1, JAM-A or VE-cadherin using live immunofluorescence imaging have used both GFP-tagged proteins (Yang et al., 2005, 2006a, 2006b) and antibodies conjugated to fluorescent molecules (Shaw et al., 2004; Yang et al., 2005) with little effect on the adhesion molecule function.

5.4.3 Tail-less ΔC E-selectin forms far fewer spontaneous clusters than full length ES or endogenous E-selectin

One interesting observation that was consistently repeatable was the expression pattern of the tail-less ΔC mutant transfected E-selectin; which only rarely formed spontaneous clusters (Figure 5.3, Figure 5.9) compared to both the full-length ES transfected E-selectin and IL-1β induced endogenous E-selectin, which often formed spontaneous clusters. The lack of spontaneous clustering of tail-less ΔC E-selectin implies that this pattern of expression involves interactions of the E-selectin intracellular region with the cytoskeleton and other intracellular pathways.

The E-selectin intracellular tail interacts with several components of the endothelial cytoskeleton, which can affect both E-selectin distribution and re-internalisation. Full-length

E-selectin is expressed on the endothelial surface in both lipid rafts, which function as platforms for signalling receptors(Kiely et al., 2003; Korade and Kenworthy, 2008; Setiadi and McEver, 2008; Tilghman and Hoover, 2002b), and clathrin-coated pits, which are associated with endocytosis of surface molecules(McMahon and Boucrot, 2011; Setiadi and McEver, 2008). Tail-less E-selectin on the other hand does not associate with clathrin-coated pits, and has impaired re-internalisation(Chuang et al., 1997; Kluger et al., 2002; Setiadi and McEver, 2008). It is unclear whether tail-less E-selectin can associate in lipid rafts, however lipid raft association is required for E-selectin signalling via the PLCγ pathway as well as interactions with cortactin and the cytoskeleton(Kiely et al., 2003; Tilghman and Hoover, 2002a, 2002b).

It is possible that the high spontaneous clustering of full-length E-selectin compared to tail-less ΔC mutant is related to its association with Clathrin pits and lipid rafts, and the subsequent interactions with the cytoskeleton that can occur with the E-selectin tail. The variation between donors may then be partially due to the differences in the composition and number of these membrane microdomains. It would be interesting to investigate this further, by using antibodies against other components that are commonly associated with clathrin pits, such as α-adaptin (Kirchhausen, 1999; Setiadi and McEver, 2008), or lipid rafts, such as Caveolin-1, flotilin, Lyn, and the IgE Fc receptor (Gassart et al., 2003; Setiadi and McEver, 2008; Tilghman and Hoover, 2002b; Wilson et al., 2004), and seeing whether this co-localises with the spontaneous E-selectin clusters seen in this experiment.

5.4.4 IL-1β induced E-selectin on HUVEC co-localises with adherent *SiaD* mutant *N.meningitidis*

60 minutes stimulation of endothelial cells with the acapsulate *SiaD N.meningitidis* mutant did not appear to induce any greater clustering of E-selectin than WT bacteria (Figure 5.10); however after 2 hours exposure to live *SiaD N.meningitidis,* co-localisation of endogenous E-selectin could be seen beneath adhered *SiaD* bacteria in Figure 5.12, and beneath both *SiaD* and WT *N.meningitidis* after 4 hours exposure in Figure 5.13. This shows direct evidence for redistribution of E-selectin due to *N.meningitidis* exposure, with much less ambiguity than the earlier experiments looking for bright E-selectin clusters in response to the bacteria, which were often masked by spontaneous clustering.

As mentioned previously, it was also noticeable that there appeared to be much fewer bright clusters seen on cells where meningococcal co-localisation with E-selectin was seen. It is possible that both the E-selectin co-localisation beneath adhered *SiaD N.meningitidis* in

Figure 5.12, as well as the increased bright clustering seen upon meningococcal stimulation in Figure 5.7 are both caused by related pathways in the endothelial cells; with both stimuli causing redistribution of E-selectin prompted by *N.meningitidis* interactions with the endothelium. This would mean that the redistribution of endothelial E-selectin in response to *N.meningitidis* can occur in different ways, perhaps based on donor variation or other confounding factors. HUVEC stained with staining method B in Figure 5.17 also showed reduced spontaneous clustering, which combined with these results may imply that the redistribution of E-selectin by either direct antibody binding or co-localisation via intracellular reorganisation has similar effects on the disruption of the spontaneous clusters.

Bacterial co-localisation with endothelial E-selectin is probably too slow for it to be due to direct binding of *N.meningitidis* bacteria to the E-selectin adhesion molecule, as occurs in leucocyte or antibody mediated E-selectin cross-linking; and indicates that the redistribution of E-selectin on the endothelial surface may be due to *N.meningitidis* binding to some other endothelial membrane component and activating an intracellular pathway that re-distributes E-selectin via signalling to the E-selectin cytoplasmic domain. WT *N.meningitidis* induces much less E-selectin co-localisation than the *SiaD* mutant, which suggests that the increased adhesiveness of the *SiaD* mutant, due to the availability of the Opa and Opc proteins, has a strong affect on E-selectin redistribution.

Intriguingly, co-localisation with *SiaD N.meningitidis* was only seen with endogenous E-selectin induced by IL-1β stimulation. Neither ES nor ΔC transfected E-selectin co-localised with adherent bacteria despite high expression of transfected E-selectin. The reasons for this difference between endogenous and transfected E-selectin were unclear; if co-localisation was solely controlled by intracellular signalling and cytoskeletal interactions with the cytoplasmic domain then full length ES E-selectin would be expected to behave in a similar way to endogenous E-selectin, however neither ES nor tail-less ΔC E-selectin co-localise with adhered *N.meningitidis*.

It is possible that the transfected ES and ΔC were expressed in a different part of the cell membrane or did not interact with the intracellular components in the same way. As discussed earlier, it has been shown that ES and ΔC E-selectin transfected into CHO cells using an adenovirus vector is expressed in clathrin pits, but has much lower expression in lipid rafts compared to endogenous E-selectin(Setiadi and McEver, 2008), it is possible that both forms of transfected E-selectin are expressed in a different membrane microdomain compared to endogenous E-selectin. Another potential explanation is that the redistribution

of E-selectin is caused by *N.meningitidis* binding to and activating a surface molecule that is upregulated by IL-1β, and is therefore not present on ES or ΔC transfected cells.

Co-localisation of adherent *N.meningitidis* bacteria with E-selectin has previously been reported using a specific serogroup C strain (Doulet et al., 2006). E-selectin, along with other endothelial CAMs and cytoskeletal associated proteins such as ezrin and moesin, form clusters beneath the microcolonies, with microvilli-like protrusions extending around and between adherent bacteria, helping to anchor them in place against the blood flow (Eugène et al., 2002; Mikaty et al., 2009). Other studies by the same group showed that this clustering could also assist traversal of the endothelial layer(Coureuil et al., 2009, 2010), and reduce the effectiveness of neutrophil migration by sequestering the majority of their endothelial ligands(Doulet et al., 2006).

My results back up some of these findings, however, they do not corroborate all of them: In Figure 5.12 E-selectin co-localisation is seen directly beneath the adhered bacteria, whereas in the confocal images from Doulet et al, reproduced in Figure 5.18, the clustering of E-selectin and CAM staining is seen between the adherent bacteria, in membrane protrusions. These protrusions were not seen between bacteria in the images presented in this chapter, although protrusions were seen around adhered neutrophils in Figure 5.4B and Figure 5.5C+D. This may however be due to the confocal microscopy z-stacks not being detailed enough to show this around the adhered bacteria.

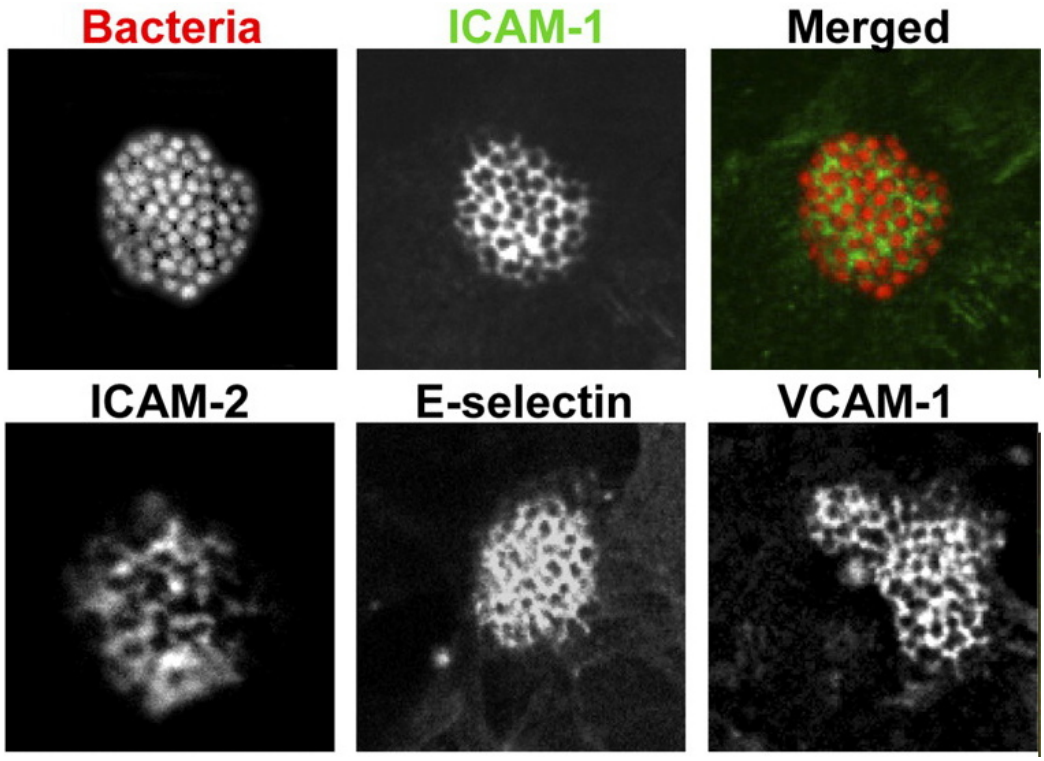

Figure 5.18: Microscopy images adapted from Figure 3 of (Doulet et al., 2006), showing recruitment and clustering of E-selectin and other adhesion molecules beneath *N.meningitidis* microcolonies.

HBMEC cells were activated with 100U/ml TNF-α for 24 hours before being infected with the 2C43 strain of *N.meningitidis* for 2 hours, fixed, and then stained for various Cell Adhesion Molecules.

Neither these co-localisation experiments nor those in other publications showing clustering beneath adhered *N.meningitidis* used a WT strain. Doulet et al, 2006, used a piliated, encapsulated, Opa-, Opc- MenC mutant (2C43) of the 8013 strain (Nassif et al., 1993; Pujol et al., 1999), whereas the strain used in the experiments presented in this chapter was a *SiaD*- Opa+, Opc+ mutant of the H44/76 MenB strain. It is interesting that co-localisation after 2 hours meningococcal exposure was seen under two very different mutant strains of *N.meningitidis*, but not with WT bacteria, although it is possible that this is due to the reduced adhesion of the WT strain.

The major difference between the WT and *SiaD* mutant H44/76 MenB bacteria used in the experiments above is the presence of capsule obscuring the outer membrane adhesins, allowing the mutant to adhere in much greater numbers to the endothelium. Doulet et al, along with others from the same group, have described the co-localisation of the 2C43 strain with endothelial adhesion molecules and cytoskeletal components as reliant on pilus expression (Brissac et al., 2012; Coureuil et al., 2009; Hoffmann et al., 2001); and in other experiments un-piliated, Opa+ strains do not produce co-localisation with cytoskeletal components despite extensive adhesion to the endothelium(Lécuyer et al., 2012). It is

possible that the E-selectin co-localisation seen in this chapter with the *SiaD* mutant H44/76 strain of *N.meningitidis* is also pilus mediated, although this would not explain why *SiaD-N.meningitidis* had greater levels of co-localisation than WT. It is possible however that the increased adhesion of the *SiaD* mutant to the endothelium facilitates a greater level of co-localisation compared to WT *N.meningitidis*.

In order to investigate the discrepancies between the co-localisation results from these two mutant strains, and to see whether the co-localisation effects were enhanced by Opa and Opc expression, future work would include obtaining a sample of the 2C43 MenC Opa- Opc- mutant used in the publications from this group, along with the WT 8013 strain, and carrying out side by side co-localisation experiments to compare the amount of bacterial adhesion and co-localisation of E-selectin caused by the H44/76 and 2C43 strains.

In conclusion, the effect of *N.meningitidis* exposure on E-selectin redistribution is still unclear. While the *SiaD* strain can adhere strongly to the endothelium and co-localise with endogenous E-selectin; co-localisation with transfected full-length or tail-less E-selectin was not observed. The reasons for this are unclear, although the differing levels of localisation of endogenous or transfected E-selectin in membrane microdomains such as lipid rafts and clathrin pits may play a role in its redistribution, and there may be additional factors induced by IL-1β stimulation that are not present in ES or ΔC transfected cells. Future work could concentrate on investigating the distribution of ES and ΔC expression in cell membrane microdomains, and examining whether the interactions of the E-selectin cytoplasmic tail affect the fractionation of ES and ΔC transfected E-selectin with the same membrane components of clathrin pits and lipid rafts as endogenous E-selectin, as well as whether the spontaneous *N.meningitidis* induced clusters co-localise with these membrane microdomains upon confocal fluorescence staining.

The differences in E-selectin co-localisation beneath the H44/76 MenB *SiaD N.meningitidis* mutant and the 2C43 MenC Opa- Opc- mutant could also be investigated, as both mutants are very different, although produce similar co-localisation results which are not seen, or seen to a lesser extent, with WT bacteria. A side-by-side comparison of E-selectin co-localisation using both of these strains with the same staining technique would allow greater insight into the contribution of the Opa and Opc adhesins into this effect. Previous reports have indicated that the co-localisation of E-selectin, as well as other adhesion molecules and cytoskeletal components, with adherent *N.meningitidis* is pilus mediated, and so the E-selectin co-localisation of H44/76 pilus mutants would also be interesting to investigate.

6 The effects of *Neisseria meningitidis* on neutrophil adhesion and transmigration through the endothelium

6.1 Introduction

In the previous chapter, E-selectin redistribution due to *N.meningitidis* exposure was studied. These results suggest that E-selectin may form clusters upon *N.meningitidis* stimulation, however the data was variable due to reasons discussed previously. Co-localisation of endogenous E-selectin beneath adherent *SiaD* mutant bacteria was observed, however it is unclear how this affects E-selectin function. In order to further understand the effects that *N.meningitidis* may have on the endothelium, some of the more functional aspects of the E-selectin response were examined, focussing specifically on recruitment and transmigration of neutrophils on the endothelium.

The major known function of E-selectin is as an adhesion molecule in the early stage of leucocyte adhesion to the endothelium. E-selectin forms weak contacts with Sialyl-Lewis X antigen ligands on leucocytes, especially granulocytes(Hidalgo et al., 2007), which slows their rolling and allows the formation of stronger integrin-mediated contacts between the rolling neutrophils and other endothelial adhesion molecules such as ICAM-1 and VCAM-1 (Smith et al., 1989; Yago et al., 2010; Zarbock et al., 2007).

Neutrophil recruitment to the endothelium is likely to be one of the major steps in the pathogenesis of meningococcal disease, as the widespread activation of neutrophils leads to the release of cytotoxic granules that cause the extensive endothelial and tissue damage associated with *meningococcal* infection (Heyderman et al., 1999; Klein et al., 1996; Westlin and Gimbrone, 1993). Low neutrophil blood counts may be due to increased neutrophil recruitment to the endothelium and emigration from the circulation, and may explain why neutropenia is a factor indicative of a poor prognosis in patients with meningococcal disease (Gedde-Dahl et al., 1990).

N.meningitidis stimulation of the endothelium has previously been shown to induce higher levels of E-selectin expression compared to stimulation by other pro-inflammatory molecules such as IL-1β or LOS, although all three stimuli induce similar levels of other endothelial CAMs (Dixon et al., 2004). Combined with experiments in the previous chapter showing E-selectin redistribution and co-localisation beneath adherent *N.meningitidis*, this implies a specific relationship between *N.meningitidis* and E-selectin that directly leads to the recruitment and activation of neutrophils that is characteristic of meningococcal infection.

6.1.1 Aims and objectives

The aims of this chapter were to investigate the functional effects of *N.meningitidis* exposure on E-selectin mediated neutrophil adhesion and subsequent transmigration through the endothelium. Furthermore, the contribution of the E-selectin intracellular domain on neutrophil adhesion and migration was explored by studying adhesion to both endogenous E-selectin, as well as ES full length and ΔC mutant transfected E-selectin.

In order to achieve this, human endothelial cells were exposed to neutrophils under both static and physiological flow conditions. Static neutrophil adhesion was measured by counting the number of adherent neutrophils on confocal microscopy images of the endothelium; while neutrophil rolling, adhesion and transmigration under physiological flow were measured by analysing time lapse video recordings of neutrophils flowing over endothelial cell monolayers in flow chambers.

6.2 Methods

6.2.1 Neutrophil isolation

Neutrophils were isolated using polymorphprep density separation, which is described in more detail in section 2.6, as well as confirmation of isolated neutrophil purity by flow cytometry.

6.2.2 Neutrophil adhesion under static conditions

Endothelial cells were grown on glass cover slips coated with fibronectin, and either transfected with the full-length ES or mutant ΔC E-selectin lentiviral constructs, or left untransfected. Once confluent, HUVEC were either exposed to 10^7 *N.meningitidis* bacteria for 60 minutes, or left unexposed. Neutrophils were added to the endothelial monolayers 15 minutes before the end of the experiment and allowed to adhere. Cover slips were washed in sterile PBS to remove non-adherent neutrophils, before being fixed with 4% PFA and stained with mouse anti-CD66b antibody followed by a FITC goat anti-mouse antibody and TO-PRO3 DNA stain. Five fields of view (1.4x1.4mm) were analysed by confocal microscopy for each stimulation condition, with a representative image shown in Figure 6.1. The number of adherent cells was then counted per field of view.

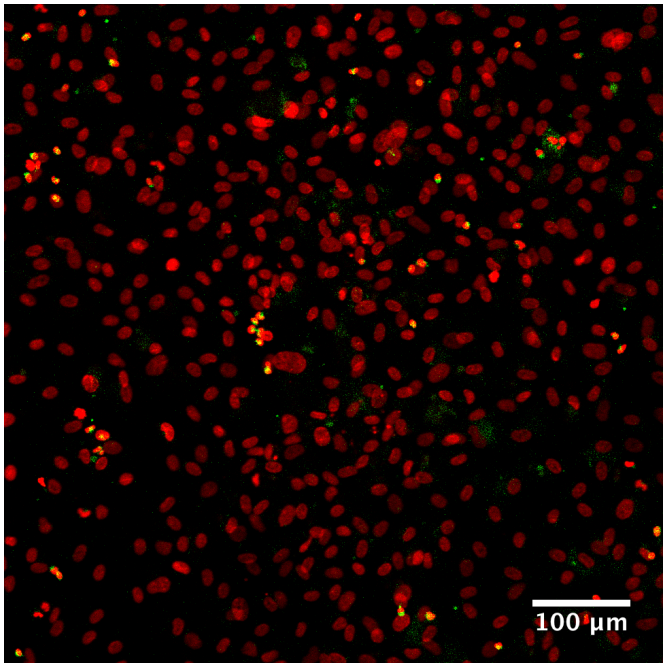

Figure 6.1: Representative confocal microscopy image showing neutrophils adhered to IL-1β stimulated endothelial cells under static conditions.

CD66b-FITC stained neutrophils (green) adhere to IL-1β stimulated HUVEC monolayers. Nuclei (red) of both HUVEC and neutrophils are stained with TO-PRO3. Adherent neutrophils appear yellow as the FITC and TO-PRO3 nuclear staining co-localise, neutrophils also have distinct multi-lobed nuclei compared to the large round endothelial nuclei.

6.2.3 Measurement of neutrophil adhesion under flow conditions using a metal parallel plate flow chamber

The metal parallel plate flow chamber was used to perform the physiological flow experiments at first as it had been inherited from a previous group member. A photograph of the metal parallel plate flow chamber is shown in Figure 6.2A, with the components arranged in the order in which they fit together. Figure 6.2B shows the order of assembly of the components, with the 0.1mm gasket forming a 0.1mm deep watertight chamber between the Thermanox cover slip and the Perspex flow channel, which contained input and output channels.

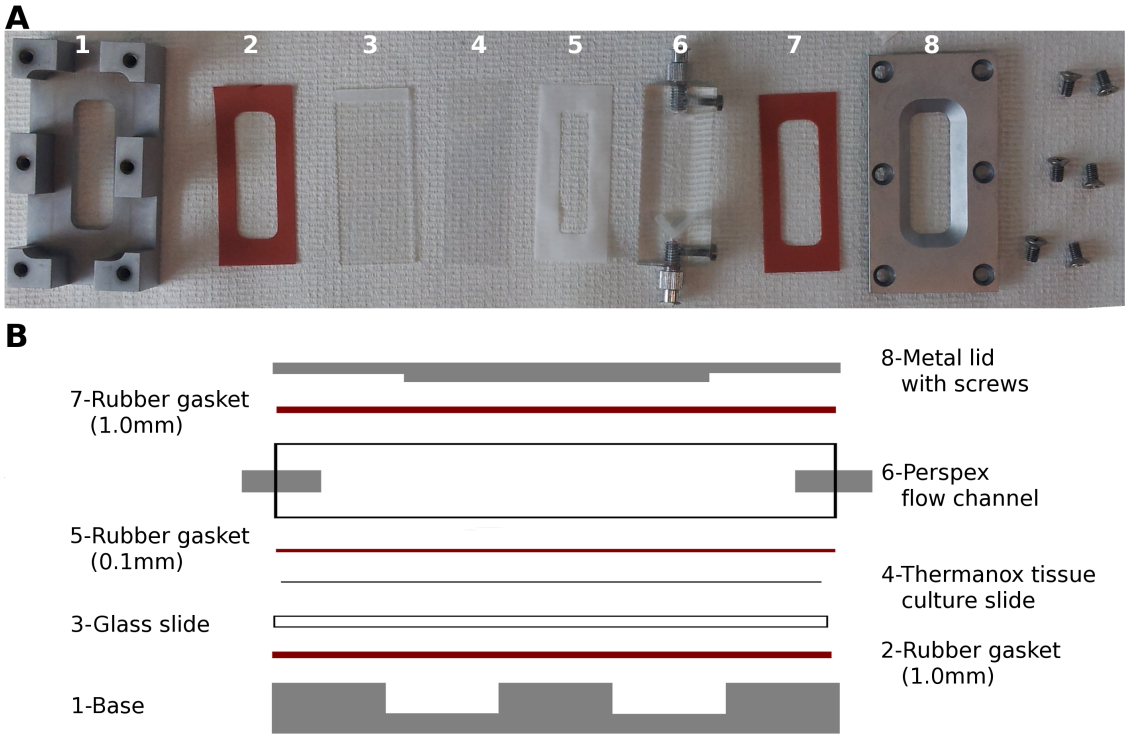

Figure 6.2: Diagram of the metal parallel plate flow chamber used to capture video of neutrophil-endothelial interactions under flow

(A) Photograph showing individual components of the metal flow chamber, and (B) Diagram showing the order of construction for the different components in order to create a watertight chamber.

Firstly a 1.0mm rubber gasket was placed inside the metal base, which provided a watertight seal at the bottom of the chamber, and the metal base provided stability when in use. A glass slide was placed on top of the rubber gasket, and a 22x60mm Thermanox (NUNC) plastic cover slip (coated in HUVEC) was placed on top of that with the cells facing up. The HUVEC were grown on disposable Thermanox cover slips as they provide a surface designed for endothelial cell growth, and are the correct size to fit inside the chamber.

A 0.1mm gasket was placed carefully on top of the HUVEC coated cover slip; the gasket contained a 10mm wide window, creating the chamber through which the neutrophil containing media flows. The Perspex flow channel was then carefully placed on top of the 0.1mm gasket, avoiding bubbles, creating a 0.1x10mm cross sectional channel with the HUVEC coated slide forming the bottom. The Perspex flow channel contained Luer-lock outlets at either end where 1mm silicone tubes could be affixed to allow fluid to pass through the chamber. A second 1mm rubber gasket was placed on top of the Perspex flow channel, and the metal lid screwed on to keep the chamber watertight and all the components in place. All the opaque components (metal chamber and rubber gaskets) contained viewing windows, so that the HUVEC and the chamber above them could be viewed with a microscope.

Once the parallel plate flow chamber was constructed with the HUVEC coated cover slip inside, Luer-lock tubes were fitted to the input and output connections of the chamber, and 20% RPMI was passed through to wash any cellular debris from the chamber. A KDS220 syringe pump (KD Scientific) holding a 50ml syringe was used to perfuse fluid at a constant rate of 6.7 ml/hour, which corresponded to a shear stress rate of 1 dyne/cm^2. The flow rate is calculated using an equation derived from Navier-Stokes equations describing fluid motion:

$$\tau = \frac{6Q\mu}{wh^2}$$

Where τ=shear stress, Q=flow rate, μ=fluid viscosity (0.076), w=width of channel and h=height of channel

The shear stress rate of 1 dyne/cm^2 is comparable to the sheer stress encountered in the bloodstream in some capillaries, which can vary between 1-10 dyne/cm^2, and is typical for post-capillary venules, which can be between 1-5 dyne/cm^2 (Sheikh et al., 2003). During inflammation, as occurs during sepsis and meningococcal disease, blood vessels also dilate, reducing both blood pressure and endothelial sheer stress, making it easier for both meningococci and leucocytes to attach and roll on the endothelium (Paize et al., 2012). The sheer stress rate of 1 dyne/cm^2 was chosen to be comparable to the flow rate conditions in the post-capillary venules during sepsis.

After a few minutes of 20% RPMI flowing through the chamber to clear debris, the pump was paused and the silicone tube clamped to prevent bubble formation while the input tube was switched to a falcon tube containing neutrophils at 5x10^5 cells/ml. The neutrophils were passed through the chamber for 4 minutes at 1 dyne/cm^2, before being switched back to plain media again.

Video was taken with a Hamamatsu Orca-ER C4742-80 camera attached to an Axiovert 135 inverted microscope, and recorded onto hard drive using Volocity 3D image analysis software (Perkin Elmer). Volocity files were exported to tiff format and analysed in FIJI ImageJ image analysis software(Schindelin et al., 2012). A basic diagram of the flow chamber and microscope setup is shown in Figure 6.3.

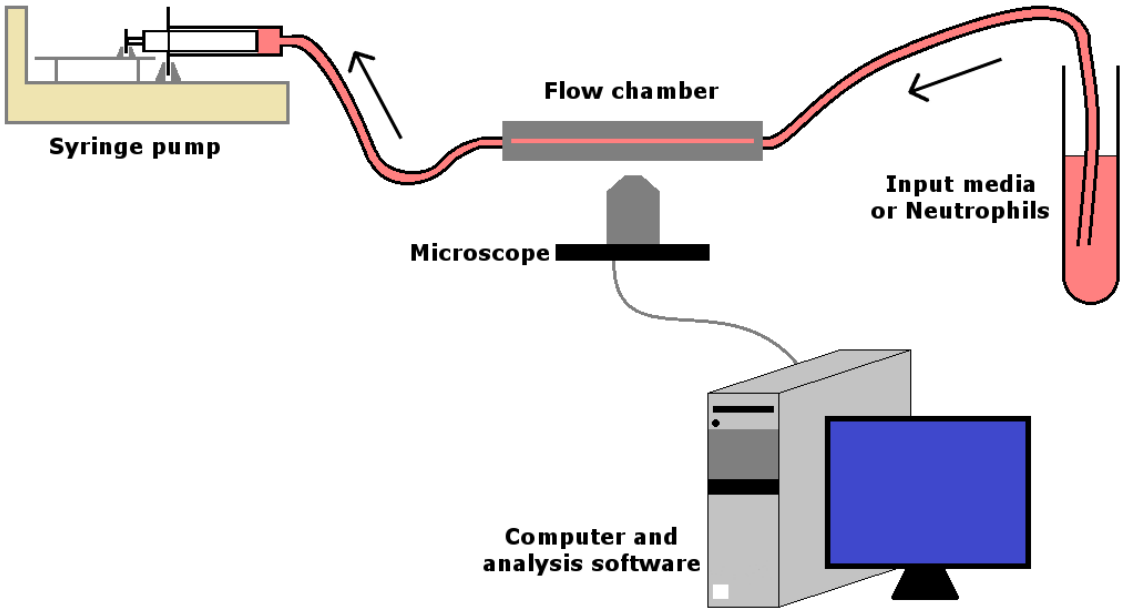

Figure 6.3: Diagram showing the basic setup of the flow chamber and video capture.

The flow chamber was attached by silicone tubing at one end to a 50ml syringe, and at the other end to a falcon tube containing either empty media or neutrophil solution. The syringe was held in a pump that filled the syringe at a constant rate, causing media or neutrophils to flow over the cells with a sheer stress of 1 dyne/cm^2. A computer connected to a microscope camera with a 10x objective lens was used to capture the time-lapse images using Volocity software.

6.2.4 Use of disposable plastic flow chambers to measure neutrophil rolling, adhesion and transmigration under flow

An alternative flow chamber technique was described involving the study of neutrophil flow on HUVEC cultured in plastic disposable flow chambers(Ganguly et al., 2012). The ibidi µ-slide VI$^{0.4}$ slides, as pictured in Figure 6.4A, each contain 6 flow channels with dimensions of 17x3.8x0.4mm, and a growth surface of 60mm^2 per channel. HUVEC were seeded into each chamber at a concentration of 2.5x10^5 cells/ml, and adhered to the bottom of the chamber as shown in Figure 6.4B. Cells were transfected with ES or ΔC lentivirus as required, and fed every day until confluent.

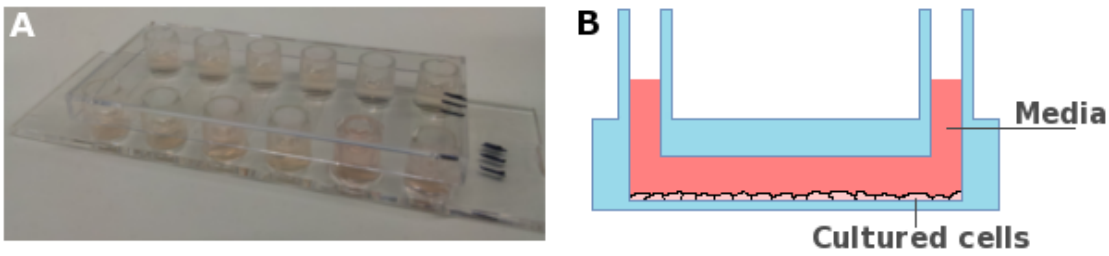

Figure 6.4: Photograph and diagram of the disposable Ibidi µ-slide VI$^{0.4}$ slides

(A) Photo of an ibidi µ-slide VI$^{0.4}$ showing the 6 chambers, each with a well at either end. (B) Cross-sectional diagram of a single chamber, showing the cultured cells lining the bottom of the chamber, and the wells either side of the chamber allowing media exchange.

The experimental protocol was the same as with the metal chamber described in section 6.2.3. Luer-lock silicone tubes were attached to both ends of the chamber, and neutrophils passed through at constant sheer stress rate of 1 dyne/cm^2 for 4 minutes, before being switched back to empty medium to wash off non-adherent cells. The disposable slide chambers did however have a larger cross-sectional area than the parallel plate flow chamber, so to get the same sheer stress of 1 dyne/cm^2 a flow rate of 0.57ml/min was required. Other brands of disposable flow chambers are available, however were not tested.

6.3 Neutrophil adhesion to both IL-1β stimulated and ES or ΔC transfected HUVEC under static conditions

The major function of E-selectin in the body is in the recruitment and activation of circulating neutrophils(Bevilacqua et al., 1989; Tedder et al., 1995). Weak E-selectin binding to ligands such as ESL-1 expressed on the neutrophil surface can activate signal pathways within the neutrophils, leading to conformational changes in other neutrophil CAMs such as LFA-1(Simon et al., 2000; Yago et al., 2010). This allows the formation of tighter bonds between the neutrophil and endothelium, causing the neutrophils to adhere tightly before initiating transmigration and diapedesis(Green et al., 2006; Zarbock et al., 2007). Microvascular studies in patients with meningococcal disease have shown reduced blood pressure and increased levels of both adhesion molecules and adherent neutrophils in small blood vessels infected with *N.meningitidis*(Paize et al., 2012). The level of neutrophil adhesion to HUVEC under a range of conditions was used as a quantitative indicator of the level of endothelial activation.

6.3.1 ES transfected HUVEC exposed to *N.meningitidis* for 60 minutes support greater neutrophil adhesion under static conditions than ΔC transfected HUVEC

In order to study the effects of *N.meningitidis* on endothelial E-selectin function, neutrophil adhesion to the endothelium was investigated initially under static conditions. Figure 6.5A shows neutrophil adherence to endothelium either transfected with ES or ΔC E-selectin, or stimulated for 4 hours with IL-1β, before exposure to *N.meningitidis* for 60 minutes. Few neutrophils adhered to untransfected HUVEC (<50/field) or HUVEC transfected with ES or ΔC E-selectin, whereas IL-1β stimulation of untransfected cells for 4 hours increased neutrophil adhesion significantly ($P<0.001$) above both untransfected and ES or ΔC transfected HUVEC (Figure 6.5B).

Upon HUVEC exposure to *N.meningitidis* for 60 minutes however, the numbers of adherent neutrophils under all conditions increased significantly, as shown in Figure 6.5A. The approximately two-fold increase in neutrophil adhesion to *N.meningitidis* exposed ΔC transfected cells was not significantly different to the increase in adhesion to *N.meningitidis* exposed untransfected cells (P=0.4469) (Figure 6.5C) showing that the presence of transfected ΔC E-selectin on the endothelium did not cause any greater neutrophil adhesion under static conditions than the untransfected endothelial control, either before or after *N.meningitidis* exposure. Conversely, the 8-fold increase in neutrophil adherence to ES transfected HUVEC upon *N.meningitidis* exposure was significantly greater than the two-fold increases in levels of neutrophil adhesion to both untransfected (P=0.0015) and ΔC transfected (P=0.0051) HUVEC upon *N.meningitidis* stimulation (Figure 6.5C). Exposure of IL-1β stimulated HUVEC to *N.meningitidis* also increased levels of neutrophil adhesion significantly (P=0.0473), up to a 4-fold increase in the levels of neutrophil adhesion triggered by IL-1β stimulation alone.

Although IL-1β is a potent proinflammatory stimulus on endothelial cells, exposure of ES transfected HUVEC to *N.meningitidis* for 60 minutes appeared to induce greater neutrophil adhesion than 4 hours IL-1β stimulation, approaching statistical significance (P=0.0633). Exposure of IL-1β stimulated HUVEC to *N.meningitidis* however, also increased neutrophil adhesion to equivalent, and slightly greater levels than those observed in ES transfected HUVEC stimulated with *N.meningitidis*, which was also approaching statistical significance (P=0.0729).

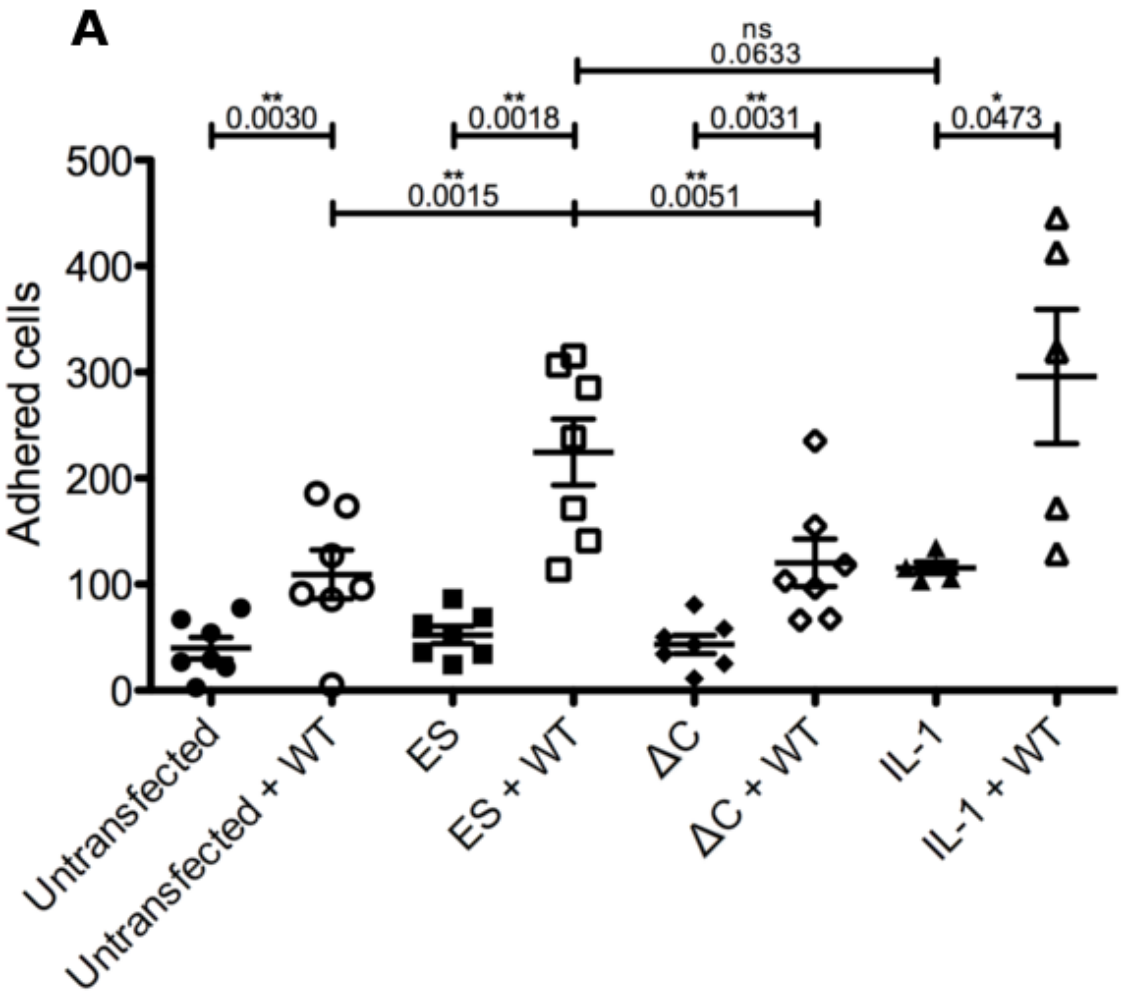

B

	Untransfected		IL-1β	
ES	0.1399	ns	0.0009	***
ΔC	0.5386	ns	0.0007	***
IL-1β	0.0005	***	n/a	n/a

C

	Untransfected + WT		ES + WT	
ES + WT	0.0015	**	n/a	n/a
ΔC + WT	0.4469	ns	0.0051	**
IL-1β + WT	0.0166	*	0.0729	ns

Figure 6.5: Graph showing neutrophil adhesion to ES and ΔC transfected HUVEC under static conditions.

(A) Graph showing neutrophil adhesion to the endothelium under static conditions. HUVEC were untransfected (●), transfected with ES (■) or ΔC (◆) E-selectin, or stimulated for 4 hours with IL-1β (▲). Open symbols represent HUVEC exposed to 10^7/ml *Neisseria meningitidis* for 60 minutes prior to the end of the experiment, while filled symbols represent unexposed HUVEC. (Mean +/- SEM, n=7 except IL-1β where n=5). Some P-values are shown on the graph, additional P-values from paired student's t-tests are shown in tables comparing non-*N.meningitidis* exposed conditions (B) and *N.meningitidis* exposed conditions (C)

In conclusion, neutrophil adhesion to endothelium under static conditions is not affected by the presence of ES or ΔC E-selectin *per se*, however neutrophil adhesion is increased by both *N.meningitidis* exposure as well as endothelial stimulation by IL-1β. 60 minutes of *N.meningitidis* exposure increased neutrophil adhesion under all conditions, however in HUVEC expressing either endogenous or transfected full-length ES E-selectin, adhesion increased by a significantly greater amount compared to those expressing ΔC or no E-selectin at all. ΔC E-selectin did not appear to cause any greater neutrophil adhesion than in

untransfected cells. These results suggest that the presence of *N.meningitidis* can mediate neutrophil adhesion to the endothelium via a process that involves full length E-selectin and its cytoplasmic tail under static conditions.

6.4 Measuring neutrophil adhesion to HUVEC under physiological flow conditions

Whilst the results from the static adhesion experiments were intriguing, it was important to investigate more physiologically relevant conditions that occur in the human body. Neutrophil and endothelium interactions occur in the bloodstream where they are under constant physiological flow, although circulating leucocytes can become static for short periods of time in narrow capillaries such as in the lung or brain microvasculature (Doerschuk et al., 1993; Lien et al., 1990; Mairey et al., 2006; Villringer et al., 1994).

To investigate neutrophil adhesion under more physiologically relevant conditions, a parallel plate flow model was used to investigate neutrophil-endothelial interactions under flow conditions. Two types of chamber were used to carry out these experiments: firstly, a metal and Perspex parallel plate flow chamber that screwed together to make a watertight seal and described in detail in section 6.2.3. In later experiments, disposable plastic chamber slides were used, and are described in section 6.2.4.

6.4.1 Use of the metal parallel plate flow chamber to study leucocyte-endothelial interactions under physiological flow conditions

6.4.1.1 Neutrophil adhesion under flow to HUVEC using the metal parallel plate flow chamber

The aim of this set of experiments using the metal parallel plate flow chamber was to measure the level of neutrophil adhesion to HUVEC under physiological flow conditions using the chamber and technique described in section 6.2.3. Figure 6.6 shows representative images of neutrophils adhered to HUVEC stimulated for 4 hours with 10^8 WT *N.meningitidis*, 100ng/ml *N.meningitidis* LOS or 10ng/ml IL-1β, after neutrophil perfusion for 4 minutes at 1 dyne/cm^2 followed by perfusion of empty RPMI media for 2 minutes to wash away non-adherent cells. These concentrations of bacteria and LOS were used as a bacterial concentration of 10^8/ml is often found in severe meningococcal sepsis(Øvstebø et al., 2004), and 10^8 *N.meningitidis* bacteria produce approximately 100ng of LOS(Sprong et al., 2001). Additional concentrations were not compared in these experiments.

The neutrophils appear as white dots standing out clearly from the dark grey HUVEC monolayer. Very few neutrophils adhered to the unstimulated HUVEC shown in Figure 6.6A,

whereas the number of adherent neutrophils was much greater on HUVEC stimulated with either *N.meningitidis*, LOS or IL-1β (Figure 6.6B, C and D).

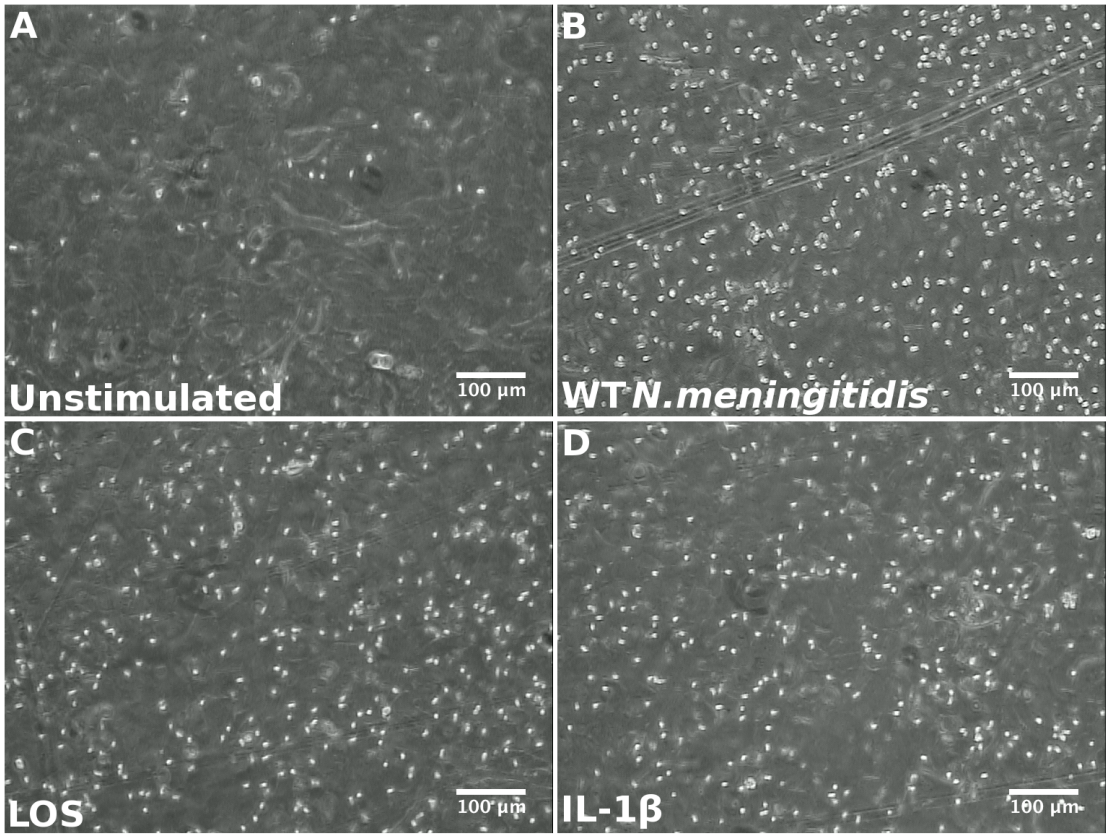

Figure 6.6: Representative images of neutrophil adhesion to HUVEC monolayers after 5 minutes neutrophil flow through the metal parallel plate flow chamber.

Neutrophils appear as white dots on the dark grey HUVEC monolayer. HUVEC were either unstimulated (A) or stimulated for 4 hours with 10^8/ml killed WT *N.meningitidis* (B), 100ng/ml LOS (C) or 10ng/ml IL-1β (D).

To quantitatively measure neutrophil adhesion to the endothelium, photographs of five non-overlapping fields of view were taken. The number of adherent neutrophils in each field was counted using Fiji ImageJ software (Schindelin et al., 2012), the image was first thresholded to separate out the white spots of the neutrophils, which were then counted automatically using the Analyse Particles feature on Fiji. The mean of these five fields of view were plotted on the graphs below. This computerised counting method was validated in the first set of experiments by additionally counting the number of adherent neutrophils manually alongside the automatic counting. The two sets of values were found to be equivalent in the first donor, and in subsequent experiments only the automatic counting method was used.

The graphs in Figure 6.7 show the level of neutrophil adhesion on several donors under flow conditions. Proinflammatory stimulation of HUVEC greatly increases neutrophil adhesion, whether due to IL-1β, LOS or whole killed *N.meningitidis* bacteria stimulation. However,

adhesion to HUVEC stimulated with *N.meningitidis* was significantly greater than adhesion to IL-1β stimulated HUVEC (Figure 6.7A P =0.0289). Neutrophil adhesion levels to HUVEC stimulated with *N.meningitidis* were also visibly greater than adhesion to LOS stimulated HUVEC (Figure 6.7B); however, it was not possible to establish significance in that case, as only 2 LOS stimulated repeats were carried out.

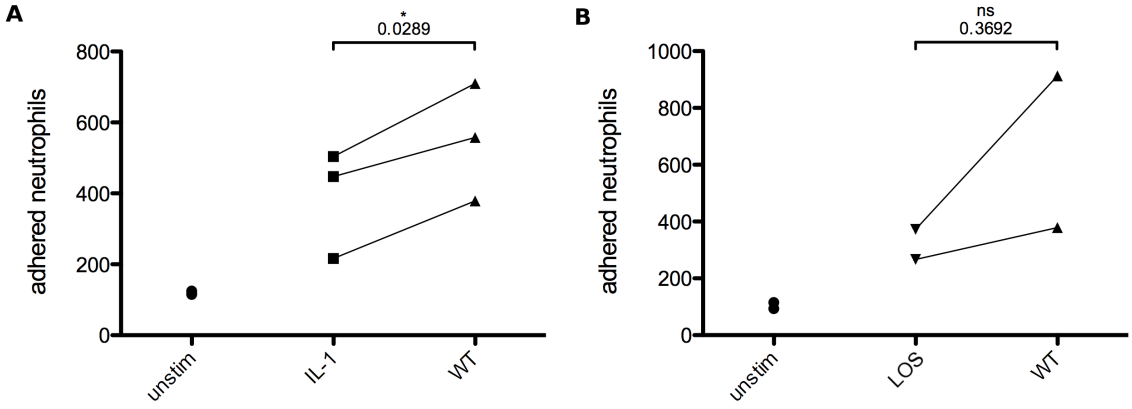

Figure 6.7: Neutrophil adhesion under flow in the metal chambers to HUVEC monolayers stimulated for 4 hours with killed WT *N.meningitidis*, IL-1β or LOS.

HUVEC were either unstimulated, or exposed for 4 hours to 10^8/ml killed WT *N.meningitidis* and either 10ng/ml IL-1β (A) or 100ng/ml LOS (B). Neutrophils were passed over the HUVEC monolayers at concentration of $5x10^5$ cells/ml at a sheer stress rate of 1 dyne/cm^2 for 4 minutes, after which media was passed through the chamber for 2 minutes to clear non-adherent neutrophils. The mean adhesion from five non-overlapping fields is shown for each donor per condition. Lines connect points corresponding to the same donor. Data from (A) 3 or (B) 2 separate human donors is shown, and significance calculated using Student's t-test.

The increased neutrophil adhesion to *N.meningitidis* stimulated HUVEC under flow conditions compared to IL-1β or LOS stimulated HUVEC is in line with previous studies from our group where it was shown that *N.meningitidis* stimulates 2-fold greater E-selectin expression on HUVEC compared to both TNF-α and LOS (Dixon et al., 1999, 2004). However the results in Figure 6.7 expand on this by showing that this may have a functional effect on neutrophil adhesion, as exposure of HUVEC to *N.meningitidis* can stimulate significantly greater neutrophil adhesion under flow conditions than other inflammatory stimuli.

6.4.1.2 Analysis of neutrophil adhesion under flow to HUVEC transfected with ES or ΔC E-selectin using the metal parallel plate flow chamber

The experiments described in Figure 6.7 showed that 4 hours of HUVEC stimulation with *N.meningitidis* induced significantly greater levels of neutrophil recruitment than IL-1β stimulation, and that this may demonstrate a functional aspect to the differential E-selectin and other adhesion molecule expression seen after meningococcal or IL-1β stimulation in previous studies(Dixon et al., 1999, 2004).

The increase in static neutrophil adhesion seen in Figure 6.5 due to *N.meningitidis* however, occurred after only 60 minutes of meningococcal exposure, and so was very unlikely to be down to increased E-selectin expression. This implies that *N.meningitidis* may have additional affects on neutrophil interactions with the endothelium that involve the E-selectin intracellular tail, and which are unrelated to increased expression of adhesion molecules.

In order to further investigate the consequences of *N.meningitidis* exposure on endothelial E-selectin mediated neutrophil recruitment, HUVEC were transfected with ES or ΔC E-selectin before being exposed to *N.meningitidis* for 60 minutes, and the neutrophil recruitment under flow recorded.

As the main known function of E-selectin is to bind to neutrophils in the circulation to slow them down and adhere to the endothelium, it was expected that both ES and ΔC transfected cells would support neutrophil rolling and adhesion without any additional stimuli required, although ΔC E-selectin has been reported to support lower levels of neutrophil adhesion under flow than full-length E-selectin(Setiadi and McEver, 2008).

Figure 6.A shows neutrophil adhesion under flow to ES and ΔC transfected HUVEC from 3 donors. Neutrophil adhesion after 5 minutes of flow appeared to be greater on both the ES and ΔC transfected cells compared to controls, however this was insignificant due to the large variation in adhesion to unstimulated cells between individual donors. In order to account for this variation the relative adhesion compared to the untransfected control was also calculated (Figure 6.B), however these values were also not significant, despite 1-2 fold increases in adhesion to the transfected cells compared to unstimulated control.

Interestingly, exposure to *N.meningitidis* did not appear to increase adhesion to either transfected or untransfected HUVEC under the flow conditions used in this experiment. This contrasts with the results from the static adhesion assay in Figure 6.5, which showed increased neutrophil adhesion after 1 hour *N.meningitidis* stimulation on untransfected and ES or ΔC transfected cells.

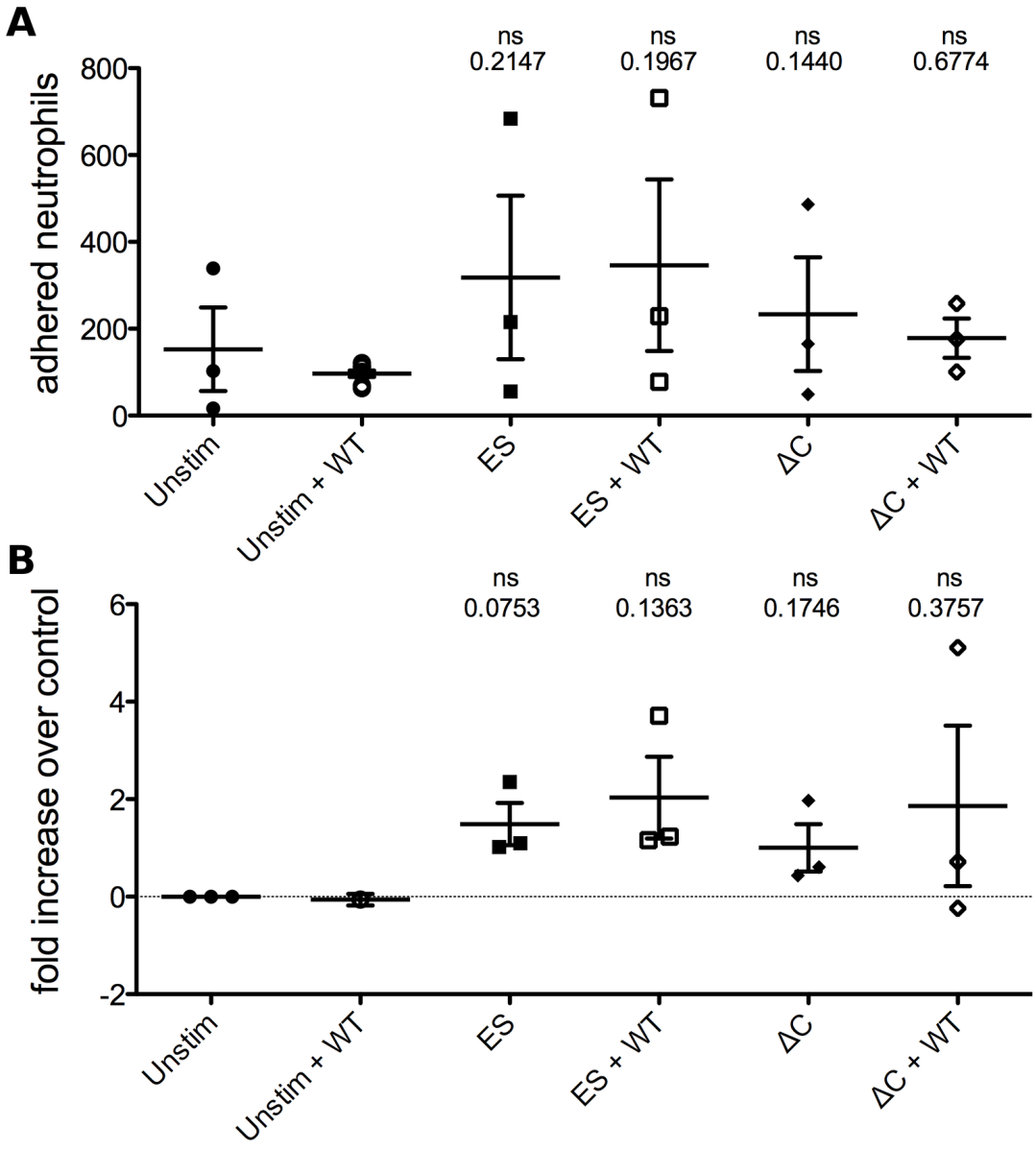

Figure 6.8: Neutrophil adhesion under flow on ES or ΔC transfected HUVEC exposed to killed *N.meningitidis* in the metal flow chamber.

HUVEC were either untransfected, or transfected with full length ES E-selectin or the tail-less mutant ΔC, and exposed to 10^8/ml killed *N.meningitidis* bacteria for 1 hour. Neutrophils were passed over the HUVEC monolayers at concentration of $5x10^5$ cells/ml at a sheer stress rate of 1 dyne/cm^2 for 4 minutes, after which media was passed through the chamber for 2 minutes to clear non-adherent cells. The mean neutrophil adhesion from five non-overlapping fields is shown for each donor per condition. Graphs are expressed in terms of (A) total number of adhered neutrophils per field, and (B) fold-increase over the unstimulated control. (Mean +/- SEM, n=3, significance values calculated by Student's t-test)

Whilst the increased numbers of adherent neutrophils was not significantly higher under any conditions compared to unstimulated control (Figure 6.A), there was a trend suggesting increased levels of neutrophils adhesion on most of the transfected HUVEC conditions when normalising the data to the unstimulated control (Figure 6.B). Further experiments and larger numbers of samples would aid in determining if this effect is real.

Despite the observable trend in Figure 6.B showing that more neutrophils adhered under flow conditions to transfected cells than to untransfected cells, the differences were not statistically significant. One of the reasons for this was the high range of neutrophil adhesion values for the untransfected negative control, which varied from 16 cells/field up to over 300 cells/field in different donors (Figure 6.A); higher than some of the transfected cells. The high variability was unusual, and reflected problems with the flow chamber technique discussed below. Although the relative increase over control was also calculated in order to attempt to filter out this range of adhesion, the results were still non-significant.

The high variability in neutrophil adhesion to the untransfected control HUVEC between donors was caused by a variety of conditions contributing to both aberrant endothelial activation and neutrophil adhesion, as well as poor quality images that made accurate neutrophil counts difficult, as demonstrated in Figure 6.9.

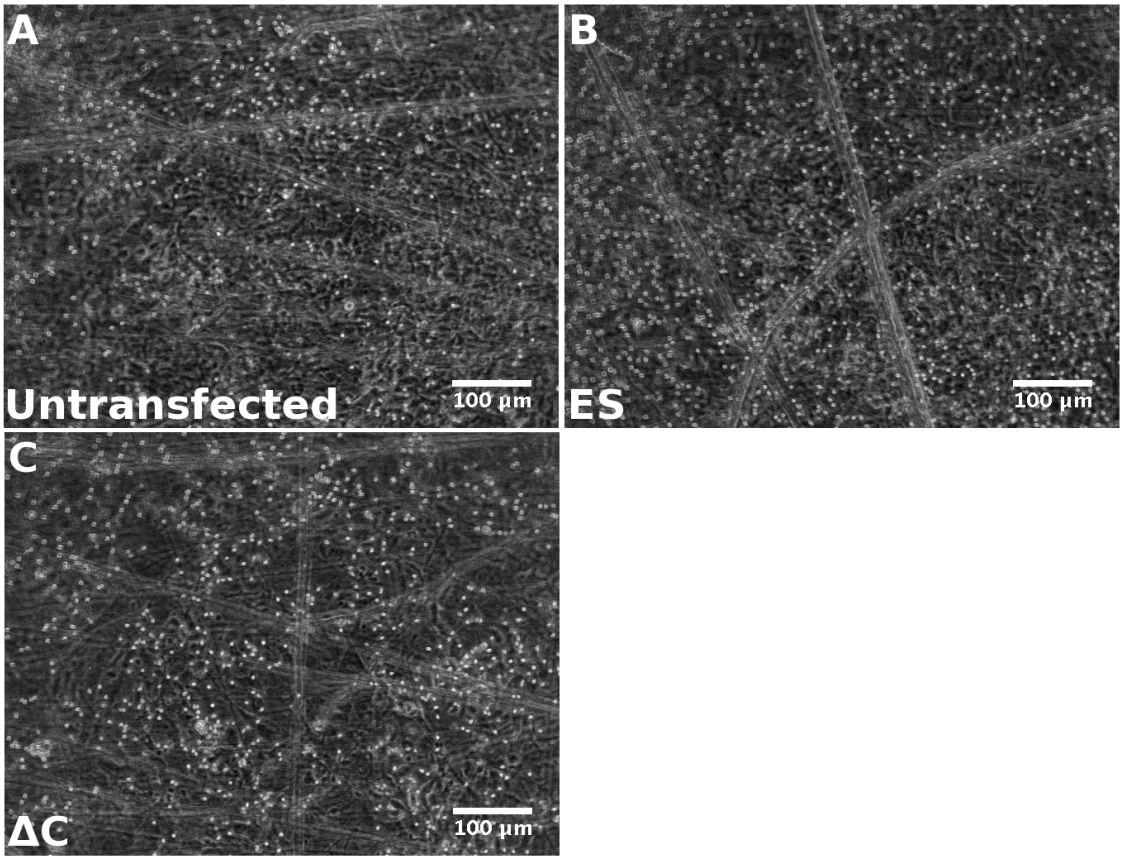

Figure 6.9: Representative images of neutrophil adhesion to HUVEC under flow using the metal flow chamber, showing difficulty focussing correctly and scratches in the Perspex flow chamber.

Images were taken after 4 minutes neutrophil flow through the parallel plate flow chamber, then a further 2 minutes of media being passed through to clear any non-adhered cells. HUVEC were either untransfected (A) or transfected with lentivirus expressing full length E-selectin ES (B) or tail-less mutant ΔC (C)

The problems encountered whilst carrying out the flow experiments using the metal chamber are discussed in more detail in section 6.7.1 of this chapter, however some of the

major problems included excessive bubble formation within the chamber during assembly, requiring excessive handling of the slide and chamber to remove them, as well as problems with scratches and focussing on the large metal chamber, which obscured the images as can be seen in Figure 6.9 and caused inaccurate neutrophil counts.

A new, disposable flow chamber system was obtained and used in order to determine if the metal flow chamber was the main contributor to the variability observed in neutrophil adhesion to control cells.

6.4.2 Use of disposable flow slides to study leucocyte-endothelial interactions under physiological flow conditions

Given the issues with the metal parallel plate flow chamber described above, an alternative, more reliable technique to study neutrophil-endothelial interactions under flow conditions was sought. A publication using a similar technique to the methods used in this chapter described the use of disposable ibidi flow chambers which used a similar technique to the one in which HUVEC could be grown and neutrophils passed through(Ganguly et al., 2012). The disposable ibidi flow chambers provided consistently sized flow chambers with much fewer parts and complications compared to the metal parallel plate flow chamber, and are described in greater detail in section 6.2.4.

The representative images of HUVEC grown in disposable flow chambers in Figure 6.10 show the HUVEC monolayers and neutrophils in much greater detail and clarity than the equivalent images taken on the metal chamber in Figure 6.6 and Figure 6.9. This allows for better analysis of the images, and more accurate assessment of neutrophil adhesion. After initial evaluation of the disposable flow chambers, they were utilised in all subsequent flow experiments.

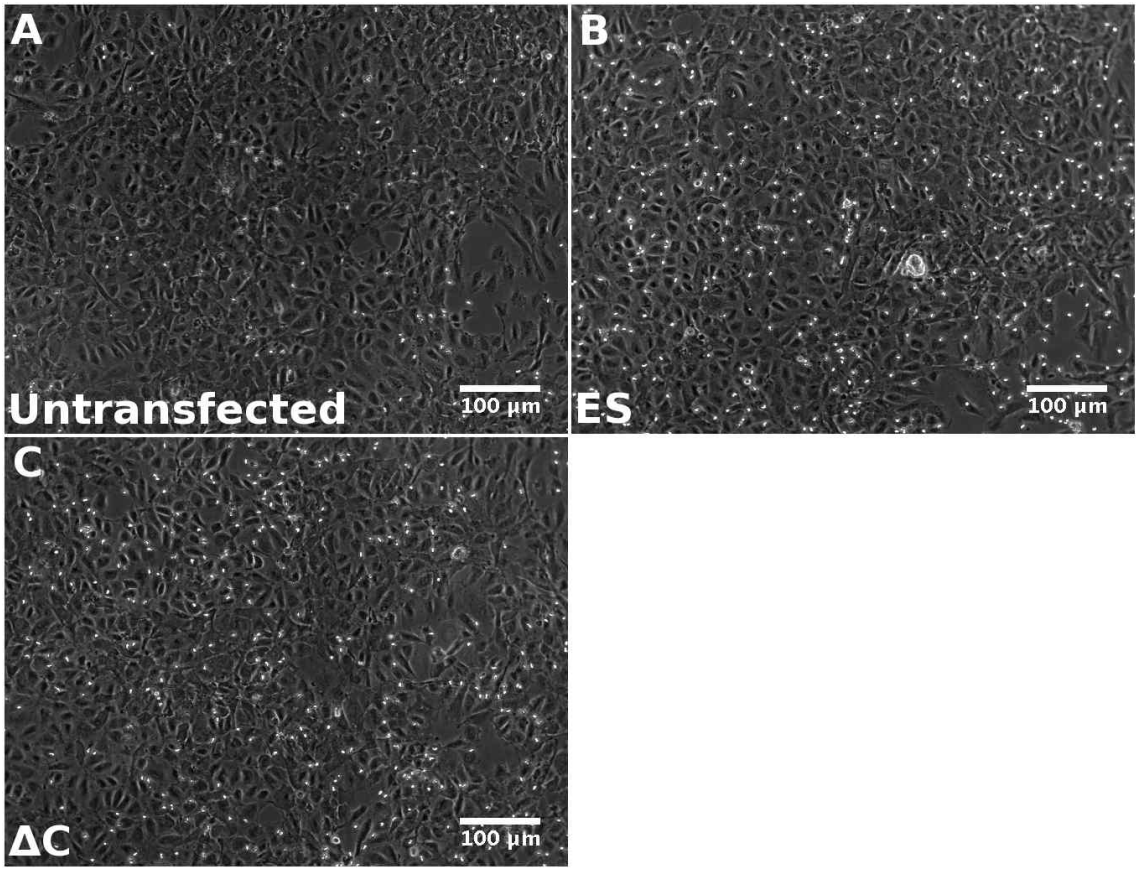

Figure 6.10: Representative images of neutrophil adhesion to HUVEC under flow in ibidi µ-slide VI$^{0.4}$ chambers.

Images were taken after 4 minutes neutrophil flow through the chamber, and then a further 2 minutes of empty media being passed through to clear any non-adherent cells. HUVEC were either untransfected (A) or transfected with lentivirus expressing full length E-selectin ES (B) or tail-less mutant ΔC (C).

6.4.2.1 Analysis of neutrophil adhesion under flow to HUVEC transfected with ES or ΔC E-selectin using disposable flow chambers

The experiment outlined in section 6.4.1.2 was repeated on HUVEC monolayers cultured inside the disposable flow chamber slides. Neutrophil adhesion under flow to HUVEC transfected with ES or ΔC, or stimulated for 4 hours with IL-1β, was significantly higher than adhesion to untransfected cells (p=0.0018, 0.0057, 0.0206, respectively) (Figure 6.11A). Exposure to *N.meningitidis* for 60 minutes, however, did not significantly increase adhesion further under any condition, and even appeared to decrease neutrophil adhesion slightly in both untransfected and ES or ΔC transfected cells. HUVEC stimulated with IL-1β for 4 hours followed by 60 minutes *N.meningitidis* exposure appeared to have similar levels of neutrophil adhesion as unexposed IL-1β stimulated cells, however the values were not significant as fewer repeats of this condition were carried out.

The pattern of neutrophil adhesion under different conditions appeared similar to that seen with the experiments carried out in the metal chamber as shown in Figure 6., more

neutrophil adhesion was seen on transfected cells compared to untransfected cells, and 60 minutes *N.meningitidis* exposure did not appear to increase neutrophil adhesion.

The size of the difference in the level of neutrophil adhesion to transfected cells compared to untransfected cells was significantly greater when using the disposable slides in Figure 6.11 compared to the metal flow chamber used in Figure 6.. One of the major reasons for this was due to the much lower background adhesion seen in the control untransfected cells; the mean/median of adhered neutrophils counted per field on untransfected cells was 59.8/36.7 in the disposable slides compared to 152/102 when using the metal chamber. The much lower negative control made the increased neutrophil adhesion to transfected cells more significant.

To show that the differences in neutrophil adhesion were due to the interaction with E-selectin, and not another endothelial factor affected by the lentivirus vector or IL-1β, the transfected HUVEC were treated with an anti-E-selectin blocking antibody for 15 minutes before neutrophil perfusion. Incubation of HUVEC transfected with ES or ΔC E-selectin, whether with or without additional 60 minutes exposure to *N.meningitidis,* with E-selectin blocking antibody significantly reduced neutrophil adhesion to levels almost equivalent with that observed in untransfected cells (Figure 6.11B). The significant reduction in adhesion (P=0.0147, Friedman test) could be seen in all conditions with the blocking antibody (Figure 6.11B).

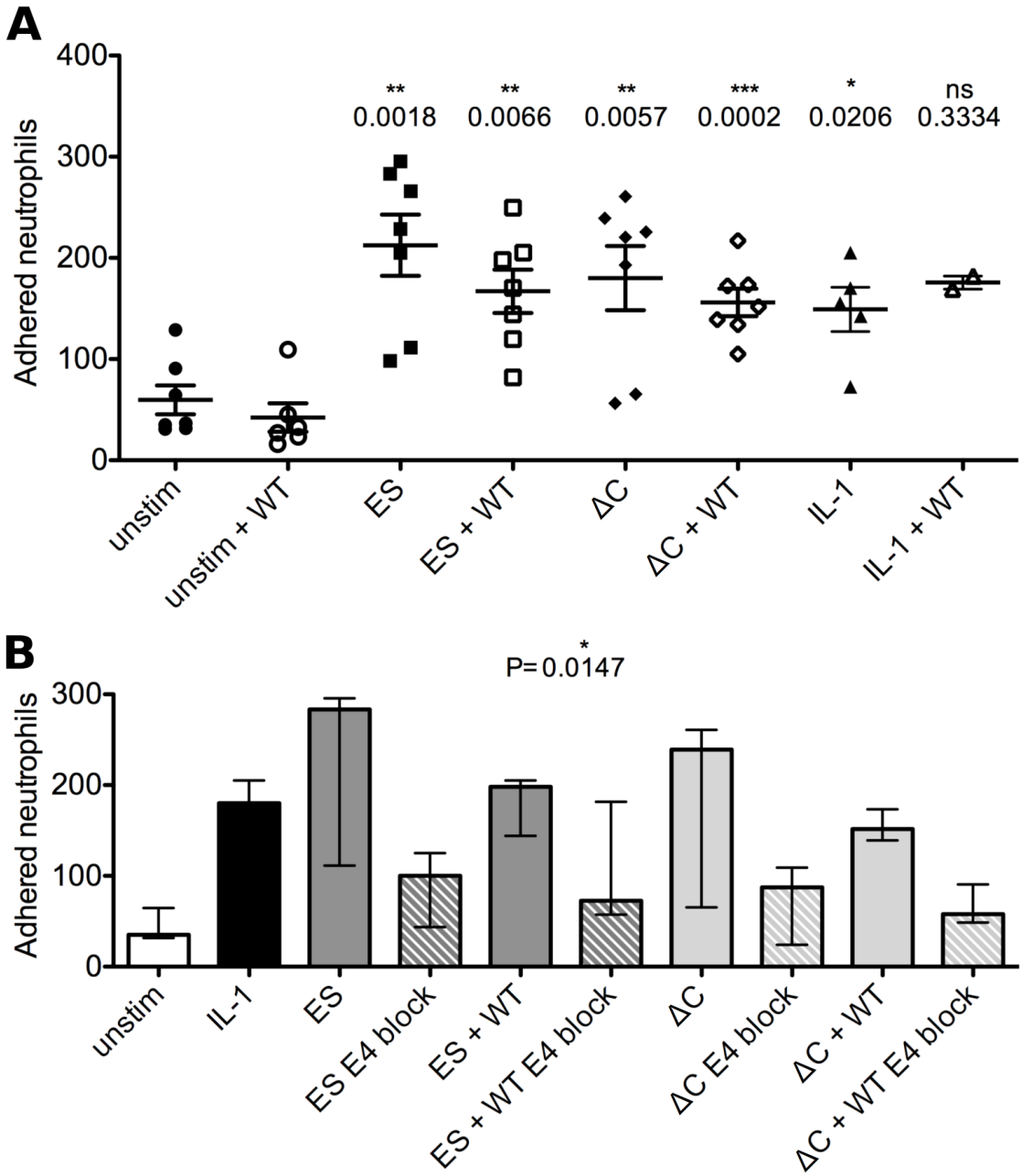

Figure 6.11: Neutrophil adhesion to ES and ΔC transfected HUVEC in disposable flow chambers after 4 minutes perfusion of 5x10^5/ml neutrophils at 1 dyne/cm^2.

(A) Neutrophil adhesion under physiological flow to HUVEC transfected with either full length (ES) or tail-less mutant (ΔC) E-selectin, or stimulated for 4 hours with IL-1β. HUVEC were then exposed to killed WT *N.meningitidis* for 60 minutes (n=7, except for IL-1β where n=5 and IL-1β + WT where n=2) (Mean +/- SEM) Significance values calculated using paired Student's t-test. (B) ES and ΔC transfected HUVEC were treated with 50μg/ml E4 E-selectin blocking antibody for 15 minutes prior to neutrophil perfusion (n=3, Median +/- Range) Significance of adhesion inhibition by blocking antibody analysed by Friedman test, P=0.0147.

In conclusion, these results show that the disposable flow chamber slides are a more reliable method for carrying out adhesion assays under flow conditions. Furthermore, neutrophil adhesion to HUVEC transfected with ES or ΔC E-selectin is significantly higher than adhesion to untransfected cells, and is equivalent to the levels of adhesion seen on HUVEC stimulated

with IL-1β. Exposure of transfected or untransfected HUVEC to WT *N.meningitidis* for 60 minutes however did not increase neutrophil adhesion at all, and even appeared to reduce adhesion slightly, which was in contrast to neutrophil adhesion seen under static conditions in Figure 6.5, and summarised in Table 6-1, where 60 minutes bacterial exposure increased neutrophil adhesion significantly.

Table 6-1: Comparison of neutrophil adhesion to either transfected or IL-1β stimulated HUVEC upon exposure to WT *N.meningitidis* under both static and flow conditions.

	Unstim	Unstim + WT	ES	ES + WT	ΔC	ΔC + WT	IL-1β	IL-1β + WT
Static	-	+	-	++	-	+	+	+++
Flow	-	-	++	++	++	++	++	++

Incubation with an E-selectin blocking antibody for 15 minutes significantly reduced neutrophil adhesion to ES and ΔC transfected cells, as well as reducing adhesion to ES and ΔC cells that had been exposed to *N.meningitidis*.

These results imply that E-selectin is vital for the adhesion of neutrophils to the endothelium under flow conditions; HUVEC transfection with ES and ΔC E-selectin produces levels of neutrophil adhesion equivalent to HUVEC stimulated with IL-1β for 4 hours, and blocking of E-selectin binding using an anti-E-selectin antibody significantly reduces neutrophil adhesion on transfected cells equivalent to the levels seen on control cells. Exposure to *N.meningitidis* for 60 minutes, however, does not significantly affect the amount of neutrophil adhesion to either transfected or untransfected HUVEC.

6.5 Rolling adhesion of neutrophils on endothelial cells

E-selectin binding to neutrophils under flow conditions results in characteristic rolling of the leucocyte along the endothelium, activating other adhesion molecules on the neutrophils and allowing them to form tighter interactions between the cells (Simon et al., 2000; Yago et al., 2010; Zarbock et al., 2007). Total adhesion of neutrophils to the endothelium was measured in section 6.4, and blocking of E-selectin was shown to almost completely abrogate neutrophil adhesion. Although firm adhesion is mostly mediated by integrin binding to endothelial adhesion molecules such as ICAM-1, adhesion under flow is reliant on the initial E-selectin binding causing slow rolling of neutrophils along the endothelium.

The rolling interactions are often fairly brief, as rolling neutrophils quickly become activated through their interactions with E-selectin, causing conformational changes in the integrin adhesion molecules allowing them to adhere tightly to the endothelium(Simon et al., 2000). As rolling velocity can be very fast, assessment of rolling interactions requires the events to

be captured as video, and played back at slower speeds to visualise rolling leucocytes. In order to record these interactions, the setup of the camera and microscope used for the adhesion experiments under flow conditions was modified to capture real time videos of the rolling cells at 16 frames per second for 3 minutes directly to the hard drive. A cropped example of the rolling adhesion videos is shown in Video 6.1 on the accompanying DVD. In other publications a higher frame rate of around 30 FPS was achieved by using a more powerful computer attached to the microscope, or by recording the video on an analogue videotape and playing it back at slower speeds (Ramachandran et al., 2001; Setiadi and McEver, 2008; Zarbock et al., 2007). The analogue videotape method was attempted, however the quality of the image obtained was very poor using our apparatus, and so digital capture at the slower 16fps was used instead.

HUVEC were grown in disposable flow chamber slides and transfected with ES or ΔC E-selectin. Neutrophils were then passed over the endothelium as previously described, and a 3 minute video of a single field per condition was recorded at 16FPS direct to the hard drive. The videos were then analysed manually using the MtrackJ plugin on Fiji ImageJ software (Meijering et al., 2012; Schindelin et al., 2012). Individual neutrophils (50 neutrophils per condition per experiment) were marked as they first adhered to the endothelium, and followed as they rolled across the field of view. When the neutrophil stopped rolling due to either firmly adhering to or dissociating from the endothelium, the distance travelled and the time between the beginning and the end of rolling was recorded in order to calculate the average rolling velocity. Neutrophils that adhered directly without rolling more than 1 cell diameter were given a velocity of zero.

Figure 6.12 shows that neutrophils rolled much faster on untransfected HUVEC compared to cells transfected with ES or ΔC E-selectin, however the rolling velocity on HUVEC stimulated with IL-1β for 4 hours was even slower than on transfected HUVEC. There did not appear to be any difference in the rolling velocity between HUVEC transfected with ES or ΔC E-selectin, and 60 minutes stimulation with IL-1β or WT *N.meningitidis* did not appear to affect the neutrophil rolling velocity under any condition.

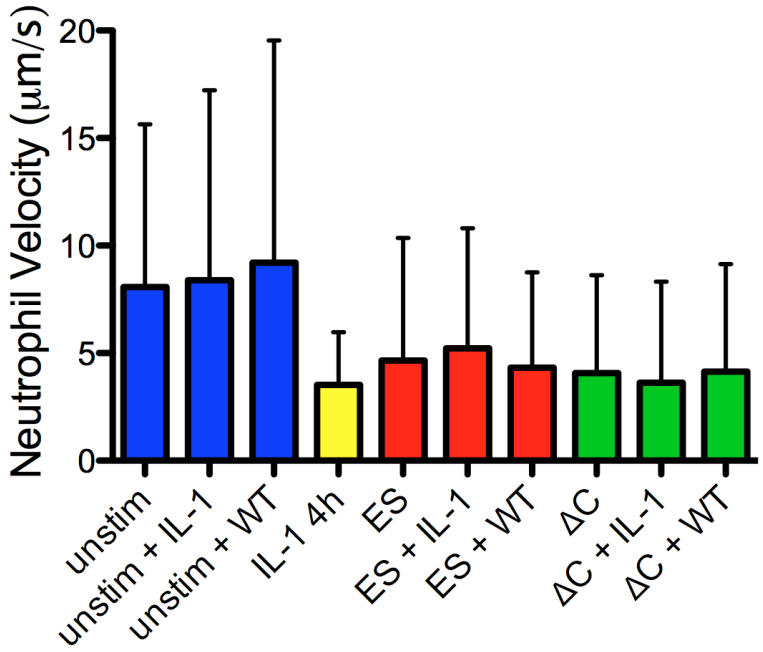

Figure 6.12: Rolling velocities (µm/s) of neutrophils on HUVEC.

HUVEC were unstimulated (blue), transfected with ES (red) or ΔC (green) E-selectin, or stimulated for 4 hours with IL-1β (yellow). HUVEC were also exposed to WT *N.meningitidis* or IL-1β for 1 hour in the columns indicated. (n=1, velocity of 50 rolling neutrophils per experiment were recorded and graph shows mean +/- SD)

There were very few rolling neutrophils on the untransfected HUVEC, and fewer than 50 rolling or adherent cells were recorded in each of the untransfected HUVEC conditions. The cells that did roll on untransfected HUVEC had much faster velocity compared to those on HUVEC that were stimulated with IL-1β or transfected with lentivirus, and the majority of them did not firmly adhere, rolling only for a short period before dissociating and re-entering the flow. This is presumably due to the lack of E-selectin expression on unstimulated HUVEC.

There did not appear to be much difference in the velocities of neutrophils rolling on HUVEC transfected with ES or ΔC E-selectin. This implies that the rolling velocity is unaffected by the presence of the E-selectin intracellular tail, although this disagrees with previous publications that have reported a faster rolling velocity on cells transfected with ΔC rather than ES E-selectin(Setiadi and McEver, 2008). The slower rolling velocity on HUVEC stimulated with IL-1β compared to transfected HUVEC was expected, as IL-1β stimulation can upregulate neutrophil activating cytokines such as IL-8, as well as adhesion molecules such as P-selectin that can also contribute to rolling adhesion alongside E-selectin (Homeister et al., 1998; Middleton et al., 1997; Sica et al., 1990).

Many of the distances travelled by the rolling neutrophils were very short, only a few cell diameters, before either detaching or adhering tightly; however some cells rolled for long

distances, and sometimes moved out of the field of view while still rolling at a consistent speed. It is unclear why these cells did not activate and adhere tightly, however, differences in neutrophil rolling speeds on the same surface can occur, and are likely to be a result of variation in expression of selectin ligands between individual neutrophils.

In conclusion, neutrophil rolling on ES or ΔC E-selectin transfected HUVEC appears to be faster than IL-1β stimulated HUVEC, although slower than on unstimulated cells. There did not appear to be any difference in rolling velocity between neutrophils rolling on ES or ΔC transfected E-selectin, and there was also no observed difference in rolling velocity on neutrophils exposed to *N.meningitidis* or IL-1β for 60 minutes.

6.6 Measuring the transmigration of neutrophils through the endothelium under flow conditions

In section 6.4, neutrophil adhesion was studied on transfected HUVEC under flow conditions. In Figure 6.11A exposure to *N.meningitidis* appeared to reduce neutrophil adhesion on both untransfected and ES or ΔC transfected cells. Upon closer examination of the cells during flow experiments, and especially in the video recordings of neutrophil rolling, bright neutrophils adherent to the HUVEC could be observed as they crawled over the endothelium before transmigrating through it and becoming phase dark. During flow analysis of ES and ΔC transfected cells there were noticeably more transmigrated neutrophils crawling beneath the HUVEC exposed to *N.meningitidis* for 60 minutes compared to unexposed HUVEC. After consultation with Dr Aleksandar Ivetic, King's College London, it was decided to study the effects of the E-selectin tail on neutrophil transmigration in greater detail.

6.6.1 Description and measurement of neutrophil transmigration

The process of transmigration is more complex than neutrophil rolling and adhesion to the endothelium, and is much slower, taking minutes rather than seconds. In order to record and measure transmigration, the time-lapse microscope was set up to capture a single image at the same position every 15 seconds over the course of 15 minutes. These images could then be played back much faster in order to watch the neutrophils crawling and migrating through the endothelium. Three fields of view were captured per chamber. Neutrophils were perfused through the flow chamber for 4 minutes as described previously, before the input tube was switched back to empty media for the remaining time.

Adherent neutrophils could be seen on phase contrast images of the endothelium as rounded white spots, which often crawled about on the surface of the endothelial cells

(Figure 6.13A). In contrast, transmigrated neutrophils appear phase-dark, and were usually more flattened as they crawled about beneath the endothelial cells (Figure 6.13B). Neutrophils could also be observed both with both phase-light and phase-dark sections, as they were captured in the process of transmigrating (Figure 6.13C). Crawling neutrophils could be distinguished from rolling neutrophils due to the much slower crawling movement, as well as the fact that crawling occurs in all directions and not just in the direction of flow, as can be seen in videos 6.2-6.7 on the accompanying DVD, which are examples of neutrophil adhesion, crawling and transmigration under different conditions.

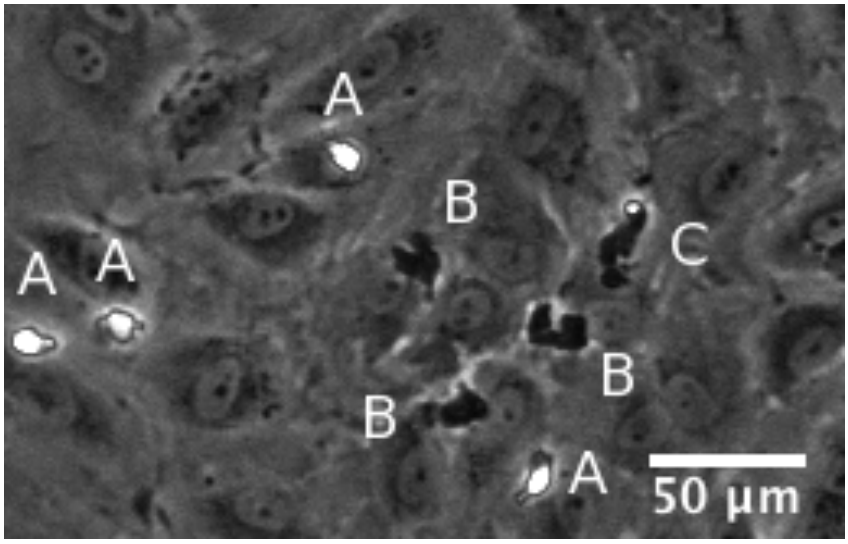

Figure 6.13: Photograph of both adherent and transmigrated neutrophils on HUVEC under flow conditions.

Phase-bright neutrophils (A) are adherent to the endothelial surface, phase-dark neutrophils (B) have transmigrated through the endothelium, and some neutrophils can be seen both phase-bright and phase-dark (C) which are in the process of transmigrating.

The number of white, adherent neutrophils on the surface of the endothelium at each 15 second time point of the video were counted using the Analyse Particles feature of Fiji ImageJ software(Schindelin et al., 2012) in the same way as in the previous adhesion experiments. Transmigrated neutrophils were harder to count automatically using computer software, as the phase-dark cells often blended in with the similarly dark grey underlying HUVEC, and could only be detected easily when they moved. The transmigrated cells were counted by hand using the Fiji "Cell Counter" plugin (De Vos, Kurt, 2008), however rather than counting every frame of the 15 minute time lapse video, only every 6th frame was counted (every 90 seconds) as this still gave a reasonable overview of the rate of transmigration while being more practical.

6.6.2 Transmigration of neutrophils through ES and ΔC transfected HUVEC in response to *N.meningitidis* exposure

The aim of the following experiments was to study the transmigration of neutrophils through the endothelium in response to *N.meningitidis* exposure on ES and ΔC transfected endothelial cells. Figure 6.14A shows the total number of adherent neutrophils at each 15 second time point over a 15 minute time period. Figure 6.14B shows the total number of transmigrated neutrophils over the same 15 minute time period.

Very few neutrophils adhered to untransfected HUVEC, or untransfected HUVEC exposed for 60 minutes to WT *N.meningitidis* (Figure 6.14A). The number of adherent neutrophils on the ES or ΔC transfected HUVEC increased at a relatively constant rate during the first 5 minutes of the experiment as neutrophils were perfused over the endothelium, reaching a peak after 5 minutes when the input tube was switched back to empty RPMI media and no new neutrophils entered the chamber (Figure 6.14A). After this time point, the total number of adherent neutrophils began to slowly decrease as some broke away from the endothelium and re-entered the flow, while others transmigrated through the endothelium and became phase dark.

Figure 6.14B shows the number of transmigrated neutrophils over the same 15 minute time period. There was very little neutrophil transmigration on untransfected cells, whether exposed to *N.meningitidis* for 60 minutes or not. This was expected, as there were very few adherent cells under these conditions, and therefore very few cells that had the potential to transmigrate through the untransfected cells. Neutrophil transmigration through ES and ΔC transfected cells was also limited, despite high levels of adhesion as seen in Figure 6.14A. However, upon WT *N.meningitidis* exposure for 60 minutes, neutrophil transmigration on both ES and ΔC transfected cells increased dramatically. Transmigration on ES transfected cells was greater than on ΔC transfected HUVEC both with and without 60 minutes of *N.meningitidis* exposure, implying that full length E-selectin may have a contributing role in neutrophil transmigration. This increased transmigration may also account for the decreasing numbers of bright adhered neutrophils over time seen on ES and ΔC transfected cells exposed to *N.meningitidis* for 60 minutes in Figure 6.14A.

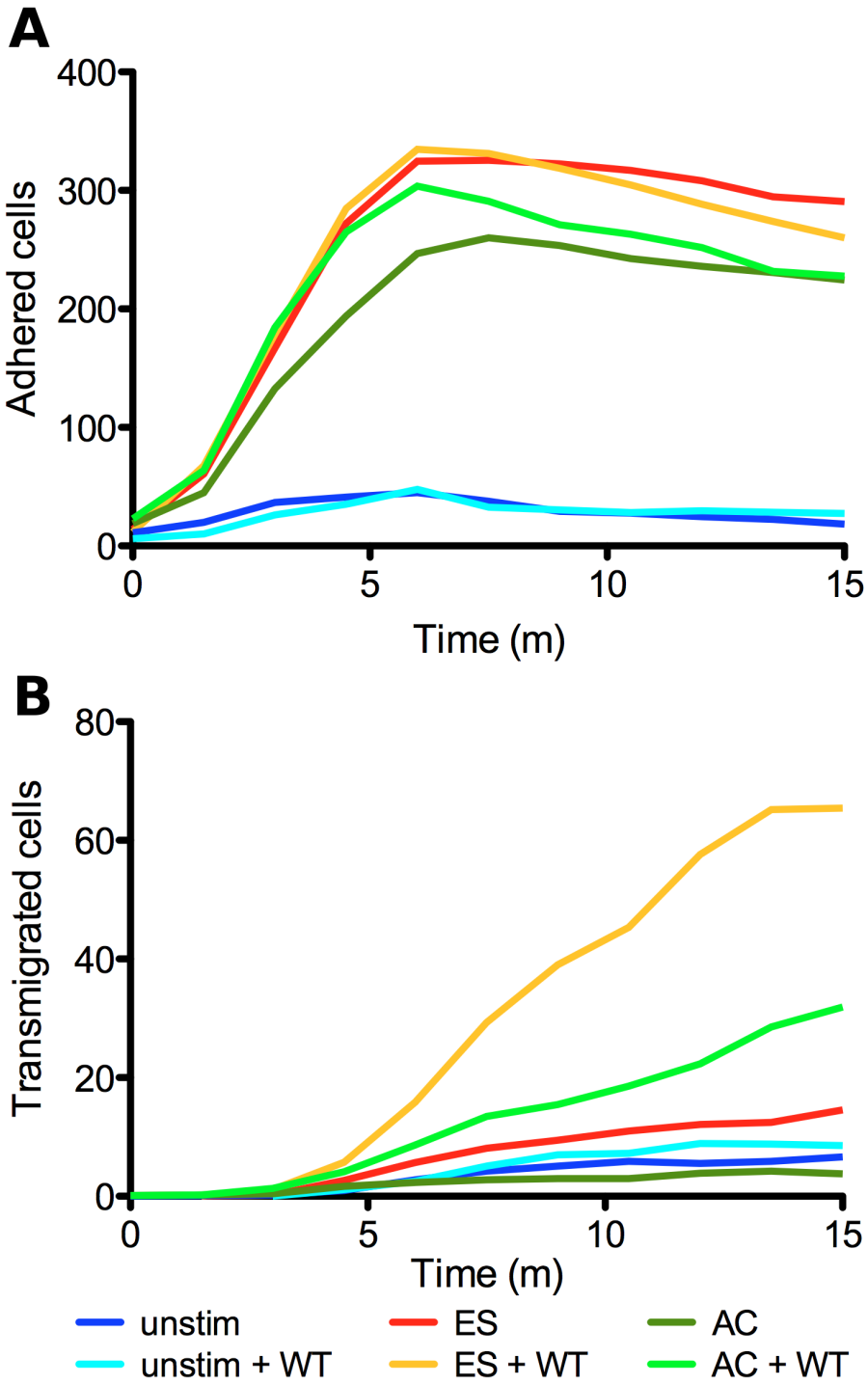

Figure 6.14: Graphs showing the number of both adherent and transmigrated neutrophils per field over time on HUVEC transfected with either ES or ΔC E-selectin in disposable flow chambers over a 15 minute time lapse experiment.

The number of adherent (A) or transmigrated (B) neutrophils on ES or ΔC transfected HUVEC, either exposed or unexposed to WT *N.meningitidis* for 60 minutes, was recorded over a 15 minute time period. The total number of adherent neutrophils per field of view was counted every 15 seconds, and transmigrated neutrophils were counted every 90 seconds. $5x10^5$/ml neutrophils at 1 dyne/cm^2 were perfused over HUVEC for 4 minutes, followed by 11 minutes empty media. Smoothed lines show the mean of three separate donors, with three separate fields of view counted per donor. Videos 6.2-6.7 show representative cropped videos of neutrophil adhesion and transmigration under each of the conditions shown in this graph.

Counting the number of adherent and transmigrated neutrophils on transfected HUVEC at regular time points over 15 minutes of flow allowed the construction of graphs showing the rate of neutrophil adhesion and transmigration on HUVEC over that time period. This showed that neutrophil transmigration begins to occur fairly soon after neutrophil adhesion, and increases at a relatively constant rate over the 15 minute time course, despite the total number of adhered neutrophils levelling out once the input tube is switched to the cell-free media.

Although 60 minutes of *N.meningitidis* exposure does not appear to have an effect on the number of neutrophils adhering to the endothelium, it does appear to increase the number of adherent neutrophils that subsequently transmigrate through the endothelial monolayer. This increase in neutrophil transmigration upon exposure to *N.meningitidis* appears to be related in part to the presence of full length E-selectin, as ES transfected HUVEC had greater levels of transmigration than ΔC transfected cells, despite both ES and ΔC having similar levels of adhesion.

6.7 Conclusions and Discussion

6.7.1 Comparison of the metal parallel plate flow chamber with the disposable ibidi μ-slide VI$^{0.4}$ chamber slides

The neutrophil adhesion results obtained in section 6.4.1 had problems with variability in neutrophil adhesion between donors, as well as high levels of adhesion in the untransfected controls; which meant that statistically significant results for neutrophil adhesion under flow were difficult to obtain using this method. Contributing to the variability were a number of factors involving the flow chamber itself, which were mainly corrected by switching to the more reliable disposable ibidi μ-slide VI$^{0.4}$ chamber slides.

The metal parallel plate flow chamber was screwed together with the HUVEC-coated cover slip inside, as seen in Figure 6.2. The cover slip had to be kept wet during assembly while ensuring no bubbles formed inside the chamber. This was difficult to achieve reliably, and the apparatus often had to be deconstructed and put back together again several times. This assembling and disassembling could lead to disruption of the HUVEC monolayer and possible activation of the cells. Bubbles were less of a problem with the disposable chamber slides however, as the cells were grown directly inside the small chambers as seen in Figure 6.4B; which meant that there were fewer parts to assemble and so fewer chances for bubbles to form. Any bubbles that did form were also much easier to remove, as the deeper cross-section of the chamber (0.4mm compared to 0.1mm) made bubbles easier to either

flush out using media or dislodge by tapping gently. As well as reducing the propensity of bubble formation, the lack of assembly enabled easier and faster switching between conditions, as well as less manipulation of the slides and potential activation of cells.

The quality and clarity of many of the images captured using the metal parallel plate chamber also caused problems when counting adherent neutrophils. Scratches on the Perspex flow chamber itself had built up over many uses, obscuring neutrophils in some areas while creating erroneous bright spots in others. In addition to this, the metal chamber itself is large, and held the HUVEC coated cover slip 5mm above the microscope stage. This meant that the microscope was operating at the limit of its focus, causing many of the images taken to be out of focus and producing inaccurate neutrophil counts. The effects of both of these problems on the clarity of the images can be seen in both Figure 6.6 and Figure 6.9. As well as the ease of use, one of the main advantages of the disposable slide system was the increase in image clarity and focus. The chambers were disposed after microscopy; therefore scratches did not build up on the chamber over several uses, and the base of the disposable slides was only 0.18mm, allowing proper focussing on both the HUVEC and neutrophils.

Finally, as well as problems with inaccurate neutrophil counting, the cover slips used in the metal flow chamber were themselves very large (22x60mm) in comparison to the area of the chamber visible through the Perspex window (10x40mm). This meant that when only a limited number of cells per donor were available, such as when using primary HUVEC at passage 1 as in these experiments, only a limited number of cover slips could be seeded per donor, meaning that multiple conditions were difficult to test in the same donor. The disposable slides however, had a much reduced growth surface area (60mm^2) compared to the large 22x60mm slides (1320mm^2), and the entire chamber surface area could be viewed under the microscope. This meant that many more conditions could be analysed for each donor, especially when the number of HUVEC isolated from a single donor was low.

Overall, the disposable flow chambers made for more detailed photographs with fewer artefacts than the metal chamber, as seen in Figure 6.10, which contributed to more accurate adhesion data and greater significance in the graphs.

6.7.2 Stimulation of HUVEC for 4 hours with WT *N.meningitidis* induces high levels of neutrophil adhesion under flow

Endothelial exposure to inflammatory stimuli for 4 hours causes high levels of neutrophil adhesion. In this study we showed that neutrophil adhesion to *N.meningitidis* stimulated

HUVEC was greater than adhesion to LOS stimulated HUVEC, and significantly greater than adhesion to HUVEC stimulated with IL-1β (Figure 6.7).

IL-1β and LOS are both potent proinflammatory molecules that can stimulate endothelial activation and initiate recruitment of neutrophils. However, these results are consistent with previous observations showing that *N.meningitidis* can induce greater levels of E-selectin expression on HUVEC after 4 hours compared to equivalent levels of LOS and other proinflammatory stimuli (Dixon et al., 1999, 2004). The increased E-selectin expression is due to signalling in the endothelial cells via the ATF-2 pathway activated by non-LOS components of the bacteria (Dixon et al., 2004; Jacobsen et al, manuscript in preparation). The results in Figure 6.7 demonstrate that *N.meningitidis* stimulation of HUVEC for 4 hours also has an increased functional effect on endothelial neutrophil recruitment as well as increasing E-selectin expression.

This increased neutrophil adhesion to HUVEC stimulated for 4 hours with *N.meningitidis* compared to IL-1β and LOS is potentially related to the increased E-selectin expression, however, other experiments described in this chapter show increased neutrophil adhesion under static conditions and increased transmigration under flow after only 60 minutes *N.meningitidis* exposure, which is too short a period to induce increased E-selectin expression. This suggests that other mechanisms may also be at work, such as increased E-selectin interactions with the cytoskeleton providing greater stability described previously in colon cancer and leucocyte activation (Sawada et al., 2001; Tilghman and Hoover, 2002a; Yoshida et al., 1996).

6.7.3 Neutrophil adhesion to ES and ΔC transfected HUVEC is different under static and physiological flow conditions

Neutrophil adhesion to ES and ΔC transfected endothelial cells was studied under both static conditions and under physiological flow. When neutrophils were added to HUVEC under static conditions, adhesion to cells transfected with either ES or ΔC was no different to untransfected cells. HUVEC stimulated with IL-1β for 4 hours however had significantly greater neutrophil adhesion than either transfected or untransfected cells (Figure 6.5).

These results are interesting. E-selectin is an important adhesion molecule in neutrophil-endothelial interactions, and has been reported to support increased neutrophil adhesion to the endothelium even under static conditions (Bevilacqua et al., 1989; Kishimoto et al., 1991; Sawada et al., 2001). However in the reported experiments from other publications the E-selectin was usually transfected into non-endothelial cell lines such as CHO or COS

cells using adenovirus vectors, and none were transfected using the much less-immunogenic lentivirus. This may go some way to explain the differences seen in this study compared to studies previously published.

Conversely, when neutrophils were perfused over HUVEC at a constant physiological flow rate, large numbers of neutrophils adhered to both ES and ΔC transfected cells, whereas relatively few adhered to untransfected cells. Neutrophil adhesion under flow to HUVEC transfected with either ES or ΔC E-selectin was equivalent to that seen on IL-1β stimulated cells (Figure 6.11A). Treatment of HUVEC with an E-selectin blocking antibody significantly inhibited neutrophil adhesion to both ES and ΔC transfected cells, showing that the increased adhesion under flow was E-selectin mediated (Figure 6.11B).

These results (summarised in Table 6-1) show that E-selectin mediated neutrophil adhesion is much more important under conditions of physiological flow than under static conditions. Under static conditions, the neutrophils have 15 minutes to interact with the endothelium, become activated and adhere. Whereas under flow conditions the neutrophils pass through the chamber and out the other side very quickly, giving them only a few seconds to interact and roll along the endothelium before adhering. The weak interactions of E-selectin with the neutrophils are therefore much more important under flow, as they are required to capture the neutrophils and slow them down to allow the formation of stronger integrin bonds; meaning that expression of E-selectin is the limiting factor in neutrophil adhesion under flow. Under static conditions however, there is no need for the weak E-selectin bonds to slow the neutrophils, and the strong contacts with ICAM-1 and VCAM-1 can be formed whether E-selectin is present or not.

These conclusions are supported by previous studies showing that blocking of E-selectin ligands such as PGSL-1 and L-selectin on neutrophils can inhibit their adhesion to E-selectin transfected CHO cells, or immobilised E-selectin and fibrin, under flow but not static conditions (Kuijper et al., 1996, 1997; Lawrence and Springer, 1993; Patel et al., 1995). Conversely, blocking the binding of leucocyte integrins inhibits adhesion under static conditions but not under flow, and also inhibits neutrophil transmigration(Lawrence et al., 1990; Smith et al., 1988).

Although E-selectin adhesion also functions to activate signalling pathways within the neutrophils which lead to firm adhesion, these can also be activated by other cytokines(Smith et al., 2004; Yago et al., 2010; Zarbock et al., 2007); therefore engagement with E-selectin is not essential for the formation of strong integrin bonds with neutrophils in

static conditions, which helps explain the lack of difference in neutrophil adhesion under static conditions between untransfected and transfected HUVEC.

Furthermore, these results also show that under both static and flow conditions, with no additional stimuli, there are no differences in neutrophil recruitment between full-length ES and tail-less ΔC E-selectin. This is in contrast with previous evidence showing that ΔC E-selectin has decreased adhesion under flow compared to ES E-selectin (Setiadi and McEver, 2008). It is unclear why my ES and ΔC neutrophil adhesion data conflicts with this previously published work, however there are some differences in the experimental procedure. In the studies presented here, a lentivirus vector was used to transfect ES and ΔC E-selectin into primary HUVEC, whereas Setiadi and McEver used the more immunogenic and less stable adenovirus vector to transfect the non-endothelial CHO cells. It is possible that other molecules expressed on endothelial cells but not CHO cells assisted in the ΔC mediated neutrophil adhesion, or that the higher and more stable ΔC expression in the lentiviral transfected cells allowed for greater neutrophil adhesion. Setiadi and McEver also noted that the transfected E-selectin in CHO cells was not expressed in lipid rafts, whereas endogenous E-selectin in HUVEC is. Therefore it is also possible that transfected E-selectin in HUVEC is expressed in the more physiologically relevant lipid raft location compared to transfected E-selectin in CHO cells, leading to greater neutrophil adhesion, although the data presented here does not indicate where the lentiviral transfected ES and ΔC is expressed in the cell.

6.7.4 *N.meningitidis* exposure increases neutrophil adhesion to all HUVEC under static conditions, but not under physiological flow

Exposure of HUVEC to *N.meningitidis* for 60 minutes increases neutrophil adhesion under static conditions (Figure 6.5). The increased adhesion was seen on all HUVEC whether adhesion was already high, such as in IL-1β stimulated HUVEC, or was similar to baseline levels as in untransfected or ES and ΔC transfected cells. When neutrophils were perfused over HUVEC under physiological flow, 60 minutes pre-exposure to *N.meningitidis* did not appear to increase the rate of adhesion in any of the endothelial conditions (Figure 6.11A, Table 6-1). Adhesion remained high and at similar levels in IL-1β stimulated cells as well as ES and ΔC transfected HUVEC. Untransfected cells continued to have the same low level of adhesion as they did before meningococcal exposure.

One potential reason for the increased adhesion due to 60 minutes of *N.meningitidis* exposure under static, but not flow, conditions is that under static conditions the

neutrophils have much more time to interact and become activated by *N.meningitidis* bacteria, whereas under flow the majority of bacteria are cleared from the flow chamber experiment as soon as the pump is turned on, preventing neutrophils from interacting with any non-adherent bacteria. Incubation of neutrophils with inflammatory stimuli, such as fMLP or *N.meningitidis*, has been shown to increase integrin and CD18 mediated adhesion to the endothelium under static conditions as well as transmigration(Klein et al., 1996; Smith et al., 1988), however this can reduce their ability to roll and adhere under flow conditions due to shedding of L-selectin, a ligand for E-selectin(Kuijper et al., 1996; Lawrence et al., 1990). Washing the endothelial cells with PBS to remove non-adherent bacteria before the addition of the neutrophils may have reduced the level of neutrophil adhesion, however the leukocytes would still have been able to interact with and be activated by *N.meningitidis* bacteria that were adherent to the endothelium.

The level of neutrophil adhesion under flow is similar for both ES and ΔC transfected cells as well as IL-1β stimulated cells; although rolling is slightly slower on IL-1β transfected cells, whereas there is no difference in neutrophil rolling velocity on ES or ΔC transfected cells. This implies that this may well be the limit of E-selectin mediated neutrophil adhesion under these flow conditions. At a certain point there may only be a certain number of adherent neutrophils that can be supported by the endothelium, no matter the stimuli. E-selectin expression is generally the limiting factor in neutrophil rolling and adhesion under flow, whereas it is less important in static adhesion.

An interesting experiment for the future may be to transfect lower concentrations of ES and ΔC lentivirus onto HUVEC, and measure the level of neutrophil rolling and adhesion and the effect of *N.meningitidis* exposure under flow conditions. It may be that the high expression of E-selectin on cells transfected in these experiments has saturated the amount of flow-mediated adhesion that is possible, preventing 60 minutes of *N.meningitidis* exposure from having an effect. This may also explain the fact that no difference in neutrophil adhesion between ES and ΔC transfected cells was seen, despite ΔC transfected cells being previously described as having lower neutrophil adhesion (Setiadi and McEver, 2008).

6.7.5 Functionality of full length ES, but not tail-less ΔC E-selectin, is increased by *N.meningitidis* exposure

The major finding of this chapter is the differing responses observed to *N.meningitidis* exposure of HUVEC transfected with ES and ΔC E-selectin, and its effects on neutrophil adhesion and activity. The increased neutrophil adhesion upon 60 minutes *N.meningitidis*

stimulation under static conditions to cells expressing transfected ES full-length E-selectin was much greater than the increased adhesion to untransfected or ΔC transfected cells (Figure 6.5A and C). The responses of untransfected and ΔC transfected cells were indistinguishable from each other, whereas adhesion to HUVEC transfected with ES increased to levels greater than seen on IL-1β stimulated HUVEC. Neutrophil adhesion to IL-1β stimulated cells also significantly increased after 60 minutes *N.meningitidis* exposure.

Interestingly, the level of neutrophil adhesion to untransfected and ΔC transfected HUVEC after 60 minutes *N.meningitidis* exposure was similar to the level of adhesion seen after 4 hours IL-1β stimulation, implying that 60 minutes *N.meningitidis* stimulation was as potent as 4 hours IL-1β stimulation at inducing neutrophil adhesion. This implies that the increased neutrophil adhesion to HUVEC due to stimulation by either IL-1β for 4 hours or *N.meningitidis* for 60 minutes is not related to increased E-selectin expression, as no endogenous E-selectin would have been induced on endothelial cells after only 60 minutes stimulation (Bevilacqua et al., 1989). The markedly increased neutrophil adhesion to ES transfected and IL-1β stimulated HUVEC after 60 minutes *N.meningitidis* stimulation, however, indicates that there is definitely some additional E-selectin intracellular domain mediated response that increases neutrophil adhesion.

Chemokine factors such as CXCL1 and IL-8 can bind to the CXCR2 receptor on the neutrophil surface, and activate the same conformational change in LFA-1 induced by E-selectin binding to its receptors such as PGSL-1 that leads to tight binding to ICAM-1 on the endothelium (Lefort and Ley, 2012; Smith et al., 2004; Yago et al., 2010), although E-selectin and CXCR2 act via different signalling pathways. It is possible that the 60 minutes of *N.meningitidis* stimulation can induce IL-8, CXCL1 and other endothelial cytokines, which then activate neutrophil binding and transmigration. The level of LFA-1 activation by E-selectin and CXCR2 signalling was however previously described as overlapping, not synergistic(Smith et al., 2004), and would not necessarily explain the greatly increased adhesion and transmigration seen upon *N.meningitidis* exposure to HUVEC expressing full-length E-selectin.

Under flow conditions, whilst 60 minutes meningococcal exposure did not increase neutrophil adhesion to the endothelium, it did increase neutrophil transmigration (Figure 6.14B). Transmigration was increased on both ES and ΔC transfected cells, although to a much greater extent on cells transfected with full-length ES E-selectin. These findings differ from those seen in some other studies showing impaired leucocyte adhesion and migration on endothelium stimulated with *N.meningitidis* for a short period (Doulet et al., 2006; Join-

Lambert et al., 2013). These studies used a MenC 2C43 *N.meningitidis* mutant that was missing the important outer membrane adhesins Opa and Opc, as discussed in Chapter 5, and was very different to the H44/76 MenB strain used in these experiments. In addition, both of these studies used live bacteria rather than killed ones. In the flow adhesion and transmigration experiments shown here, killed *N.meningitidis* bacteria were used, due to laboratory restrictions on the use of live *N.meningitidis* bacteria. Live and killed *N.meningitidis* have previously been shown to have differential effects on Dendritic cell maturation (Jones et al., 2007), as well as on the mucosal epithelium(Tezera et al., 2011; Wong et al., 2011). It is conceivable that live bacteria could also actively manipulate the endothelial-neutrophil interactions in ways that killed bacteria cannot, and large quantities of both live and killed bacteria are found in the bloodstream of patients with meningococcal disease (Øvstebø et al., 2004).

The results in this chapter imply that HUVEC expressing full-length ES E-selectin respond to short-term (60 minutes) *N.meningitidis* exposure in a different way to HUVEC expressing tail-less ΔC E-selectin. The E-selectin intracellular domain has previously been shown to have both signalling abilities and interactions with the cytoskeleton. E-selectin clustering by leucocyte or antibody adhesion can activate ERK/MAPK, Phospholipase Cγ and induce tighter contacts with the actin cytoskeleton (Hu et al., 2000; Kiely et al.; Yoshida et al., 1996). The E-selectin intracellular domain is also important for the re-internalisation and recycling of E-selectin (Chuang et al., 1997; Kluger et al., 2002; Yoshida et al., 1998), which is controlled differently in different endothelial lineages(Kluger et al., 1997, 2002).

The ERK/MAPK pathway in particular has been implicated in neutrophil transmigration in the past (Stein et al., 2003), and E-selectin signalling via ERK and p38 has also been implicated in the transmigration of metastasising colon cancer cells (Tremblay et al., 2006, 2008), as well as activating β_1-integrin receptors in the endothelial cells (Sawada et al., 2001). Endothelial transmigration of HL-60 cells, an E-selectin-ligand expressing cell line, has also been shown to be inhibited by anti-E-selectin, anti-ICAM-1 or anti-VE-Cadherin blocking antibodies(Yoshida et al., 2000). However, in most current theories, ICAM-1 and other integrin receptors are considered the major transmigration mediators(Muller, 2009; Yang et al., 2005), and E-selectin is often considered to be less important after initial neutrophil tethering to the endothelium. The data presented here supports the idea that E-selectin signalling has a role to play in the transmigration of neutrophils, which has not previously been directly explored.

In summary, results presented in this chapter have shown that 60 minutes exposure of E-selectin expressing HUVEC to *N.meningitidis* has greatly differing effects on neutrophil-endothelial interactions depending on the presence of E-selectin cytoplasmic domain. HUVEC expressing full length E-selectin have increased adhesion to neutrophils under static conditions, as well as increased neutrophil transmigration under physiological flow conditions compared to HUVEC transfected with tail-less E-selectin. These results suggest a hitherto poorly studied yet important role for the E-selectin intracellular domain in control of neutrophil adhesion and transmigration upon *N.meningitidis* stimulation.

Although these results showed increased neutrophil transmigration upon 60 minutes *N.meningitidis* exposure on the endothelium, and hinted at a potential role for E-selectin signalling in the increased activation of neutrophils in meningococcal disease, the experiments carried out so far were not conclusive. It is currently unclear whether the additional transmigration caused by 60 minutes of *N.meningitidis* exposure on the endothelium was a general response to proinflammatory factors, or specific to *N.meningitidis*. The most pressing future work, therefore, is to investigate whether exposure of ES and ΔC transfected HUVEC to other inflammatory stimuli such as IL-1β or LOS for 60 minutes produces the same response in increased neutrophil static adhesion and transmigration under flow. Additionally, given the results in chapter 5 showing E-selectin clustering beneath microcolonies of *SiaD* mutant bacteria on the endothelium, it would be interesting to look at neutrophil adhesion and transmigration under flow to endothelial cells stimulated with the *N.meningitidis* mutant, as well as live *N.meningitidis* bacteria.

Some of these experiments were attempted, however problems were encountered which hindered the gathering of these results in time for inclusion in this thesis. Unexpected activation of freshly isolated neutrophils in some later experiments led to large amounts of adhesion and transmigration under all conditions. In several experiments large amounts of adhesion was seen on untransfected cells, or virtually all adhered bacteria under all conditions underwent transmigration, an effect only previously seen in control experiments where the endothelium was stimulated for 4 hours with large quantities of IL-1β.

Other researchers isolating neutrophils in the same laboratory also experienced similar problems with highly activated neutrophils after isolation, and as these neutrophil transmigration experiments were carried out towards the end of this thesis; there was unfortunately not enough time to properly investigate the IL-1β and LOS controls that would show whether the increased transmigration on ES transfected cells was *N.meningitidis* specific, or a general response to 60 minutes of inflammatory stimulus.

The rolling velocity experiments shown in Figure 6.12 were also incomplete, as only one donor was fully analysed in time for this thesis. The data from this experiment did not show any differences in rolling velocity between ES and ΔC transfected cells, although did appear to show slower rolling on IL-1β stimulated cells. The second most important experiments to carry out in the future are these experiments looking into rolling velocity, as leucocyte rolling is a known role of E-selectin activity in a way that neutrophil transmigration is only beginning to be considered as.

More functionally, it would be interesting to investigate a potential mechanism for the increased adhesion and transmigration seen on ES transfected HUVEC after 60 minutes *N.meningitidis* stimulation. Several pathways have been described that involve the E-selectin tail, including Cortactin activation, ERK/MAPK and PLCγ signalling. Investigating and blocking these pathways individually in ES and ΔC transfected cells to see what effect they have on E-selectin mediated neutrophil transmigration may expose a signalling mechanism activated by the E-selectin intracellular domain that assists neutrophil transmigration. On the other side of the adhesion mechanism, it would also be interesting to investigate activation by 60 minutes *N.meningitidis* exposure of neutrophil adhesion and transmigration on the endothelium by CXCR2 signalling; blocking the CXCR2 signalling pathway in neutrophils would distinguish between increased neutrophil adhesion effects due to E-selectin or CXCR2 signalling.

It would also be interesting to compare neutrophil adhesion and transmigration on ES or ΔC E-selectin transfected into a non-endothelial cell line, such as CHO cells, in order to discern any interference that other endothelial specific molecules may be having on E-selectin meditated neutrophil adhesion. This may increase the differences between full length and tail-less E-selectin, as there is normally some crossover between the functions of the three selectin molecules (Homeister et al., 1998; Jung and Ley, 1999), which would become less important on cells which did not express P-selectin or expressed fewer L-selectin ligands.

7 Final Discussion

The aim of the studies described in this thesis was to investigate the ability of the pathogenic bacterium *Neisseria meningitidis* to influence the distribution of the endothelial adhesion molecule E-selectin on the endothelial cell surface, as well as the consequences for E-selectin function in both neutrophil adhesion and intracellular signalling.

In order to do this, I developed lentiviral vectors containing cDNA coding for both full-length ES and tail-less mutant ΔC E-selectin, and validated their transfection efficiency and inflammatory potential in the HMEC-1 cell line as well as primary HUVEC. I used these lentiviral vectors to investigate the distribution of transfected ES and ΔC mutant E-selectin on the endothelial surface, and showed that the tail-less ΔC mutant E-selectin is expressed in a different, more diffuse pattern compared to full length E-selectin. I also showed that while clustering of E-selectin by *N.meningitidis* stimulation is variable and difficult to reproduce, exposure to an unencapsulated *SiaD*- mutant of *N.meningitidis* could cause co-localisation of endogenous, but not transfected, E-selectin beneath adherent colonies.

I also investigated a more functional link between *N.meningitidis* and E-selectin cytoplasmic signalling in the intense neutrophil recruitment and activation seen in meningococcal disease. I used the ES and ΔC lentiviral constructs to show that 60 minutes meningococcal exposure to HUVEC expressing full-length E-selectin can induce greater neutrophil adhesion to the endothelium under static conditions than tail-less E-selectin, as well as increased neutrophil transmigration under flow conditions. In order to investigate these neutrophil-endothelial interactions under physiological flow conditions I developed a reliable and reproducible *in vitro* flow chamber system to investigate neutrophil adhesion, rolling and transmigration.

7.1 The development and future uses of lentiviral vectors containing full length and tail-less E-selectin genes

The ES and ΔC lentiviral vectors developed and used throughout this thesis are useful tools for examining the contribution of E-selectin and its cytoplasmic tail to neutrophil adhesion and transmigration, and will certainly be valuable instruments in future experiments investigating other properties of E-selectin. Previous studies that involved the transfection of E-selectin into endothelial cells have used adenovirus vectors, which cannot transfect non-dividing cells, and can cause inflammatory stimulation of endothelial cells (Copreni et al., 2009; Gerszten et al., 1996; Nayak and Herzog, 2010). Although the lentiviral vector was shown to cause a slight increase in ICAM-1 expression during the validation stage of the viral

transfection method investigation, no other inflammatory CAMs were upregulated at the concentrations of virus used in later experiments. Furthermore, the levels of increased ICAM-1 expression were much lower than that seen on adenovirus transfected cells (Gerszten et al., 1996; Rafii et al., 2001).

The development of this less inflammatory and more stable lentiviral vector system enabled the efficient transfection and study of E-selectin expression and function in primary endothelial cells. Furthermore, the development of this model should facilitate a greater range of experiments investigating E-selectin signalling and adhesion in the future, which would be less influenced by additional activation of other inflammatory pathways and without the disadvantage of the transient nature of E-selectin expression in response to stimuli such as IL-1β. I have already used the lentiviral vector system to transfect cells of the HMEC-1 and HeLa cell lines, and have prepared and stored aliquots of cells that continue to stably express both ES and ΔC E-selectin after several passages.

Cell lines that stably express ES and ΔC E-selectin could be used as a direct comparison to HUVEC expressing both endogenous and transfected E-selectin. As HMEC-1 cells or other cell lines do not express endogenous E-selectin upon inflammatory stimulation, all E-selectin present on the surface of the HMEC-1 cells must therefore be the transfected ES or ΔC, whereas in transfected HUVEC there may be uncertainty over whether some of the expressed E-selectin is endogenous, especially after *N.meningitidis* stimulation. A preliminary experiment has already shown that HMEC-1 cells transfected with ES and ΔC have adhesion and transmigration responses to *N.meningitidis* that are similar to that seen in transfected HUVEC as in Figure 6.14, and the ES and ΔC transfected HMEC-1 cell line may be a useful tool to study E-selectin responses without donor variation and aberrant endogenous E-selectin expression in the future.

7.2 The role of the E-selectin intracellular tail in the distribution and function of E-selectin

Throughout the experiments shown in Chapter 5, it could consistently be seen that HUVEC transfected tail-less ΔC E-selectin formed much fewer spontaneous clusters than HUVEC expressing full length endogenous or transfected ES E-selectin (Figure 5.3). However both tail-less and full length E-selectin clustered beneath and around adherent neutrophils (Figure 5.4 and 5.5), as well as forming bright clusters upon antibody cross-linking (Figure 5.6). The implication of these observations is that the E-selectin cytoplasmic domain is

required for spontaneous E-selectin clustering, however clustering due to binding of the extracellular domain is unaffected by the presence of the E-selectin tail.

In addition to increasing spontaneous clustering, experiments in Chapter 6 showed that the cytoplasmic tail of E-selectin also has functional effects on leucocyte recruitment and transmigration. In response to 60 minutes *N.meningitidis* exposure, HUVEC transfected with full length E-selectin had significantly increased neutrophil adhesion under static conditions, and increased levels of neutrophil transmigration under physiological flow. HUVEC expressing tail-less E-selectin however, supported no more static neutrophil adhesion than unstimulated cells upon 60 minutes *N.meningitidis* stimulation, and lower transmigration under flow conditions than ES transfected cells.

These observations show the strong functional effect that the short 31 amino acid long tail has on E-selectin function; both in terms of the expression pattern on the plasma membrane, and functionally in the response to 60 minutes *N.meningitidis* stimulation by increasing the ability of neutrophils to adhere and transmigrate through the HUVEC monolayer. Although the intracellular tail is involved in both these responses, they are not necessarily controlled by the same mechanism; both the linkage of E-selectin to the cytoskeleton, and signalling via the ERK/MAPK pathway are known to be activated by the phosphorylation state of two different residues on the E-selectin tail (Hu et al., 2001; Kluger et al., 2002; Yoshida et al., 1998). A potential future set of experiments would be to use site-directed mutagenesis to create a series of E-selectin mutants with substitutions of the specific cytoplasmic tail residues that are known to be important in specific signalling pathways, and then testing their ability to support neutrophil adhesion and transmigration in response to *N.meningitidis*. This would make it possible to determine which of the pathways activated by the intracellular tail might be important in the increased adhesion and transmigration seen on ES E-selectin.

Interactions of the E-selectin intracellular domain have previously been shown to be important for linkage to the actin cytoskeleton (Lorenzon et al., 1998; Tilghman and Hoover, 2002a; Yoshida et al., 1996, 1998), and these intracellular linkages are also important for the endocytosis of E-selectin, and its transport around the cell(Chuang et al., 1997; Lamaze et al., 1997; Setiadi and McEver, 2008). The fact that these spontaneous clusters are commonly seen with full length endogenous or transfected ES, but not tail-less ΔC, E-selectin, implies that the interactions of E-selectin cytoplasmic domain with the cytoskeleton can act in two directions. Either outside-in, via binding of leucocytes or anti-E-selectin antibodies causing clustering and subsequent intracellular signalling and cytoskeletal linkage; or inside-out,

when E-selectin localisation on the endothelial surface is controlled by rearrangement of the cytoskeleton caused by other factors. E-selectin signalling has also previously been implicated in the transmigration of metastasising colon cancer cells, for which the p38 and ERK signalling pathways were shown to be important (Sawada et al., 2001; Stein et al., 2003; Tremblay et al., 2006, 2008). The ERK/MAPK pathway has also been shown to be activated by cross-linking of both E-selectin and ICAM-1(Gardiner and D'Souza, 1999; Hu et al., 2000, 2001; Sithu et al., 2007), leading to activation of the transcription factor c-fos (Hu et al., 2000; Thompson et al., 2002). It is likely that signalling via both E-selectin and ICAM-1 activates similar pathways to increase neutrophil transmigration across the endothelium, which may explain why some transmigration is also seen on ΔC transfected HUVEC which still express ICAM-1.

Another possibility is that the interaction of *N.meningitidis* with the endothelium causes greater activation of the conformational changes in the neutrophil integrins, which then bind to ICAM-1 and are required for efficient crawling and transmigration. This could occur via either increased activation of the Syk and p38 signalling pathways initiated by E-selectin binding to PSGL-1 and CD44 on the leucocyte surface(Yago et al., 2010; Zarbock et al., 2007), or by increased release of cytokines such as IL-8 or CXCL1 from the endothelium that activate neutrophils via the CXCR2 receptor(Lefort and Ley, 2012; Smith et al., 2004). Blocking of the CXCR2 receptor on neutrophils would allow the determination of which of pathway is more important in the increased neutrophil adhesion and transmigration due to *N.meningitidis* stimulation of the ES transfected endothelium.

It is unclear how the presence of the E-selectin tail would cause greater activation of neutrophils, however full-length E-selectin that is linked to the cytoskeleton via the intracellular domain does have a greater mechanical stiffness in response to magnetic twisting than tail-less E-selectin (Yoshida et al., 1996), and the transmission of force to the E-selectin ligands on neutrophils is required to activate the pathways leading to conformational change in integrins (Chase et al., 2012). Additionally, E-selectin linkage to the cytoskeleton under sheer flow conditions increases both the leucocyte transmigration and the activation of endothelial ERK/MAPK signalling due to E-selectin cross-linking (Cuvelier et al., 2005), implying that the mechanical force acting on E-selectin under sheer flow is important in activating the pathways leading to increased transmigration.

The possibility that this phenomenon may occur with other inflammatory conditions is also an intriguing one. Although meningococcal disease incurs a particularly strong inflammatory response, if the increased neutrophil recruitment and migration seen on full-length E-

selectin is also found under other inflammatory conditions, it could reveal a novel target pathway for treatment of many other instances of acute inflammation in addition to meningococcal disease.

There are of course other potential explanations for the increased static adhesion and transmigration under flow; notably that the 60 minutes exposure to *N.meningitidis* induces expression of cytokines (including IL-8 and CXCL1 mentioned previously), other adhesion molecules, and activation of multiple other inflammatory signalling pathways within the endothelial cells(Christodoulides et al., 2002; Constantin et al., 2004; Robinson et al., 2004; Schubert-Unkmeir et al., 2007; Sokolova et al., 2004). Although these undoubtedly play a role in the adhesion and transmigration of neutrophils, they do not explain the notable differences between ES and ΔC transfected cells. Whether the cause of this increased transmigration and adhesion is specific to *N.meningitidis* or not, this work has highlighted a previously under-appreciated role in neutrophil transmigration for E-selectin and E-selectin signalling.

7.3 Co-localisation of E-selectin with *N.meningitidis* and its effect on redistribution

The other major finding from this project was the co-localisation of E-selectin beneath adherent *SiaD N.meningitidis* microcolonies. Although co-localisation of E-selectin, as well as other endothelial cell adhesion molecules and cytoskeletal components, was also seen under adherent *N.meningitidis* in another study(Doulet et al., 2006); a very different, Opa-Opc- encapsulated MenC mutant (2C43) was used. In future work it would be interesting to obtain this 2C43 mutant and compare the co-localisation and clustering of E-selectin caused by 2C43 and the *SiaD* strain of the H44/76 strain used in my experiments.

Co-localisation of adherent *N.meningitidis* bacteria with E-selectin in the experiments in this thesis was only seen on endogenous E-selectin after IL-1β or meningococcal stimulation, and not with lentiviral transfected ES or ΔC. The reasons for this were unclear, as the sequence of ES transfected E-selectin is the same as endogenous E-selectin. It is possible that this is related to a different protein in endothelial cells that is upregulated by IL-1β stimulation but is not present on ES or ΔC transfected cells, and which then participates in a signalling pathway leading to co-localisation of E-selectin with adherent bacteria. The clustering of cytoskeletal components beneath adherent 2C93 *N.meningitidis* bacteria however, occurs without any additional stimulation by IL-1β (Doulet et al., 2006; Eugène et al., 2002; Hoffmann et al., 2001), implying that additional proinflammatory

stimulation of the endothelium is not necessarily required for *N.meningitidis* mediated signalling leading to cytoskeletal rearrangement.

It is also possible that the lack of *N.meningitidis* co-localisation with transfected E-selectin may be related to the localisation of E-selectin in different microdomains within the plasma membrane. As mentioned previously, endogenous E-selectin is expressed in both lipid rafts and clathrin pits (Kiely et al., 2003; Setiadi and McEver, 2008; Tilghman and Hoover, 2002b), however ES and ΔC E-selectin transfected into Chinese Hamster Ovary (CHO) cells using an adenovirus vector was only expressed in clathrin pits, and not in lipid rafts(Setiadi and McEver, 2008). It is unclear whether ES or ΔC E-selectin transfected into HUVEC would be located in the same microdomains as endogenous E-selectin, or merely a subset as was seen in transfected CHO cells. Signalling via PLCγ requires the localisation of E-selectin into lipid rafts, although ERK/MAPK signalling does not(Kiely et al., 2003). If ES and ΔC separate into different microdomains compared to endogenous E-selectin then this may affect the signalling required to co-localise with adhered bacteria. It is also possible that ES and ΔC separate into different microdomains from each other, which may influence the formation of the spontaneous clusters seen in ES but not ΔC E-selectin.

7.4 Future work

There are several avenues of research to be investigated regarding E-selectin localisation, function and interactions with *N.meningitidis* that stem from the work done in this thesis. Firstly I would like to further investigate the neutrophil transmigration and rolling experiments on transfected HUVEC. Exciting results were observed with increased neutrophil transmigration on full length ES transfected HUVEC exposed to *N.meningitidis* for one hour compared to the lower transmigration seen in cells transfected with tail-less ΔC E-selectin. However, it is still not known whether this response is specific to *N.meningitidis,* or due to general inflammatory stimulation. It will be necessary to investigate whether the same phenomenon occurs when stimulating ES and ΔC transfected HUVEC with IL-1β or LOS instead of *N.meningitidis* bacteria for 60 minutes. Nonetheless, the fact that meningococci can apparently influence the function of E-selectin, even indirectly, is an important observation and worthy of additional study, and E-selectin blockers may have additional implications for the treatment of other forms of acute inflammation if IL-1β or LPS produce a similar response as *N.meningitidis*.

Other studies have reported lower neutrophil migration on the endothelium in response to *N.meningitidis* stimulation, which is the opposite to the results seen in this thesis(Doulet et

al., 2006; Join-Lambert et al., 2013). However these publications used live *N.meningitidis* bacteria, whereas the neutrophil flow experiments in this thesis used killed bacteria due to restrictions on the use of live *N.meningitidis* in this laboratory. Differences in the immune response to live and killed *N.meningitidis*, as well as other bacteria, have been seen previously (Ivanov and Roy, 2013; Jones et al., 2007; Tezera et al., 2011; Wong et al., 2011), and it is an exciting possibility that live and killed *N.meningitidis* could also differentially affect the neutrophil-endothelium interactions. In order to test this, ES and ΔC transfected HUVEC would be exposed to live or killed *N.meningitidis* for 60 minutes before investigating neutrophil transmigration under flow. These experiments would not be able to be carried out in this laboratory under the current restrictions on using live *N.meningitidis*, however a collaboration with another laboratory which has access to a time lapse microscope at the correct microbiological containment level would allow for the effect of live and killed *N.meningitidis* on neutrophil migration to be investigated fully.

In addition to further studies on neutrophil transmigration, further work is also required to fully investigate the influence of the E-selectin tail on neutrophil rolling. Due to time constraints, only a limited number of donors were analysed for rolling velocity; and while decreased neutrophil velocity was seen on ES and ΔC transfected cells, as well as cells stimulated with IL-1β for 4 hours, there was no obvious difference in rolling velocity seen between ES and ΔC transfected cells or upon 60 minutes *N.meningitidis* or IL-1β stimulation. I would like to complete these rolling experiments by using additional donors in order to get a better picture of the difference in neutrophil rolling velocity between ES and ΔC transfected cells. As well as this, the neutrophil rolling velocity on HUVEC stimulated for 4 hours with *N.meningitidis* or with LOS would be studied. *N.meningitidis* stimulation of HUVEC for 4 hours in Figure 6.7 showed significantly increased compared to IL-1β or LOS stimulation, and it would be interesting to confirm whether this difference in neutrophil adhesion is also true for neutrophil rolling velocity as well as transmigration. Neutrophil rolling velocity measurements are especially important to gather given that neutrophil rolling is governed solely by E-selectin interactions, whereas adhesion and transmigration involve many different adhesion molecules and signalling pathways. Rolling velocity on *N.meningitidis* stimulated HUVEC would be especially interesting to investigate given that the bacteria has previously been shown to induce much greater E-selectin expression, but similar ICAM-1 and VCAM-1 expression, on HUVEC compared to IL-1β or LOS stimulation(Dixon et al., 2004).

One hypothesis that was also raised in the above discussion was the similar signalling pathways initiated by clustering of E-selectin and ICAM-1 (Schmid et al., 1995; Simon et al., 2000; Thompson et al., 2002; Tilghman and Hoover, 2002a, 2002b). Both of these endothelial adhesion molecules form clusters upon either leucocyte or antibody binding, and both have been shown to initiate ERK/MAPK signalling and c-fos activation (Hu et al., 2000; Thompson et al., 2002). ERK/MAPK activation from ICAM-1 signalling has been shown to be involved in monocyte transmigration (Gardiner and D'Souza, 1999; Sithu et al., 2007), while E-selectin signalling through the same pathway has been shown to mediate transmigration of a colon cancer cell line (Tremblay et al., 2006, 2008).

A novel method to investigate the relative contributions of E-selectin and ICAM-1 signalling in neutrophil transmigration would be to create a tail-less mutant of ICAM-1 in the same way as the ΔC E-selectin mutant was created in this project(Yoshida et al., 1996). Co-transfection of full length E-selectin and tail-less ICAM-1, or vice versa, into a cell line that does not express endogenous ICAM-1 or E-selectin such as CHO cells, would allow the relative contributions of E-selectin and ICAM-1 intracellular domains on neutrophil adhesion and transmigration under flow conditions to be determined; as well as allow the relative contributions of E-selectin and ICAM-1 to activation of ERK/MAPK and other signalling pathways upon leucocyte adhesion and cross-linking to be investigated. Antibody blocking of leucocyte-mediated adhesion molecule clustering would be a difficult way to investigate these interactions, as both E-selectin and ICAM-1 have essential neutrophil adhesion functions as well as signalling function, and antibody blocking of the extracellular clustering of one adhesion molecule would severely inhibit study of the other.

Specific inhibitors of ERK signalling would allow the contribution of this signalling pathway to the increased transmigration in response to *N.meningitidis* stimulation to be determined. Pull-down assays could also be used to co-immunoprecipitate the receptor complexes and cytoskeletal elements bound to the intracellular domains of E-selectin and ICAM-1 upon neutrophil binding or cross-linking, and investigate whether the two adhesion molecules form similar, or associated signalling complexes.

The other major element of this project that would be interesting to investigate further is the clustering and distribution of E-selectin on the endothelial cell surface. I had a great deal of trouble during these experiments with spontaneous clustering of full length E-selectin in many donors. As mentioned previously, I would like to investigate whether the E-selectin clusters are associated with specific plasma membrane microdomains such as lipid rafts or clathrin pits. Antibodies to components of clathrin pits and lipid rafts, such as α-actinin,

caveolin-1 and the IgE Fc receptor FcεRI (Kirchhausen, 1999; Setiadi and McEver, 2008; Wilson et al., 2004) could be used to examine their co-localisation with E-selectin under fluorescent confocal microscopy. It would be especially interesting to look at the differences in the spontaneous clusters seen with full length endogenous or ES E-selectin or tail-less ΔC E-selectin, as well as the co-localisation seen beneath adherent *SiaD* microcolonies. In order to examine the localisation of membrane components in more detail, a common technique is to isolate the lipid rafts by detergent solubilisation of the cell membrane followed by centrifugation in a sucrose gradient, and then examine co-localisation of E-selectin with membrane components of lipid rafts via western blotting (Setiadi and McEver, 2008; Wilson et al., 2004). This would confirm the localisation of transfected ES and ΔC E-selectin on the plasma membrane compared to endogenous E-selectin, and give interesting insight into the link between localisation on the plasma membrane and E-selectin function.

I would also like to examine the redistribution of E-selectin upon *N.meningitidis* stimulation. During the project I had trouble distinguishing between E-selectin redistribution due to *N.meningitidis* exposure and spontaneous clustering. It is possible that the pattern of distribution, and redistribution, of E-selectin is different on different donors, and that fixed time points may not capture the transient redistribution of E-selectin upon *N.meningitidis* stimulation on different donors. In order to get around this, the distribution of E-selectin on the endothelial surface could be studied in real time with live cell imaging, using either fluorescently linked ES and ΔC transfected E-selectin, or antibody labelled endogenous E-selectin. Linkage to a large fluorescent protein such as GFP could interfere in the function of the short E-selectin intracellular domain, but a shorter synthetic fluorescent tag may allow study of E-selectin redistribution in real time using a time lapse microscope(Chen et al., 2013; Wombacher and Cornish, 2011). This technique could be used to study transient events in E-selectin redistribution upon *N.meningitidis* stimulation that may have been missed when fixing the cells at specific time points.

7.5 Final Summary

The studies in this thesis have shown clear differences in both neutrophil adhesion and transmigration on full length and tail-less E-selectin in response to *N.meningitidis*. These results have strong ramifications for the current understanding of meningococcal sepsis, as a clear role for the E-selectin tail in increased neutrophil transmigration under *N.meningitidis* stimulation has not previously been shown. This data has wider implications than just meningococcal sepsis, as the involvement of the E-selectin intracellular domain in neutrophil

adhesion and transmigration has broad ramifications for both other forms of bacterial sepsis as well as the inflammatory state of the endothelium. The contribution of the E-selectin intracellular domain to leucocyte transmigration has previously been poorly studied, however this is an area of research that now deserves greater attention. E-selectin is already well understood to be central to neutrophil rolling adhesion, and it will be vital to understand in greater detail the adhesion molecule's novel function in neutrophil transmigration by investigating E-selectin's intracellular signalling pathways and their consequences. The tools and techniques described in this thesis can be used to investigate this further by investigating neutrophil transmigration on ES and ΔC transfected cells under other stimuli and conditions. Other questions can also now be addressed such as the contribution of E-selectin intracellular signalling to other aspects of the neutrophil recruitment pathway, and the behaviour of the endothelium during inflammation in general. As stated previously, it is possible that the functions of E-selectin intracellular signalling overlap with ICAM-1 signalling, and currently the ERK/MAPK pathway appears to be the primary candidate for further investigation as it is known to be activated by both E-selectin and ICAM-1, and has been implicated previously in the transmigration of colon cancer cells. Additionally the tools developed in this thesis, notably the ES and ΔC lentiviral constructs, have the potential be used in other, different studies looking at endothelial inflammation in areas unrelated to sepsis.

8 Appendix

Appendix A: Additional figures showing confirmation of ES and ΔC cDNA clones from Chapter 3

A-1 Restriction digest of the six lentiviral clones containing ES cDNA

The six ES clones that were positive for inserted ES cDNA as determined by colony PCR using the primer pair a-b in Figure 3.7A were amplified by miniprep, and incubated with the restriction enzymes BamHI and SspI, before being run on a 1% Agarose gel containing GelRed. Results are shown in Appendix Figure A-1. Clones 6, 40 and 56 have the insert in the wrong direction, as two bands of around 3700bp and 3136bp can be seen, while clones 33 and 64 have the insert in the correct direction, as they show three DNA fragments of around 2537bp, 3700bp and 4386bp. Clone 44 either has no insert at all (which would contradict the colony PCR results in Figure 3.8) or there was a problem with the experiment at either the amplification or restriction digestion stages.

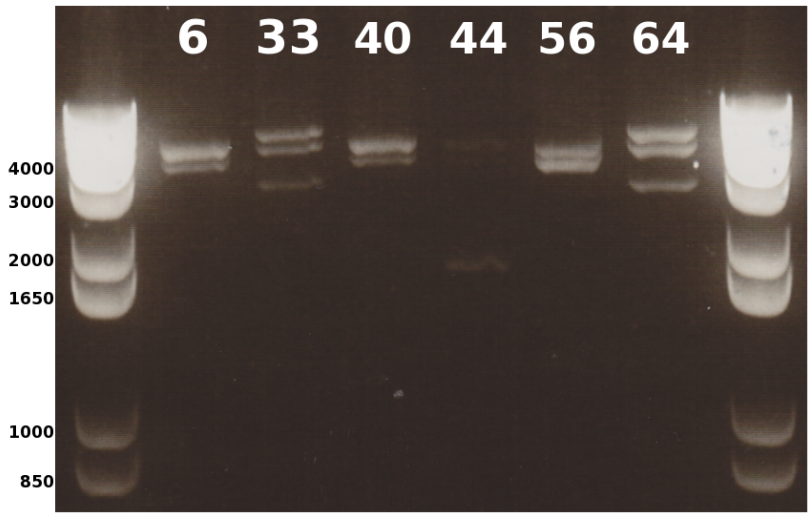

Appendix Figure A-1: Restriction digest using enzymes BamHI and SspI of the 6 ampicillin resistant transformants that were confirmed to contain the wild type ES E-selectin sequence, as confirmed by colony PCR.

A-2 Colony PCR of two lentiviral clones containing ΔC cDNA

Two of the ΔC clones that were positive for inserted ΔC cDNA underwent colony PCR using the three combinations of primer pairs shown in Figure 3.7. Results are shown in Appendix Figure A-2. Both clones produced a heavy PCR product with primer pair a-b (lanes 1+4), while clone ΔC-3 produced a smaller product with the primers a-c (lane 5), but not b-c (lane 6), and ΔC-4 produced a PCR product with b-c (lane 3) but not a-c (lane 2). This indicates that clone ΔC-4 has the ΔC insert ligated in the correct direction, while ΔC-3 has it inserted in the reverse direction. Confirming the restriction digest results in Figure 3.6.

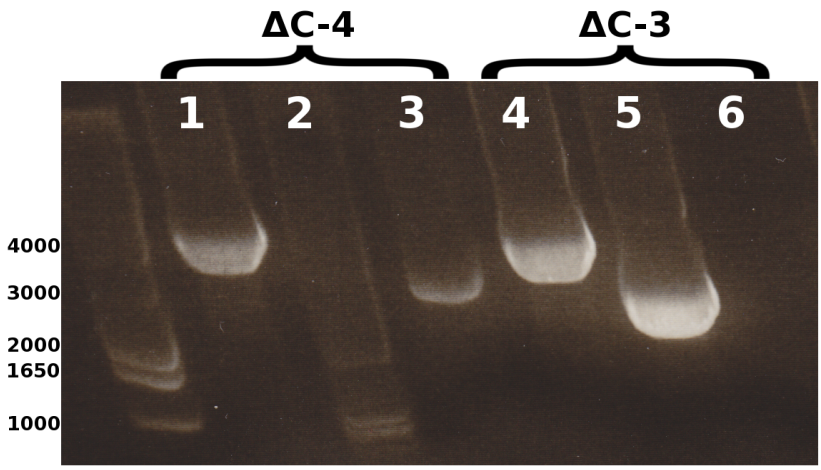

Appendix Figure A-2: Colony PCR results of two transformants, ΔC-4 (lanes 1-3) and ΔC-3 (lanes 4-6), using the primer pairs outlined in Figure 3.7A. Lanes 1+4 were amplified with primer pair a-b, lanes 2+5 with a-c and lanes 3+6 with b-c.

Appendix B: Full published E-selectin coding sequence aligned with the sequences of ES and ΔC cDNA inserts

```
E-selectin      ATGATTGCTTCACAGTTTCTCTCAGCTCTCACTTTGGTGCTTCTCATTAAAGAGAGTGGA 60
ES              ATGATTGCTTCACAGTTTCTCTCAGCTCTCACTTTGGTGCTTCTCATTAAAGAGAGTGGA 60
AC              ATGATTGCTTCACAGTTTCTCTCAGCTCTCACTTTGGTGCTTCTCATTAAAGAGAGTGGA 60
                ************************************************************

E-selectin      GCCTGGTCTTACAACACCTCCACGGAAGCTATGACTTATGATGAGGCCAGTGCTTATTGT 120
ES              GCCTGGTCTTACAACACCTCCACGGAAGCTATGACTTATGATGAGGCCAGTGCTTATTGT 120
AC              ATGATTGCTTCACAGTTTCTCTCAGCTCTCACTTTGGTGCTTCTCATTAAAGAGAGTGGA 120
                ************************************************************

E-selectin      CAGCAAAGGTACACACACCTGGTTGCAATTCAAAACAAAGAAGAGATTGAGTACCTAAAC 180
ES              CAGCAAAGGTACACACACCTGGTTGCAATTCAAAACAAAGAAGAGATTGAGTACCTAAAC 180
AC              GCCTGGTCTTACAACACCTCCACGGAAGCTATGACTTATGATGAGGCCAGTGCTTATTGT 180
                ************************************************************

E-selectin      TCCATATTGAGCTATTCACCAAGTTATTACTGGATTGGAATCAGAAAAGTCAACAATGTG 240
ES              TCCATATTGAGCTATTCACCAAGTTATTACTGGATTGGAATCAGAAAAGTCAACAATGTG 240
AC              TCCATATTGAGCTATTCACCAAGTTATTACTGGATTGGAATCAGAAAAGTCAACAATGTG 240
                ************************************************************

E-selectin      TGGGTCTGGGTAGGAACCCAGAAACCTCTGACAGAAGAAGCCAAGAACTGGGCTCCAGGT 300
ES              TGGGTCTGGGTAGGAACCCAGAAACCTCTGACAGAAGAAGCCAAGAACTGGGCTCCAGGT 300
AC              TGGGTCTGGGTAGGAACCCAGAAACCTCTGACAGAAGAAGCCAAGAACTGGGCTCCAGGT 300
                ************************************************************

E-selectin      GAACCCAACAATAGGCAAAAAGATGAGGACTGCGTGGAGATCTACATCAAGAGAGAAAAA 360
ES              GAACCCAACAATAGGCAAAAAGATGAGGACTGCGTGGAGATCTACATCAAGAGAGAAAAA 360
AC              GAACCCAACAATAGGCAAAAAGATGAGGACTGCGTGGAGATCTACATCAAGAGAGAAAAA 360
                ************************************************************

E-selectin      GATGTGGGCATGTGGAATGATGAGAGGTGCAGCAAGAAGAAGCTTGCCCTATGCTACACA 420
ES              GATGTGGGCATGTGGAATGATGAGAGGTGCAGCAAGAAGAAGCTTGCCCTATGCTACACA 420
AC              GATGTGGGCATGTGGAATGATGAGAGGTGCAGCAAGAAGAAGCTTGCCCTATGCTACACA 420
                ************************************************************

E-selectin      GCTGCCTGTACCAATACATCCTGCAGTGGCCACGGTGAATGTGTAGAGACCATCAATAAT 480
ES              GCTGCCTGTACCAATACATCCTGCAGTGGCCACGGTGAATGTGTAGAGACCATCAATAAT 480
AC              GCTGCCTGTACCAATACATCCTGCAGTGGCCACGGTGAATGTGTAGAGACCATCAATAAT 480
                ************************************************************

E-selectin      TACACTTGCAAGTGTGACCCTGGCTTCAGTGGACTCAAGTGTGAGCAAATTGTGAACTGT 540
ES              TACACTTGCAAGTGTGACCCTGGCTTCAGTGGACTCAAGTGTGAGCAAATTGTGAACTGT 540
AC              TACACTTGCAAGTGTGACCCTGGCTTCAGTGGACTCAAGTGTGAGCAAATTGTGAACTGT 540
                ************************************************************

E-selectin      ACAGCCCTGGAATCCCCTGAGCATGGAAGCCTGGTTTGCAGTCACCCACTGGGAAACTTC 600
ES              ACAGCCCTGGAATCCCCTGAGCATGGAAGCCTGGTTTGCAGTCACCCACTGGGAAACTTC 600
33-I            ACAGCCCTGGAATCCCCTGAGCATGGAAGCCTGGTTTGCAGTCACCCACTGGGAAACTTC 600
                ************************************************************

E-selectin      AGCTACAATTCTTCCTGCTCTATCAGCTGTGATAGGGGTTACCTGCCAAGCAGCATGGAG 660
ES              AGCTACAATTCTTCCTGCTCTATCAGCTGTGATAGGGGTTACCTGCCAAGCAGCATGGAG 660
AC              AGCTACAATTCTTCCTGCTCTATCAGCTGTGATAGGGGTTACCTGCCAAGCAGCATGGAG 660
                ************************************************************

E-selectin      ACCATGCAGTGTATGTCCTCTGGAGAATGGAGTGCTCCTATTCCAGCCTGCAATGTGGTT 720
ES              ACCATGCAGTGTATGTCCTCTGGAGAATGGAGTGCTCCTATTCCAGCCTGCAATGTGGTT 720
AC              ACCATGCAGTGTATGTCCTCTGGAGAATGGAGTGCTCCTATTCCAGCCTGCAATGTGGTT 720
                ************************************************************

E-selectin      GAGTGTGATGCTGTGACAAATCCAGCCAATGGGTTCGTGGAATGTTTCCAAAACCCTGGA 780
ES              GAGTGTGATGCTGTGACAAATCCAGCCAATGGGTTCGTGGAATGTTTCCAAAACCCTGGA 780
AC              GAGTGTGATGCTGTGACAAATCCAGCCAATGGGTTCGTGGAATGTTTCCAAAACCCTGGA 780
                ************************************************************

E-selectin      AGCTTCCCATGGAACACAACCTGTACATTTGACTGTGAAGAAGGATTTGAACTAATGGGA 840
ES              AGCTTCCCATGGAACACAACCTGTACATTTGACTGTGAAGAAGGATTTGAACTAATGGGA 840
AC              AGCTTCCCATGGAACACAACCTGTACATTTGACTGTGAAGAAGGATTTGAACTAATGGGA 840
                ************************************************************

E-selectin      GCCCAGAGCCTTCAGTGTACCTCATCTGGGAATTGGGACAACGAGAAGCCAACGTGTAAA 900
ES              GCCCAGAGCCTTCAGTGTACCTCATCTGGGAATTGGGACAACGAGAAGCCAACGTGTAAA 900
AC              GCCCAGAGCCTTCAGTGTACCTCATCTGGGAATTGGGACAACGAGAAGCCAACGTGTAAA 900
                ************************************************************

E-selectin      GCTGTGACATGCAGGGCCGTCCGCCAGCCTCAGAATGGCTCTGTGAGGTGCAGCCATTCC 960
ES              GCTGTGACATGCAGGGCCGTCCGCCAGCCTCAGAATGGCTCTGTGAGGTGCAGCCATTCC 960
AC              GCTGTGACATGCAGGGCCGTCCGCCAGCCTCAGAATGGCTCTGTGAGGTGCAGCCATTCC 960
                ************************************************************

E-selectin      CCTGCTGGAGAGTTCACCTTCAAATCATCCTGCAACTTCACCTGTGAGGAAGGCTTCATG 1020
ES              CCTGCTGGAGAGTTCACCTTCAAATCATCCTGCAACTTCACCTGTGAGGAAGGCTTCATG 1020
AC              CCTGCTGGAGAGTTCACCTTCAAATCATCCTGCAACTTCACCTGTGAGGAAGGCTTCATG 1080
```

```
                ************************************************************

E-selectin      TTGCAGGGACCAGCCCAGGTTGAATGCACCACTCAAGGGCAGTGGACACAGCAAATCCCA 1080
ES              TTGCAGGGACCAGCCCAGGTTGAATGCACCACTCAAGGGCAGTGGACACAGCAAATCCCA 1080
AC              TTGCAGGGACCAGCCCAGGTTGAATGCACCACTCAAGGGCAGTGGACACAGCAAATCCCA 1080
                ************************************************************

E-selectin      GTTTGTGAAGCTTTCCAGTGCACAGCCTTGTCCAACCCCGAGCGAGGCTACATGAATTGT 1140
ES              GTTTGTGAAGCTTTCCAGTGCACAGCCTTGTCCAACCCCGAGCGAGGCTACATGAATTGT 1140
AC              GTTTGTGAAGCTTTCCAGTGCACAGCCTTGTCCAACCCCGAGCGAGGCTACATGAATTGT 1140
                ************************************************************

E-selectin      CTTCCTAGTGCTTCTGGCAGTTTCCGTTATGGGTCCAGCTGTGAGTTCTCCTGTGAGCAG 1200
ES              CTTCCTAGTGCTTCTGGCAGTTTCCGTTATGGGTCCAGCTGTGAGTTCTCCTGTGAGCAG 1200
AC              CTTCCTAGTGCTTCTGGCAGTTTCCGTTATGGGTCCAGCTGTGAGTTCTCCTGTGAGCAG 1200
                ************************************************************

E-selectin      GGTTTTGTGTTGAAGGGATCCAAAAGGCTCCAATGTGGCCCCACAGGGGAGTGGGACAAC 1260
ES              GGTTTTGTGTTGAAGGGATCCAAAAGGCTCCAATGTGGCCCCACAGGGGAGTGGGACAAC 1260
AC              GGTTTTGTGTTGAAGGGATCCAAAAGGCTCCAATGTGGCCCCACAGGGGAGTGGGACAAC 1260
                ************************************************************

E-selectin      GAGAAGCCCACATGTGAAGCTGTGAGATGCGATGCTGTCCACCAGCCCCCGAAGGGTTTG 1320
ES              GAGAAGCCCACATGTGAAGCTGTGAGATGCGATGCTGTCCACCAGCCCCCGAAGGGTTTG 1320
AC              GAGAAGCCCACATGTGAAGCTGTGAGATGCGATGCTGTCCACCAGCCCCCGAAGGGTTTG 1320
                ************************************************************

E-selectin      GTGAGGTGTGCTCATTCCCCTATTGGAGAATTCACCTACAAGTCCTCTTGTGCCTTCAGC 1380
ES              GTGAGGTGTGCTCATTCCCCTATTGGAGAATTCACCTACAAGTCCTCTTGTGCCTTCAGC 1380
AC              GTGAGGTGTGCTCATTCCCCTATTGGAGAATTCACCTACAAGTCCTCTTGTGCCTTCAGC 1380
                ************************************************************

E-selectin      TGTGAGGAGGGATTTGAATTATATGGATCAACTCAACTTGAGTGCACATCTCAGGGACAA 1440
ES              TGTGAGGAGGGATTTGAATTATATGGATCAACTCAACTTGAGTGCACATCTCAGGGACAA 1440
AC              TGTGAGGAGGGATTTGAATTATATGGATCAACTCAACTTGAGTGCACATCTCAGGGACAA 1440
                ************************************************************

E-selectin      TGGACAGAAGAGGTTCCTTCCTGCCAAGTGGTAAAATGTTCAAGCCTGGCAGTTCCGGGA 1500
ES              TGGACAGAAGAGGTTCCTTCCTGCCAAGTGGTAAAATGTTCAAGCCTGGCAGTTCCGGGA 1500
AC              TGGACAGAAGAGGTTCCTTCCTGCCAAGTGGTAAAATGTTCAAGCCTGGCAGTTCCGGGA 1500
                ************************************************************

E-selectin      AAGATCAACATGAGCTGCAGTGGGGAGCCCGTGTTTGGCACTGTGTGCAAGTTCGCCTGT 1560
ES              AAGATCAACATGAGCTGCAGTGGGGAGCCCGTGTTTGGCACTGTGTGCAAGTTCGCCTGT 1560
AC              AAGATCAACATGAGCTGCAGTGGGGAGCCCGTGTTTGGCACTGTGTGCAAGTTCGCCTGT 1560
                ************************************************************



E-selectin      CCTGAAGGATGGACGCTCAATGGCTCTGCAGCTCGGACATGTGGAGCCACAGGACACTGG 1620
ES              CCTGAAGGATGGACGCTCAATGGCTCTGCAGCTCGGACATGTGGAGCCACAGGACACTGG 1620
AC              CCTGAAGGATGGACGCTCAATGGCTCTGCAGCTCGGACATGTGGAGCCACAGGACACTGG 1620
                ************************************************************

E-selectin      TCTGGCCTGCTACCTACCTGTGAAGCTCCCACTGAGTCCAACATTCCCTTGGTAGCTGGA 1680
ES              TCTGGCCTGCTACCTACCTGTGAAGCTCCCACTGAGTCCAACATTCCCTTGGTAGCTGGA 1680
AC              TCTGGCCTGCTACCTACCTGTGAAGCTCCCACTGAGTCCAACATTCCCTTGGTAGCTGGA 1680
                ************************************************************

E-selectin      CTTTCTGCTGCTGGACTCTCCCTCCTGACATTAGCACCATTTCTCCTCTGGCTTCGGAAA 1740
ES              CTTTCTGCTGCTGGACTCTCCCTCCTGACATTAGCACCATTTCTCCTCTGGCTTCGGAAA 1740
AC              CTTTCTGCTGCTGGACTCTCCCTCCTGACATTAGCACCATTTCTCCTCTGGCTTCGGTAA 1740
                ************************************************** **

E-selectin      TGCTTACGGAAAGCAAAGAAATTTGTTCCTGCCAGCAGCTGCCAAAGCCTTGAATCAGAC 1800
ES              TGCTTACGGAAAGCAAAGAAATTTGTTCCTGCCAGCAGCTGCCAAAGCCTTGAATCAGAC 1800
AC              TGCTTACGGAAAGCAAAGAAATTTGTTCCTGCCAGCAGCTGCCAAAGCCTTGAATCAGAC 1800
                ************************************************************

E-selectin      GGAAGCTACCAAAAGCCTTCTTACATCCTTTAA                              1833
ES              GGAAGCTACCAAAAGCCTTCTTACATCCTTTAA                              1833
AC              GGAAGCTACCAAAAGCCTTCTTACATCCTTTAT                              1833
                *********************************
```

Appendix Figure B-1: Full sequence of the E-selectin coding region aligned with the sequence of the ES and ΔC inserts used in the lentivirus. Mutations from the published sequence are highlighted in red. ES and ΔC sequences sequenced by the UCL Wolfson institute of Biomedical Research.

Appendix C: E-selectin spontaneous clustering and cross-linking was also seen using alternative primary and secondary antibodies

In order to investigate whether the spontaneous E-selectin clustering seen when HUVEC were stained using the Method A staining technique outlined in Methods section 2.9 and in Figure 5.2 were an artefact caused by the antibodies used, several additional primary and secondary antibodies were tested to see if they produced the same staining results.

The antibodies used in all confocal images seen in Chapter 5 were the BBIG-E6 anti-E-selectin primary antibody and the Sigma FITC linked goat anti-mouse IgG antibody, as seen in Appendix Figure C-1A. In Appendix Figure C-1B an alternative primary antibody, BBIG-E4, was used to stain E-selectin, using the same secondary antibody. In Appendix Figure C-1C and D, the BBIG-E6 primary antibody was once again used but in conjunction with the Alexa Fluor 546 or 568 secondary antibodies, respectively.

All four different antibody combinations show the same staining effects, spontaneous clustering of IL-1β induced E-selectin on HUVEC and E-selectin cross-linking when stained with both antibodies before fixation of the cells.

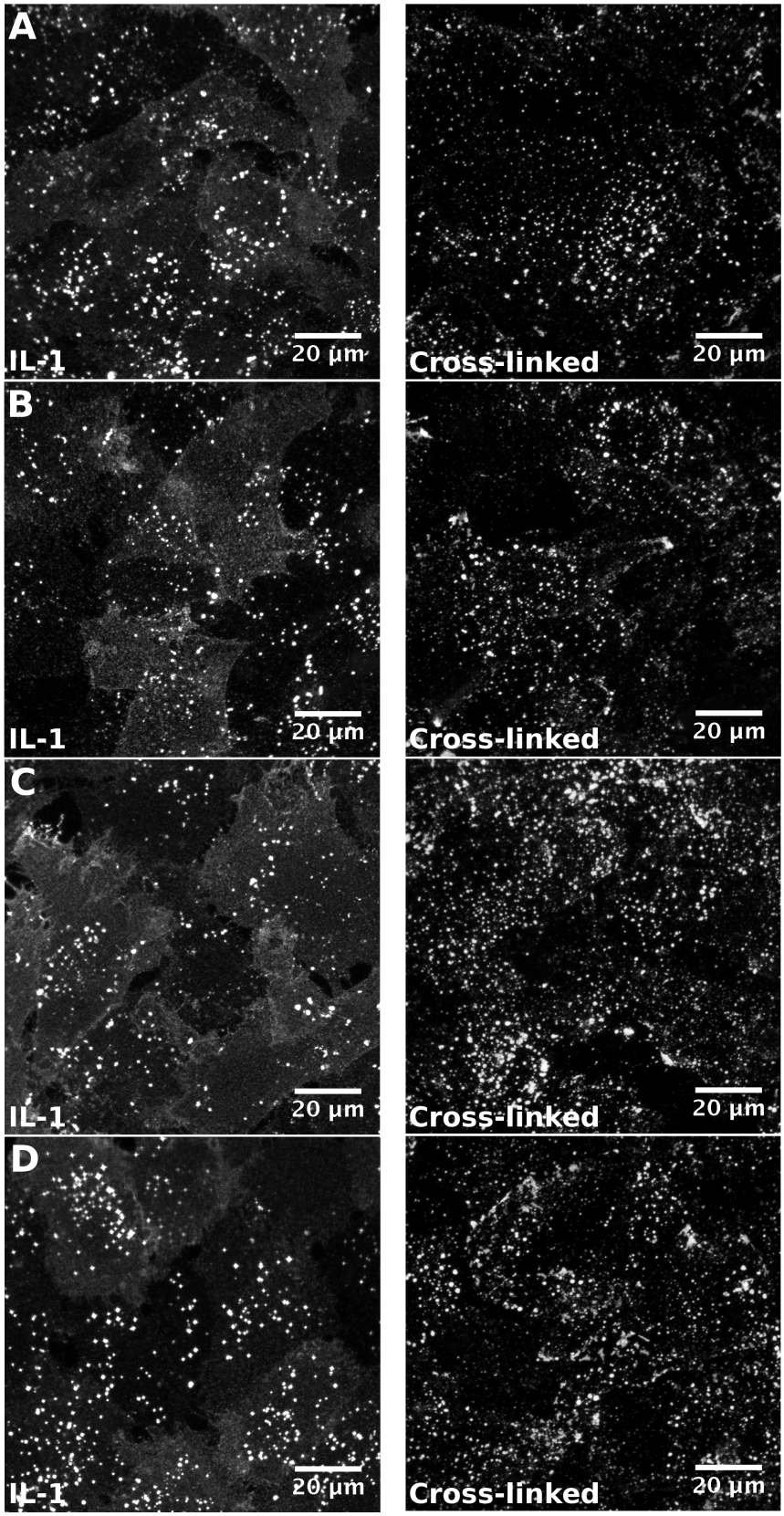

Appendix Figure C-1: E-selectin expression on HUVEC stimulated with IL-1β (column 1) and subsequently cross-linked with primary and secondary antibodies (column 2). HUVEC were stained using different combinations of antibodies. Cells were stained with either BBIG-E6 (A, C, D) or BBIG-E4 (B) primary antibody from R&D systems, followed by either Sigma FITC-linked goat anti-mouse antibody (A, B), or Molecular Probes Alexa-Fluor 546 (C) or Alexa-Fluor 568 (D) linked goat anti-mouse antibody.

References

Ades, E.W., Candal, F.J., Swerlick, R.A., George, V.G., Summers, S., Bosse, D.C., and Lawley, T.J. (1992). HMEC-1: establishment of an immortalized human microvascular endothelial cell line. J. Invest. Dermatol. *99*, 683–690.

Aho, E.L., Dempsey, J.A., Hobbs, M.M., Klapper, D.G., and Cannon, J.G. (1991). Characterization of the opa (class 5) gene family of Neisseria meningitidis. Mol. Microbiol. *5*, 1429–1437.

Aird, W.C. (2003). The role of the endothelium in severe sepsis and multiple organ dysfunction syndrome. Blood *101*, 3765–3777.

Aird, W.C. (2006). Mechanisms of Endothelial Cell Heterogeneity in Health and Disease. Circ. Res. *98*, 159–162.

Albiger, B., Johansson, L., and Jonsson, A.-B. (2003). Lipooligosaccharide-deficient Neisseria meningitidis shows altered pilus-associated characteristics. Infect. Immun. *71*, 155–162.

Von Asmuth, E.J.U., Smeets, E.F., Ginsel, L.A., Onderwater, J.J.M., Leeuwenberg, J.F.M., and Buurman, W.A. (1992). Evidence for endocytosis of E-selectin in human endothelial cells. Eur. J. Immunol. *22*, 2519–2526.

Baggiolini, M. (1993). Novel aspects of inflammation: interleukin-8 and related chemotactic cytokines. Clin. Investig. *71*, 812–814.

Banerjee, A., and Ghosh, S.K. (2003). The role of pilin glycan in neisserial pathogenesis. Mol. Cell. Biochem. *253*, 179–190.

Bernard, S.C., Simpson, N., Join-Lambert, O., Federici, C., Laran-Chich, M.-P., Maïssa, N., Bouzinba-Ségard, H., Morand, P.C., Chretien, F., Taouji, S., et al. (2014). Pathogenic Neisseria meningitidis utilizes CD147 for vascular colonization. Nat. Med. *advance online publication*.

Bevilacqua, M.P. (1993). Endothelial-leukocyte adhesion molecules. Annu. Rev. Immunol. *11*, 767–804.

Bevilacqua, M.P., Pober, J.S., Majeau, G.R., Fiers, W., Cotran, R.S., and Gimbrone, M.A. (1986). Recombinant tumor necrosis factor induces procoagulant activity in cultured human vascular endothelium: characterization and comparison with the actions of interleukin 1. Proc. Natl. Acad. Sci. *83*, 4533–4537.

Bevilacqua, M.P., Stengelin, S., Gimbrone, M.A., and Seed, B. (1989). Endothelial leukocyte adhesion molecule 1: an inducible receptor for neutrophils related to complement regulatory proteins and lectins. Science *243*, 1160–1165.

Birkness, K.A., Swisher, B.L., White, E.H., Long, E.G., Ewing, E.P., and Quinn, F.D. (1995). A tissue culture bilayer model to study the passage of Neisseria meningitidis. Infect. Immun. *63*, 402–409.

Bjerknes, R., Guttormsen, H.K., Solberg, C.O., and Wetzler, L.M. (1995). Neisserial porins inhibit human neutrophil actin polymerization, degranulation, opsonin receptor expression, and phagocytosis but prime the neutrophils to increase their oxidative burst. Infect. Immun. *63*, 160–167.

Blömer, U., Naldini, L., Kafri, T., Trono, D., Verma, I.M., and Gage, F.H. (1997). Highly efficient and sustained gene transfer in adult neurons with a lentivirus vector. J. Virol. *71*, 6641–6649.

Bochner, B.S. (2000). Road signs guiding leukocytes along the inflammation superhighway. J. Allergy Clin. Immunol. *106*, 817–828.

Bochner, B.S., Sterbinsky, S.A., Bickel, C.A., Werfel, S., Wein, M., and Newman, W. (1994). Differences between human eosinophils and neutrophils in the function and expression of sialic acid-containing counterligands for E-selectin. J. Immunol. Baltim. Md 1950 *152*, 774–782.

Borg, J., Christie, D., Coen, P.G., Booy, R., and Viner, R.M. (2009). Outcomes of Meningococcal Disease in Adolescence: Prospective, Matched-Cohort Study. Pediatrics *123*, e502–e509.

Borregaard, N., and Cowland, J.B. (1997). Granules of the Human Neutrophilic Polymorphonuclear Leukocyte. Blood *89*, 3503–3521.

Boulton, I.C., Gorringe, A.R., Gorinsky, B., Retzer, M.D., Schryvers, A.B., Joannou, C.L., and Evans, R.W. (1999). Purified meningococcal transferrin-binding protein B interacts with a secondary, strain-specific, binding site in the N-terminal lobe of human transferrin. Biochem. J. *339*, 143–149.

Bradley, C.J., Griffiths, N.J., Rowe, H.A., Heyderman, R.S., and Virji, M. (2005). Critical determinants of the interactions of capsule-expressing Neisseria meningitidis with host cells: the role of receptor density in increased cellular targeting via the outer membrane Opa proteins. Cell. Microbiol. *7*, 1490–1503.

Van Brakel, M.J.M., van Vught, A.J., and Gemke, R.J.B.J. (2000). Pediatric risk of mortality (PRISM) score in meningococcal disease. Eur. J. Pediatr. *159*, 232–236.

Brandtzaeg, P. (2006). Pathogenesis and Pathophysiology of Invasive Meningococcal Disease. In Handbook of Meningococcal Disease, tthias Frosch, and rtin C. J.iden, eds. (Wiley-VCH Verlag GmbH & Co. KGaA), pp. 427–480.

Brandtzaeg, P., Kierulf, P., Gaustad, P., Skulberg, A., Bruun, J.N., Halvorsen, S., and Sørensen, E. (1989). Plasma endotoxin as a predictor of multiple organ failure and death in systemic meningococcal disease. J. Infect. Dis. *159*, 195–204.

Brandtzaeg, P., Bjerre, A., Øvstebø, R., Brusletto, B., Joø, G.B., and Kierulf, P. (2001). Invited review: Neisseria meningitidis lipopolysaccharides in human pathology. J. Endotoxin Res. *7*, 401–420.

Brissac, T., Mikaty, G., Duménil, G., Coureuil, M., and Nassif, X. (2012). The meningococcal minor pilin PilX is responsible for type IV pilus conformational changes associated with signaling to endothelial cells. Infect. Immun. *80*, 3297–3306.

Brock, R., Hamelers, I.H.L., and Jovin, T.M. (1999). Comparison of fixation protocols for adherent cultured cells applied to a GFP fusion protein of the epidermal growth factor receptor. Cytometry *35*, 353–362.

Bröker, M., Jacobsson, S., DeTora, L., Pace, D., and Taha, M.-K. (2012). Increase of meningococcal serogroup Y cases in Europe: A reason for concern? Hum. Vaccines Immunother. *8*, 685–688.

Cartwright, K. (2006). Historical Aspects. In Handbook of Meningococcal Disease, tthias Frosch, and rtin C. J.iden, eds. (Wiley-VCH Verlag GmbH & Co. KGaA), pp. 1–13.

Cartwright, K.A., Stuart, J.M., Jones, D.M., and Noah, N.D. (1987). The Stonehouse survey: nasopharyngeal carriage of meningococci and Neisseria lactamica. Epidemiol. Infect. *99*, 591–601.

Caugant, D.A., H?iby, E.A., Rosenqvist, E., Fr?holm, L.O., and Selander, R.K. (1992). Transmission of Neisseria meningitidis among asymptomatic military recruits and antibody analysis. Epidemiol. Infect. *109*, 241–253.

Caugant, D.A., Høiby, E.A., Magnus, P., Scheel, O., Hoel, T., Bjune, G., Wedege, E., Eng, J., and Frøholm, L.O. (1994). Asymptomatic carriage of Neisseria meningitidis in a randomly sampled population. J. Clin. Microbiol. *32*, 323–330.

Chan, E., Schaller, T., Eddaoudi, A., Zhan, H., Tan, C.P., Jacobsen, M., Thrasher, A.J., Towers, G.J., and Qasim, W. (2012). Lentiviral Gene Therapy Against Human Immunodeficiency Virus Type 1, Using a Novel Human TRIM21-Cyclophilin A Restriction Factor. Hum. Gene Ther. *23*, 1176–1185.

Chase, S.D., Magnani, J.L., and Simon, S.I. (2012). E-selectin ligands as mechanosensitive receptors on neutrophils in health and disease. Ann. Biomed. Eng. *40*, 849–859.

Chen, Z., Cornish, V.W., and Min, W. (2013). Chemical tags: inspiration for advanced imaging techniques. Curr. Opin. Chem. Biol. *17*, 637–643.

Chi, J.-T., Chang, H.Y., Haraldsen, G., Jahnsen, F.L., Troyanskaya, O.G., Chang, D.S., Wang, Z., Rockson, S.G., van de Rijn, M., Botstein, D., et al. (2003). Endothelial cell diversity revealed by global expression profiling. Proc. Natl. Acad. Sci. *100*, 10623–10628.

Christensen, H., Hickman, M., Edmunds, W.J., and Trotter, C.L. (2013). Introducing vaccination against serogroup B meningococcal disease: An economic and mathematical modelling study of potential impact. Vaccine *31*, 2638–2646.

Christodoulides, M., Makepeace, B.L., Partridge, K.A., Kaur, D., Fowler, M.I., Weller, R.O., and Heckels, J.E. (2002). Interaction of Neisseria meningitidis with Human Meningeal Cells Induces the Secretion of a Distinct Group of Chemotactic, Proinflammatory, and Growth-Factor Cytokines. Infect. Immun. *70*, 4035–4044.

Chuang, P.I., Young, B.A., Thiagarajan, R.R., Cornejo, C., Winn, R.K., and Harlan, J.M. (1997). Cytoplasmic Domain of E-selectin Contains a Non-tyrosine Endocytosis Signal. J. Biol. Chem. *272*, 24813–24818.

Cohn, A.C., MacNeil, J.R., Harrison, L.H., Hatcher, C., Theodore, J., Schmidt, M., Pondo, T., Arnold, K.E., Baumbach, J., Bennett, N., et al. (2010). Changes in Neisseria meningitidis Disease Epidemiology in the United States, 1998–2007: Implications for Prevention of Meningococcal Disease. Clin. Infect. Dis. *50*, 184–191.

Constantin, D., Cordenier, A., Robinson, K., Ala'Aldeen, D.A.A., and Murphy, S. (2004). Neisseria meningitidis-induced death of cerebrovascular endothelium: mechanisms triggering transcriptional activation of inducible nitric oxide synthase. J. Neurochem. *89*, 1166–1174.

Copreni, E., Nicolis, E., Tamanini, A., Bezzerri, V., Castellani, S., Palmieri, L., Giri, M.G., Vella, A., Colombatti, M., Rizzotti, P., et al. (2009). Late generation lentiviral vectors: Evaluation of inflammatory potential in human airway epithelial cells. Virus Res. *144*, 8–17.

Cornelissen, C.N., and Sparling, P.F. (1994). Iron piracy: acquisition of transferrin-bound iron by bacterial pathogens. Mol. Microbiol. *14*, 843–850.

Cotran, R.S., and Pober, J.S. (1990). Cytokine-endothelial interactions in inflammation, immunity, and vascular injury. J. Am. Soc. Nephrol. *1*, 225–235.

Coureuil, M., Mikaty, G., Miller, F., Lécuyer, H., Bernard, C., Bourdoulous, S., Duménil, G., Mège, R.-M., Weksler, B.B., Romero, I.A., et al. (2009). Meningococcal Type IV Pili Recruit the Polarity Complex to Cross the Brain Endothelium. Science *325*, 83–87.

Coureuil, M., Lécuyer, H., Scott, M.G.H., Boularan, C., Enslen, H., Soyer, M., Mikaty, G., Bourdoulous, S., Nassif, X., and Marullo, S. (2010). Meningococcus Hijacks a [beta]2-Adrenoceptor/[beta]-Arrestin Pathway to Cross Brain Microvasculature Endothelium. Cell *143*, 1149–1160.

Coureuil, M., Join-Lambert, O., Lécuyer, H., Bourdoulous, S., Marullo, S., and Nassif, X. (2012). Mechanism of meningeal invasion by Neisseria meningitidis. Virulence *3*, 154–162.

Criss, A.K., and Seifert, H.S. (2012). A bacterial siren song: intimate interactions between Neisseria and neutrophils. Nat. Rev. Microbiol. *10*, 178–190.

Cuvelier, S.L., Paul, S., Shariat, N., Colarusso, P., and Patel, K.D. (2005). Eosinophil adhesion under flow conditions activates mechanosensitive signaling pathways in human endothelial cells. J. Exp. Med. *202*, 865–876.

Darton, T., Guiver, M., Naylor, S., Jack, D.L., Kaczmarski, E.B., Borrow, R., and Read, R.C. (2009). Severity of Meningococcal Disease Associated with Genomic Bacterial Load. Clin. Infect. Dis. *48*, 587–594.

Daugla, D., Gami, J., Gamougam, K., Naibei, N., Mbainadji, L., Narbé, M., Toralta, J., Kodbesse, B., Ngadoua, C., Coldiron, M., et al. (2014). Effect of a serogroup A meningococcal conjugate vaccine (PsA–TT) on serogroup A meningococcal meningitis and carriage in Chad: a community study. The Lancet *383*, 40–47.

Degel, J., and Shokrani, M. (2010). Validation of the efficacy of a practical method for neutrophils isolation from peripheral blood. Clin. Lab. Sci. J. Am. Soc. Med. Technol. *23*, 94–98.

Deghmane, A.-E., Giorgini, D., Larribe, M., Alonso, J.-M., and Taha, M.-K. (2002). Down-regulation of pili and capsule of Neisseria meningitidis upon contact with epithelial cells is mediated by CrgA regulatory protein. Mol. Microbiol. *43*, 1555–1564.

Dejana, E. (2004). Endothelial cell-cell junctions: happy together. Nat. Rev. Mol. Cell Biol. *5*, 261–270.

Delrieu, I., Yaro, S., Tamekloé, T.A.S., Njanpop-Lafourcade, B.-M., Tall, H., Jaillard, P., Ouedraogo, M.S., Badziklou, K., Sanou, O., Drabo, A., et al. (2011). Emergence of Epidemic Neisseria meningitidis Serogroup X Meningitis in Togo and Burkina Faso. PLoS ONE *6*, e19513.

Demaison, C., Parsley, K., Brouns, G., Scherr, M., Battmer, K., Kinnon, C., Grez, M., and Thrasher, A.J. (2002). High-level transduction and gene expression in hematopoietic repopulating cells using a human immunodeficiency [correction of imunodeficiency] virus type 1-based lentiviral vector containing an internal spleen focus forming virus promoter. Hum. Gene Ther. *13*, 803–813.

Deng, D.X.-F., Tsalenko, A., Vailaya, A., Ben-Dor, A., Kundu, R., Estay, I., Tabibiazar, R., Kincaid, R., Yakhini, Z., Bruhn, L., et al. (2006). Differences in Vascular Bed Disease Susceptibility Reflect Differences in Gene Expression Response to Atherogenic Stimuli. Circ. Res. *98*, 200–208.

Denk, A., Goebeler, M., Schmid, S., Berberich, I., Ritz, O., Lindemann, D., Ludwig, S., and Wirth, T. (2001). Activation of NF-κB via the IκB Kinase Complex Is Both Essential and Sufficient for Proinflammatory Gene Expression in Primary Endothelial Cells. J. Biol. Chem. *276*, 28451–28458.

Derrick, J., Heckels, J.E., and Virji, M. (2006). Major Outer Membrane Proteins of Meningococci. In Handbook of Meningococcal Disease, tthias Frosch, and rtin C. J.iden, eds. (Wiley-VCH Verlag GmbH & Co. KGaA), pp. 181–215.

Van Deuren, M., van der Ven-Jongekrijg, J., Bartelink, A.K., van Dalen, R., Sauerwein, R.W., and van der Meer, J.W. (1995). Correlation between proinflammatory cytokines and antiinflammatory mediators and the severity of disease in meningococcal infections. J. Infect. Dis. *172*, 433–439.

Van Deuren, M., Brandtzaeg, P., and van der Meer, J.W.M. (2000). Update on Meningococcal Disease with Emphasis on Pathogenesis and Clinical Management. Clin. Microbiol. Rev. *13*, 144–166.

DeVoe, I.W., Gilka, F., Gilchrist, J.E., and Yu, E. (1977). Pathology in rabbits treated with leukocyte-degraded meningococci in combination with meningococcal endotoxin. Infect. Immun. *16*, 271–279.

De Vos, Kurt (2008). Cell Counter Plugin - http://fiji.sc/Cell_Counter.

Dishart, K.L., Denby, L., George, S.J., Nicklin, S.A., Yendluri, S., Tuerk, M.J., Kelley, M.P., Donahue, B.A., Newby, A.C., Harding, T., et al. (2003). Third-generation lentivirus vectors efficiently transduce and phenotypically modify vascular cells: implications for gene therapy. J. Mol. Cell. Cardiol. *35*, 739–748.

Dixon, G.L.J., Heyderman, R.S., Kotovicz, K., Jack, D.L., Andersen, S.R., Vogel, U., Frosch, M., and Klein, N. (1999). Endothelial Adhesion Molecule Expression and Its Inhibition by Recombinant Bactericidal/Permeability-Increasing Protein Are Influenced by the Capsulation and Lipooligosaccharide Structure of Neisseria meningitidis. Infect Immun *67*, 5626–5633.

Dixon, G.L.J., Newton, P.J., Chain, B.M., Katz, D., Andersen, S.R., Wong, S., Ley, P. van der, Klein, N., and Callard, R.E. (2001). Dendritic Cell Activation and Cytokine Production Induced

by Group B Neisseria meningitidis: Interleukin-12 Production Depends on Lipopolysaccharide Expression in Intact Bacteria. Infect. Immun. *69*, 4351–4357.

Dixon, G.L.J., Heyderman, R.S., van der Ley, P., and Klein, N.J. (2004). High-level endothelial E-selectin (CD62E) cell adhesion molecule expression by a lipopolysaccharide-deficient strain of Neisseria meningitidis despite poor activation of NF-kappaB transcription factor. Clin. Exp. Immunol. *135*, 85–93.

Doerschuk, C.M., Beyers, N., Coxson, H.O., Wiggs, B., and Hogg, J.C. (1993). Comparison of neutrophil and capillary diameters and their relation to neutrophil sequestration in the lung. J. Appl. Physiol. Bethesda Md 1985 *74*, 3040–3045.

Doulet, N., Donnadieu, E., Laran-Chich, M.-P., Niedergang, F., Nassif, X., Couraud, P.O., and Bourdoulous, S. (2006). Neisseria meningitidis infection of human endothelial cells interferes with leukocyte transmigration by preventing the formation of endothelial docking structures. J. Cell Biol. *173*, 627–637.

Edwards, U., Müller, A., Hammerschmidt, S., Gerardy-Schahn, R., and Frosch, M. (1994). Molecular analysis of the biosynthesis pathway of the alpha-2,8 polysialic acid capsule by Neisseria meningitidis serogroup B. Mol. Microbiol. *14*, 141–149.

Erickson, L., and De Wals, P. (1998). Complications and sequelae of meningococcal disease in Quebec, Canada, 1990-1994. Clin. Infect. Dis. Off. Publ. Infect. Dis. Soc. Am. *26*, 1159–1164.

Estabrook, M.M., Jack, D.L., Klein, N.J., and Jarvis, G.A. (2004). Mannose-binding lectin binds to two major outer membrane proteins, opacity protein and porin, of Neisseria meningitidis. J. Immunol. Baltim. Md 1950 *172*, 3784–3792.

Eugène, E., Hoffmann, I., Pujol, C., Couraud, P.-O., Bourdoulous, S., and Nassif, X. (2002). Microvilli-like structures are associated with the internalization of virulent capsulated Neisseria meningitidis into vascular endothelial cells. J. Cell Sci. *115*, 1231–1241.

European Centre for Disease Prevention and Control (2013). Annual epidemiological report Reporting on 2010 surveillance data and 2011 epidemic intelligence data 2012.

Faust, S.N., Levin, M., Harrison, O.B., Goldin, R.D., Lockhart, M.S., Kondaveeti, S., Laszik, Z., Esmon, C.T., and Heyderman, R.S. (2001). Dysfunction of endothelial protein C activation in severe meningococcal sepsis. N. Engl. J. Med. *345*, 408–416.

Finne, J., Bitter-Suermann, D., Goridis, C., and Finne, U. (1987). An IgG monoclonal antibody to group B meningococci cross-reacts with developmentally regulated polysialic acid units of glycoproteins in neural and extraneural tissues. J. Immunol. *138*, 4402–4407.

Frosch, M., and Vogel, U. (2006). Structure and Genetics of the Meningococcal Capsule. In Handbook of Meningococcal Disease, tthias Frosch, and rtin C. J.iden, eds. (Wiley-VCH Verlag GmbH & Co. KGaA), pp. 145–162.

Ganguly, A., Zhang, H., Sharma, R., Parsons, S., and Patel, K.D. (2012). Isolation of Human Umbilical Vein Endothelial Cells and Their Use in the Study of Neutrophil Transmigration Under Flow Conditions. J. Vis. Exp.

Gardiner, E.E., and D'Souza, S.E. (1999). Sequences within Fibrinogen and Intercellular Adhesion Molecule-1 (ICAM-1) Modulate Signals Required for Mitogenesis. J. Biol. Chem. *274*, 11930–11936.

Gassart, A. de, Géminard, C., Février, B., Raposo, G., and Vidal, M. (2003). Lipid raft-associated protein sorting in exosomes. Blood *102*, 4336–4344.

Gedde-Dahl, T.W., Bjark, P., Høiby, E.A., Høst, J.H., and Bruun, J.N. (1990). Severity of meningococcal disease: assessment by factors and scores and implications for patient management. Rev. Infect. Dis. *12*, 973–992.

Gerszten, R.E., Luscinskas, F.W., Ding, H.T., Dichek, D.A., Stoolman, L.M., Gimbrone, M.A., and Rosenzweig, A. (1996). Adhesion of Memory Lymphocytes to Vascular Cell Adhesion Molecule-1 Transduced Human Vascular Endothelial Cells Under Simulated Physiological Flow Conditions In Vitro. Circ. Res. *79*, 1205–1215.

Gold, R., Goldschneider, I., Lepow, M.L., Draper, T.F., and Randolph, M. (1978). Carriage of Neisseria meningitidis and Neisseria lactamica in Infants and Children. J. Infect. Dis. *137*, 112–121.

Goldschneider, I., Gotschlich, E.C., and Artenstein, M.S. (1969a). Human Immunity to the Meningococcus I. the Role of Humoral Antibodies. J. Exp. Med. *129*, 1307–1326.

Goldschneider, I., Gotschlich, E.C., and Artenstein, M.S. (1969b). Human Immunity to the Meningococcus Ii. Development of Natural Immunity. J. Exp. Med. *129*, 1327–1348.

Goldschneider, I., Lepow, M.L., and Gotschlich, E.C. (1972). Immunogenicity of the Group A and Group C Meningococcal Polysaccharides in Children. J. Infect. Dis. *125*, 509–519.

Gorringe, A.R., and Pajón, R. (2012). Bexsero: a multicomponent vaccine for prevention of meningococcal disease. Hum. Vaccines Immunother. *8*, 174–183.

Gotschlich, E.C., Goldschneider, I., and Artenstein, M.S. (1969a). Human immunity to the meningococcus. IV. Immunogenicity of group A and group C meningococcal polysaccharides in human volunteers. J. Exp. Med. *129*, 1367–1384.

Gotschlich, E.C., Goldschneider, I., and Artenstein, M.S. (1969b). Human Immunity to the Meningococcus V. the Effect of Immunization with Meningococcal Group C Polysaccharide on the Carrier State. J. Exp. Med. *129*, 1385–1395.

Goujon, M., McWilliam, H., Li, W., Valentin, F., Squizzato, S., Paern, J., and Lopez, R. (2010). A new bioinformatics analysis tools framework at EMBL–EBI. Nucleic Acids Res. *38*, W695–W699.

Graham, F.L., Smiley, J., Russell, W.C., and Nairn, R. (1977). Characteristics of a human cell line transformed by DNA from human adenovirus type 5. J. Gen. Virol. *36*, 59–74.

Granoff, D.M., Welsch, J.A., and Ram, S. (2009). Binding of Complement Factor H (fH) to Neisseria meningitidis Is Specific for Human fH and Inhibits Complement Activation by Rat and Rabbit Sera. Infect. Immun. *77*, 764–769.

Gray, S.J., Trotter, C.L., Ramsay, M.E., Guiver, M., Fox, A.J., Borrow, R., Mallard, R.H., and Kaczmarski, E.B. (2006). Epidemiology of meningococcal disease in England and Wales

1993/94 to 2003/04: contribution and experiences of the Meningococcal Reference Unit. J. Med. Microbiol. *55*, 887–896.

Gray-Owen, S.D., and Schryvers, A.B. (1993). The interaction of primate transferrins with receptors on bacteria pathogenic to humans. Microb. Pathog. *14*, 389–398.

Green, C.E., Schaff, U.Y., Sarantos, M.R., Lum, A.F.H., Staunton, D.E., and Simon, S.I. (2006). Dynamic shifts in LFA-1 affinity regulate neutrophil rolling, arrest, and transmigration on inflamed endothelium. Blood *107*, 2101–2111.

Griffiths, N.J., Bradley, C.J., Heyderman, R.S., and Virji, M. (2007). IFN-γ amplifies NFκB-dependent Neisseria meningitidis invasion of epithelial cells via specific upregulation of CEA-related cell adhesion molecule 1. Cell. Microbiol. *9*, 2968–2983.

Griffiths, N.J., Hill, D.J., Borodina, E., Sessions, R.B., Devos, N.I., Feron, C.M., Poolman, J.T., and Virji, M. (2011). Meningococcal surface fibril (Msf) binds to activated vitronectin and inhibits the terminal complement pathway to increase serum resistance. Mol. Microbiol. *82*, 1129–1149.

Hackett, S.J., Guiver, M., Marsh, J., Sills, J.A., Thomson, A.P.J., Kaczmarski, E.B., and Hart, C.A. (2002). Meningococcal bacterial DNA load at presentation correlates with disease severity. Arch. Dis. Child. *86*, 44–46.

Hafezi-Moghadam, A., Thomas, K.L., Prorock, A.J., Huo, Y., and Ley, K. (2001). L-Selectin Shedding Regulates Leukocyte Recruitment. J. Exp. Med. *193*, 863–872.

Halperin, S.A., Bettinger, J.A., Greenwood, B., Harrison, L.H., Jelfs, J., Ladhani, S.N., McIntyre, P., Ramsay, M.E., and Sáfadi, M.A.P. (2012). The changing and dynamic epidemiology of meningococcal disease. Vaccine *30, Supplement 2*, B26–B36.

Hammarström, S. (1999). The carcinoembryonic antigen (CEA) family: structures, suggested functions and expression in normal and malignant tissues. Semin. Cancer Biol. *9*, 67–81.

Hammerschmidt, S., Birkholz, C., Zähringer, U., Robertson, B.D., van Putten, J., Ebeling, O., and Frosch, M. (1994). Contribution of genes from the capsule gene complex (cps) to lipooligosaccharide biosynthesis and serum resistance in Neisseria meningitidis. Mol. Microbiol. *11*, 885–896.

Hammerschmidt, S., Hilse, R., van Putten, J.P., Gerardy-Schahn, R., Unkmeir, A., and Frosch, M. (1996). Modulation of cell surface sialic acid expression in Neisseria meningitidis via a transposable genetic element. EMBO J. *15*, 192–198.

Hauck, C.R., Meyer, T.F., Lang, F., and Gulbins, E. (1998). CD66-mediated phagocytosis of Opa52 Neisseria gonorrhoeae requires a Src-like tyrosine kinase- and Rac1-dependent signalling pathway. EMBO J. *17*, 443–454.

Hazelzet, J.A. (2005). Diagnosing meningococcemia as a cause of sepsis. Pediatr. Crit. Care Med. J. Soc. Crit. Care Med. World Fed. Pediatr. Intensive Crit. Care Soc. *6*, S50–S54.

Hellerud, B.C., Stenvik, J., Espevik, T., Lambris, J.D., Mollnes, T.E., and Brandtzaeg, P. (2008). Stages of Meningococcal Sepsis Simulated In Vitro, with Emphasis on Complement and Toll-Like Receptor Activation. Infect Immun *76*, 4183–4189.

Heyderman, R.S., Ison, C.A., Peakman, M., Levin, M., and Klein, N.J. (1999). Neutrophil response to Neisseria meningitidis: inhibition of adhesion molecule expression and phagocytosis by recombinant bactericidal/permeability-increasing protein (rBPI21). J. Infect. Dis. *179*, 1288–1292.

Hidalgo, A., Peired, A.J., Wild, M.K., Vestweber, D., and Frenette, P.S. (2007). Complete Identification of E-Selectin Ligands on Neutrophils Reveals Distinct Functions of PSGL-1, ESL-1, and CD44. Immunity *26*, 477–489.

Hill, D.J., Griffiths, N.J., Borodina, E., and Virji, M. (2010). Cellular and molecular biology of Neisseria meningitidis colonization and invasive disease. Clin Sci (Lond) *118*, 547–564.

Hixenbaugh, E.A., Goeckeler, Z.M., Papaiya, N.N., Wysolmerski, R.B., Silverstein, S.C., and Huang, A.J. (1997). Stimulated neutrophils induce myosin light chain phosphorylation and isometric tension in endothelial cells. Am. J. Physiol. *273*, H981–H988.

Hoffmann, I., Eugène, E., Nassif, X., Couraud, P.-O., and Bourdoulous, S. (2001). Activation of ErbB2 receptor tyrosine kinase supports invasion of endothelial cells by Neisseria meningitidis. J. Cell Biol. *155*, 133–144.

Holten, E. (1979). Serotypes of Neisseria meningitidis isolated from patients in Norway during the first six months of 1978. J. Clin. Microbiol. *9*, 186–188.

Homeister, J.W., Zhang, M., Frenette, P.S., Hynes, R.O., Wagner, D.D., Lowe, J.B., and Marks, R.M. (1998). Overlapping functions of E- and P-selectin in neutrophil recruitment during acute inflammation. Blood *92*, 2345–2352.

Hu, Y., Kiely, J.-M., Szente, B.E., Rosenzweig, A., and Gimbrone, M.A. (2000). E-Selectin-Dependent Signaling Via the Mitogen-Activated Protein Kinase Pathway in Vascular Endothelial Cells. J Immunol *165*, 2142–2148.

Hu, Y., Szente, B., Kiely, J.-M., and Gimbrone, M.A. (2001). Molecular Events in Transmembrane Signaling via E-selectin. J. Biol. Chem. *276*, 48549–48553.

Humphries, H.E., Triantafilou, M., Makepeace, B.L., Heckels, J.E., Triantafilou, K., and Christodoulides, M. (2005). Activation of human meningeal cells is modulated by lipopolysaccharide (LPS) and non-LPS components of Neisseria meningitidis and is independent of Toll-like receptor (TLR)4 and TLR2 signalling. Cell. Microbiol. *7*, 415–430.

Ishii, H., Salem, H., Bell, C., Laposata, E., and Majerus, P. (1986). Thrombomodulin, an endothelial anticoagulant protein, is absent from the human brain. Blood *67*, 362–365.

Ivanov, S.S., and Roy, C.R. (2013). Pathogen signatures activate a ubiquitination pathway that modulates the function of the metabolic checkpoint kinase mTOR. Nat. Immunol. *14*, 1219–1228.

Jack, D.L., Dodds, A.W., Anwar, N., Ison, C.A., Law, A., Frosch, M., Turner, M.W., and Klein, N.J. (1998). Activation of complement by mannose-binding lectin on isogenic mutants of Neisseria meningitidis serogroup B. J. Immunol. Baltim. Md 1950 *160*, 1346–1353.

Jafri, R.Z., Ali, A., Messonnier, N.E., Tevi-Benissan, C., Durrheim, D., Eskola, J., Fermon, F., Klugman, K.P., Ramsay, M., Sow, S., et al. (2013). Global epidemiology of invasive meningococcal disease. Popul. Health Metr. *11*, 17.

Jarva, H., Ram, S., Vogel, U., Blom, A.M., and Meri, S. (2005). Binding of the Complement Inhibitor C4bp to Serogroup B Neisseria meningitidis. J. Immunol. *174*, 6299–6307.

Jarvis, G.A., and Vedros, N.A. (1987). Sialic acid of group B Neisseria meningitidis regulates alternative complement pathway activation. Infect. Immun. *55*, 174–180.

Jennings, M.P., Srikhanta, Y.N., Moxon, E.R., Kramer, M., Poolman, J.T., Kuipers, B., and Ley, P. van der (1999). The genetic basis of the phase variation repertoire of lipopolysaccharide immunotypes in Neisseria meningitidis. Microbiology *145*, 3013–3021.

Johansson, L., Rytkönen, A., Wan, H., Bergman, P., Plant, L., Agerberth, B., Hökfelt, T., and Jonsson, A.-B. (2005). Human-Like Immune Responses in CD46 Transgenic Mice. J. Immunol. *175*, 433–440.

Johswich, K.O., McCaw, S.E., Islam, E., Sintsova, A., Gu, A., Shively, J.E., and Gray-Owen, S.D. (2013). In Vivo Adaptation and Persistence of Neisseria meningitidis within the Nasopharyngeal Mucosa. PLoS Pathog *9*, e1003509.

Join-Lambert, O., Lecuyer, H., Miller, F., Lelievre, L., Jamet, A., Furio, L., Schmitt, A., Pelissier, P., Fraitag, S., Coureuil, M., et al. (2013). Meningococcal Interaction to Microvasculature Triggers the Tissular Lesions of Purpura Fulminans. J. Infect. Dis.

Jones, D.M., Borrow, R., Fox, A.J., Gray, S., Cartwright, K.A., and Poolman, J.T. (1992). The lipooligosaccharide immunotype as a virulence determinant in Neisseria meningitidis. Microb. Pathog. *13*, 219–224.

Jones, H.E., Uronen-Hansson, H., Callard, R.E., Klein, N., and Dixon, G.L.J. (2007). The differential response of human dendritic cells to live and killed Neisseria meningitidis. Cell. Microbiol. *9*, 2856–2869.

Jones, H.E., Copland, A., Hamstra, H.J., Cohen, J., Brown, J., Klein, N., van der Ley, P., and Dixon, G. (2014). LOS oligosaccharide modification enhances dendritic cell responses to meningococcal native outer membrane vesicles expressing a non-toxic lipid A. Cell. Microbiol. *16*, 519–534.

Jung, U., and Ley, K. (1999). Mice Lacking Two or All Three Selectins Demonstrate Overlapping and Distinct Functions for Each Selectin. J. Immunol. *162*, 6755–6762.

Kahler, C.M., Martin, L.E., Shih, G.C., Rahman, M.M., Carlson, R.W., and Stephens, D.S. (1998). The (α2→8)-Linked Polysialic Acid Capsule and Lipooligosaccharide Structure Both Contribute to the Ability of Serogroup B Neisseria meningitidis To Resist the Bactericidal Activity of Normal Human Serum. Infect. Immun. *66*, 5939–5947.

Källström, H., Islam, M.S., Berggren, P.-O., and Jonsson, A.-B. (1998). Cell Signaling by the Type IV Pili of Pathogenic Neisseria. J. Biol. Chem. *273*, 21777–21782.

Kaplanski, G., Farnarier, C., Benoliel, A.M., Foa, C., Kaplanski, S., and Bongrand, P. (1994). A Novel Role for E- and P-Selectins: Shape Control of Endothelial Cell Monolayers. J. Cell Sci. *107*, 2449–2457.

Kay, M.A., Glorioso, J.C., and Naldini, L. (2001). Viral vectors for gene therapy: the art of turning infectious agents into vehicles of therapeutics. Nat. Med. *7*, 33–40.

Kempe, S., Kestler, H., Lasar, A., and Wirth, T. (2005). NF-κB controls the global pro-inflammatory response in endothelial cells: evidence for the regulation of a pro-atherogenic program. Nucleic Acids Res. *33*, 5308–5319.

Kiely, J.-M., Hu, Y., García-Cardeña, G., and Gimbrone, M.A., Jr (2003). Lipid raft localization of cell surface E-selectin is required for ligation-induced activation of phospholipase C gamma. J. Immunol. Baltim. Md 1950 *171*, 3216–3224.

Kiely, J.-M., Luscinskas, F.W., and Gimbrone, M.A. Leukocyte-Endothelial Monolayer Adhesion Assay (Static Conditions). In Adhesion Protein Protocols, (New Jersey: Humana Press), pp. 131–136.

Kinlin, L.M., Spain, C.V., Ng, V., Johnson, C.C., White, A.N.J., and Fisman, D.N. (2009). Environmental Exposures and Invasive Meningococcal Disease: An Evaluation of Effects on Varying Time Scales. Am. J. Epidemiol. *169*, 588–595.

Kirchhausen, T. (1999). Adaptors for Clathrin-Mediated Traffic. Annu. Rev. Cell Dev. Biol. *15*, 705–732.

Kirchner, M., and Meyer, T.F. (2005). The PilC adhesin of the Neisseria type IV pilus – binding specificities and new insights into the nature of the host cell receptor. Mol. Microbiol. *56*, 945–957.

Kirchner, M., Heuer, D., and Meyer, T.F. (2005). CD46-Independent Binding of Neisserial Type IV Pili and the Major Pilus Adhesin, PilC, to Human Epithelial Cells. Infect. Immun. *73*, 3072–3082.

Kishimoto, T.K., Warnock, R.A., Jutila, M.A., Butcher, E.C., Lane, C., Anderson, D.C., and Smith, C.W. (1991). Antibodies against human neutrophil LECAM-1 (LAM-1/Leu-8/DREG-56 antigen) and endothelial cell ELAM-1 inhibit a common CD18-independent adhesion pathway in vitro. Blood *78*, 805–811.

Klein, N.J., Ison, C.A., Peakman, M., Levin, M., Hammerschmidt, S., Frosch, M., and Heyderman, R.S. (1996). The influence of capsulation and lipooligosaccharide structure on neutrophil adhesion molecule expression and endothelial injury by Neisseria meningitidis. J. Infect. Dis. *173*, 172–179.

Kluger, M., Johnson, D., and Pober, J. (1997). Mechanism of sustained E-selectin expression in cultured human dermal microvascular endothelial cells. J Immunol *158*, 887–896.

Kluger, M.S., Shiao, S.L., Bothwell, A.L.M., and Pober, J.S. (2002). Cutting Edge: Internalization of Transduced E-Selectin by Cultured Human Endothelial Cells: Comparison of Dermal Microvascular and Umbilical Vein Cells and Identification of a Phosphoserine-Type Di-leucine Motif. J. Immunol. *168*, 2091–2095.

Korade, Z., and Kenworthy, A.K. (2008). Lipid rafts, cholesterol, and the brain. Neuropharmacology *55*, 1265–1273.

Koumaré, B., Ouedraogo-Traoré, R., Sanou, I., Yada, A.A., Sow, I., Lusamba, P.-S., Traoré, E., Dabal, M., Santamaria, M., Hacen, M.-M., et al. (2007). The first large epidemic of meningococcal disease caused by serogroup W135, Burkina Faso, 2002. Vaccine *25, Supplement 1*, A37–A41.

Kristiansen, P.A., Diomandé, F., Ba, A.K., Sanou, I., Ouédraogo, A.-S., Ouédraogo, R., Sangaré, L., Kandolo, D., Aké, F., Saga, I.M., et al. (2013). Impact of the Serogroup A Meningococcal Conjugate Vaccine, MenAfriVac, on Carriage and Herd Immunity. Clin. Infect. Dis. *56*, 354–363.

Kuijper, P.H., Torres, H.G., Linden, J. van der, Lammers, J.W., Sixma, J.J., Koenderman, L., and Zwaginga, J.J. (1996). Platelet-dependent primary hemostasis promotes selectin- and integrin- mediated neutrophil adhesion to damaged endothelium under flow conditions. Blood *87*, 3271–3281.

Kuijper, P.H.M., Torres, H.I.G., Linden, J.A.M. van der, Lammers, J.-W.J., Sixma, J.J., Zwaginga, J.J., and Koenderman, L. (1997). Neutrophil Adhesion to Fibrinogen and Fibrin Under Flow Conditions Is Diminished by Activation and L-Selectin Shedding. Blood *89*, 2131–2138.

Lacy, P., and Eitzen, G. (2008). Control of granule exocytosis in neutrophils. Front. Biosci. J. Virtual Libr. *13*, 5559–5570.

Ladhani, S.N., Lucidarme, J., Newbold, L.S., Gray, S.J., Carr, A.D., Findlow, J., Ramsay, M.E., Kaczmarski, E.B., and Borrow, R. (2012). Invasive Meningococcal Capsular Group Y Disease, England and Wales, 2007-2009. Emerg. Infect. Dis. *18*, 63–70.

Lamaze, C., Fujimoto, L.M., Yin, H.L., and Schmid, S.L. (1997). The Actin Cytoskeleton Is Required for Receptor-mediated Endocytosis in Mammalian Cells. J. Biol. Chem. *272*, 20332–20335.

Lambotin, M., Hoffmann, I., Laran-Chich, M.-P., Nassif, X., Couraud, P.O., and Bourdoulous, S. (2005). Invasion of endothelial cells by Neisseria meningitidis requires cortactin recruitment by a phosphoinositide-3-kinase/Rac1 signalling pathway triggered by the lipo-oligosaccharide. J. Cell Sci. *118*, 3805–3816.

Lappann, M., Danhof, S., Guenther, F., Olivares-Florez, S., Mordhorst, I.L., and Vogel, U. (2013). In vitro resistance mechanisms of Neisseria meningitidis against neutrophil extracellular traps. Mol. Microbiol. *89*, 433–449.

Larkin, M.A., Blackshields, G., Brown, N.P., Chenna, R., McGettigan, P.A., McWilliam, H., Valentin, F., Wallace, I.M., Wilm, A., Lopez, R., et al. (2007). Clustal W and Clustal X version 2.0. Bioinformatics *23*, 2947–2948.

Lawrence, M., and Springer, T. (1993). Neutrophils roll on E-selectin. J Immunol *151*, 6338–6346.

Lawrence, M.B., Smith, C.W., Eskin, S.G., and McIntire, L.V. (1990). Effect of venous shear stress on CD18-mediated neutrophil adhesion to cultured endothelium. Blood *75*, 227–237.

Lécuyer, H., Nassif, X., and Coureuil, M. (2012). Two Strikingly Different Signaling Pathways Are Induced by Meningococcal Type IV Pili on Endothelial and Epithelial Cells. Infect. Immun. *80*, 175–186.

Lefort, C.T., and Ley, K. (2012). Neutrophil arrest by LFA-1 activation. Chemoattractants *3*, 157.

Lewis, L.A., Ram, S., Prasad, A., Gulati, S., Getzlaff, S., Blom, A.M., Vogel, U., and Rice, P.A. (2008). Defining targets for complement components C4b and C3b on the pathogenic neisseriae. Infect. Immun. *76*, 339–350.

Lewis, L.A., Ngampasutadol, J., Wallace, R., Reid, J.E.A., Vogel, U., and Ram, S. (2010). The Meningococcal Vaccine Candidate Neisserial Surface Protein A (NspA) Binds to Factor H and Enhances Meningococcal Resistance to Complement. PLoS Pathog *6*, e1001027.

Lewis, L.A., Carter, M., and Ram, S. (2012). The relative roles of fHbp, NspA and lipooligosaccharide sialylation in regulation of the alternative pathway of complement on meningococci. J. Immunol. Baltim. Md 1950 *188*, 5063–5072.

Ley, P. van der, and Steeghs, L. (2003). Lessons from an LPS-deficient Neisseria meningitidis mutant. J. Endotoxin Res. *9*, 124–128.

Lien, D.C., Worthen, G.S., Capen, R.L., Hanson, W.L., Checkley, L.L., Janke, S.J., Henson, P.M., and Wagner, W.W. (1990). Neutrophil Kinetics in the Pulmonary Microcirculation: Effects of Pressure and Flow in the Dependent Lung. Am. Rev. Respir. Dis. *141*, 953–959.

Liu, J.W., Pernod, G., Dunoyer-Geindre, S., Fish, R.J., Yang, H., Bounameaux, H., and Kruithof, E.K.O. (2006). Promoter Dependence of Transgene Expression by Lentivirus-Transduced Human Blood–Derived Endothelial Progenitor Cells. STEM CELLS *24*, 199–208.

Lorenzon, P., Vecile, E., Nardon, E., Ferrero, E., Harlan, J.M., Tedesco, F., and Dobrina, A. (1998). Endothelial cell E- and P-selectin and vascular cell adhesion molecule-1 function as signaling receptors. J. Cell Biol. *142*, 1381–1391.

Ma, Y.-Q., Plow, E.F., and Geng, J.-G. (2004). P-selectin binding to P-selectin glycoprotein ligand-1 induces an intermediate state of αMβ2 activation and acts cooperatively with extracellular stimuli to support maximal adhesion of human neutrophils. Blood *104*, 2549–2556.

Mackinnon, F.G., Borrow, R., Gorringe, A.R., Fox, A.J., Jones, D.M., and Robinson, A. (1993). Demonstration of lipooligosaccharide immunotype and capsule as virulence factors for Neisseria meningitidis using an infant mouse intranasal infection model. Microb. Pathog. *15*, 359–366.

Madico, G., Welsch, J.A., Lewis, L.A., McNaughton, A., Perlman, D.H., Costello, C.E., Ngampasutadol, J., Vogel, U., Granoff, D.M., and Ram, S. (2006). The Meningococcal Vaccine Candidate GNA1870 Binds the Complement Regulatory Protein Factor H and Enhances Serum Resistance. J. Immunol. Baltim. Md 1950 *177*, 501–510.

Maiden, M.C.J., and Caugant, D.A. (2006). The Population Biology of Neisseria meningitidis: Implications for Meningococcal Disease, Epidemiology and Control. In Handbook of Meningococcal Disease, tthias Frosch, and rtin C. J.iden, eds. (Wiley-VCH Verlag GmbH & Co. KGaA), pp. 17–35.

Mairey, E., Genovesio, A., Donnadieu, E., Bernard, C., Jaubert, F., Pinard, E., Seylaz, J., Olivo-Marin, J.-C., Nassif, X., and Dumenil, G. (2006). Cerebral microcirculation shear stress levels determine Neisseria meningitidis attachment sites along the blood-brain barrier. J. Exp. Med. *203*, 1939–1950.

Mamdouh, Z., Chen, X., Pierini, L.M., Maxfield, F.R., and Muller, W.A. (2003). Targeted recycling of PECAM from endothelial surface-connected compartments during diapedesis. Nature *421*, 748–753.

Mann, A.P., Somasunderam, A., Nieves-Alicea, R., Li, X., Hu, A., Sood, A.K., Ferrari, M., Gorenstein, D.G., and Tanaka, T. (2010). Identification of thioaptamer ligand against E-selectin: potential application for inflamed vasculature targeting. PloS One *5*.

Mantovani, A., Bussolino, F., and Introna, M. (1997). Cytokine regulation of endothelial cell function: from molecular level to the bedside. Immunol. Today *18*, 231–240.

Marc LaForce, F., Ravenscroft, N., Djingarey, M., and Viviani, S. (2009). Epidemic meningitis due to Group A Neisseria meningitidis in the African meningitis belt: A persistent problem with an imminent solution. Vaccine *27, Supplement 2*, B13–B19.

Marzouk, O., Thomson, A.P., Sills, J.A., Hart, C.A., and Harris, F. (1991). Features and outcome in meningococcal disease presenting with maculopapular rash. Arch. Dis. Child. *66*, 485–487.

Mathew, S., and Overturf, G.D. (2006). Complement and Properidin Deficiencies in Meningococcal Disease: Pediatr. Infect. Dis. J. *25*, 255–256.

McCaw, S.E., Schneider, J., Liao, E.H., Zimmermann, W., and Gray-Owen, S.D. (2003). Immunoreceptor tyrosine-based activation motif phosphorylation during engulfment of Neisseria gonorrhoeae by the neutrophil-restricted CEACAM3 (CD66d) receptor. Mol. Microbiol. *49*, 623–637.

McMahon, H.T., and Boucrot, E. (2011). Molecular mechanism and physiological functions of clathrin-mediated endocytosis. Nat. Rev. Mol. Cell Biol. *12*, 517–533.

Meijering, E., Dzyubachyk, O., and Smal, I. (2012). Methods for cell and particle tracking. Methods Enzymol. *504*, 183–200.

Melican, K., Michea Veloso, P., Martin, T., Bruneval, P., and Duménil, G. (2013). Adhesion of Neisseria meningitidis to Dermal Vessels Leads to Local Vascular Damage and Purpura in a Humanized Mouse Model. PLoS Pathog *9*, e1003139.

Merz, A.J., Rifenbery, D.B., Arvidson, C.G., and So, M. (1996). Traversal of a polarized epithelium by pathogenic Neisseriae: facilitation by type IV pili and maintenance of epithelial barrier function. Mol. Med. *2*, 745–754.

Merz, A.J., So, M., and Sheetz, M.P. (2000). Pilus retraction powers bacterial twitching motility. Nature *407*, 98–102.

Middleton, J., Neil, S., Wintle, J., Clark-Lewis, I., Moore, H., Lam, C., Auer, M., Hub, E., and Rot, A. (1997). Transcytosis and Surface Presentation of IL-8 by Venular Endothelial Cells. Cell *91*, 385–395.

Mikaty, G., Soyer, M., Mairey, E., Henry, N., Dyer, D., Forest, K.T., Morand, P., Guadagnini, S., Prévost, M.C., Nassif, X., et al. (2009). Extracellular Bacterial Pathogen Induces Host Cell Surface Reorganization to Resist Shear Stress. PLoS Pathog *5*, e1000314.

Mirlashari, M.R., Høiby, E.A., Holst, J., and Lyberg, T. (2001). Outer membrane vesicles from Neisseria meningitidis: effects on tissue factor and plasminogen activator inhibitor-2 production in human monocytes. Thromb. Res. *102*, 375–380.

Molesworth, A.M., Thomson, M.C., Connor, S.J., Cresswell, M.P., Morse, A.P., Shears, P., Hart, C.A., and Cuevas, L.E. (2002). Where is the meningitis belt? Defining an area at risk of epidemic meningitis in Africa. Trans. R. Soc. Trop. Med. Hyg. *96*, 242–249.

Molesworth, A.M., Cuevas, L.E., Connor, S.J., Morse, A.P., and Thomson, M.C. (2003). Environmental Risk and Meningitis Epidemics in Africa. Emerg. Infect. Dis. *9*, 1287–1293.

Moore, K.L., Andreoli, S.P., Esmon, N.L., Esmon, C.T., and Bang, N.U. (1987). Endotoxin enhances tissue factor and suppresses thrombomodulin expression of human vascular endothelium in vitro. J. Clin. Invest. *79*, 124–130.

Morand, P.C., and Rudel, T. (2006). Genetics, Structure and Function of Pili. In Handbook of Meningococcal Disease, tthias Frosch, and rtin C. J.iden, eds. (Wiley-VCH Verlag GmbH & Co. KGaA), pp. 235–254.

Muenzner, P., Dehio, C., Fujiwara, T., Achtman, M., Meyer, T.F., and Gray-Owen, S.D. (2000). Carcinoembryonic Antigen Family Receptor Specificity of Neisseria meningitidis Opa Variants Influences Adherence to and Invasion of Proinflammatory Cytokine-Activated Endothelial Cells. Infect. Immun. *68*, 3601–3607.

Mukaida, N. (2003). Pathophysiological roles of interleukin-8/CXCL8 in pulmonary diseases. Am. J. Physiol. - Lung Cell. Mol. Physiol. *284*, L566–L577.

Mulks, M.H., Plaut, A.G., Feldman, H.A., and Frangione, B. (1980). IgA proteases of two distinct specificities are released by Neisseria meningitidis. J. Exp. Med. *152*, 1442–1447.

Muller, W.A. (2009). Mechanisms of Transendothelial Migration of Leukocytes. Circ. Res. *105*, 223–230.

Müller, A.M., Hermanns, M.I., Skrzynski, C., Nesslinger, M., Müller, K.-M., and Kirkpatrick, C.J. (2002). Expression of the Endothelial Markers PECAM-1, vWf, and CD34 in Vivo and in Vitro. Exp. Mol. Pathol. *72*, 221–229.

Nassif, X., Lowy, J., Stenberg, P., O'Gaora, P., Ganji, A., and So, M. (1993). Antigenic variation of pilin regulates adhesion of Neisseria meningitidis to human epithelial cells. Mol. Microbiol. *8*, 719–725.

Nayak, S., and Herzog, R.W. (2010). Progress and prospects: immune responses to viral vectors. Gene Ther. *17*, 295–304.

Neal, K.R., Nguyen-Van-Tam, J.S., Jeffrey, N., Slack, R.C.B., Madeley, R.J., Ait-Tahar, K., Job, K., Wale, M.C.J., and Ala'Aldeen, D.A.A. (2000). Changing carriage rate of Neisseria meningitidis among university students during the first week of term: cross sectional study. BMJ *320*, 846–849.

Ngampasutadol, J., Ram, S., Blom, A.M., Jarva, H., Jerse, A.E., Lien, E., Goguen, J., Gulati, S., and Rice, P.A. (2005). Human C4b-binding protein selectively interacts with Neisseria gonorrhoeae and results in species-specific infection. Proc. Natl. Acad. Sci. U. S. A. *102*, 17142–17147.

Ngampasutadol, J., Ram, S., Gulati, S., Agarwal, S., Li, C., Visintin, A., Monks, B., Madico, G., and Rice, P.A. (2008). Human factor H interacts selectively with Neisseria gonorrhoeae and results in species-specific complement evasion. J. Immunol. Baltim. Md 1950 *180*, 3426–3435.

Nikulin, J., Panzner, U., Frosch, M., and Schubert-Unkmeir, A. (2006). Intracellular survival and replication of Neisseria meningitidis in human brain microvascular endothelial cells. Int. J. Med. Microbiol. IJMM *296*, 553–558.

Nottebaum, A.F., Cagna, G., Winderlich, M., Gamp, A.C., Linnepe, R., Polaschegg, C., Filippova, K., Lyck, R., Engelhardt, B., Kamenyeva, O., et al. (2008). VE-PTP maintains the endothelial barrier via plakoglobin and becomes dissociated from VE-cadherin by leukocytes and by VEGF. J. Exp. Med. *205*, 2929–2945.

Oftung, F., Løvik, M., Andersen, S.R., Frøholm, L.O., and Bjune, G. (1999). A mouse model utilising human transferrin to study protection against Neisseria meningitidis serogroup B induced by outer membrane vesicle vaccination. FEMS Immunol. Med. Microbiol. *26*, 75–82.

Orr, H.J., Gray, S.J., Macdonald, M., and Stuart, J.M. (2003). Saliva and Meningococcal Transmission. Emerg Infect Dis *9*, 1314–1315.

Øvstebø, R., Brandtzaeg, P., Brusletto, B., Haug, K.B.F., Lande, K., Høiby, E.A., and Kierulf, P. (2004). Use of robotized DNA isolation and real-time PCR to quantify and identify close correlation between levels of Neisseria meningitidis DNA and lipopolysaccharides in plasma and cerebrospinal fluid from patients with systemic meningococcal disease. J. Clin. Microbiol. *42*, 2980–2987.

Pace, D., Pollard, A.J., and Messonier, N.E. (2009). Quadrivalent meningococcal conjugate vaccines. Vaccine *27, Supplement 2*, B30–B41.

Paize, F., Sarginson, R., Makwana, N., Baines, P.B., Thomson, A.P.J., Sinha, I., Hart, C.A., Riordan, A., Hawkins, K.C., Carrol, E.D., et al. (2012). Changes in the sublingual microcirculation and endothelial adhesion molecules during the course of severe meningococcal disease treated in the paediatric intensive care unit. Intensive Care Med. *38*, 863–871.

Patel, K.D., Moore, K.L., Nollert, M.U., and McEver, R.P. (1995). Neutrophils use both shared and distinct mechanisms to adhere to selectins under static and flow conditions. J. Clin. Invest. *96*, 1887–1896.

Pathan, N., Faust, S., and Levin, M. (2003). Pathophysiology of meningococcal meningitis and septicaemia. Arch. Dis. Child. *88*, 601–607.

Pollard, A.J., and Nadel, S. (2006). Course of Disease and Clinical Management. In Handbook of Meningococcal Disease, tthias Frosch, and rtin C. J.iden, eds. (Wiley-VCH Verlag GmbH & Co. KGaA), pp. 481–517.

Pridmore, A.C., Wyllie, D.H., Abdillahi, F., Steeghs, L., van der Ley, P., Dower, S.K., and Read, R.C. (2001). A Lipopolysaccharide-Deficient Mutant of Neisseria meningitidis Elicits Attenuated Cytokine Release by Human Macrophages and Signals via Toll-like Receptor (TLR) 2 but Not via TLR4/MD2. J. Infect. Dis. *183*, 89–96.

Pron, B., Taha, M.-K., Rambaud, C., Fournet, J.-C., Pattey, N., Monnet, J.-P., Musilek, M., Beretti, J.-L., and Nassif, X. (1997). Interaction of Neisseria meningitidis with the Components of the Blood-Brain Barrier Correlates with an Increased Expression of PilC. J. Infect. Dis. *176*, 1285–1292.

Public Health England, PHE (2014). Invasive meningococcal infections laboratory reports, England and Wales by capsular group & epidemiological year, 1998/99-2012/13 (Public Health England).

Pujol, C., Eugène, E., de Saint Martin, L., and Nassif, X. (1997). Interaction of Neisseria meningitidis with a polarized monolayer of epithelial cells. Infect. Immun. *65*, 4836–4842.

Pujol, C., Eugène, E., Marceau, M., and Nassif, X. (1999). The meningococcal PilT protein is required for induction of intimate attachment to epithelial cells following pilus-mediated adhesion. Proc. Natl. Acad. Sci. *96*, 4017–4022.

Pusztaszeri, M.P., Seelentag, W., and Bosman, F.T. (2006). Immunohistochemical Expression of Endothelial Markers CD31, CD34, von Willebrand Factor, and Fli-1 in Normal Human Tissues. J. Histochem. Cytochem. *54*, 385–395.

Rafii, S., Dias, S., Meeus, S., Hattori, K., Ramachandran, R., Feuerback, F., Worgall, S., Hackett, N.R., and Crystal, R.G. (2001). Infection of Endothelium With E1-E4+, but Not E1-E4- , Adenovirus Gene Transfer Vectors Enhances Leukocyte Adhesion and Migration by Modulation of ICAM-1, VCAM-1, CD34, and Chemokine Expression. Circ. Res. *88*, 903–910.

Ram, S., and Vogel, U. (2006). Role of Complement in Defense Against Meningococcal Infection. In Handbook of Meningococcal Disease, tthias Frosch, and rtin C. J.iden, eds. (Wiley-VCH Verlag GmbH & Co. KGaA), pp. 273–293.

Ram, S., Cox, A.D., Wright, J.C., Vogel, U., Getzlaff, S., Boden, R., Li, J., Plested, J.S., Meri, S., Gulati, S., et al. (2003). Neisserial Lipooligosaccharide Is a Target for Complement Component C4b INNER CORE PHOSPHOETHANOLAMINE RESIDUES DEFINE C4b LINKAGE SPECIFICITY. J. Biol. Chem. *278*, 50853–50862.

Ram, S., Lewis, L.A., and Rice, P.A. (2010). Infections of people with complement deficiencies and patients who have undergone splenectomy. Clin. Microbiol. Rev. *23*, 740–780.

Ram, S., Lewis, L.A., and Agarwal, S. (2011). Meningococcal Group W-135 and Y Capsular Polysaccharides Paradoxically Enhance Activation of the Alternative Pathway of Complement. J. Biol. Chem. *286*, 8297–8307.

Ramachandran, V., Yago, T., Epperson, T.K., Kobzdej, M.M.A., Nollert, M.U., Cummings, R.D., Zhu, C., and McEver, R.P. (2001). Dimerization of a selectin and its ligand stabilizes cell rolling and enhances tether strength in shear flow. Proc. Natl. Acad. Sci. *98*, 10166–10171.

Ray, N., Kuwahara, M., Takada, Y., Maruyama, K., Kawaguchi, T., Tsubone, H., Ishikawa, H., and Matsuo, K. (2006). c-Fos suppresses systemic inflammatory response to endotoxin. Int. Immunol. *18*, 671–677.

Reisinger, K.S., Black, S., and Stoddard, J.J. (2010). Optimizing Protection Against Meningococcal Disease. Clin. Pediatr. (Phila.) *49*, 586–597.

Reller, L.B., MacGregor, R.R., and Beaty, H.N. (1973). Bactericidal Antibody after Colonization with Neisseria meningitidis. J. Infect. Dis. *127*, 56–62.

Ricklin, D., Hajishengallis, G., Yang, K., and Lambris, J.D. (2010). Complement - a key system for immune surveillance and homeostasis. Nat. Immunol. *11*, 785–797.

Rio, D.C., Clark, S.G., and Tjian, R. (1985). A mammalian host-vector system that regulates expression and amplification of transfected genes by temperature induction. Science *227*, 23–28.

Robinson, K., Taraktsoglou, M., Rowe, K.S.J., Wooldridge, K.G., and Ala'Aldeen, D.A.A. (2004). Secreted proteins from Neisseria meningitidis mediate differential human gene expression and immune activation. Cell. Microbiol. *6*, 927–938.

Rosenstein, N.E., Perkins, B.A., Stephens, D.S., Lefkowitz, L., Cartter, M.L., Danila, R., Cieslak, P., Shutt, K.A., Popovic, T., Schuchat, A., et al. (1999). The Changing Epidemiology of Meningococcal Disease in the United States, 1992–1996. J. Infect. Dis. *180*, 1894–1901.

Rosenstein, N.E., Perkins, B.A., Stephens, D.S., Popovic, T., and Hughes, J.M. (2001). Meningococcal Disease. N. Engl. J. Med. *344*, 1378–1388.

Ross, S.C., and Densen, P. (1984). Complement deficiency states and infection: epidemiology, pathogenesis and consequences of neisserial and other infections in an immune deficiency. Medicine (Baltimore) *63*, 243–273.

Rowe, H.A., Griffiths, N.J., Hill, D.J., and Virji, M. (2007). Co-ordinate action of bacterial adhesins and human carcinoembryonic antigen receptors in enhanced cellular invasion by capsulate serum resistant Neisseria meningitidis. Cell. Microbiol. *9*, 154–168.

Rubanyi, G.M. (1993). The role of endothelium in cardiovascular homeostasis and diseases. J. Cardiovasc. Pharmacol. *22 Suppl 4*, S1–S14.

Runnels, J.M., Zamiri, P., Spencer, J.A., Veilleux, I., Wei, X., Bogdanov, A., and Lin, C.P. (2006). Imaging Molecular Expression on Vascular Endothelial Cells by In Vivo Immunofluorescence Microscopy. Mol. Imaging *5*, 31–40.

Sadarangani, M., Pollard, A.J., and Gray-Owen, S.D. (2011). Opa proteins and CEACAMs: pathways of immune engagement for pathogenic Neisseria. FEMS Microbiol. Rev. *35*, 498–514.

Sa E Cunha, C., Griffiths, N.J., Murillo, I., and Virji, M. (2009). Neisseria meningitidis Opc invasin binds to the cytoskeletal protein alpha-actinin. Cell. Microbiol. *11*, 389–405.

Sa E Cunha, C., Griffiths, N.J., and Virji, M. (2010). Neisseria meningitidis Opc Invasin Binds to the Sulphated Tyrosines of Activated Vitronectin to Attach to and Invade Human Brain Endothelial Cells. PLoS Pathog *6*, e1000911.

Sarantis, H., and Gray-Owen, S.D. (2007). The specific innate immune receptor CEACAM3 triggers neutrophil bactericidal activities via a Syk kinase-dependent pathway. Cell. Microbiol. *9*, 2167–2180.

Sawada, T., Yoshida, M., Yasukouchi, Y., Watanabe, M., and Numano, F. (2001). Colon Cancer Cell Adhesion to Endothelial E-Selectin Inhibits Detachment of Endothelial Cells through Activation of β1-Integrin. Biochem. Biophys. Res. Commun. *286*, 20–27.

Schindelin, J. (2008). Fiji Is Just ImageJ (Batteries included).

Schindelin, J., Arganda-Carreras, I., Frise, E., Kaynig, V., Longair, M., Pietzsch, T., Preibisch, S., Rueden, C., Saalfeld, S., Schmid, B., et al. (2012). Fiji: an open-source platform for biological-image analysis. Nat. Methods *9*, 676–682.

Schmid, E., MüLler, T.H., Budzinski, R.-M., Binder, K., and Pfizenmaier, K. (1995). Signaling by E-selectin and ICAM-1 Induces Endothelial Tissue Factor Production via Autocrine Secretion of Platelet-Activating Factor and Tumor Necrosis Factor α. J. Interferon Cytokine Res. *15*, 819–825.

Schmitter, T., Agerer, F., Peterson, L., Münzner, P., and Hauck, C.R. (2004). Granulocyte CEACAM3 Is a Phagocytic Receptor of the Innate Immune System that Mediates Recognition and Elimination of Human-specific Pathogens. J. Exp. Med. *199*, 35–46.

Schneider, M.C., Exley, R.M., Ram, S., Sim, R.B., and Tang, C.M. (2007). Interactions between Neisseria meningitidis and the complement system. Trends Microbiol. *15*, 233–240.

Schneider, M.C., Prosser, B.E., Caesar, J.J.E., Kugelberg, E., Li, S., Zhang, Q., Quoraishi, S., Lovett, J.E., Deane, J.E., Sim, R.B., et al. (2009). Neisseria meningitidis recruits factor H using protein mimicry of host carbohydrates. Nature *458*, 890–893.

Schnell, U., Dijk, F., Sjollema, K.A., and Giepmans, B.N.G. (2012). Immunolabeling artifacts and the need for live-cell imaging. Nat. Methods *9*, 152–158.

Scholten, R.J.P.M., Kuipers, B., Valkenburg, H.A., Dankert, J., Zollinger, W.D., and Poolman, J.T. (1994). Lipo-oligosaccharide immunotyping of Neisseria meningitidis by a whole-cell ELISA with monoclonal antibodies. J. Med. Microbiol. *41*, 236–243.

Schorer, A.E., Moldow, C.F., and Rick, M.E. (1987). Interleukin 1 or endotoxin increases the release of von Willebrand factor from human endothelial cells. Br. J. Haematol. *67*, 193–197.

Schryvers, A.B., and Morris, L.J. (1988). Identification and characterization of the transferrin receptor from Neisseria meningitidis. Mol. Microbiol. *2*, 281–288.

Schubert-Unkmeir, A., Sokolova, O., Panzner, U., Eigenthaler, M., and Frosch, M. (2007). Gene Expression Pattern in Human Brain Endothelial Cells in Response to Neisseria meningitidis. Infect. Immun. *75*, 899–914.

Setiadi, H., and McEver, R.P. (2008). Clustering endothelial E-selectin in clathrin-coated pits and lipid rafts enhances leukocyte adhesion under flow. Blood *111*, 1989–1998.

Sharip, A., Sorvillo, F., Redelings, M.D., Mascola, L., Wise, M., and Nguyen, D.M. (2006). Population-Based Analysis of Meningococcal Disease Mortality in the United States: 1990???2002. Pediatr. Infect. Dis. J. *25*, 191–194.

Shaw, S.K., Ma, S., Kim, M.B., Rao, R.M., Hartman, C.U., Froio, R.M., Yang, L., Jones, T., Liu, Y., Nusrat, A., et al. (2004). Coordinated Redistribution of Leukocyte LFA-1 and Endothelial Cell ICAM-1 Accompany Neutrophil Transmigration. J. Exp. Med. *200*, 1571–1580.

Sheikh, S., Rainger, G.E., Gale, Z., Rahman, M., and Nash, G.B. (2003). Exposure to fluid shear stress modulates the ability of endothelial cells to recruit neutrophils in response to tumor necrosis factor-α: a basis for local variations in vascular sensitivity to inflammation. Blood *102*, 2828–2834.

Sica, A., Matsushima, K., Van Damme, J., Wang, J.M., Polentarutti, N., Dejana, E., Colotta, F., and Mantovani, A. (1990). IL-1 transcriptionally activates the neutrophil chemotactic factor/IL-8 gene in endothelial cells. Immunology *69*, 548–553.

Simon, S.I., Hu, Y., Vestweber, D., and Smith, C.W. (2000). Neutrophil Tethering on E-Selectin Activates β2 Integrin Binding to ICAM-1 Through a Mitogen-Activated Protein Kinase Signal Transduction Pathway. J. Immunol. *164*, 4348–4358.

Simonis, A., Hebling, S., Gulbins, E., Schneider-Schaulies, S., and Schubert-Unkmeir, A. (2014). Differential Activation of Acid Sphingomyelinase and Ceramide Release Determines Invasiveness of Neisseria meningitidis into Brain Endothelial Cells. PLoS Pathog *10*, e1004160.

Sinclair, D., Preziosi, M.-P., Jacob John, T., and Greenwood, B. (2010). The epidemiology of meningococcal disease in India. Trop. Med. Int. Health *15*, 1421–1435.

Sipehia, R., and Martucci, G. (1995). High-Efficiency Transformation of Human Endothelial Cells by Apo E-Mediated Transfection with Plasmid DNA. Biochem. Biophys. Res. Commun. *214*, 206–211.

Sithu, S.D., English, W.R., Olson, P., Krubasik, D., Baker, A.H., Murphy, G., and D'Souza, S.E. (2007). Membrane-type 1-Matrix Metalloproteinase Regulates Intracellular Adhesion Molecule-1 (ICAM-1)-mediated Monocyte Transmigration. J. Biol. Chem. *282*, 25010–25019.

Sjölinder, H., and Jonsson, A.-B. (2007). Imaging of Disease Dynamics during Meningococcal Sepsis. PLoS ONE *2*, e241.

Slevogt, H., Zabel, S., Opitz, B., Hocke, A., Eitel, J., N'Guessan, P.D., Lucka, L., Riesbeck, K., Zimmermann, W., Zweigner, J., et al. (2008). CEACAM1 inhibits Toll-like receptor 2–triggered antibacterial responses of human pulmonary epithelial cells. Nat. Immunol. *9*, 1270–1278.

Smith, C.W., Rothlein, R., Hughes, B.J., Mariscalco, M.M., Rudloff, H.E., Schmalstieg, F.C., and Anderson, D.C. (1988). Recognition of an endothelial determinant for CD 18-dependent human neutrophil adherence and transendothelial migration. J. Clin. Invest. *82*, 1746–1756.

Smith, C.W., Marlin, S.D., Rothlein, R., Toman, C., and Anderson, D.C. (1989). Cooperative interactions of LFA-1 and Mac-1 with intercellular adhesion molecule-1 in facilitating adherence and transendothelial migration of human neutrophils in vitro. J. Clin. Invest. *83*, 2008–2017.

Smith, M.L., Olson, T.S., and Ley, K. (2004). CXCR2- and E-Selectin–induced Neutrophil Arrest during Inflammation In Vivo. J. Exp. Med. *200*, 935–939.

Snape, M.D., Saroey, P., John, T.M., Robinson, H., Kelly, S., Gossger, N., Yu, L.-M., Wang, H., Toneatto, D., Dull, P.M., et al. (2013). Persistence of bactericidal antibodies following early infant vaccination with a serogroup B meningococcal vaccine and immunogenicity of a preschool booster dose. Can. Med. Assoc. J. *185*, E715–E724.

Sokolova, O., Heppel, N., Jägerhuber, R., Kim, K.S., Frosch, M., Eigenthaler, M., and Schubert-Unkmeir, A. (2004). Interaction of Neisseria meningitidis with human brain microvascular endothelial cells: role of MAP- and tyrosine kinases in invasion and inflammatory cytokine release. Cell. Microbiol. *6*, 1153–1166.

Sotto, M.N., Langer, B., Hoshino-Shimizu, S., and de Brito, T. (1976). Pathogenesis of Cutaneous Lesions in Acute Meningococcemia in Humans: Light, Immunofluorescent, and Electron Microscopic Studies of Skin Biopsy Specimens. J. Infect. Dis. *133*, 506–514.

Spinosa, M.R., Progida, C., Tala, A., Cogli, L., Alifano, P., and Bucci, C. (2007). The Neisseria meningitidis Capsule Is Important for Intracellular Survival in Human Cells. Infect. Immun. *75*, 3594–3603.

Springer, T.A. (1994). Traffic signals for lymphocyte recirculation and leukocyte emigration: The multistep paradigm. Cell *76*, 301–314.

Sprong, T., Stikkelbroeck, N., Ley, P. van der, Steeghs, L., Alphen, L. van, Klein, N., Netea, M.G., Meer, J.W.M. van der, and Deuren, M. van (2001). Contributions of Neisseria meningitidis LPS and non-LPS to proinflammatory cytokine response. J. Leukoc. Biol. *70*, 283–288.

Steeghs, L., den Hartog, R., den Boer, A., Zomer, B., Roholl, P., and van der Ley, P. (1998). Meningitis bacterium is viable without endotoxin. Nature *392*, 449–449.

Steeghs, L., de Cock, H., Evers, E., Zomer, B., Tommassen, J., and van der Ley, P. (2001). Outer membrane composition of a lipopolysaccharide-deficient Neisseria meningitidis mutant. EMBO J. *20*, 6937–6945.

Stein, B.N., Gamble, J.R., Pitson, S.M., Vadas, M.A., and Khew-Goodall, Y. (2003). Activation of Endothelial Extracellular Signal-Regulated Kinase Is Essential for Neutrophil Transmigration: Potential Involvement of a Soluble Neutrophil Factor in Endothelial Activation. J. Immunol. *171*, 6097–6104.

Stein-Zamir, C., Shoob, H., Sokolov, I., Kunbar, A., Abramson, N., and Zimmerman, D. (2014). The Clinical Features and Long Term Sequelae of Invasive Meningococcal Disease in Children. Pediatr. Infect. Dis. J.

Stephens, D.S., Greenwood, B., and Brandtzaeg, P. (2007). Epidemic meningitis, meningococcaemia, and Neisseria meningitidis. Lancet *369*, 2196–2210.

Stevens, T., Rosenberg, R., Aird, W., Quertermous, T., Johnson, F.L., Garcia, J.G.N., Hebbel, R.P., Tuder, R.M., and Garfinkel, S. (2001). NHLBI workshop report: endothelial cell phenotypes in heart, lung, and blood diseases. Am. J. Physiol. - Cell Physiol. *281*, C1422–C1433.

Sutherland, T.C., Quattroni, P., Exley, R.M., and Tang, C.M. (2010). Transcellular Passage of Neisseria meningitidis across a Polarized Respiratory Epithelium. Infect. Immun. *78*, 3832–3847.

Swartley, J.S., Marfin, A.A., Edupuganti, S., Liu, L.-J., Cieslak, P., Perkins, B., Wenger, J.D., and Stephens, D.S. (1997). Capsule switching of Neisseria meningitidis. Proc. Natl. Acad. Sci. *94*, 271–276.

Tedder, T.F., Steeber, D.A., Chen, A., and Engel, P. (1995). The selectins: vascular adhesion molecules. FASEB J. Off. Publ. Fed. Am. Soc. Exp. Biol. *9*, 866–873.

Tezera, L.B., Hampton, J., Jackson, S.K., and Davenport, V. (2011). Neisseria lactamica attenuates TLR-1/2-induced cytokine responses in nasopharyngeal epithelial cells using PPAR-γ. Cell. Microbiol. *13*, 554–568.

Thompson, M.J., Ninis, N., Perera, R., Mayon-White, R., Phillips, C., Bailey, L., Harnden, A., Mant, D., and Levin, M. (2006). Clinical recognition of meningococcal disease in children and adolescents. Lancet *367*, 397–403.

Thompson, P.W., Randi, A.M., and Ridley, A.J. (2002). Intercellular Adhesion Molecule (ICAM)-1, But Not ICAM-2, Activates RhoA and Stimulates c-fos and rhoA Transcription in Endothelial Cells. J. Immunol. *169*, 1007–1013.

Thorson, L.M., Turkalj, A., and Hung, J.C. (1995). In vitro evaluation of neutrophil viability after exposure to a hypotonic medium. Nucl. Med. Commun. *16*, 615–620.

Tilghman, R.W., and Hoover, R.L. (2002a). The Src-cortactin pathway is required for clustering of E-selectin and ICAM-1 in endothelial cells. FASEB J. Off. Publ. Fed. Am. Soc. Exp. Biol. *16*, 1257–1259.

Tilghman, R.W., and Hoover, R.L. (2002b). E-selectin and ICAM-1 are incorporated into detergent-insoluble membrane domains following clustering in endothelial cells. FEBS Lett. *525*, 83–87.

Del Tordello, E., Vacca, I., Ram, S., Rappuoli, R., and Serruto, D. (2014). Neisseria meningitidis NalP cleaves human complement C3, facilitating degradation of C3b and survival in human serum. Proc. Natl. Acad. Sci. U. S. A. *111*, 427–432.

Totsugawa, T., Kobayashi, N., Okitsu, T., Noguchi, H., Watanabe, T., Matsumura, T., Maruyama, M., Fujiwara, T., Sakaguchi, M., and Tanaka, N. (2002). Lentiviral Transfer of the LacZ Gene Into Human Endothelial Cells and Human Bone Marrow Mesenchymal Stem Cells. Cell Transplant. *11*, 481–488.

Tremblay, P.-L., Auger, F.A., and Huot, J. (2006). Regulation of transendothelial migration of colon cancer cells by E-selectin-mediated activation of p38 and ERK MAP kinases. Oncogene *25*, 6563–6573.

Tremblay, P.-L., Huot, J., and Auger, F.A. (2008). Mechanisms by which E-Selectin Regulates Diapedesis of Colon Cancer Cells under Flow Conditions. Cancer Res. *68*, 5167–5176.

Trotter, C.L., and Greenwood, B.M. (2007). Meningococcal carriage in the African meningitis belt. Lancet Infect. Dis. *7*, 797–803.

Trotter, C.L., Chandra, M., Cano, R., Larrauri, A., Ramsay, M.E., Brehony, C., Jolley, K.A., Maiden, M.C.J., Heuberger, S., and Frosch, M. (2007). A surveillance network for meningococcal disease in Europe. FEMS Microbiol. Rev. *31*, 27–36.

Turowski, P., Martinelli, R., Crawford, R., Wateridge, D., Papageorgiou, A.-P., Lampugnani, M.G., Gamp, A.C., Vestweber, D., Adamson, P., Dejana, E., et al. (2008). Phosphorylation of vascular endothelial cadherin controls lymphocyte emigration. J. Cell Sci. *121*, 29–37.

Tyski, S., Grzybowska, W., Dulny, G., Berthelsen, L., and Lind, I. (2001). Phenotypical and genotypical characterization of Neisseria meningitidis carrier strains isolated from Polish recruits in 1998. Eur. J. Clin. Microbiol. Infect. Dis. Off. Publ. Eur. Soc. Clin. Microbiol. *20*, 350–353.

Tzeng, Y.-L., Ambrose, K.D., Zughaier, S., Zhou, X., Miller, Y.K., Shafer, W.M., and Stephens, D.S. (2005). Cationic Antimicrobial Peptide Resistance in Neisseria meningitidis. J. Bacteriol. *187*, 5387–5396.

Uchida, E., Mizuguchi, H., Ishii-Watabe, A., and Hayakawa, T. (2002). Comparison of the efficiency and safety of non-viral vector-mediated gene transfer into a wide range of human cells. Biol. Pharm. Bull. *25*, 891–897.

Unkmeir, A., Latsch, K., Dietrich, G., Wintermeyer, E., Schinke, B., Schwender, S., Kim, K.S., Eigenthaler, M., and Frosch, M. (2002). Fibronectin mediates Opc-dependent internalization of Neisseria meningitidis in human brain microvascular endothelial cells. Mol. Microbiol. *46*, 933–946.

Urban, C.F., Lourido, S., and Zychlinsky, A. (2006). How do microbes evade neutrophil killing? Cell. Microbiol. *8*, 1687–1696.

Varki, A., Chrispeels, M.J., and National Center for Biotechnology Information (U.S.) (c1999). Chapter 31: C-type Lectins. In Essentials of Glycobiology, (Cold Spring Harbor, N.Y.: Cold Spring Harbor Laboratory Press),.

Villringer, A., Them, A., Lindauer, U., Einhäupl, K., and Dirnagl, U. (1994). Capillary perfusion of the rat brain cortex. An in vivo confocal microscopy study. Circ. Res. *75*, 55–62.

Virji, M. (2009). Pathogenic neisseriae: surface modulation, pathogenesis and infection control. Nat. Rev. Microbiol. *7*, 274–286.

Virji, M., Kayhty, H., Ferguson, D.J.P., Alexandrescu, C., Heckels, J.E., and Moxon, E.R. (1991). The role of pili in the interactions of pathogenic Neisseria with cultured human endothelial cells. Mol. Microbiol. *5*, 1831–1841.

Virji, M., Makepeace, K., Ferguson, D.J., Achtman, M., Sarkari, J., and Moxon, E.R. (1992). Expression of the Opc protein correlates with invasion of epithelial and endothelial cells by Neisseria meningitidis. Mol. Microbiol. *6*, 2785–2795.

Virji, M., Makepeace, K., Ferguson, D.J., Achtman, M., and Moxon, E.R. (1993). Meningococcal Opa and Opc proteins: their role in colonization and invasion of human epithelial and endothelial cells. Mol. Microbiol. *10*, 499–510.

Virji, M., Makepeace, K., and Moxon, E.R. (1994). Distinct mechanisms of interactions of Opc-expressing meningococci at apical and basolateral surfaces of human endothelial cells; the role of integrins in apical interactions. Mol. Microbiol. *14*, 173–184.

Virji, M., Makepeace, K., Peak, I., Ferguson, D.J.P., Jennings, M.P., and Moxon, E.R. (1995a). Opc- and pilus-dependent interactions of meningococci with human endothelial cells: molecular mechanisms and modulation by surface polysaccharides. Mol. Microbiol. *18*, 741–754.

Virji, M., Makepeace, K., Peak, I., Payne, G., Saunders, J.R., Ferguson, D.J.P., and Moxon, H.R. (1995b). Functional implications of the expression of PilC proteins in meningococci. Mol. Microbiol. *16*, 1087–1097.

Virji, M., Watt, S.M., Barker, S., Makepeace, K., and Doyonnas, R. (1996). The N-domain of the human CD66a adhesion molecule is a target for Opa proteins of Neisseria meningitidis and Neisseria gonorrhoeae. Mol. Microbiol. *22*, 929–939.

Virji, M., Evans, D., Hadfield, A., Grunert, F., Teixeira, A.M., and Watt, S.M. (1999). Critical determinants of host receptor targeting by Neisseria meningitidis and Neisseria gonorrhoeae : identification of Opa adhesiotopes on the N-domain of CD66 molecules. Mol. Microbiol. *34*, 538–551.

Vogel, U., Weinberger, A., Frank, R., Müller, A., Köhl, J., Atkinson, J.P., and Frosch, M. (1997). Complement factor C3 deposition and serum resistance in isogenic capsule and lipooligosaccharide sialic acid mutants of serogroup B Neisseria meningitidis. Infect. Immun. *65*, 4022–4029.

Vogel, U., Taha, M.-K., Vazquez, J.A., Findlow, J., Claus, H., Stefanelli, P., Caugant, D.A., Kriz, P., Abad, R., Bambini, S., et al. (2013). Predicted strain coverage of a meningococcal multicomponent vaccine (4CMenB) in Europe: a qualitative and quantitative assessment. Lancet Infect. Dis. *13*, 416–425.

Voges, M., Bachmann, V., Kammerer, R., Gophna, U., and Hauck, C.R. (2010). CEACAM1 recognition by bacterial pathogens is species-specific. BMC Microbiol. *10*, 117.

De Vries, F.P., Cole, R., Dankert, J., Frosch, M., and Van Putten, J.P.M. (1998). Neisseria meningitidis producing the Opc adhesin binds epithelial cell proteoglycan receptors. Mol. Microbiol. *27*, 1203–1212.

Vu, D.M., Shaughnessy, J., Lewis, L.A., Ram, S., Rice, P.A., and Granoff, D.M. (2012). Enhanced Bacteremia in Human Factor H Transgenic Rats Infected by Neisseria meningitidis. Infect. Immun. *80*, 643–650.

Vyse, A., Woltor, J.M., Chen, J., Ng, T., and Soriano-Gabarro, M. (2011). Meningococcal disease in Asia: an under-recognized public health burden. Epidemiol. Infect. *139*, 967–985.

Westlin, W.F., and Gimbrone, M.A. (1993). Neutrophil-mediated damage to human vascular endothelium. Role of cytokine activation. Am. J. Pathol. *142*, 117–128.

Wilder-Smith, A., Barkham, T.M.S., Earnest, A., and Paton, N.I. (2002). Acquisition of W135 meningococcal carriage in Hajj pilgrims and transmission to household contacts: prospective study. BMJ *325*, 365–366.

Wilson, B.S., Steinberg, S.L., Liederman, K., Pfeiffer, J.R., Surviladze, Z., Zhang, J., Samelson, L.E., Yang, L., Kotula, P.G., and Oliver, J.M. (2004). Markers for Detergent-resistant Lipid Rafts Occupy Distinct and Dynamic Domains in Native Membranes. Mol. Biol. Cell *15*, 2580–2592.

Witko-Sarsat, V., Rieu, P., Descamps-Latscha, B., Lesavre, P., and Halbwachs-Mecarelli, L. (2000). Neutrophils: Molecules, Functions and Pathophysiological Aspects. Lab. Invest. *80*, 617–653.

Wójciak-Stothard, B., Williams, L., and Ridley, A.J. (1999). Monocyte adhesion and spreading on human endothelial cells is dependent on Rho-regulated receptor clustering. J. Cell Biol. *145*, 1293–1307.

Woltmann, G., McNulty, C.A., Dewson, G., Symon, F.A., and Wardlaw, A.J. (2000). Interleukin-13 induces PSGL-1/P-selectin-dependent adhesion of eosinophils, but not neutrophils, to human umbilical vein endothelial cells under flow. Blood *95*, 3146–3152.

Wombacher, R., and Cornish, V.W. (2011). Chemical tags: Applications in live cell fluorescence imaging. J. Biophotonics *4*, 391–402.

Wong, H.E.E., Li, M.-S., Kroll, J.S., Hibberd, M.L., and Langford, P.R. (2011). Genome Wide Expression Profiling Reveals Suppression of Host Defence Responses during Colonisation by Neisseria meningitides but not N. lactamica. PLoS ONE *6*, e26130.

Woodfin, A., Voisin, M.-B., Imhof, B.A., Dejana, E., Engelhardt, B., and Nourshargh, S. (2009). Endothelial cell activation leads to neutrophil transmigration as supported by the sequential roles of ICAM-2, JAM-A, and PECAM-1. Blood *113*, 6246–6257.

World Health Organisation (2011). Weekly epidemiological record: meningococcal vaccines.

Wright, J.C., Plested, J.S., and Moxon, E.R. (2006). Genetics, Structure and Function of Lipopolysaccharide. In Handbook of Meningococcal Disease, tthias Frosch, and rtin C. J.iden, eds. (Wiley-VCH Verlag GmbH & Co. KGaA), pp. 163–179.

Writer, M.J., Marshall, B., Pilkington-Miksa, M.A., Barker, S.E., Jacobsen, M., Kritz, A., Bell, P.C., Lester, D.H., Tabor, A.B., Hailes, H.C., et al. (2004). Targeted gene delivery to human airway epithelial cells with synthetic vectors incorporating novel targeting peptides selected by phage display. J. Drug Target. *12*, 185–193.

Yago, T., Shao, B., Miner, J.J., Yao, L., Klopocki, A.G., Maeda, K., Coggeshall, K.M., and McEver, R.P. (2010). E-selectin engages PSGL-1 and CD44 through a common signaling pathway to induce integrin αLβ2-mediated slow leukocyte rolling. Blood *116*, 485–494.

Yang, L., Froio, R.M., Sciuto, T.E., Dvorak, A.M., Alon, R., and Luscinskas, F.W. (2005). ICAM-1 regulates neutrophil adhesion and transcellular migration of TNF-α-activated vascular endothelium under flow. Blood *106*, 584–592.

Yang, L., Kowalski, J.R., Yacono, P., Bajmoczi, M., Shaw, S.K., Froio, R.M., Golan, D.E., Thomas, S.M., and Luscinskas, F.W. (2006a). Endothelial Cell Cortactin Coordinates Intercellular Adhesion Molecule-1 Clustering and Actin Cytoskeleton Remodeling during Polymorphonuclear Leukocyte Adhesion and Transmigration. J. Immunol. *177*, 6440–6449.

Yang, L., Kowalski, J.R., Zhan, X., Thomas, S.M., and Luscinskas, F.W. (2006b). Endothelial cell cortactin phosphorylation by Src contributes to polymorphonuclear leukocyte transmigration in vitro. Circ. Res. *98*, 394–402.

Yi, K., Stephens, D.S., and Stojiljkovic, I. (2003). Development and evaluation of an improved mouse model of meningococcal colonization. Infect. Immun. *71*, 1849–1855.

Yoshida, M., Westlin, W.F., Wang, N., Ingber, D.E., Rosenzweig, A., Resnick, N., and Gimbrone, M.A. (1996). Leukocyte adhesion to vascular endothelium induces E-selectin linkage to the actin cytoskeleton. J. Cell Biol. *133*, 445–455.

Yoshida, M., Szente, B.E., Kiely, J.-M., Rosenzweig, A., and Gimbrone, M.A. (1998). Phosphorylation of the Cytoplasmic Domain of E-Selectin Is Regulated During Leukocyte-Endothelial Adhesion. J Immunol *161*, 933–941.

Yoshida, M., Chien, L.-J., Yasukochi, Y., and Numano, F. (2000). Differentiation-Induced Transmigration of HL60 Cells across Activated HUVEC Monolayer Involves E-selectin-Dependent Mechanisma. Ann. N. Y. Acad. Sci. *902*, 307–310.

Yoshida, M., Takano, Y., Sasaoka, T., Izumi, T., and Kimura, A. (2003). E-Selectin Polymorphism Associated With Myocardial Infarction Causes Enhanced Leukocyte-Endothelial Interactions Under Flow Conditions. Arter. Thromb Vasc Biol *23*, 783–788.

Zarantonelli, M.-L., Szatanik, M., Giorgini, D., Hong, E., Huerre, M., Guillou, F., Alonso, J.-M., and Taha, M.-K. (2007). Transgenic mice expressing human transferrin as a model for meningococcal infection. Infect. Immun. *75*, 5609–5614.

Zarbock, A., Lowell, C.A., and Ley, K. (2007). Spleen Tyrosine Kinase Syk Is Necessary for E-Selectin-Induced αLβ2 Integrin-Mediated Rolling on Intercellular Adhesion Molecule-1. Immunity *26*, 773–783.

Zhou, L., Somasundaram, R., Nederhof, R.F., Dijkstra, G., Faber, K.N., Peppelenbosch, M.P., and Fuhler, G.M. (2012). Impact of Human Granulocyte and Monocyte Isolation Procedures on Functional Studies. Clin. Vaccine Immunol. CVI *19*, 1065–1074.